An investigation of the expression of glucose regulated genes -crystallin and Molybdenum Cofactor Sulfurase C-Terminal in Diabetic Nephropathy

Mirzaei, Saman

Awarding institution:
King's College London

An investigation of the expression of glucose regulated genes μ-crystallin and Molybdenum Cofactor Sulfurase C-Terminal in Diabetic Nephropathy

A thesis submitted by

Saman Mirzaei

For the degree of Doctor of Philosophy from

King's College London

Diabetes Research Group

Division of Diabetes & Nutritional Sciences

School of Medicine

King's College London

February 2014

Abstract

Diabetic Nephropathy (DN), a major cause of end stage renal failure, is believed to result from hyperglycaemia-induced pathways in the kidney. We previously identified μ-crystalline (CRYM) and Molybdenum Cofactor Sulfurase C-terminal domain-containing protein 2 (MOSC2) as two of several hyperglycaemia-induced renal genes in the Goto-Kakizaki (GK) rat, and showed that both were regulated by glucose *in vitro* in human mesangial cells (HMCs). In the current thesis, we investigated their expression in models of diabetes as well as in circulating cells from DN patients, in order to evaluate these genes as potential biomarkers and to explore their possible roles in the pathophysiology of DN. The expression of CRYM and MOSC were examined in tissues obtained from *in vivo* mouse models including a streptozotocin (STZ)-induced model of diabetes reversible through islet transplantation, renal cells cultured in normal (5mM) and high (25mM) glucose, and blood samples from diabetic patients with and without nephropathy (n= 97)/ retinopathy (n= 36). mRNA levels were determined using qPCR relative to reference genes, and protein location/ abundance was determined using immunofluorescence. Functional analysis included N-hydroxylation assays.

Both CRYM and MOSC2 mRNAs increased during hyperglycaemia in the diabetic kidneys of the STZ-induced mice and this increase was attenuated by treatment of diabetes ($P<0.05$). Immunohistochemistry revealed an abundant expression of both proteins in tubular cells, and very low expression in mesangial cells. The hyperglycaemia-induced increase in renal CRYM was specific as we could not demonstrate any change in cardiac CRYM, and similarly no change in expression was found under diabetic conditions *in vitro* in Molybdenum Cofactor Sulfurase C-terminal domain-containing protein 1 (MOSC1), a homolog of MOSC2. Surprisingly, in high glucose (HG), CRYM and MOSC2 mRNA levels showed a slight decrease in cultured tubular cells, whereas they showed a significant increase in HMCs. Biochemical analysis of MOSC protein showed that hyperglycaemia increased the N-reductive activity of MOSC2 protein. To evaluate CRYM and MOSC mRNA levels as potential biomarkers of DN, we examined their expression in the peripheral blood of diabetic patients. We could detect low levels of CRYM but there was no expression of MOSC2. However, the closely related homolog MOSC1 was expressed in the peripheral blood though its mRNA levels did not change in association with DN. CRYM mRNA levels were 7.4-fold increased in patients with type 2 nephropathy and this effect was strongest in patients with a well controlled nephropathy compared to those with proteinuria. However, we found that circulating CRYM mRNA was reduced in patients with retinopathy. Therefore it is currently unclear if circulating CRYM is associated with nephropathy and its low levels of expression suggest it may not be a useful biomarker.

Our data suggest that diabetes leads to an increased expression of renal CRYM and MOSC2 mRNAs, and although there are high levels of both mRNAs in tubular cells, the up-regulation may be taking place in mesangial or other renal cells. Circulating CRYM mRNA levels showed changes in patients with nephropathy and retinopathy but MOSC1 remained unchanged. CRYM or MOSC1/2 are unlikely to be useful biomarkers for DN but may be involved in the pathways that lead to DN.

Acknowledgments

It would have been impossible to finish my study if it wasn't for the help and unlimited support of many people who were closely involved with my project. First and foremost, I would like to express my special thanks to Dr Afshan Malik whom I had the honour to have as my supervisor. Her unconditional support in every aspect and all her contributions of time and ideas made my PhD experience productive and stimulating. The joy and enthusiasm that she had for this research was so inspirational that it motivated me at all times even during tough times. Her patience is also greatly appreciated specially during my thesis-writing.

I thank Professor Peter Jones who contributed immensely to my PhD. I would like to thank to Dr Antje Havemeyer, and Heyka Jacob (Kiel University, Germany) for their collaboration with the MOSC work. I also thank Dr Luigi Gnudi (Cardiovascular Division, KCL) and Dr Sobha Sivaprasad (DNS, KCL) for making it possible to have access to patient samples, Dr Aileen King and Dr Chloe Chapman (Diabetes Research Group, KCL) for access to their streptozotcin mouse model tissues, and to Dr Sachin Supale and Professor Pierre Miescheler (University of Geneva, Switzerland) for providing the ß-Prohibitin 2 knockout mouse model tissues. I would also like to thank everyone in Diabetes Research Group for providing a stimulating and fun environment. Particularly, Professor Fasih Ansari, Dr Rojeen Shahni, Anna Czajka and Dr Saima Ajaz for their help in the lab and Kiran Hoolsy for proofreading the thesis.

Last but not least I would like to thank my family for all their love and encouragement. My parents have always valued my interests and talents and have devoted their lives to their children's success. My beloved grandfather, who I always looked up to, enlightened my life with his moral support and best of advice, in a way that despite no longer being with us, I always feel him near me at every step of my success. My dearest Delaram, who is the best sister any one could ever have.

Table of Contents

List of Figures

List of tables

Chapter 1

General Introduction

Chapter 1. General introduction

1.1. Diabetic mellitus

Worldwide, approximately 347 million people have been diagnosed with diabetes mellitus (Danaei et al., 2011). Recent surveys have predicted that by 2030, diabetes mellitus will be the seventh leading cause of death in the world (WHO, 2011). Diabetes mellitus is a disease caused by an inappropriately high blood sugar (hyperglycaemia) resulting from insulin deficiency or insulin resistance. There are two factors which are central to the pathophysiology of diabetes: the pancreatic-β cells and the secretory insulin. In the standard definition, diabetic mellitus occurs as a result of excessive glucose in the blood of diabetic patients. The new definition of diabetes considers diabetic symptoms as well as three criteria: a random plasma sugar level greater than 11mmol/l (millimoles per litre); a fasting plasma sugar level greater than or equal to 7 mmol/l (or 6.1 mmol/l in whole blood); a plasma sugar level greater than 11 mmol/l two hours after drinking 75 grams of glucose dissolved in water in an oral glucose tolerance test (OGTT; Rubin and Jarvis, 2011). In 1679 the English physician, Thomas Willis was the first person who reported that diabetic urine contained sugar and Matthew Dobson demonstrated that the urine and blood of patients with diabetes contained sugar (Dobson, 1776). In 1921, Fredrick Banting (1891-1941) and Charles Best (1899-1978) found that insulin is in the pancreas islets (Pick up and Williams, 2003).

In 1985, the World Health Organization categorized diabetes into two groups: insulin dependent mellitus (IDDM), or type I and non-insulin dependent diabetes mellitus (NIDDM), or type II, based on clinical symptoms, lifestyle and the type of treatment applied. Type 1 diabetes mellitus (T1DM) cause a deficiency of insulin and is categorized by the loss of the insulin-producing β cells of the islets of langerhans in the pancreas. In 1997, the American Diabetes Association (ADA) characterised diabetes into four characterisations based on the etiology of the disease: type 1 diabetes mellitus (T1DM); type 2 diabetes mellitus (T2DM); the secondary type of diabetes that can stem from genetic syndromes, surgery, drugs, malnutrition, infections and other illness; and gestational diabetes mellitus which appears during pregnancy (ADA, 2004).

T1DM is characterised by the loss of insulin-producing β cells of the islets of Langerhans in the pancreas, caused by an autoimmune T-cell-mediated mechanism and which results in insufficient insulin production (Rother 2007). This type of diabetes is more common under 40 but it can appear at any age and is triggered by various factors such as viruses, diet or chemicals in genetically predisposed people (Burno et al., 2005). About 10-15% of diabetic people are affected with type 1 and they are treated by exogenous insulin injections to replace the missing hormone (Bruno et al., 2005).

T2DM was formerly known as non-insulin-dependent or adult-onset (WHO, 1999), it is also known as obesity associated diabetes and is a metabolic disorder which is categorized by insulin resistance, relative insulin deficiency and hyperglycaemia (Kahn, 2000). This type of diabetes is very common and affects about 85-90% of diabetic people (Rizivi, 2004).

T1DM and T2DM have some different phenotypic variations although they share common symptoms, such as hyperglycaemia, glucose intolerance, hyperlipidaemia as well as similar complications; however, their pathogenesis is different from each other (Brownlee 2001). Hyperglycaemia alone leads to changes in several systems in the body, such as altered glucose, fat and protein metabolism, which can make microenvironment alteration in various cells and tissues. These effects are long-term and can result in diabetic complications (Ryan et al., 2009).

1.2. Complication of diabetes

Diabetic complications are the major cause of morbidity and mortality in patients with diabetes mellitus. Diabetic patients have a much higher risk of complications that involve many different systems within the body. Diabetic complications can be classified into two groups, acute and chronic. Acute complications of diabetes include diabetic ketoacidosis, and non-ketotic. Chronic complications are related to vascular disease and they are classified as macrovascular disease (affecting arteries that supply the heart and brain) and microvascular disease (due to damage to the small blood vessels) (Weiss and Sumpio, 2006). Diabetes-specific microvascular disease can lead to one or more of the following complications: diabetic retinopathy, which is proposed to be the most common ischaemic disorder and presents as an ocular manifestation of the retina, typically affecting patients who have had diabetes over 15

years (Chistiakov, 2011; Pardinato et al., 2005). Indeed, diabetic retinopathy is the result of damage to the blood vessels in the retina which can lead to blindness; diabetic nephropathy, caused by damage to the kidney, which can lead to chronic renal failure; and diabetic neuropathy, which is the result of high blood glucose levels and which can damage nerves throughout the body. Worldwide, Diabetes mellitus (DM) has been identified as the most common cause of renal failure (ADA, 2006).

Chronic hyperglycaemia is linked to diabetes and can be the cause of structural and functional alterations in the retina, nerves, kidneys, and blood vessels (Table 1: Williams et al., 2002). As described previously, many complications of diabetes are considered to be due to persistently increased levels of blood glucose and are far less common and less severe in people who have well-controlled blood sugar levels (Nathan et al., 2006). Indeed, intensive control of hyperglycaemia reduces the progression of retinopathy, neuropathy and nephropathy in diabetic patients (Cefalu, 2005; DCCT/EDIC, 2005; UKPDS, 1998; DCCT, 1993).

1.3. Diabetic nephropathy

Diabetic nephropathy (DN) is one of the most serious complications among diabetic patients (including T1DM & T2DM) and occurs in up to 40% of cases (ADA, 2004). Diabetic nephropathy is a non-immune disease and is the major cause of end stage renal disease; it is this progressive renal disease which develops within 10-30 years of the onset of diabetes in the western world (Schena and Gesualdo, 2005; ADA, 2004). It is also the leading cause of chronic kidney disease in patients and although both diabetic groups can lead to end stage renal disease, it is more common in patients with T2DM (Ritz and Tang, 2001).

Diabetic nephropathy is closely associated with cardiovascular disease and blood vessel disease. High blood pressure is a common factor in diabetes which can involve diabetic nephropathy by damaging the kidneys. Indeed, heart disease, high blood pressure and cholesterol levels raise the risk of diabetic nephropathy, although hyperglycaemia may also play a role in its development (Rubin and Jarvis, 2011).

Table 1. The chronic complications of diabetes (modified from Williams et al., 2002)

Organ affected	Disease
Eyes	Retinopathy, Glaucoma
	Cataracts
	Blindness
Blood vessels	Coronary artery disease (CAD)
	Cerebral vascular disease (CVD)
	Peripheral vascular disease (PVD)
	Hypertension
Kidneys	Renal insufficiency
	Kidney failure
Skin, Muscle, Bone	Advanced infections
	Cellulitis
	Gangrene
	Amputation

At the time of a diabetic diagnosis, major functional changes occur in patients with T1D and T2D. Theses functional changes include an increase in kidney size, reversible albuminuria and an increase in the glomerular hyperfiltration rate (GFR). At the early stages in the development of the onset of diabetes, renal biopsies are normal. Within 1½ to 2½ years, glomerular basement membrane (a filmentous network of collagen IV and laminin) thickening appears. Each kidney has a structure which is called the glomerulus; it has the capacity to filter and clean the blood. The blood is filtered by passing through the glomerular capillaries, which have intimate contact with tubules. When the filtrate passes into the tubules, most of the water and small solutes within the blood are reabsorbed. Meanwhile a small amount of water and solutes passes from the kidney into the ureter and finally forms urine (Rubin and

Jarvis, 2011; Border et al., 1966). The expanding membranes begin to reduce the space occupied by the capillaries within the glomeruli. Thus, this process prevents blood filtration. In addition to GBM thickening, there are other changes such as: nodular and diffuse forms of intracapillary glomerulosclerosis, the fibrin cap, the capsular drop lesion and mesangila matrix expansion (Greenberg, 1998).

The estimated glomerular filtration rate (eGFR) and microalbuminuria are the first indicators for patients with DN. The eGFR is calculated on the basis of age and the creatinine level in the blood and is the most popular test used to check the kidney function. However, microalbuminuria is an alternative test which can reveal early signs of kidney damage when the eGFR is still normal. Less than 30 mg/24h albumin is detected in normal urine and about 20% of renal plasma is filtered at glumerulus over the duration of one day. Any filtered proteins are reabsorbed into peritubular capillaries (Gudehithlu et al., 2004). Patients with DN have increased urinary albumin excretion of 300 mg/24h. Under normal conditions, albumin accounts for 60% of protein in plasma and only tiny amounts of albumin are filtered at glumerulus. With the microalbuminuria test, those patients at risk of DN which have a urinary albumin excretion between 30 and 300 mg/24h can be identified. The presence of microalbuminuria in patients with DN is highly predictive of the development of DN over the next 10 to 15 years (Greenberg, 1998). Should it be undetected for more than 15 years, the damage may become so severe that it can lead to kidney failure (Rubin and Jarvis, 2011). Figure 1 shows the normal management of albumin by the glomerulus.

The progression of DN goes from relatively minor to end stage renal disease and includes five stages (Moregensen, 1989) namely hyperfiltration, microalbuminuria, proteinuria, advanced clinical nephropathy and end-stage renal failure (Rubin and Jarvis, 2011). At the first stage (hyperfiltration), a huge amount of glucose enters the kidneys and draws a large amount of water. Therefore, the blood flow through the glomeruli increases and the kidneys become enlarged. The second stage (microalbuminuria) usually occurs 10-30 years after diagnosis. During this stage, the filtration rate increases and the glomeruli show signs of damage.

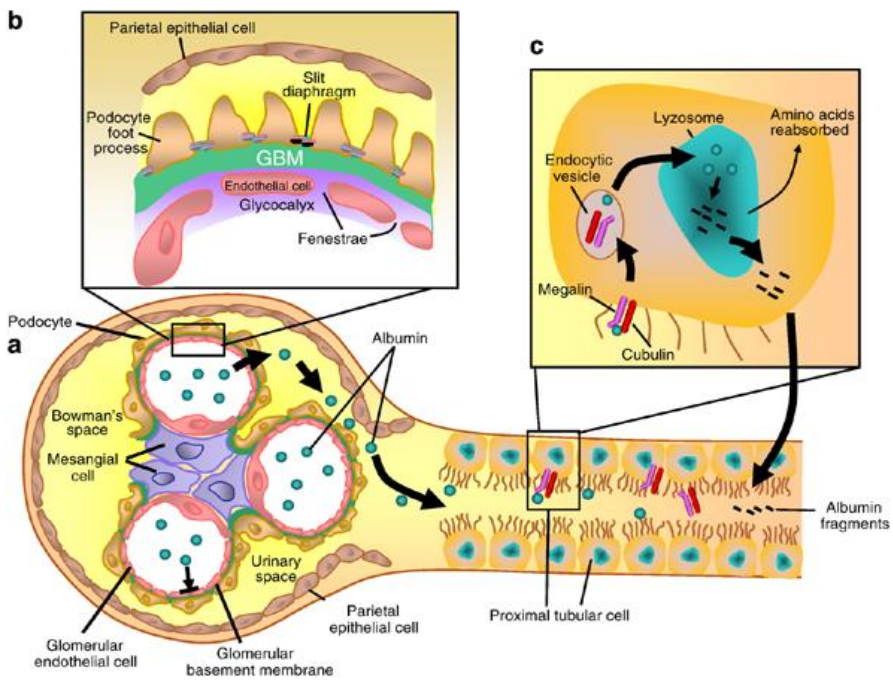

Figure 1.Normal renal management of albumin.

a) Normal glomerulus and proximal tubule. The individual cells and constituents of the glomerulus and proximal tubules are shown. Albumin (represented by green spheres). b) Glomerular filtration barrier. c) Proximal tubule. The albumin that is physiologically filtered at the level of glomerulus into the urinary space is taken up by the megalin/cubulin receptor lining the brush border of proximal tubular cells. Albumin is internalized by vesicles, and upon lysozyme action, the resultant fragments are either reabsorbed or secreted back into the tubular lumen as albumin fragments .Taken from Jefferson et al., 2008.

This damage provides the conditions for a small amount of albumin to leak into the urine. However, there is no diagnostic test, as the amount of urinary albumin is less than the estimated amount and therefore a number of patients continue at this stage for the remainder of their lives (silent stage).

In the third stage, levels of creatinine and urea increase because of reduced ability of the glomeruli to filter. In this stage, patients show a decline in microalbuminuria and the GFR. In the fourth stage (advanced clinical nephropathy), there is a significant amount of albumin in the urine (AER; normal range =<30 mg/day), a gradual GFR decline and high levels of creatinine and urea in the serum. The elevation in AER and

reduction in GFR lead to extensive glomerular closure that marks end-stage renal that marks end-stage renal disease. During this stage, kidneys continue to supply residual function, even when dialysis has commenced (Morgensen, 1989). Table 2 represents the stages in the progression of DN.

Table 2. Stages in the progression of diabetic nephropathy (DN)

Stages	Designation	Characteristics	GFR	Albumin Excretion	Chronology
Stage 1	Hyper-function/ hypertrophy	Glomerular Hyperfiltration	Increased in type 1 and type 2	May be increased	Present at diagnosis
Stage 2	Silent stage	Thickend Basement Membrane Expanded Mesangium	Normal	Type 1 normal Type 2 <30-300mg/dL	First 5 years
Stage 3	Incipient Stage	Microalbuminuria	GFR begins to fall	30-300 mg/dL	6-15 years
Stage 4	Overt diabetic nephropathy	Macroalbuminuria	Reduced GFR	> 380 mg/dL	15-25 years
Stage 5	Uremic	ESRD (End Stage Renal Disease)	0-10	Decreasing	24-30 years

The histological changes in the glomeruli of patients with DN are: first-mesangial expansion, which correlates with creatinine clearance and is induced directly by hyperglycaemia, perhaps via increased matrix production or glycosylation of matrix proteins; second-glomerular basement membrane (GBM) thickening; third-glomerular sclerosis as the result of intraglomerular hypertension. The expanded mesangium is the cause of diffuse glomerulosclerosis, which ultimately leads to a decrease in the density of capillaries and in the glomerular filtration surface area. Permeability of the filtration barrier falls and consequently GFR declines. Extracellular matrix (ECM) also builds up in the tubular BM and the interstitial compartment (Osterby, 1992; Vestra et al., 2000). In the diabetic kidney, tubulointerstitial fibrosis and glomerular sclerosis occur. Indeed, tubulointerstitial fibrosis is described by an excess of ECM accumulation in the renal interstitium (Iwano et al., 2004). These hemodynamic alterations lead to DN progression as a result of shear stress on the endothelial and mesangial cell, which is countered by increasing growth factor, cytokine and ECM

production (Raptis and Viberti, 2001). Figure 2 shows the histological changes in the glomeruli of patients with DN.

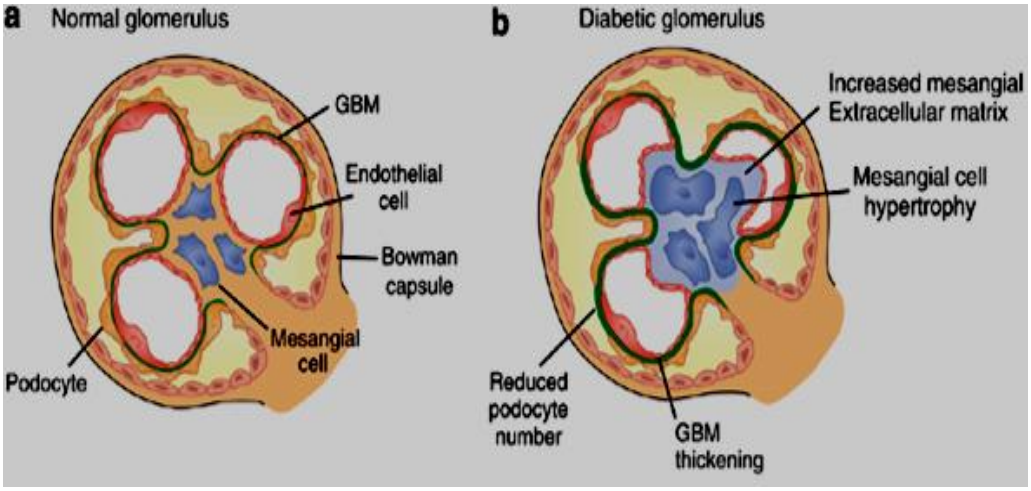

Figure 2. Characteristic glomerular changes of diabetic nephropathy (DN).

a) Normal glomerulus. Cells of the glomerular tuft (mesangial cells, endothelial cells, and podocytes) and extracapillary glomerulus (parietal epithelial cells) are shown, along with the GBM. (b) Diabetic kidney. In the diabetic kidney, characteristic glomerular changes include thickening of GBM and mesangial expansion. Taken from Jefferson et al., 2008.

1.4. Risk factors for DN

1.4.1. Hyperglycaemia

It is well established that most microvascular complications as a result of diabetes, such as diabetic nephropathy, are associated to the degree and length of exposure of hyperglycaemia. Indeed, hyperglycaemia is the main factor initiating the progression of nephropathy and other diabetic complications (Unnikrishnan et al., 2011). A number of clinical studies have highlighted the role and the value of early glycemic control in the prevention of the development of diabetic complications. The Diabetes Control and Complications Trial (DCCT) was the longest and largest prospective study to confirm the importance of optimising glycaemic control in T1DM (DCCT, 1993).

In this study, a total number of 1,441 subjects, aged 13 to 39, with T1DM were enrolled from 26 health centres in the US and Canada between 1983 and 1989. This

study was designed in two groups and both groups of patients were monitored for a mean period of 6.5 years. The first group (a primary-preventative cohort) was called the standard treatment group which included 726 subjects who were recruited within 1-5 years after developing diabetes, had no diabetic nephropathy and had a urinary albumin excretion of <40 mg/day. The second group (a secondary-preventative cohort) was called the intensive treatment group which included 715 subjects who had been living for 1-15 years after developing diabetes and they had mild-to-moderate background diabetic retinopathy with a urinary albumin excretion of <200mg/day.

In the standard treatment group, intensive therapy decreased the adjusted mean risk for the progression of retinopathy by 76% as compared with conventional therapy. In the intensive treatment group, intensive therapy slowed the development of retinopathy by 54% and decreased the progression of proliferative retinopathy (PDR) or nonproliferative retinopathy (NPDR) by 74%. In the combined groups, intensive therapy decreased the incidence of microalbuminuria (urinary albumin excretion of ≥ 40 mg per 24 hours) by 39% and that of albuminuria (urinary albumin excretion of ≥ 300 mg per 24 hours) by 54%, and it also reduced the occurrence of clinical neuropathy by 60%. This study concluded that intensive therapy efficiently delays and slows the development of diabetic complications in patients with T1DM (DCCT, 1993).

The DCCT demonstrated that improved glucose control in patients with T1DM had beneficial effects and decreased risks for the progression of microvascular complications. Following the DCCT study, the Epidemiology of Diabetes Interventions and Complications (EDIC) study began in January 1994. This study investigated the interactions between established and putative risk factors for long-term microvascular complications and cardiovascular disease of patients with T1DM as well as prior treatments of diabetes and the level of glycemic control during the DCCT (EDIC, 1999).

For the EDIC study, 28 out of 29 DCCT clinics contributed. The EDIC studies have shown that intensive blood glucose control reduced the risk of cardiovascular events by 42% and it also decreased the event of death as a result of cardiovascular causes, non-fatal heart attack and stroke by 57%.

The conclusion of DCCT and its follow-up observational study (EDIC) showed that intensive therapy reduces the development and progression of all diabetic-specific complications. The long-term results of the DCCT/EDIC demonstrated that intensive therapy reduced the risk of kidney dysfunction by 50% (DCCT/EDIC, 2003). Furthermore, data reported by the DCCT/EDIC (2003) indicated that intensive therapy decreased the risk for albuminuria during the DCCT and throughout the first eight years of the EDIC study. In addition, a review of the DCCT/EDIC (2011) reported that the intensive therapy also reduced the risk for an impaired glomerular filtration rate by 50%.

Based on the DCCT trial which indicated that strict control reduces complications in patients with T1DM, the results of the long-awaited UK prospective Diabetes Study (UKPDS) demonstrated that the risk of diabetic complications can be decreased significantly in patients with T2DM. The UKPDS trial recruited 5,102 patients with newly diagnosed T2DM and it ran for twenty years (1977 to 1991) in 23 clinical centres based in England, Northern Ireland and Scotland. 4,209 subjects were randomly allocated to receive either conventional therapy (dietary restriction) or intensive therapy (either sulfonylurea or insulin, or metformin in overweight patients) for the control of glucose.

In this study, patients were monitored for a mean follow up time of 10 years to demonstrate whether the intensive pharmacological therapy to lower blood glucose levels can reduce the occurrence and progression of cardiovascular and microvascular complications. The second aim was designed to test the therapeutic advantages or disadvantages of the usage of numerous sulfonylurea drugs, the biguanide drug Metformin, or insulin. The UKPDS data revealed that diabetic complications such as nephropathy, retinopathy and neuropathy are benefitted by better blood glucose control in T2DM with intensive therapy and their overall rate was decreased by 25%. These results also established that hyperglycaemia is the major contributor to these complications. The study demonstrated that better blood pressure control (a mean of 144/82 mmHg) in the majority of patients notably reduced the risk of death from long-term diabetic complications, stroke, heart failure and visual loss (UKPDS, 1998).

Therefore, these results confirm previous conclusions that hyperglycaemia is the initiating cause of diabetic tissue damage including diabetic nephropathy (DCCT,

1993; UKPDS, 1998). However, this process is modified by both genetic and independent accelerating factors such as hypertension (Brownlee, 2001).

1.4.2. Metabolic memory

As described previously, hyperglycaemia is a main factor in the development of diabetic nephropathy. Despite strict glucose control, vascular complications still develop in most diabetic patients. For instance, the UKPDS was unable to show a significant effect of tight glycaemic control in the prevention of cardiovascular disease, whereas a recent follow-up of the same study seems to confirm the usefulness of long-term glycaemia in patients with T2DM. Taken together, it was suggested that the control of hyperglycaemia is not enough to completely reduce complications (Ceriello et al., 2009).

The first theory of metabolic memory was reported 20 years ago in the retina of diabetic dogs who were switched to good hyperglycaemia control after either 2 months or 2.5 years of poor glycaemic control. The animals which were switched to good hyperglycaemia control after 2 months of poor glycaemic control had little sign of retinopathy. Conversely, the animals that were switched to good glucose control after 2.5 years of poor glucose control showed similar signs of retinopathy (Engerman and Kern, 1987). Following this study, Lorenzi's research group showed that in isolated endothelial cells and in the kidneys of streptozotocin (STZ)-induced diabetic rats there was a memory of basement membrane (collagen IV, fibronectin) mRNA induction one week after glucose normalisation, after two weeks of high glucose condition (Roy et al., 1990).

The metabolic memory phenomenon emerged clinically, to describe the fact that despite good glycemic control, T1DM patients in the DCCT-EDIC trial still had a higher occurrence of microvascular diabetic complications. The follow-up of the UKPDS results showed that patients with T2DM could also develop microvascular and cardiovascular complications during their intensive therapy. Therefore, these observations suggest that early metabolic control has continued beneficial consequences in both types of diabetes. The metabolic memory theory explains that an early glycaemic environment is memorised in the target organs such as the heart, kidney and extremities. This theory also mentions that good glycaemic control should start from an early age in order to prevent the development of diabetic complications

(Cerielo et al., 2009). There are various factors including oxidative stress and age that are involved in this phenomenon, as well as hyperglycaemia (Sell, 1990).

1.4.3. Hypertention and hyperlipidemia

Aggressive control of blood pressure and cholesterol can reduce the progression of microvascular disease in patients with T1DM and T2DM (Grossman and Messerli, 2008). The studies during the DCCT showed that hypertension and hyperlipidaemia can influence the progression of microvascular disease by altering glycaemia (DCCT, 1993). Data from the follow-up of the UKPDS established that an increase of 38.7 mg/dL in low density lipoprotein (LDL) cholesterol (1.00 mmol/L) was related to disease of the artery increasing by 57%, whereas an increase of 4mg/dL (0.10 mmol/L) in high density lipoprotein (HDL) cholesterol was correlated with a 15% reduction in disease of the artery (KPDS, 1998). Furthermore, this study showed that high levels of LDL-C, low levels of HDL-C and hypertension are all risk factors for disease of the artery in T2DM patients as well as hyperglycaemia.

Parallel to hyperlipidaemia, there was additional evidence that showed the effect of hypertension in microvascular disease. Ravid et al. (1993) revealed that patients with blood pressure show an annual decline in GFR, which is close to a normal average and the development of microalbuminuria is rare in this group. Conversely, diabetic patients who had hypertension (130/80-140/90 mm Hg) showed a larger decline in GFR and the microalbuminuria or macroalbuminuria had developed in 30% of these patients after 12-15 years. A year after this study, Tarnow et al. (1994) reported that there was an association between the progression of diabetic nephropathy with hypertension and the incidence of hyperglycaemia increased in those patients who developed diabetic complications.

In the kidney, the process of high blood pressure to hypertension results in an increase in intraglomerular capillary pressure (Hosteller et al., 1982). The increase of intraglomerular blood pressure leads to the progression of glomerular sclerosis. This procedure is illustrated by an extracellular matrix accumulation within the glomerulus (Yasuda et al., 1996). Due to the elastic property of the glomeruli, this increase in pressure leads to changes in overall glomerular volume, which leads to a stretch and relaxation of cells, such as mesangial cells (Cortes et al., 1996). As a result, hypertension is an important risk factor in the progression of diabetic nephropathy.

1.5. Glucose transport inside the cells

Glucos is used as a primary source of energy and a metabolic intermediate inside the cells. Therefore, glucose acts as a precursor for the synthesis of triglycerides, glycoproteins and glycogen. Glucose is directly absorbed into the bloodstream and the kidneys reabsorb the filtered glucose back into the blood. Due to the nature of glucose, it does not readily disperse across the hydrophobic plasma membrane. Thus, it requires specific molecules to mediate the specific uptake of this sugar (Oslon and Pessin, 1996).

Glucose transport inside the cells through specific glucose transporters is the first step of the glucose signalling pathway. Glucose can be transported into the cells through specific glucose transporters which belong to a family of proteins (Haneda et al., 2003). Glucose transporters identified in glomeruli include GluT1, GluT2, GluT3, and GluT4. These transporter isoforms have been cloned and explored specifically for glucose transport: GluT1 is ubiquitously distributed and displays constitutive transport activity; GluT2 is present in various organs such as the liver, gut and pancreatic islets; GluT3 is present in the brain and the central nervous system; and GluT4 is present in insulin-responsive tissues, skeletal muscle, adipose tissue and the heart (Bell et al., 1993).

High glucose activates various signalling pathways inside the cell (Heilig, 2013). Heilig et al. (1997) demonstrated that GluT1 synthesis and expression increased in mesangial cells, when exposed to high glucose. They also looked at the effects of elevated extracellular glucose on the regulation of a facilitative glucose transporter in rat mesangial cells. They found that GluT1 is the only transporter isoform which is detected and its mRNA and protein expression up-regulated in the presence of high glucose rather than normal glucose. Consequently, Glut1 easily facilitated the transport of excessive extracellular glucose from DM into the cells (Brousius and Heilig, 2005).

In the kidney, GluT1 plays an important role in this process by regulating glucose movement through the cells in which it acts as a primary gatekeeper for this process (Heillig et al., 2013). The studies indicated that GluT1 facilitated the transport of glucose, which activates Protein Kinase C (PKC) and Transforming growth factor beta (TGF-β) and leads to glomerulosclerosis (Heilig et al., 1995; Heilig et al., 2004).

Therefore, GluT1 activity could be a factor in the progression of fibrosis in DN. In support of this argument, overexpression of GluT1 in cultured mesangial cells in normal glucose results in elevation in glucose uptake and consumption, as well as excessive production of ECM proteins (Weigert et al., 2003). Additionally, *in vivo* studies showed that overexpression of GluT1 in transgenic mice lead to development of glomerulosclerosis and nephropathy, regardless of normoglycaemia (Heilig et al., 1995). Thus, the GluT1 transporter seems to be a regulator of ECM production in both cultured mesangial cells and glomeruli cells.

Studies have also been carried out to establish the correlation between polymorphisms of GluT1 with DN. Liu et al. (1999) found that GluT1 Xba1 (-) allele was associated with a higher occurrence of diabetic nephropathy. Another study in Poland showed that XbaI (+) genotype was more frequent in patients with DN when compared with patients without DN. They suggested an association between GluT1 polymorphism with DN (Grzeszczak, 2001).

Understanding the mechanism of GluT1 is important since it appears that the expression of GluT1 gene leads to morphologic features of DN. A number of studies showed that GluT1 is regulated in the presence of high glucose in mesangial cells and its regulation activates various signalling pathways. Indeed, after glucose transportation through the cells, it is metabolized mainly by the glycolytic pathway. However, when present in excess, glucose is also metabolized by other pathways and activate numerous signalling pathways as indicated in Figure 3. It has been observed that there is an increase in glucose entry into the polyol pathway, the diacylglycerol (DAG) synthesis pathway, and the hexosamine pathway when mesangial cells are exposed to high glucose. For instance, chronic overexpression of GluT1 stimulates the polyol pathway activation (Henry et al., 1999) as well as PKCα and β1 activation (Henry et al., 1999; Weigert et al., 2003). Therefore, the metabolism of glucose through the polyol pathway can result in the synthesis of diacylglycerol and phosphaditic acid, which may lead to an increase of PKC levels and its activation in mesangial cells (Whiteside et al., 2002).

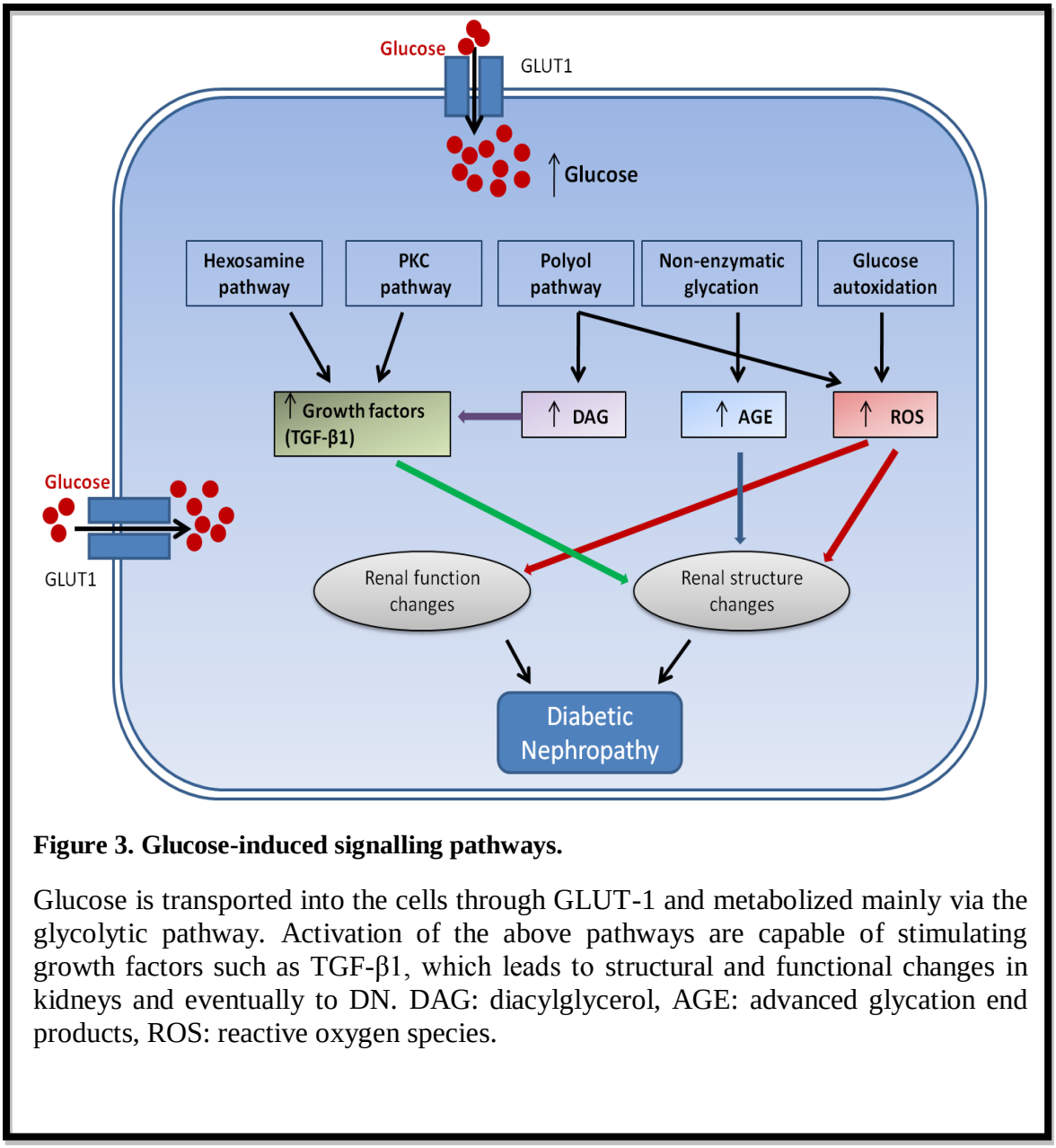

Figure 3. Glucose-induced signalling pathways.

Glucose is transported into the cells through GLUT-1 and metabolized mainly via the glycolytic pathway. Activation of the above pathways are capable of stimulating growth factors such as TGF-β1, which leads to structural and functional changes in kidneys and eventually to DN. DAG: diacylglycerol, AGE: advanced glycation end products, ROS: reactive oxygen species.

1.5.1. Metabolic factors

It appears that DN results from the interaction between various factors namely: metabolic, hemodynamic, intracellular factors, growth factors and cytokines (Ritz et al., 2001). Metabolic factors are effectively glucose dependent pathways which are activated in diabetic renal tissues. These pathways include the polyol pathway, accumulation of advanced glycated end-products (AGEs), hexosamine flux and oxidative stress (Brownlee, 2001). Hyperglycaemia has been shown to alter the activities and expression of transcription factors and intracellular factors (Djk and

Berl, 2004). Figure 4 presents a schematic diagram of numerous factors which are involved in hyperglycaemia-induced tissue damage.

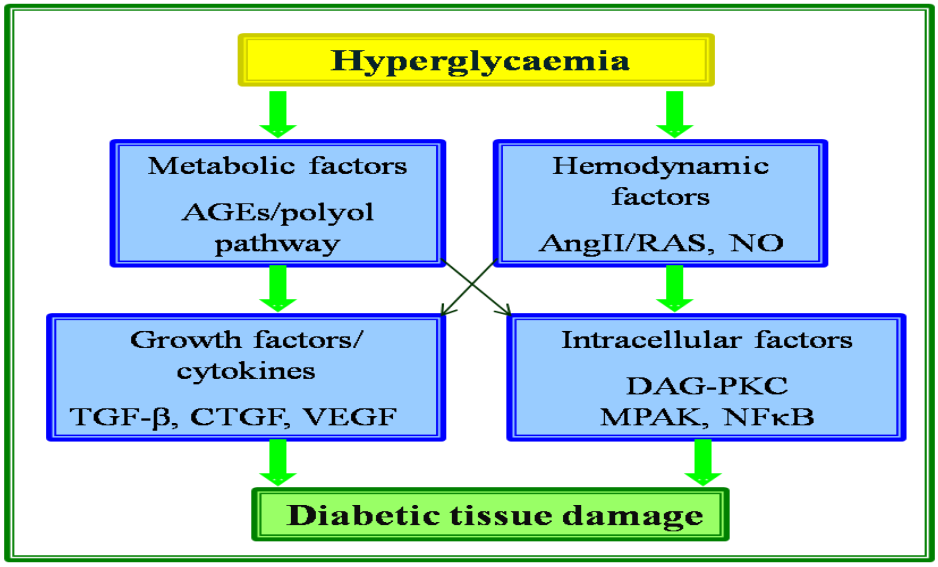

Figure 4. Glucose induced signalling pathways of diabetic microvascular damage. AGEs: Advanced glycated end products, AngII: angiotensin II, RAs: rennin angiotensin system, NO: nitric oxide, TGF-β: transforming growth factor β, CTGF: connective tissue growth factor, VEGF: vascular endothelial growth factor, DAG-PKC: diacylglycerol-protein kinase c, MAKP: MAP kinase, NF-κB: nuclear factor-Kappa B (Modified from Schrijvers et al., 2004**).**

● ***The polyol pathway***

The polyol pathway is one of the key pathways in the development of DN. Aldose reductase (AR) is the main enzyme in the polyol pathway which converts glucose to sorbitol. In converting glucose to sorbitol, the co-factor nicotinamide adenine dinucleotide phosphate (NADPH), and sorbitol dehydrogenase (SDH) with co-factor NAD+, is used to convert sorbitol to fructose (Figure 5; Djk and Berl, 2004). Under normal glucose conditions, only a small amount of glucose enters through the pathway as opposed to a diabetic state, with significant increase of 3% and upto 30% being observed. Cellular accumulation of sorbitol is associated with depletion of

myoinositol. There is evidence that shows the cellular accumulation of sorbitol and the depletion of myoinositol are linked to the progression of DN (Greene et al., 1987).

The polyol pathway is involved in the reduction of oxidative stress in different ways. Under hyperglycaemic condition, a depletion of NADPH co-factor to AR causes reduction of reduced glutathione (GSH). Therefore, the cells become susceptible to intracellular oxidative stress (Brownlee, 2005). Indeed, excessive activation of the polyol pathway results in an increase in intracellular and extracellular sorbitol concentration and is also a cause of increased ROS and decreased glutathione levels (Brownlee, 2001). In addition, fructose and its metabolites when glycosylated, have a powerful effect on AGE-induced oxidative stress (Chung et al., 2003). Each of these imbalances can damage cells (Brownlee, 2001).

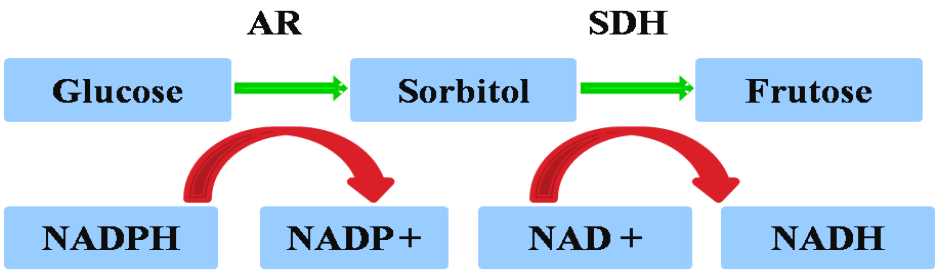

Figure 5. The polyol pathway.
Aldose reductase (AR) reduce glucose to sorbitol with the aid of its co-factor NADPH. This reaction oxidises NADPH to NADP+ and sorbitol dehydrogenase (SDH) can then oxidise sorbitol to fructose (Modified from Djk and Berl, 2004).

Several studies have reported the role of polyol pathway in the development of DN. Bank et al (1989) showed that that polyol pathway metabolism plays a role in glomerular hyperperfusion in IDDM of Streptozotocin-induced diabetic rats, by using aldose reductase inhibitors which is a specific inhibitor for the polyol pathway. Results showed that using the aldose reductase inhibitor sorbinil in STZ rats prevented the glomerular hyperfusion. *In vivo* studies have also shown the effect of aldose reductase. In this study, diabetic dogs were treated with aldose reductase

inhibitors for 5 years and it was found that diabetes induced deficiencies in nerve conduction velocity were prevented (Engerman et al., 1994). An additional study in transgenic mice over-expressing human aldose reductase revealed that the mice developed pathological alterations such as thrombosis of renal vessels deposits in Bowman's capsules in the kidney (Yamaoka et al., 1995).

● ***Advanced glycation end products (AGEs) Activation***

Advanced glycation end products (AGEs) are complex, heterogenous molecules that are formed non-enzymatically by the interaction of extracellular proteins and glucose (Yashpal et al., 2008; Ahmed, 2005). Various studies show evidence that AGEs accumulate *in vivo* in the renal cortex of diabetic rats (Mitsuhashi et al., 1993) and also increase in sclerosing glomeruli of patients with diabetes (Witztum et al., 1997). A further patient study indicated that increased AGEs are associated with the severity of DN (Tanji et al., 2000). Therefore, AGEs are important pathogenetic mediators in the development of DN and the accumulation of AGEs may lead to ESRD (Djk and Berl, 2004). AGEs appear to damage cells through receptor-dependent and receptor-independent pathways. AGEs interact with receptors such as RAGE and RAGE regulates the uptake and clearance of AGE (Wendt et al., 2003). It also appears that intracellular AGEs is the primary initiating feature in generating various signal events by activation PKC, MAP kinase and transcription factors. This would increase the activity of growth factors such as TGF-β and CTGF and thereby modify the regulation of expression of ECM proteins, which is a cause of renal hypertrophy and accumulation of extracellular matrix components (Jakus et al., 2004). In addition, it increases the synthesis of proteins which are involved in the regulation of gene transcription (Shinohara et al., 1998).

Interestingly, AGEs have the capability to covalently bind with proteins and induce deleterious effects in various tissues. Indeed, AGE precursors have the ability to diffuse outside of the cell and alter circulating proteins within the blood, including albuminuria, or bind to cell-associated proteins that trigger abnormal cellular function (Vlassara and palace, 2002). Vittorio et al. (2007) revealed that urine and plasma AGEs increase in patients with DN compared to healthy subjects. *In vitro* studies by Chen et al (2001) showed that AGE-rich proteins and glycated albumin increase the activity of PKC and expression of ECM proteins and TGF-β levels in both cultured

glomerular and endothelial mesangial cells. Furthermore, it has been shown that AGEs can mediate their effect via AGE receptor (RAGE), resulting in formation of ROS (Tan et al., 2007).

● ***Hexosamine pathway activity***

Under high glucose conditions, the excessive glucose is metabolized through glycolysis, going first to glucose-6 phosphate via hexokinase, which subsequently converts to fructose 6-phosphate and then continues through the rest of the glycolytic pathway. However, only some fructose-6-phosphate gets diverted in the signalling pathway by an enzyme called GFAT (glutamine: fructose-6 phosphate amidotransferase). Fructose-6 phosphate further converts to glucosamine-6 phosphate and finally to UPD-GlcNAc (uridine-5diphosphate-N-acetyglucosamine). Subsequently, the N-acetylglucosamine is added to serine and threonine residues of TGF-β (Brownlee, 2005). This procedure often results in changes in gene expression including the elevation of TGF-β levels, which is involved in the pathogenesis of DN (Du et al., 2000).

Studies by Weigert et al. (2003) reported that the activation of the hexosamine biosynthetic pathway has been implicated in an elevated expression of TGF-β in mesangial cells, leading to mesangial matrix expansion and diabetic glumerulosclerosis. Additionally, Singh and Crook (2000) showed that the activity of Protein kinase C through the hyperglycaemia-induced hexoamine pathway also contributed to the synthesis of ECM proteins in mesangial cells. Taken together, the activation of the hexosamine pathway via hyperglycaemia may produce various changes in both gene expression and protein function, which together leads to the pathogenesis of DN (Brownlee, 2001).

1.5.2. Hemodynamic factors

● ***The reactive oxygen species (ROS) pathway***

Reactive oxygen species (ROS) seem to have been an interesting topic in all areas of biology for many years. ROS are reduced forms of oxygen which are in a more reactive state when compared with molecular oxygen (Hancock et al., 2001). Normal metabolism of oxygen results in the formation of ROS, a natural byproduct which includes free radicals (Djk and Tomas et al., 2004). ROS are key signalling molecules which play a central role in cell signalling (Hancock et al., 2001). However, stress can

dramatically increase the levels of ROS in the cells which causes damage to cell structure. This relative overload of oxidant and reduction of antioxidants is known as oxidative stress (Vittorio et al., 2007; Valko et al., 2006). Oxidative stress causes a harmful consequence on cells including severe damage to DNA, proteins, and lipids (Valko et al., 2006).

It has been shown that hyperglycaemia induces vascular injury through complex overlapping pathways, including enzymatic and nonenzymatic processes such as ROS. Several *in vivo* and *in vitro* studies strongly suggest an important role of ROS in the initiation and progression of DN, by affecting the intracellular redox balance of the cell (Schafer and Buettner, 2001). Studies by Lee et al. (2003) showed that high glucose induces ROS in both mesangial and tubular epithelial cells. Lee et al. (2003) concluded that ROS activates signal transduction cascade and transcription factors resulting in an increase in the expression of genes involved in the expansion of glomerular and mesangial cells (Figure 6). Studies (Vittorio et al., 2007) also revealed that AGEs, together with hyperglycaemia and ROS, generate growth factors and cytokines which all result in renal hypertrophy and increased expression of extracellular matrix components.

NADPH oxidase is the major enzymatic source for ROS generation in renal mesangial and tubular cells (Griendling et al., 2000; Shiose et al., 2001). A study by Guzik et al (2000) reported that hyperglycaemia independently correlated with NADPH oxidase-derived ROS generation in diabetic patients. Generally, hyperglycaemia resulted in elevated ROS both via NADPH oxidase and through electron leakage from the mitochondrial electron transport chain (Lee et al., 2003). NADPH oxidase is one of the most important enzymes for controlled release of ROS. However, the exact function of ROS and their internal role as signals in the face of a barrage of antioxidants still require more research studies (Hancock et al., 2001). It has been suggested that modulation of ROS production in biochemical pathways may prove to be a promising step in the prevention of DN progression (Djk and Berl, 2004).

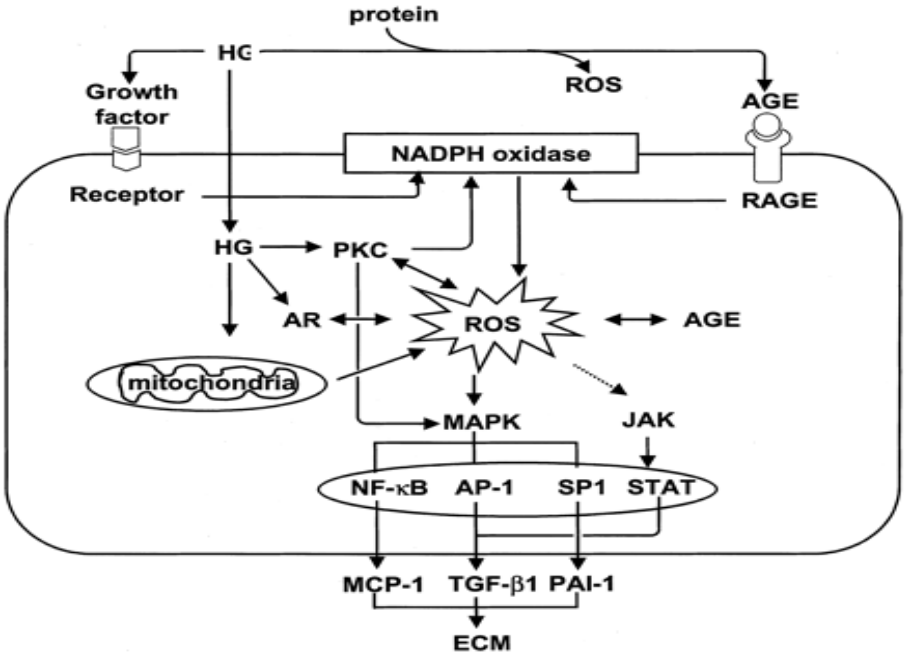

Figure 6. ROS-regulated signalling in renal cells cultured under high glucose.

Mitochondrial electron transfer chain and receptor-stimulated NADPH oxidases are important sources of intracellular ROS generation under high glucose conditions. High glucose-induced ROS activate signal transduction cascades and transcription factors, leading to up-regulation of expression of genes and proteins involved in ECM remodelling in the kidney. HG: high glucose, MCP-1: monocyte chemoattractant protein-1, RAGE: receptors for advanced glycation end products, Sp1: specificity protein 1. Taken from Lee et al., 2003.

.

Various *in vivo* and *in vitro* studies show the up-regulation of Ang II and Renin activity in DN. *In vitro* studies by Zhang et al. (1999) reported the up-regulation of angiotensinogen mRNA and protein in proximal tubular epithelial cells exposed to high glucose. Another study by Chouinard et al (2002) showed increased expression levels of AngII production in rat mesangial cells cultured in high glucose. *In vivo* studies have also confirmed the involvement of Ang II in DN. For instance, STZ-induced diabetic rats showed higher levels of plasma Ang II than control and insulin treated rats (Zimplmann et al., 2000).

Clinical studies were also performed in parallel with *in vivo* and *in vitro* studies and support previous findings. A clinical study in both hypertensive patients with DN by Lai et al. (1998), highlighted stronger signals of angiotensinogen, renin and ACE mRNA in both epithelial and mesangial cells. A study by Andersen et al. (1996)

showed up-regulation of different components of the renin-angiotensin system (RAS) in the diabetic kidney. Furthermore, a number of studies suggested the activation of RAS in diabetes and they showed that DN has an increased sensitivity to AngII (Kennefic TM, 1996). Zhang et al. (2006) showed that RAS plays a role in the pathogenesis of DN by regulating the PKC isoforms activity. These findings postulate the involvement of Ang II and the RAS system in the progression of DN.

● ***Nitric oxide (NO)***

Nitric oxide (NO) is a signalling molecule which plays a role in the renal structure and function in diabetes. NO is derived from L-arginine (L-Arg) in macrophages and other cell types (Marletta, 1989). This reaction is catalyzed by several nitric oxide syntheses (NOS) isoenzymes. These NO isoforms include neuronal (nNOS), endothelial (eNOS) and inducible (iNOS), which have been identified in mammalian tissues (Komers et al., 2003) and all are expressed in the kidney. NO plays an important role in renal functions including the excretion of sodium, regulation and the maintenance of renal structural integrity (Kone et al., 1997). There are extensive studies which demonstrate that abnormalities of NO production modulates renal function.

A number of *in vitro* studies showed that high glucose has an influence on NO bioavailability in cultured mesangial cells, which may involve the action of the prostanoid thromboxane A_2 and PKC activation (Trachtman et al., 1998; Noh et al., 2002). *In vivo* studies by Choi et al. (1997) reported the elevation of renal cortical expression of all NOS isoforms in STZ diabetic rats. However, in medulla of the same samples there was no difference in their expression with respect to controls. Another study by Ishi (2001) indicated no change in NO synthase isoform protein levels in the renal cortex of the STZ rat.

1.5.3. Intracellular factors

● ***Protein kinase C activation***

Hyperglycaemia concentrations inside the cells lead to the activation of PKC through increased glucose metabolism (Brownlee, 2005). PKCs family includes at least 11 isoforms of which some, such as Protein kinase-C, -β, -δ and –α, are activated by diacylglycerol (DAG ; Way et al., 2001; Idris et al., 2001) and are also generated from ROS following interaction between AGE and RAGE (Tan et al., 2007). The

activation of PKC via intracellular hyperglycaemia results in various effects on gene expression in an abnormal way (Brownlee, 2005). PKC appears to be involved in the pathogenesis of DN (Li and Gobe, 2006). PKC activation contributes to the regulation of a number of vascular functions, such as cell proliferation and synthesis of extracellular matrix proteins and growth factors; it also leads to decreased NO production (Inoguchi, 2000). In renal glomeruli, *in vitro* studies have shown an evidence of hyperglycaemia-induced PKC activity in mesangial cells.

Hyperglycaemia has been shown to be the cause of PKC activity, which in turn is linked to an increase in the expression of TGF-β as one of the main factors in regulation of ECM protein accumulation in DN (Kreisburg et al., 1994). PKC activity increased the expression of type IV collagen under high glucose which is the main component in capillary basement membrane thickening (Fumo et al., 1994). In addition to the effect of hyperglycaemia-induced PKC activity in mesangial cells, Koya et al. (1997) also reported the effect of hyperglycaemia in the activation of PKC in mesangial cells and they suggested that the activation of PKC, particularly the PKC (β) isoform can change gene expression and functions of glomerular cells which are involved in the progression of DN.

Moreover, increased activation of PKC was also exhibited in the STZ diabetic rat during the early stages of diabetes (2 weeks) through to long term (24 weeks) diabetes (Carven et al., 1990). Changes in the subcellular distribution of PKC activity in the glomeruli of short term diabetic rats were also noted (Carven et al., 1990). The clinical study by Ceolloto et al. (1999) showed that the activity of the PKC membrane is increased with high concentration of plasma glucose in a patient with T2DM. It was also suggested that hyperglycaemia-induced changes in monocyte PKC activity might be associated with the progression of DN (Ceolloto et al., 1999).

1.5.4. The role of growth factors

- ***Transforming growth factor β (TGF-β)***

The AGEs, hexosamines, ROS and DAG/PKC described above are likely candidates that activate TGF-β signalling through hyperglycaemia (Leask, 2004). TGF-β is one effector molecule that has been reported as a major mediator of the pathologic changes in diabetic kidney disease (Ziyadeh et al., 1998). TGF-β stimulates the

synthesis of ECM proteins including type I collagen, type IV collagen, fibronectin and laminin (Sharma and Ziyadeh, 1997).

TGF-β also reduces matrix degradation via the activation of protease inhibitors and inhibition of proteases (Ziyadeh, 1994). Several *in vitro* studies have demonstrated that hyperglycaemia stimulates hypertrophy of both mesangial and proximal tubular cells through the up-regulation of TGF-β expression (Ziyadeh, 1994; Han et al., 1999; Hoffman, 1998; Rocco, 1992). Furthermore, extensive studies in experimental models of diabetes indicated increased expression of TGF-β mRNA and protein in both glomerular and tubular cells compartments of diabetic rats and mice (Hill et al., 2000; Hong et al., 2001). Hill et al. (2000) reported that TGF-β protein was increased in tubules of the diabetic rat, whereas it was reduced in glomeruli. Immunohistochemical staining and *in situ* hybridisation studies detected an increase of TGF-β type II mRNA and protein in both glomerular and tubular cells in the db/db mice (Hong et al., 2001). An increase of glomerular TGF-β1 expression was also determined in a patient with T1DN (Yammoto et al., 1996). Therefore, all of these studies show the regulation of TGF-β in glucose-induced renal injury pathways.

● ***Vascular endothelial growth factor (VEGF)***

Vascular endothelial growth factor (VEGF) is a secreted mitogen which is highly specific for endothelial cells. VEGF was first identified as a potent permeability factor in 1983 (Senger et al., 1983). VEGFR-1 (Flt-1) and VEGFR-2 (KDR/Flk-1) are two VEGF receptor tyrosine kinases which have their own biological and biochemical functions. VEGFR-2 meditates most of the endothelial cell responses, whereas VEGF-1 appears to be more elusive (Robinson and Stringer, 2001). Inside the cells, VEGF is involved in various functions including stimulating endothelial cell proliferation, increasing vascular permeability, mediating endothelium-dependent vasodilation, playing a cardinal role in physiological and pathological angiogenesis and modulating leukocyte kinetics (Neufeld et al., 1999).

It has been suggested that VEGF and its receptors play a role in the development of DN in both *in vitro* and *in vivo* studies (Cooper, 1999; Hovind, 2000). Many growth factors and cytokines relevant to the pathogenesis of DN have also been reported to promote VEGF regulation. These include TGF-β and IGF-I (Neufeld et al., 1999). *In vitro* studies have shown that hyperglycaemia can induce VEGF expression. Williams

et al. (1997) reported that VEGF expression is stimulated by hyperglycaemia in vascular smooth-muscle cells via the PKC pathway. It has also been shown that VEGF expression is induced via AGEs (Hirata, 1997) and Ang II (Puppili, 1999) in human mesangial cells; its secretion leading to proliferation (Thomas et al., 2000) and induction of collagen synthesis (Amemiya et al., 1999).

In vivo, VEGF was found to be increased in the kidney of the STZ diabetic rats (Cooper et al., 1999). The up-regulation of VEGF expression was reported to occur at an early stage in diabetic rats (Cooper et al., 1999). This is evidenced by an increase in VEGF mRNA and protein expression at up to 32 weeks after onset of diabetes. However, some studies have shown a reduction in the STZ diabetic rats after only 1 week following onset (Singh et al., 2004).

Assessing circulating VEGF expression also provided evidence for the role of VEGF in DN. One large study of patients with T1DN showed that circulating VEGF levels in plasma were increased in nephropathy patients compared to normoalbuminuric patients. However, this difference was mostly owing to the elevated levels found in T1DN men, as there was no significant difference between the female patients (Hovind et al., 2000). Wasada et al (1998) also reported higher levels of plasma VEGF in patients with T2DM (Wasada et al., 1998). VEGF's urinary excretion has been examined in some patient studies with DN (Cha et al., 2000). In this study, VEGF's urinary excretion was elevated with the development of DN which was associated with serum creatinine, microalbuminuria and proteinuria levels (Cha et al., 2000). The biopsy study found that VEGF levels were high in glomerular podocytes and distal tubular cells in patients with mild DN, whereas VEGF expression was low in tubules and especially the proximal segment in patients with advanced DN (Cha et al., 2000). Therefore, it is clear that VEGF and its receptors are vital for the progression of DN.

● ***Connective tissue growth factor (CTGF)***

Connective tissue growth factor (CTGF) is a 38 kDa cysteine-rich secreted protein, which was originally isolated from conditioned media of human umbilical vein endothelial cells (Bork, 1993; Bradham, 1991). CTGF is a member of cysteine-rich growth factors (CCN family). This family of proteins is involved in various cellular effects such as mitogenesis, apoptosis, regulation of ECM physiology, osteogenesis, embryogenesis, angiogenesis, and tumourigenesis. CTGF is a highly conserved gene

in humans, mice and rats which shows approximately 90% identity (Bork, 1993). It seems that CTGF transcription is mainly induced by TGF-β and is linked to the pathogenesis of fibrosis (Grotendorst et al., 1997). However, its physiological function remains unknown.

Several lines of evidence show that hyperglycaemia induces CTGF mRNA and protein levels in humans and cultured rat mesangial cells (MC), and they also revealed that CTGF is involved in the progression of glomerulosclerosis and tubulointerstitial injury in the kidneys (Murphy, 1999; Riser, 2000).

Several different factors including hyperglycaemia, AGEs, TGF-β and ROS are involved in the increased CTGF mRNA and protein levels in renal cells in DN (Murphy et al., 1999; Reiser et al., 2000; Wahab, 2001). Riser et al. (2000) indicated that hyperglycaemia increased the CTGF mRNA levels in mesangial cells and the addition of CTGF stimulates cultured mesangial cells to induce the expression of main components of ECM, such as fibronectin and collagen I. Another study by Liu et al. (2007) showed that in human vascular smooth muscle cells (VSMC) hyperglycaemia-induced CTGF expression and is associated with the accumulation of fibronectin and collagen I. Murphy et al. (1999) reported that in addition to hyperglycaemia, TGF-β1 stimulated CTGF expression in primary human mesangial cells, whereas the addition of an anti-TGF-β1 antibody inhibits the induction of CTGF in exposed mesangial cells. Moreover, Murphy et al (1999) revealed that PKC inhibitor inhibited the induction of CTGF, as well as TGF-β1 and concluded that hyperglycaemia-induced TGF-β1 and PKC pathways are involved in the expression of CTGF.

To further determine CTGF function in the presence of hyperglycaemia, James et al. (2013) showed that hyperglycaemia increased the expression of ECM components such as collagen I, IV and XVIII as well as fibronectin and thrombospondin (TSP1) in cultured MEF from CTGF wild type mice. However, the activation of these components under hyperglycaemic conditions was attenuated in heterozygous mice. They also suggested that CTGF expression directly modulates the progression of DN.

1.6. Hyperglycaemia-induced gene expression in DN

High-throughput gene expression profiling is an important, integrative tool that provides global views into the regulatory pathways of DN (Liang et al., 2003). Several likely genes contributing to DN were identified by examining the changes in expression of a variety of mRNA transcripts throughout the course of diabetes. Gene expression profiling has been applied to demonstrate the regulated changes of genes inside a cell under different conditions. In DN, over 200 genes have been identified which are regulated differentially in mesangial cells grown in high glucose (Murphy et al., 1999). Furthermore, Clarkson et al. (2002) recognised 200 mesangial cell genes which are up or down regulated in the presence of high glucose.

The results from various strategies may be analysed together to rationalize a collection of possible markers. For instance, caldesmon is a gene which is highly expressed in mesangial cells exposed to high glucose (Murphy et al., 1999) and is placed on chromosome 7q35in a region previously connected to vulnerability from DN in two independent genome-wide screens (Imperatore et al., 1998; Fogarty et al., 1999). In addition to these results, a number of glucose regulated novel genes have been demonstrated (Wada et al., 2002). Gremlin (Dolan et al., 2003), serum glucocorticoid regulated kinase (Feng et al., 2005), beta-defensin-1 (Page and Malik, 2003) and NSA2 (Shahni et al., 2011) are examples of glucose regulated genes in both *in vivo* rodent models of diabetes and *in vitro* studies. The isolation and recognition of glucose regulated genes could lead to recognition of potential therapies for DN. Therefore, it is interesting to consider the regulation of various genes in diabetic environments in an attempt to find a novel therapeutic target for DN.

- **Gremlin (IHG-2)**

Gremlin (IHG-2) was identified as a gene that is regulated by high glucose in human mesangial cells (Murphy et al., 1999). It is a 184 amino acid protein and a member of the cysteine knot superfamily. Gremlin influences various steps in growth, differentiation and development (Murphy, 2002). Gremlin expression has been detected in a number of kidney disease models in humans, but was almost undetectable in healthy kidneys (McMahon, 2000). It was also expressed in human mesangial cells cultured in high glucose, in those exposed to TGF-β *in vitro* (Murphy et al., 1999) and in kidneys isolated from STZ diabetic rats *in vivo* (McMahon, 2000). McMahon (2000) also

reported that the mRNA expression of gremlin was increased in the renal cortex of STZ-induced diabetic rats and they were regulated in response to high extracellular glucose and mechanical strain. Studies in kidney biopsy specimens from patients with DN showed that gremlin levels were increased in DN patients compared to those with normal kidneys (Dolan et al., 2005).

A high level of gremlin expression was observed in the tubular compartment of patients with advanced DN. Interestingly, gremlin was co-localised with TGF-β1 in proximal tubular cells, suggesting that TGF-β1 might be modulating gremlin expression in the tubulointerstitial compartment. Additionally, gremlin mRNA expression was associated directly with increased serum creatinine levels and renal fibrosis in patients with DN. Therefore, they suggest a role for gremlin in the pathogenesis of DN (Dolan et al., 2005).

- **NSA2**

CDK105 or NSA2 (Nop-seven-associated 2) was one of the candidate genes which was isolated by differential screening as it exhibited a strong hybridisation signal in kidneys of a GK rat diabetic for 40 weeks (Malik et al., 1997). Northern blot analysis using total RNA from GK rat kidneys at different ages (6-,16-,26- and 40- week-old) and aged-matched Wistar control kidneys showed up- regulation of CDK105 in GK rat kidneys diabetic for 40 weeks (Ziadi, 1997). CDK105 is a highly conserved gene in humans, mice and rats which encodes a 260 amino acid protein in humans (El Mahdi, 1995). The CDK 105 coding region shares 100% identity to the TGF-β inducible nuclear protein 1 (TINP1, AF077615) and 99% identity to hairy cell leukemia (HCL, AF372458).

CDK105 is identical to NSA2 (Nop seven associated 2) and is also identified as TINP1 (TGF-β inducible nuclear protein 1) and hairy cell leukemia protein 1 (HCL-G1). The NSA2 homologue in yeast is thought to be involved in ribosome biogenesis and it has been defined as a nuclear protein which includes numerous nuclear localisation signals (Laberton, 2006; Andersen, 2005). The human homologue NSA2 was first recognised as one of the putative tumour suppressor genes involved in the pathogenesis of HCL1; it has been reported that it contributes to the regulation of cell cycle and cell proliferation (Wu et al., 1999; Zhang et al., 2010).

Studies by Zhang et al. (2010) showed that NSA2 is regulated at higher levels in the kidneys, placenta, thymus and is also regulated at lower levels in most human tissues. Additional studies by Shahni et al. (2011) showed that renal NSA2 mRNA is increased in human mesangial cells exposed to high glucose. They also found that renal NSA2 is up-regulated in response to hyperglycaemia in the kidneys of both the GK rat and the streptozotocin-induced diabetic mice. Circulating NSA2 mRNA levels were increased in patients with albuminuria compared with nonalbuminuric patients and diabetic controls. These studies suggest that NSA2 may play a role in the pathogenesis of DN.

1.7. Model systems to study Diabetic nephropathy

1.7.1. *In vitro*: cultured kidney cells

● ***Mesangial cells***

Mesangial cells are specialized cells which are located around intercapillary space in the kidney (Shigeta and Kikkawa, 1991). They play a key role in maintaining glomeruli structure and function (Wada, 2001). They also have a central role in the pathogenesis of glomerular injury (Wada, 2001) and are considered to be key mediators of glomerular inflammation and fibrosis (Wani et al., 2007). Therefore, human mesangial cells are a useful *in vitro* model for studying the early stages of DN. Progression of diabetic nephropathy is associated with glomerular hypertrophy, mesangial expansion and thickened glomerular basement membrane, which leads to glomerulosclerosis (Greenberg, 1998). The diabetic glomerulosclerosis is categorized by mesangial accumulation of extracellular matrix proteins such as laminin, collagen IV and fibronectin genes. Functional abnormalities such as glomerular hyperfilteration and hypertension, as well as alteration in metabolic pathways or the action of polypeptide growth factors may also contribute to diabetic glomerulopathy and renal failure in DN (Ziyadeh, 1998).

A number of *in vitro* studies have suggested that high concentrations of glucose modify mesangial cell function and are a major stimulus for mesangial cell matrix production in diabetic nephropathy (Murphy, 1999). Studies by Wolf et al (1992) suggested a biphasic effect on proliferation when murine mesangial cells were exposed to elevated glucose levels. Exposure of mesangial cells to high glucose also increased the amount of type IV collagen which is the major component of GBM,

suggesting an induced production or decreased degradation of type IV collagen as a result of high glucose (Shigeta and Kikkawa, 1991). Philip et al. (1999) reported that exposing glomerular mesangial cells to high glucose may alter cell proliferation and/ or ECM turnover.

Activation of many pathways have been shown to regulate mesangial cell function leading to renal injury including: stimulation of TGF-β1 (Selliti et al., 2007); PKC activation (Portilla et al., 2000); increased formation of AGEs (Matsui et al., 2007), Ang II and RAS (Yano et al., 2007); oxygen free radicals (Lee et al., 2003) and up-regulation of the thiol antioxidative pathway as an adaptational response of human mesangial cells to high glucose (Morrison et al., 2004). Moreover, there is evidence that high glucose activates an intrinsic pathway of proapoptotic signalling in cultured human mesangial cells. Additionally, an intrinsic pathway of apoptosis signalling is activated in *db/db* kidneys *in vivo,* which is correlated with apoptosis of glomerular cells (Mishra, 2005).

The growth of human mesangial cells at high concentration of glucose has been used to determine glucose-regulated genes. Studies by Murphy (1999) have demonstrated that 15 novel genes are differentially induced when primary human mesangial cells are exposed in high glucose. Consistently, MOSC2 (CDK7) (Malik et al., 2007), CRYM (Al-kafaji and Malik, 2010) and NSA2 (Shahni et al., 2011) were included in this category as they are all up-regulated by high glucose in human mesangial cells.

- ***Tubular cells***

Diabetic nephropathy is considered to be primarily a glomerular disease and there is less research about the pathogenesis of the tubulointerstitial changes in DN. Histological studies have widely shown that the deterioration of renal function in chronic kidney disease (CKD) is associated more with tubular and interstitial changes when compared with glomerular changes (Gilbert &Cooper, 1999). Indeed, the progression of renal disease is characterised by pathogenic mechanisms that lead to progressive interstitial fibrosis, peritubular capillary loss and destruction of functioning nephrons due to tubular atrophy (Eddy, 2005).

Various *in vitro* studies have established that albumin and other urinary proteins such as immunoglobulin G can stimulate proximal tubular cells to produce chemokines and inflammatory molecules (Lai, 2007; Tang, 2001). In addition to inflammation, interstitial fibrosis is a major determinant of progressive renal disease. For instance, albumin stimulated proximal tubular epithelial cells (PTECs) to produce TGF-β which is the most effective cytokine for renal fibrogenesis (Liu, 2006). AGEs and RAGE pathways activate secondary messenger pathways such as PKC, and increase production of fibrogenic growth factors and inflammatory cytokines such as TGF-β and CTGF, which lead to interstitial fibrogenesis via tubular EMT induction (Tang and Lai, 2012).

High glucose is the main component of diabetic milieu that can cause direct damage to tubular cells, alongside an accumulation of glycated proteins, increased intrarenal angiotensin II and oxidative stress (Singh, 2008; Tang and Lai, 2012). Studies by Phillip (1999) demonstrated that type IV collagen and fibronectin secretion was increased when human renal proximal tubular cells were exposed to high glucose. Ziyadeh et al. (1990) determined that growing mouse proximal epithelial cells in high glucose induces cellular hypertrophy and stimulates ECM production. They also found that type I collagen is stimulated by elevated glucose levels in PTECs. Studies have also demonstrated that high glucose caused an increase of TGF-β and VEGF in proximal tubular cells (Rocco, 1992). Furthermore, the polyol pathway is a potential mediator which meditates high glucose-induced collagen synthesis in proximal tubular cells (Blayer, 1994).

1.7.2. *In vivo*: Rodent models

- ***Streptozotocin C57BL/6 mice***

Streptozotocin-induced pancreatic injury is a widely accepted technique which is used to create rodent models of T1DM and expand renal injury with similarities to human DN. This model can be used to examine the molecular mechanisms and genetic susceptibility in the progression of DN (Tesch and Allen, 2007). Streptozotocin (STZ) is a D-glucopyranose derivative of N-methyl-N-nitrosourea (MNU) which is readily transported into pancreatic β-cells by Glut-2 and causes β-cell toxicity and results in deficiency of insulin. The diabetogenic agent STZ selectively inhibits the activity of

β-cell O-GlcNAcase. This causes irreversible O-glycosylation of intracellular proteins and results in the apoptosis of β-cells (Lee et al., 2006).

C57BL/6 mice are extensively used for studies of kidney disease which are typically made diabetic by an injection of STZ, as it results in the destruction of the pancreatic β-cells. In humans, diabetic nephropathy is clinically characterised by the development of microalbuminuria and a decline in renal function. These clinical parameters are observed in the rodent models, although the albuminuria level and renal dysfunction are less severe when compared with a patient with DN (Tesch and Allen, 2007). The STZ diabetic mice typically develop albuminuria and also have extreme hyperglycaemia and insulin deficiency which can be observed between weeks 1-2. Breyer et al. (2005) reported that there are associations between doses of STZ with microalbuminuria, as those mice receiving a high-dose of STZ developed more albuminuria in comparison with STZ mice receiving a low-dose. It is also possible the hemodynamic changes are involved in the progression of albuminuria at this early time point (Breyer et al., 2005). As time progresses (15-30 weeks of hyperglycaemia), the development of mesangial expansion and mesangial sclerosis are seen in the STZ diabetic mice. However, this severity is usually milder than patients with DN (Tesch & Allen, 2007).

Although, the use of STZ is a robust technique for inducing diabetes in rodent models, the progression of DN in these animals is less compared to DN patients. There are also additional issues when using these rodent models. Firstly, STZ has a toxic effect on kidneys, especially the tubular epithelium and this may be a significant cofounder when DN is studied in STZ–treated mice. Secondly, one of the key features in humans is that diabetic complications develop gradually, occurring in patients 15 to 25 years after the onset of diabetes (Caramori et al., 2000). However, most of the DN studies in mice, such as the progression of albuminuria and histopathologic changes have focused on the earlier indication of DN due to cost and convenience; they have not openly used renal deficiency as an end point (Sharma et al., 2003). In our experiments, we are investigating the effect of hyperglycaemia on CRYM and MOSC1/MOSC2 genes in mouse kidneys as an indication of early change in diabetes which may be involved in diabetic nephropathy.

● **ß-*phb2* KO mice**

Prohibitins are highly conserved proteins which assume a main role in the maintenance of mitochondrial function and architecture. Their dysfunction is correlated with various disorders such as cancer, obesity, aging and inflammation. However, their function in ß-cells of the pancreas is unclear. Ablation in a sequence of *Phb2* in a mouse ß-cell caused mitochondrial dysfunction, impairment of insulin secretion, loss of ß-cells, progressive change of glucose homeostasis, and ultimately severe diabetes (Supale et al., 2013). ß-cell-specific *Phb2* knockout mice were used to investigate the role of *Phb2* in this endocrine cell type. These mice became diabetic at later age i.e. 11 weeks (>25 mM) and they suffered weight loss (Supale et al., 2013). *In vivo* studies by Supale et al (2013) demonstrated that the deletion of *phb2* in these mice resulted in abnormalities of mitochondria, including a decrease in mtDNA copy number with changes in mitochondrial function and a reduction of complex IV levels. These events ultimately led to ß-cell loss and dysfunction which resulted in severe diabetes in this type of mouse. This model represents spontaneous diabetes progression, through a series of molecular events which appear after 3 weeks and does not require administration of chemicals such as STZ. Therefore, we used this spontaneous model of diabetes to examine the expression of our genes of interest in under hyperglycaemic conditions parallel to STZ models.

1.8. Background of study

In the Malik laboratory identified several candidate diabetes associated kidney cDNA clones in GK rat kidneys at progressive stages and they were isolated by differential screening (Page et al., 1997; Morris, 1997). Some of these clones showed transcriptional changes in GK rat kidneys during the progression of diabetes (Table 3). Consequently, CDK108 (CRYM) and CDK7 (MOSC2) were selected as glucose regulated candidate genes and their expressions were further investigated during the course of diabetes through *in vivo* and *in vitro* studies

1.8.1. CRYM

CDK108 (CRYM) was one of several differentially expressed candidate genes from diabetic rat kidneys which displayed a strong hybridisation signal in 40-week-old diabetic kidneys of progressively hyperglycaemic GK rat compared to 6-week-old GK rat kidneys (Malik et al., 1997). Northern blot analysis using total RNA from the GK

rat kidneys of 6, 16, 26 and 40 weeks old and aged-matched Wistar normoglycaemic kidneys showed CDK108 mRNA expression at higher levels in the kidneys of the GK rat at 40 weeks (Zaidi, 1997). The DNA sequence of rat CDK108 showed that it represents CRYM (μ-crystallin), an abundant protein normally detected in the eye (Zaidi, 1997). CRYM is also known as μ-crystallin or NADP-regulated thyroid hormone-binding protein (THBP) (Vie et al., 1997), and for the purposes of this study we will refer to this gene as CRYM.

Northen blot analysis of human tissues showed that human CRYM mRNA is abundant in the kidney, heart, brain and skeletal muscle and neural tissue whereas there is less in the liver and lung (Kim et al., 1992). Studies have shown high expression of human CRYM in cochlear vestibular tissues in the inner ear (Abe et al., 2003). In adult kangaroo, CRYM mRNA is most abundant in the lens, whereas it was expressed at lower levels in retina and brain (Kim et al., 1992). Among the mouse tissues, CRYM mRNA is most abundant in the skin, whereas its level is lower but detectable in the brain, eye, heart, kidney, liver and lung (Aoki et al., 2006). In the rat, the mRNA expression of CRYM has been detected in a number of tissues such as the kidney (Vie et al., 1996) and brain (Beslin et al., 1995).

CRYM was originally identified as a major structural protein in the lenses of kangaroos (Chen et al., 1992). CRYM has been proposed to have enzymatic function due to its structural homology to bacterial enzymes including alanine dehydrogenase and ornitine cyclodeminase (Kim et al., 1992). Mutations in CRYM can be the cause of non-syndromic deafness (Abe et al., 2003; Oshima et al., 2006) and expression changes of CRYM mRNA has been shown in glioblastoma (Khalil, 2007), prostate cancer (Mousses et al., 2002), and breast cancer (Forti et al., 2002). Additionally, altered CRYM expression has been associated with diseases where oxidative stress plays a role such as cardiovascular disease (Yang et al., 2000) and muscular dystrophy (Reed et al., 2007; Fukada et al., 2007). Furthermore, CRYM has been proposed to be a cytosolic thyroid binding protein which is regulated by binding to NADPH (Vie et al., 1997; Suzuki et al., 2007). There is much evidence which show that patients with uncontrolled diabetes have disturbed thyroid metabolism (Patrisia, 2000). Sub-clinical hypothyroidism has a greater prevalence in patients with type 2

diabetes, and it has been suggested to be an independent risk marker for nephropathy events (Bando, 2002; Chen, 2007).

In renal cells as described previously, hyperglycaemia elevates the cytosolic glucose concentrations, which leads to an abnormal activation of signalling pathways and biochemical dysfunction (Lee et al., 2003; Brownlee, 2001). For instance, hyperglycaemia results in an increase of ROS production as one of the hemodynamic factors which activates the pathways leading to the damage found in diabetic complications (Brownlee, 2001; Brownlee, 2005; Nishikawa, 2000). Much of this damage is considered to be a consequence of elevated production of ROS by either the mitochondrial respiratory chain or membrane bound NADPH oxidase, during hyperglycaemia leading to oxidative stress (Lee et al., 2003). The fact that the CRYM gene has the capability to bind to NADPH directly before being activated as a thyroid hormone binding protein is important in DN (Hashizume et al., 1989). NADPH is an essential component of the cellular antioxidation system and has been proposed as a central mediator of the fundamental biological processes containing energy metabolism and oxidative stress (Yan et al., 2006).

A study by Al-kafaji (2010) reported that CRYM mRNA levels increased in the diabetic kidneys and hearts of GK rats in response to hyperglycaemia when compared to normo-glycaemic age-matched Wistar rats. Al-kafaji and Malik (2010) reported a significant increase in CRYM mRNA and protein levels of renal mesangial cells exposed to high glucose, as well as increased intracellular ROS. Al-kafaji and Malik (2010) also showed that over expression of CRYM resulted in a decrease of glucose-induced intracellular ROS in mesangial cells. It was concluded that CRYM is a glucose-regulated gene *in vivo* in diabetic models of rats and *in vitro* in renal human mesangial cells and thus, CRYM could play a role in the oxidative response of the cell in DN (Al-Kafaji and Malik, 2010).

Taken together, we consider that there might be a link between CRYM expression and the mechanism of damage in DN. Thus, it is important to investigate the effect of high glucose on CRYM expression in different animal models *in vivo* and in vitro in different renal cell types to investigate the potential function of CRYM in DN.

1.8.2. MOSC2 (CDK7)

MOSC2 (CDK7) was one of several differentially expressed genes from diabetic kidneys (Malik et al., 2007). Increased MOSC2 mRNA expression was found in a 40-week-old GK rat kidney (Table 3; Page et al., 1997) and in human mesangial cells exposed to high glucose (Malik et al., 2007). The MOSC2 gene has been located on human chromosome 1q42 (near a diabetes susceptibility gene and linked to numerous diseases: e.g schizophrenia, prostate cancer, and diabetes). Sequence analysis of MOSC2 protein demonstrated that the MOSC2 contained Molybdenum cofactor Sulphurase C-terminal (MOSC) and MOSC_N, domain and a Cystine-Proline-Argenine-Cystine (CPRC) motif, which is conserved in 15 diverse species (Malik et al., 2007). The CPRC region of MOSC2 may have a redox function, as the CPRC domain indicated a similarity to a redox protein structure (thioredoxin; Nordberg, 2001).

There is growing evidence that hyperglycaemia can induce ROS during the inhibition of thioredoxin function by interacting with thioredoxin protein (Schulze et al., 2004). Thioredoxin plays a central role in the redox regulation of the cell (Nordberg, 2001). A study by Ceriello et al. (2000) indicated that antioxidant genes have defective role in diabetic patients. Glyn-Jones et al. (2007) suggested that the protective effect of thioredoxin in experimental DN could be used as an antioxidant therapy for the treatment of DN (Glyn-Jones et al., 2007). In addition to this study, another study by Morrison et al. (2004) showed that altered thiol protein expression is linked to the progression of DN, and also the antioxidant response inside the cell has been shown to be defective in DN (Hodgkingson et al., 2003). Thiol groups also have the capability to modify protein functions in response to ROS. The high conservation of the CPRC domain in all MOSC2 homologue and its similarity to the catalytic thioredoxin domain (Schulze, 2004), are proposed to be a functional correlation between thioredoxin-like proteins and MOSC2 (Malik et al., 2007).

According to these findings, MOSC2 may be involved in the cellular response to hyperglycaemia-induced oxidative stress and play a role in DN by the regulation of ROS levels in the mitochondria. Therefore, the functional characterization of MOSC2 and its participation in renal cellular response to oxidative stress could provide a novel treatment therapy for DN in the future.

In 2010, the Havemayer group found that MOSC2 is a mitochondrial amidoxime reducing component-2 (MARC2). They also indicated that MOSC2 is the fourth molybdenum enzyme and it is part of a three component enzyme system which is located at the outer mitochondrial membrane. MOSC2 has the potential to reduce N-hydroxylated compounds and is involved in the N-reductive pathway. As MOSC2 is involved in N-hydroxylation and plays an important role in the reductive biotransformation of N-hydroxy compounds, they suggested that MOSC2 could be used for drug therapy in diseases with rheumatic inflammation, pain and fever (Havmayer et al., 2010). Therefore, the functional study of MOSC2 (CDK7) can also provide a novel therapeutic target for DN in the future.

Table 3. Differentially expressed clones from kidneys of the Goto-Kakizaki (GK) rat (Morris, 1997)

Clone	Corresponding gene	Expression in DN
CDK1	LDH, Lactase dehydrogenase	High
CDK3	Epithelial sodium channel, alpha subunit	Low
CDK4	Beta defensin	High
CDK6	Megalin	High
CDK7	Novel	High
CDK9	Phosphate inhibitor	High
CDK101	Novel	Low
CDK102	H-protein	High
CDK104	Novel	High
CDK105	Novel	High
CDK106	Zfnl, novel	High
CDK107	**MOSC2**	High
CDK108	**CRYM**	High
CDK111	GPX	High
CDK112	Novel	High
CDK113	Invariant chain-MHC	Low
CDK114	Rat thiazide sensitive sodium chloride channel-like	High
CDK115	PDE1, pyruvate dehydrogenase E alphasubunit	Low

1.9. Aims and objectives

In the current thesis we investigated CRYM and MOSC2/MOSC1 expression in models of diabetes as well as in circulating cells from DN patients, in order to evaluate these genes as potential biomarkers and to explore their possible roles in the pathophysiology of DN. The specific objectives are as follows:

1) To investigate whether CRYM is a glucose regulated gene and if it is expressed abnormally in hyperglycaemia in two rodent models of diabetes: Streptozotocin C57BL/6 mice and ß-*phb2* KO mice. The C57BL/6 mice can be made diabetic with STZ and where the diabetes can be reversed with islet transplantation to allow us to examine the effect of hyperglycaemia and corrected hyperglycaemia on renal and cardiac CRYM mRNA expression. We will also use ß-*phb2* KO mice to test the effect of glucose on renal and cardiac CRYM expression in models of spontaneous diabetes progression.

2) To investigate the location of CRYM protein in control and diabetic kidneys of

Streptozotocin C57BL/6 mice and also examine the CRYM protein expression in renal tissues of control and diabetic Streptozotocin C57BL/6 mice.

3) To further investigate glucose regulation of CRYM, we will use *in vitro* models of diabetic nephropathy. This *in vitro* study includes human renal tubular cells and human renal embryonic kidney cells. CRYM mRNA expression will be examined in human renal tubular cells in three different conditions, normal glucose, high glucose and normal glucose with mannitol. The cellular localisation of CRYM will be determined in normal glucose and high glucose of human renal tubular cells.

4) To examine whether CRYM could be used as a possible diagnostic and therapeutic marker, CRYM mRNA expression will be measured and analysed in two different patient's studies: 1) the study of patients with only type 2 diabetes, with and without retinopathy, 2) the study in patients with type 2 diabetes, with and without nephropathy.

5) To confirm and extend previous findings that MOSC2 is a glucose regulated gene by using *in viv*o mouse models of diabetes and *in vitro* models. MOSC2 mRNA and protein expression will be examined in kidneys of STZ C57BL/6 mice and also in

kidneys of ß-*phb2* KO mice. The MOSC2 mRNA and protein expression also will be measured in human renal cells (mesangial cells, embryonic kidney cells and tubular cells). MOSC2 localisation will be demonstrated in control and diabetic kidneys of STZ mice.

6) To determine if MOSC1 is regulated by glucose *in vivo* and *in vitro* models. Renal MOSC1 mRNA expression will be measured in STZ C57BL/6 mice and renal MOSC1 mRNA and protein expression will be examined in human renal cells.

7) To investigate if MOSC N-reductive activity (associated to MOSC2 and MOSC1) is increased in the presence of hyperglycaemia *in vivo* and *in vitro.*

8) To examine if MOSC2 and MOSC1 is a biomarker in the circulating blood of patients with type 2 diabetic nephropathy and compare their mRNA expression against patients without nephropathy.

These experimental studies will provide further information as to whether CRYM and MOSC homologues (MOSC2/MOSC1) have a functional role in the progression of diabetic nephropathy in response to hyperglycaemia.

Chapter 2

Materials and Methods

Chapter 2. Materials and Methods

2.1. Chemical and reagents

The chemicals and reagents used in this study were of molecular biology grade unless otherwise stated. A list of the chemicals and reagents along with their suppliers are shown in appendix 1.

2.2. Solutions and buffers

The solutions and buffers were prepared according to the manufacturer's instructions or made up according to the laboratory manual (Sambrook et al., 1989) and were sterilized by autoclaving, except those supplied in kits. Through the entire thesis, the symbol 'X' is used to describe the buffer working concentrations unless otherwise stated in the relevant chapters. Table 4a shows the buffers and reagents that were prepared according to the manufacturer's instructions.

2.3. Cell culture

2.3.1 Culturing of renal cells

Three types of human renal cells were used; human mesangial cells (HMCs), human embryonic kidney cells (HEK293) and human tubular (HTC) cells. All renal cells (HMCs, HEK293, and HTC) grow as monolayers on negatively charged tissue culture plastic and were cultured in DMEM (Sigma, UK). The growth medium was made up as follows in 500ml of DMEM (Sigma, UK): 50ml of Foetal bovine serum (FBS), 1ml of 5µg/ml Insulin-Transferin-Selenium (Sigma, UK), 5ml of 2mM L-glutamine, 6ml of $NaHCO_3$, 1ml of Amphotericin B, 10ml of 1M HEPES buffer. The cells were incubated in 5ml of the complete growth medium, in culture flasks, in a humidified atmosphere of 5% CO_2 with 95% air at 37°C. The cells were passaged every 3-4 days.

Table 4a. Preparation of reagents and buffers

Solution	Chemical components
0.5M EDTA pH 8.0/ 500ml	Disodium ethylenediaminetetra-acetate.$2H_2O$ 186.1g (pH 8.0 adjusted with NaOH)
10X Tris-borate (TBE)/L	Tris base 108g, boric acid 55g, 0.5M EDTA (pH 8.0)
10X Tris-acetate (TAE)/L	Tris base 108g, glacial acetic acid 11.42g, 0.5 M EDTA (pH 8.0)
1M Tris/ 500ml	Tris-base 60.55g pH 7.0, 70ml HCl added
10% (w/v) SDS/ 500ml	Electrophoresis-grade SDS 50g, pH 7.2 with few drops of HCl
DNA loading dye	0.25% (w/v) bromophenol blue, 0.25% (w/v) xylene cyanol FF, 30% (v/v) glycerol in water
Ethidium bromide (10mg/ ml)	Ethidium bromide 1g in 100ml ddH_2O (stored in dark bottle at room temperature)
Ampicillin 50 mg/ml	Ampicillin 0.5g dissolved in 10ml ddH_2O (filter sterilized using 0.2μM filter prior to storage at -20°C)
LB broth/L	10g NaCl, 10g tryptone, 5g yeast extract, ddH_2O to final volume of 1 litre (pH 7.0)
LB Agar/L	10g agar dissolved in 1 litre LB broth pH 7.0 (autoclave sterilized)
LB/ Ampicillin agar/L	5ml of ampicillin (50 mg/ ml) was added to autoclaved litre of LB/Agar after cooling to 55°C (25 ml/ mm-plate)

2.3.2. Subculturing

The cells were maintained in culture and the media was replaced every 72 hours. Upon reaching 70% confluence, the culture flasks were removed from the incubator, media was removed and the cells were washed twice with 5ml pre-warmed PBS. Then, 3ml of Trypsin-EDTA 0.25% (w/v) which was warmed previously added to each flask and incubated for 3 mins at 37ºC to detach the cells from the flask. Cell detachment was observed under microscope. Trypsin actively digests the anchorage sites between the cells and the growing surface, and EDTA binds to Ca^{2+} that is required for Ca^{2+}-dependent adhesion due to its divalent ion chelating property. 5ml

of media was then added to the flask to neutralize trypsin-EDTA solution. The mixture was transferred into a fresh falcon tube and centrifuged at 10,000xg for 3 minutes. The supernatant was removed and the pellet was re-suspended with 10ml of fresh normal glucose (5mM) complete growth medium (Sigma, UK). The cell suspension was then transferred into culture flasks and incubated for 48 hours. Next, the media was changed and cells were seeded in triplicate with normal glucose (5mmol/L glucose), high glucose (25mmol/L glucose) and normal glucose with mannitol (5mmol/L glucose + 20mmol/L mannitol) for 3-4 days.

2.3.3. Counting the cells

The haemocytometer (Neubauer chamber) and the vital dye, trypan blue (Sigma, UK) was used to count the cells under study. The haemocytometer consisted of a thick glass microscope slide with two counting chambers. A cover-slip sits on top of it enclosing both chambers which are 0.1mm in depth (Figure 7). Reactivity of trypan blue is based on the fact that the chromophore is negatively charged and does not interact with the cell unless the membrane is damaged. Therefore, all the cells which exclude the dye are viable. A volume of 0.1ml of cell suspension was placed in a screw cap test tube and 0.1ml of 0.4% (w/v) trypan blue stain was then added and mixed thoroughly. The mixture was allowed to stand for five minutes at room temperature. The haemocytometer was covered with a precision ground coverslip and a few drops of the stained cell suspension were placed at the edge of the coverslip. Under a microscope, the stained non-viable cells and viable cells that excluded the stain were observed. The cells touching the right and upper lines in each chamber of the haemocytometer were counted and the average cell number was calculated using the following formula:

Cell number per ml = average cell number per $0.1mm^3$ x dilution factor (e.g. 5 for 1 in 5 dilution) x 10^4

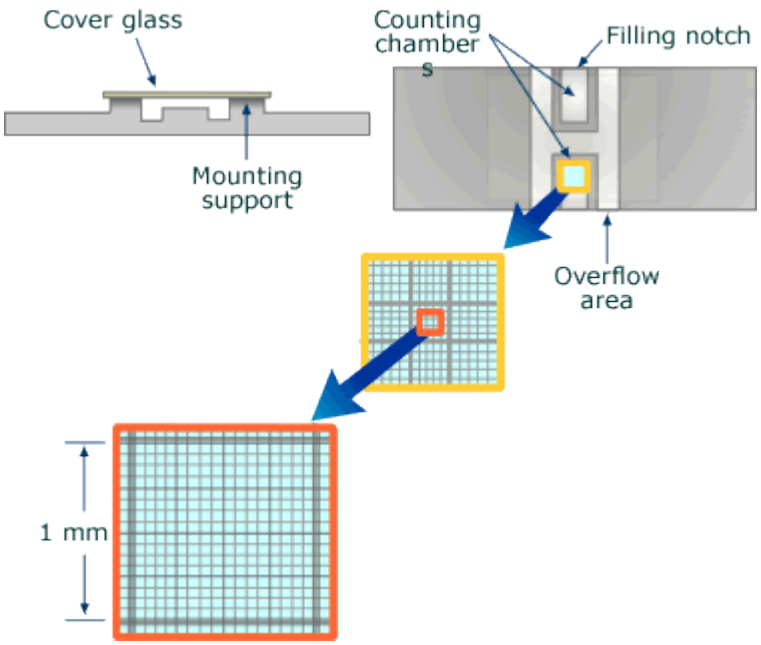

Figure 7. Cell number estimation with Neubuer haemocytometer.
The haemocytometer has a rectangular chamber etched with a grid of perpendicular lines and each grid consists of 9 primary squares, each of which measures $1mm^2$ with the plane of the grid rests 0.1mm below 2 ridges supporting a cover-slip. Since the area of the corner squares and the depth of the chamber are known, by counting the number of cells in this volume of fluid ($0.1mm^3$) the total number of cells in the original sample can be obtained.
(http://toolboxes.flexiblelearning.net.au/demosites/series4/412/laboratory/studynotes/SNHaemo.htm)

2.3.4. Freezing down and thawing of cells

Cells which are in the logarithmic phase of growth and just approaching confluency (early passage 3 or 4) were harvested as previously described and re-suspended with freezing medium containing warmed DMEM 5% (v/v), 1ml DMSO 10% (v/v) and 1ml FBS 85% (v/v). Cell suspension was dispensed in 1ml aliquots into sterile freezer Cryo-vials. The Cryo-vials were placed in a Nalgene Cryo freezing container filled with appropriate volume of isopropanol and placed at -80^oC overnight (ideally, the temperature should decrease by 1^oC per minute). Frozen vials were then stored in liquid nitrogen for permanent storage. Cells can be recovered from the frozen stage by rapid thawing in a 37˚C water bath and then transferring into a $25cm^2$ tissue culture flask. Cells were incubated with the same culture condition as previously described.

2.4. Mouse kidney samples

ß-*Phb2* KO mice: The ß-*Prohibitin2* knockout mice described in the work were set up and maintained by Prof Pierre Mieschler and his team according to local ethical rules (Department of Cell Physiology and Metabolism, Geneva). The ß-*Phb2* KO mice were bred by crossing flox-Phb2-flox mice with rat-insulin promoter driven Cre mice so that *Phb2* is specifically deleted in pancreatic beta cells. Therefore they were able to investigate its role in beta cells. The ß-*Phb*2 KO mice became diabetic (blood glucose >11.1mM) as glucose (2g/kg body weight) was administered intraperitoneally in 6h-fasted mice before the measurement of glucose levels on blood collected from the tail vein at indicated times using a glucometer (Accu-check, Roche Diagnostics, Rotkreuz, Switzerland) at the age of 5-6 weeks. The mice become diabetic at later age i.e. 11 weeks, when they have extensive polyurea and these mice die between the ages of 12-15 weeks. The kidneys and hearts from control and KO mice were collected at 11 weeks of age; at this age KO mice had glycaemia ranging between 30-40 mM. Samples were snap frozen after collection.

Streptozotocin mice: The mouse model described in the work has been set up and maintained by Dr Aileen King and her team (Diabetes Research Group, KCL). All animal procedures were conducted in accordance with the UK Home Office Animals (Scientific Procedures) Act 1986. Eight week old male C57/BL6 mice were made diabetic with an injection of 180mg/kg streptozotocin (STZ, Sigma-Aldrich). The blood glucose concentrations were determined using an Accu-Check glucose meter (Roche). Five days after STZ, the diabetic mice (>20mM) received a suboptimal islet graft of 150 islets transplanted under the left kidney isolated from the pancreases of C57/BL6 mice, as previously described (King et al., 2007). Four weeks after transplantation, the kidneys and hearts were obtained from the following: mice which had not been treated and thus remained diabetic throughout the study (blood glucose level> 20 mmol/L), treated mice (blood glucose level < 11 mmol/L for 4 weeks after transplantation) and 12 week-old non-transplanted, non diabetic control mice (glucose level < 11 mmol/L). The right kidneys and the hearts were removed and immediately frozen in liquid nitrogen, and stored at -70º C until processed.

2.5. Patient blood samples

Diabetic nephropathy patient blood samples: Patients with diabetes (SEEDA/JJ study) were recruited with written informed consent from both Guy's and St Thomas' hospital clinics under ethical approval from the regional Research Ethics Committee (REC ref number 07/H0806/120). The study adhered to the Ethical Principles for Medical Research Involving Human Subjects, World Medical Association Declaration of Helsinki. The patients' blood samples were collected and preserved in RNA later solution (Ambion) to avoid degradation of the mRNA.

Type 2 diabetes (T2D) was defined as an onset of diabetes after the age of 35, who were controlled by a healthy diet or oral hypoglycaemic treatment and/or insulin. Diabetic nephropathy (DN) has been classically defined by the presence of albuminuria in the absence of any other renal disease, though in the presence of retinopathy. For T2D, we defined a control group of patients from subjects with the onset of T2D who had suffered a long duration of diabetes (with ≥10 years) with normoalbuminuria, normal serum creatinine, normal blood pressure (≤130/80 mmHg) and taking no antihypertensive agents.

Overweight patients were defined as those with a BMI of 25-30 kg/m^2; obese patients were diagnosed as having a BMI ≥30 kg/m^2 (using BMI measurements). Hypertension was identified as a blood pressure reading of ≥130/80 mmHg and mean blood pressure of ≥80 mmHg. The amount of glucose being carried by the red blood cells is indicated by HbA1c (glycated haemoglobin) and fructosamine measurements. A patient with ≥7.5 % HbA1C was considered diabetic. A random blood glucose level of ≥11.1 or a fasting blood glucose level of ≥7 mmol/l was considered to be indicative of diabetes. Cholesterol level of ≥4 mmol/l was considered to be above the normal range.

In patients with diabetes, renal dysfunction was assessed by measuring albuminuria, serum creatinine (SCr), the albumin/creatinine (A/C) ratio and the glomerular filtration rate (eGFR). Diabetic nephropathy was classified when the Scr level was ≥115 mmol/l, albuminuria was between 30-300mg/day (microalbuminuria), the A/C ratio was ≤3.5 mg/mmol (female) or ≤2.5 mg/mmol(male) and the eGFR was < 90 $ml/min/1.73m^2$.

Diabetic retinopathy patient blood samples: Patient samples were obtained from the study 07/H0806/120 recruited by Dr Sobha Sivaprasad. Patients were recruited with written informed consent from King's College Hospital under NHS Research Ethics Committee approval (REC; ref numbers 07/H0806/120) and from Guy's and St Thomas' hospital clinics under ethical approval from the regional Research Ethics Committee (REC; ref number 07/H0806/120). The study adhered to the Ethical Principles for Medical Research Involving Human Subjects, and the World Medical Association Declaration of Helsinki. A random blood glucose level of ≥11.1 or a fasting blood glucose level of ≥7 mmol/l was considered to be indicative of diabetes. T2D was defined as onset after age 35, controlled by diet, or established oral hypoglycaemic treatment and/or insulin.

- ***Grading of diabetic retinopathy***

The patients underwent 2-field digital photographs for each eye, one centreed on the optic disc and the other centreed on the macula after dilation of the pupils. Photographs were graded in a standardised manner, and DR severity was categorized according to the ETDRS (Early Treatment Diabetic Retinopathy Study) severity system. Consequently, the following categories were created, based on the more severely involved eye: no DR (DR-0) defined as ETDRS <20, mild NPDR (DR-m) defined as ETDRS 35-43, severe NPDR and PDR (DR-s) defined as ETDRS 47 and above.

2.6. Gene expression

2.6.1. Total RNA extraction

In living cells, RNA has four major types: messenger RNA (mRNA), transfer RNA (tRNA), ribosomal RNA (rRNA) and microRNA (miRNA). A high yield of total RNA of relatively high purity is essential to determine gene expression specifically by cDNA amplification using polymerase chain reaction (PCR). For the experiments described in this thesis, RNAs were extracted from mouse tissues, human cultured renal cells and patients' blood samples. All glassware and plastic ware were autoclaved before the RNA extraction. The work was carried out in a designated RNA area (DNA free) and the bench was cleaned with an RNase decontamination solution (RNase*Zap*, Ambion UK). The RNA extraction method used is based on the disruption of tissues or cells in a solution containing guanidinium thiocyanate, a

strong chaotropic denaturant which lyses cell membranes and rapidly inactivates cellular ribonucleases.

● ***RNA Extraction from the tissue***

Total RNA was extracted from various mouse tissues using the QIAzol® Lysis Reagent (Ambion, UK) according to manufacturer guidelines. Approximately 0.5-1g of tissue was ground in liquid nitrogen using a pre-chilled mortar and pestle, and was transferred to a 50ml Falcon tube. The liquid nitrogen was allowed to evaporate and a denaturing solution (10ml) was added and the mixture shaken vigorously until the tissue dissolved. Samples were sonicated on ice for 2-5 minutes using an MSE Soniprep 150 Ultrasonic disintegrator for 15 seconds to shear high molecular mass DNA and placed into the QIAzol Lysis Reagen tube. RNA was separated from protein and DNA by adding 0.2ml chloroform per 1ml QIAzol Lysis Reagent, mixed vigorously and placed at 37°C for 2-3 minutes.

Samples were centrifuged for 15 minutes at 5,590xg at 4°C and the aqueous phase was transferred to a fresh nuclease-free tube. Isopropanol (0.5ml per 1m QIAzol Lysis Reagent) was added to allow precipitation of RNA, followed by incubation at 37°C for 10 minutes. The aqueous layer containing RNA was recovered by centrifugation at 5,590xg for 10 minutes at 4°C and carefully transferred to a fresh RNase-free tube (without transferring any material at or below the interface). RNA pellets were washed with 75% (v/v) chilled ethanol (1ml) and pellets were re-precipitated by centrifugation (5,590xg, 5 minutes, 4°C) and left to air dry to remove the ethanol. RNA was re-suspended in 50µl RNase-free water and stored at - 80 °C.

● ***RNA extraction from cell culture***

For the extraction of RNA from cultured human renal cells, RNeasy mini kit (QIAGEN, UK) was used. Culture media was removed and the cells were washed twice with PBS. The PBS wash was removed and the cells were disrupted by adding 300 µl of lysis/ binding solution (300µl per $1x10^6$ cells) and mixed by vigorous pipetting. The lysate was transferred to a QIAshredder spin column and vigorously vortexed to completely homogenise the sample. 600 µl of ethanol 70% (v/v) was added to homogenised lysate and mixed thoroughly by gently pipetting and 700µl of lysate/ ethanol mixture was applied to an RNeasy mini column (placed in a 2ml collection tube) and centrifuged for 15 seconds at 9,000xg. The flow-through was

discarded and several washing steps were carried out using 700µl and 500µl of wash solution and then were added to the filter cartridge followed by centrifugation for 2 minutes at 9,000xg. Pellets were left on the vacuum manifold for 10-30 seconds to remove the last traces of wash solutions. To elute the RNA, 50µl of elution solution (pre-heated at 95°C) was applied to the centre of the filter, elute was recovered by centrifugation (1 minute, 9,0000xg) and the RNA samples were stored at -80°C.

● ***RNA extraction from patient blood samples***

For DN patients (n= 99), we used a developed homemade method by using TRIzol ® LS Reagent (Ambion, UK). Total RNA was extracted from TRIzol® LS Reagent (Ambion, UK) according to manufacturer's guidelines. 500µl of patients' blood stored in RNAlater solution was used. The RNAlater solution was removed from blood after centrifugation. The blood cells were lysed in 1ml of TRIzol (pre-warmed to 56°C) and vigorously vortexed to completely homogenise the sample. The RNA was extracted with 200µl of 25:24:1 mixture of Phenol: Chloroform: Isoamylalcohol and the aqueous phase containing the RNA was recovered in a fresh 2 ml tube. 500µl of 100% chilled Isopropanol was added to the recovered aqueous and centrifuged for 10 minutes at 7,000xg. The pellet was washed with 500µl of chilled 75% (v/v) ethanol and centrifuged for 5 minutes at 7,000xg. The 50µl of RNaese-free water was added to the pellet and then treated with DNase-1 enzyme.

2.6.2. DNase-1 treatment of RNA

No RNA isolation procedure can guarantee the complete removal of trace amounts of DNA below the limit of detection by RT-PCR. Therefore, a DNA inactivation kit based on DNase I treatment (Sigma, UK) was used to effectively remove trace DNA contamination from RNA. 8µl RNA was mixed gently with 1µl of 10X reaction buffer (Tris-HCl, pH 7.5) containing $MgCl_2$, 1µl of Amplification Grade DNase I and incubated at 37°C for 15 minutes. 1µl of stop solution was then added to bind the calcium and magnesium ions and to inactivate the DNase I. Afterwards, the sample was heated at 70°C for 10 minutes to denature the DNase I. The samples were incubated on ice for a few minutes and finally, the treated RNA samples were kept at -80 °C.

2.6.3. Determination of RNA concentration

The concentration of RNA was measured by using the ND1000 spectrophotometer (Nanodrop). This device has the capability to measure 260 and 280nm absorbance from samples in only 2µl of sample. A_{260nm} is automatically converted to give an accurate estimation of RNA content in ng/µl. Furthermore, the ratio of A_{260nm}/A_{280nm} can be used for indicating quality of RNA. Generally speaking, a ratio of <1.6 indicates contamination of samples with protein, phenol or other compounds which absorb at 280nm. Sample RNAs with $A_{260}nm/A_{280nm}$ >1.6 were stored at -80˚C and used subsequently for cDNA synthesis (Section 2.3.2).

2.6.4. cDNA synthesis

DNA-free RNA (up to 9µl) was reverse transcribed to cDNA using a High Capacity RNA-to-cDNA kit (Applied Biosystems, UK). According to the protocol provided with the kit, cDNA synthesis was carried out as follows:

Preparation of RNA: RT reaction mix:

A reaction mix of 2X RT-buffer (10µl), 20X Enzyme mix (1µl) and RNA sample (10µg) was prepared in a final volume of 20µl nuclease–free H_2O. The RT reaction mix was transferred into 1.5ml tubes and were briefly centrifuged in 10,000x g for 30 seconds to spin down the contents and then placed on ice until they were ready for reverse transcription reaction. The reaction mix was incubated at 37°C for 60 minutes. The mixture was then heated at 95°C for 5 minutes and then held at 4°C. The cDNA samples were stored at -20°C.

2.7. Reverse-Transcriptase Polymerase chain reaction (RT-PCR)

Polymerase chain reaction (PCR) is a widely used method, employed to accurately and rapidly amplify a specific DNA sequence of interest from nanogram amounts of DNA template (Saiki et al., 1988). In the experiments described in this thesis, RT-PCR was performed with cDNAs from mouse tissues (kidney and heart), patient blood samples and human cultured renal cells (HMCs, HEK293, HTC). Specific sets of primers were designed and selected using the Roche Universal ProbeLibrary programme and used to amplify mRNAs of interest (*http://www.roche-applied-science.com/sis/rtpcr/upl/ezhome.html*).

Corresponding annealing temperatures for various products were optimised by first running the reactions under temperature gradients at 3˚C from the predicted optimum annealing temperature. PCR reaction was performed in 0.2ml PCR tubes and the reaction mix was prepared by combining the following components which were provided by Promega, UK. A list of primers used in this thesis is shown in Table 5a and 5b.

10X reaction reaction Tris-HCl (PH 8.3) buffer containing 500mM KCl; 15mM $MgCl_2$; 0.01% (w/v) gelatin (5µl), PCR Nucleotide Mix containing 10mM of sodium salts (pH 7.5), dNTP (1µl), 50 ng/µl forward and reverse prime (1µl each), DNA template (1µl) and 5 u/µl *Taq* DNA polymerase (0.3µl). DEPC water was added to make a final volume of 25µl. The reaction was spun in 17,900xg for 30 seconds to mix and PCR was carried out in a thermal cycler (Table 4b; Gene Amp System 2400, Applied Biosystems, UK).

Table 4b. Thermocycler program

Protocol	**Temprature**	**Duration**
Initial denaturation	94°C	15 minutes
Amplification	Denaturation 94°C Annealing 62°C Extension 72°C	30 seconds 30 seconds x 30 cycles 1 minute + 30 seconds
Incubation	72°C	7 minutes
Cooling	4°C	

PCR amplification was carried out in the PCR thermal cycler (GeneAmp PCR Systems 2400, Applied Biosystem, UK) and took approximately 2.5 hours for 30 cycles.

Once the amplifications had been completed, 10µl of each PCR product was analysed by agarose gel electrophoresis using a 1% (w/v) agarose gel and 1X TBE buffer. The agarose was melted in a microwave oven (medium power, 5 minutes) and cooled to approximately 60°C. Once cooled down, ethidium bromide (0.5 µg/ml) was added. The ethidium bromide stained gel was then cast to a thickness of 5mM comb. The gel

was placed in a horizontal gel electrophoresis apparatus and covered with 1X TBE buffer. A loading buffer (3µl) was added to each DNA sample (10µl), mixed and loaded into the well of the agarose gel. Electrophoresis (50-100V, 1-2 hours) was carried out to allow sufficient separation of the DNA fragments. Ethidium bromide stained agarose gels were then placed on a UV transilluminator and photographed.

Table 5a. Human reference gene primers

Gene Bank	**Accession number**	**Product size**	**Primer**	**Sequence** (5' to 3')
Human CRYM	L02950	62bp	hCRYM F_1	gcc ctg aag gag tct gag g
			hCRYM R_1	tct ccc agc tca gca aag at
Human MOSC1	NM_022746	78bp	hMOSC1F_1	cca cag tgg acc cag aca c
			hMOSC1R_1	ggt cac act ggc gat aac tct
Human MOSC2	NM_017898	187bp	hMOSC2 F_1	gac aca tgg tca ctg cc
			hMOSC2 R_1	ttg cca cag tct ctg c
Human β-actin	NM-001101	64bp	hβeta-actinF_1	cca acc gcg aga aga tga
			hβeta-actin R_1	cca gag gcg tac agg gat tag
Human Phosphoglycerate kinase (PGK)	NM-000291	121bp	hPGK F_1	gag aaa gcc tgt gcc aac c
			hPGK R_1	ctg gct cgg ctt taa cct t
Human Peptidylprolyl isomerase B (PPIB)	NM-000942	112bp	hPPIB F_1	ccc agt tct tca tca cga ca
			hPPIB R_1	gtc ttg gtg ctc tcc acc tt

5b. Mouse reference gene primers

Gene Bank	Accession number	Product size	Primer	Sequence (5' to 3')
Mouse CRYM	NM-016669	61 bp	mCRYMF$_1$ mCRYMR$_1$	ggg gct caa tca atg ct gct cgt cat cca gtt ctc g
Mouse MOSC1	NM-001081361	60bp	mMOSC1F$_1$ mMOSC1R$_1$	gtt gtc atc cgg gat gtg g tcc aat gag aac ctc gtt cc
Mouse MOSC2	NM-133684	67bp	hMOSC2F$_1$ hMOSC2R$_1$	gga tcc cat ggc tga cac gga aga tgg cca tga gga
Mouse β-actin	NM-007393	91bp	mβ-actin F$_1$ mβ-actin R$_1$	att ggc aat gag cgg ttc tga agg tag ttt cgt gga tga
Mouse PGK phosphoglycerate kinase	NM-18735	65bp	mPGK F$_1$ mPGK R$_1$	tac ctg ctg gct gga tgg cac agc ctc ggc ata ttt ct
Mouse PPIB	NM-011149	144bp	mPPIB F$_1$ mPPIB R$_1$	ttc ttc ata acc aca gtc aag ac acc ttc cgt acc aca tcc at
Mouse TBP TATA box binding protein	NM-013684	90bp	mTBP F$_1$ mTBP R$_1$	ggg aga atc atg gac gag aa gat ggg aat tcc agg gag tca
Mouse Rn28s1 28S ribosomal RNA	NM-016844	70 bp	mRn28s1F$_1$ mRn28s1R$_1$	ata tcc gca gca ggt ctc c gcc gac ttc cct tac
Mouse glyceraldehyde-3-phosphate dehydrogenase (GAPDH)	NM-008084	124bp	mGAPDH F$_1$ mGAPDH R$_1$	cct cgt ccc gta gac aaa atg gcc atc aac gac ccc ttc a

2.8. Purification of DNA from the gel band

DNA was extracted using a Qiagen Gel Extraction Kit. The DNA fragment was excised from the agarose gel using a sterile scalpel with minimum exposure to UV light. A capture buffer (10µl/ 10mg of band weight) was added and vigorously mixed with the gel slice. The capture buffer is a chaotropic agent that denatures proteins, dissolves agarose and promotes the binding of double-standard DNA to a glass fibre matrix. The complete melting and dissolving of the agarose gel slice was achieved by

incubating the samples at 60°C for 5-10 minutes. DNA bound to the glass fibre matrix was recovered by passing the samples through a GFX column and the flow-through was discarded after brief centrifugation at 10,000xg for 30 seconds. To remove the residual salts and contaminants, the matrix-bound DNA was washed with 500µl of washing buffer (previously mixed with 48ml absolute ethanol) and centrifuged at 10,000xg for 30 seconds. The purified DNA was eluted in 40µl of sterile endonuclease-free water as required**.**

The extracted DNAs were sequenced by DNA Sequencing Services at UCL. Sequence homology alignment and analysis were used to compare the homology between predicted sequences and actual sequences of products amplified by PCR.

2.9. Real time quantitative PCR (qPCR)

A quantitative real-time polymerase chain reaction (qPCR) is a sensitive and specific technique used to measure the level of the genes under study. In qPCR, the gene is amplified by means of a standard PCR reaction. Hence, the quantity of the amplicon was first quantified by Nanodrop, and the copy numbers were calculated on the basis of the molecular weight of each particular gene amplicon. Subsequently, serial dilutions of this amplicon have been tested by qPCR to produce a gene specific standard curve. The assay can be quickly and easily utilised to quantitate real-time levels of any gene product (Gentle et al., 2001). qPCR is broadly applied to accurately measure the gene activity by determining mRNA levels. It has the capacity to determine and quantify a very low amount of DNA and RNA, and clearly distinguished between samples including PCR products and non-template controls. The assays are easy to perform and they can merge reliable specificity with high sensitivity. Sensitive quantification of PCR product relies on detection of a fluorescent signal proportional to the amount of product by use of SYBR green binding dye, which binds only to double-stranded DNA. The amount of PCR product was directly measured in real time using the LightCycler ™ system that is able to carry out 30 PCR cycles in less than 20 minutes with real-time fluorimetric detection of PCR products. The system can perform continuous sampling with results displayed at once on the computer screen. To verify specificity, melting-curve analysis was applied where the temperature was raised slowly to the melting point of duplex DNA and the fluorescence was monitored (Gentle et al., 2001; Tichopad et al., 2003).

2.9.1. Standard preparation

It is necessary that the dilution series from which the standard curve is produced be carefully prepared. The units utilised to describe the dilution series are relative, not absolute values, are based on the dilution factor, and can be expressed either relatively as e.g. 1 fold, 10 fold, 100 fold, 1000 fold, etc or expressed as equivalent mass amounts e.g. 100 ng, 10 ng, 1 ng, etc. To prepare standards for a generation of standard curves, PCR products were purified applying a QIAquick Gel Extraction Kit (QIAGEN, UK). The amount of DNA present was determined by electrophoresis of the PCR products against a 100 bp DNA ladder (Promega, UK). The exact copy numbers of the purified PCR product were calculated using Avogadro's number. Dilution series including 10^9, 10^8,10^7,10^6,10^5,10^4,10^3 and 10^2 copies/µl of the gene were quantified and prepared in the presence of carrier transfer ribonucleic acid (tRNA, 10 mg/ml; Sigma, UK). Subsequently, they were utilised as a calibration curve in every run with Roche light cycler.

2.9.2. Quantification

Serially diluted standards prepared for a target gene and a reference gene were utilised to establish standard curves by amplification in 10-fold dilutions of PCR product of each gene to be quantified. A qPCR was performed using the FastStart DNA Master ^{plus} SYBR Green 1 Kit (Roche Molecular Biochemical, Germany). A qPCR was carried out in a total volume of 10µl containing 50 ng/µl forward and reverse primers (0.5µl each), Fast Start DNA Master SYBR Green 1^{plus} probe (2µl), DNA template (2 µl) and nuclease free water (5µl). The reactions were performed in the Roche Light Cycler instrument using the following 4-cycle program protocol: pre-incubation at 95°C for 10 minutes, amplification at 95°C for 10 seconds, annealing at 60°C (or optimum temperature) for 20 seconds, and 72°C for 10 seconds for 40 cycles, melting at 95°C for 0 seconds, 65°C for 30 seconds, and 95°C for 0 seconds and cooling at 40°C for 30 seconds. The data were analysed using the Roche Molecular Biochemical Light Cycler software, version 3.5. The mean crossing point of each sample was compared with the standard curve of the target gene or the reference gene. Fluorescence detection was used immediately at the end of each annealing step and the purity of the amplification was confirmed by analysing the melting curves.

2.10. Protein extraction

1) Preparation of cell lysates

Cells were maintained as monolayers in 10 cm^2 Petri dishes up to 75% confluency. The cells were harvested by trypsinisation, spun down and stored at -80°C. Frozen cell pellets were washed with PBS at room temperature and collected by low-speed centrifugation (13.975xg, 5 minutes). The pellets were lysed in 100µl lysis buffer (Table 6) supplemented with protease and phosphatase inhibitors to protect the proteins from being degraded and dephosphorylated, on ice for 10 minutes. The samples were sonicated on ice (20 seconds, 3 times) using an MSE soniprep 150 Ultrasonic disintegrator and centrifuged at 11,000xg for 10 minutes at 4°C. The supernatant was the total cell lysate which was then transferred to a new micro-centrifuge tube. The protein content of samples was quantified using 10µl of each cell lysate (section 2.11). The remaining protein extracts were kept at -20˚C in 2X NuPAGE® sample buffer (contains lithium dodecyl sulfate, pH 8.4), which contains denaturing agents, prior to electrophoresis on polyacrylamide gels.

2) Preparation of mouse tissues

Kidneys from STZ mice were homogenised using liquid N_2 before being lysed in (30 µl) of lysis buffer (Table 6), vigorously vortexed and kept on ice for 10 minutes. The samples were boiled at 90°C for 5 minutes and centrifuged at 6,000xg for 3 minutes. The supernatant containing the protein was recovered and assayed for total protein.

Table 6. Preparation of lysis buffer (RIPA buffer)

Reagent	Amount for 100ml	Final Conc.
Tris-base	790mg	50mM
NaCl	900mg	150mM
NP-40 (10%) (v/v)	10ml	1% (v/v)
Sodium-deoxycholate (10%) (v/v)	2.5ml	0.25% (v/v)
EDTA (100 mM)	1ml	1mM

790mg Tris-base and 900 mg NaCl were first dissolved in 75ml DI H_2O, the pH was adjusted to 7.4 with concentrated HCl followed by an addition of NP-40, Na-deoxycholate and EDTA. DI H_2O was then added to make up the final volume to 100ml. The RIPA buffer was stored at 2-8°C for further use.

2.11. Determination of protein concentration

To ensure equal loading for SDS-PAGE, the concentration of protein samples was measured by the BCA Protein Assay Kit (Pierce; distributed by Thermofisher Scientific, Cramlington, UK). This colourimetric method is based on bicinchoninic acid (BCA) and it combines the reduction of Cu^{2+} to Cu^{+} by protein in an alkaline medium and the formation of a purple-coloured reaction product by the subsequent chelation of the reduced Cu^{+} with BCA. The amount of protein in the sample is directly proportional to the amount of purple coloured reaction complex.

A stock solution of 2 mg/ml bovine serum albumin (BSA) was made by dissolving BSA (Sigma, UK) in the lysis buffer used and was diluted to provide final concentrations of 0.2, 0.4, 0.6, 0.8, 1.2 and 1.6 mg/ml. Lysates were further diluted 1:4 in the lysis buffer. The working reagent was prepared for each sample by combining 50 parts reagent A (containing BCA in a 0.1M sodium hydroxide solution) with 1 part reagent B (containing 4 % cupric sulphate).

10µl of standards and samples were added in triplicate to the wells of a 96 well plate, followed by the addition of 200µl of working reagent to each well. The plate was thoroughly mixed on a plate shaker for 30 seconds and incubated at 37^{o}C for 30

minutes. The plate was cooled to room temperature and the absorbance read at 570 nm on a spectrophotometer (Macroplate Autoreader; Bio-Tek Instruments, Potton, UK). The absorbances of each standard point were plotted and a standard curve was used to detect the protein concentration of each unknown sample.

2.12. Sodium dodecyl sulfate polyacrylamide gel electrophoresis (SDS-PAGE)

SDS-PAGE is the most widely used method for separating proteins across an electric field based on their molecular weight. SDS is an anionic detergent that binds to a protein sample to linearise proteins and apply a negative charge. In the presence of an electric field, the negatively charged proteins migrate across the gel towards the positive electrode through a porous gel matrix of polyacrylamide. The amount of polyacrylamide determines the pore size, and each biomolecule will move according to their size.

The NuPAGE Bis-Tris electrophoresis system was utilised in the experiments described in this thesis. Equal amounts of total protein was loaded on to a 10% (w/v) Bis-Tris-HCl buffered (pH 6.4) polyacrylamide gel. The gel was set and divided in the Xcel Surelock mini cell apparatus, and the inner chamber containing sample proteins was filled with antioxidant-supplemented MOPS running buffer (Table 7). The outer chamber was filled with approximately 600ml of MOPS running buffer and the gel was subjected to electrophoresis at 200V for 50 minutes. A Rainbow® coloured protein molecular weight marker was included and analysed in parallel to the protein samples for demonstration of sample protein molecular weights.

Table 7. Preparation of 3-(N-morpholino) propanesulfonic acid (MOPS) running buffer

Reagent	Amount for 500ml	Final Conc.
MOPS	104.6g	1M
Tris Base	66.6g	1M
SDS	10g	69.3Mm
EDTA	3g	20.5mM

The reagents listed above were dissolved in 400ml DI H_2O and adjusted to a final volume of 500ml. The 20X MOPS running buffer was kept at 4˚C and diluted 1 in 20 (50ml 20X MOPS running buffer in 950ml DI H_2O) before use.

The MOPS running buffer was made up by adding 500µl of 15ml NuPAGE® Antioxidant to 200ml 1X MOPS running buffer.

2.13. Western blotting

After SDS-PAGE, the gel was carefully removed and the separated proteins were transferred to a suitable membrane such as polyvinylidene difluoride (PVDF) to allow access of specific antibodies for the immune-detection of proteins of interest. The transfer process is performed using a trans-blot sandwich which presses the polyacrylamide gel and PVDF membrane among layers of filter paper soaked in transfer buffer (Table 8). The transfer was carried out using the electroblotter system (BioRad, UK) to tranfer the proteins from the gel onto the PVDF membrane (Figure 8).

Table 8. Preparation of 1X Transfer buffer

Reagent	Volume
DI H_2O	849ml
20X NuPAGE transfer buffer (Invitrogen)	50ml
NuPAGE sample antioxidant	1ml
Methanol	100ml

After immunoblotting, the membrane was placed in the clean tray containing 10 ml of blocking buffer [(5% w/v skimmed milk powder dissolved in 10 mM TBS-T (Tris-HCl PH 8.0, 0.15 M sodium chloride, 0.2% (v/v) Tween-20)], and incubated for 1 hour at room temperature to block non-specific binding sites. Following the blocking process, the membrane was washed in TBS-T (3 times, 5 minutes) and incubated with an appropriate primary antibody (diluted in blocking buffer to increase specificity) overnight at 4°C. The membrane was subsequently washed in TBS-T (2 times, 10 minutes) to remove any unbound primary antibodies.

The membrane was then incubated for 1 hour in a horseradish peroxidase-conjugated secondary antibody (diluted in blocking buffer) at room temperature. After 5 washes with TBST (3 times, 5 minutes), immunoreactive proteins were identified with the chemilumimescence (ECL) detection system. Photographic film, which determines light signals, was utilised and protein recognition was performed by comparing the

immunoreactive bands with those of the Rainbow® markers loaded during SDS-PAGE.

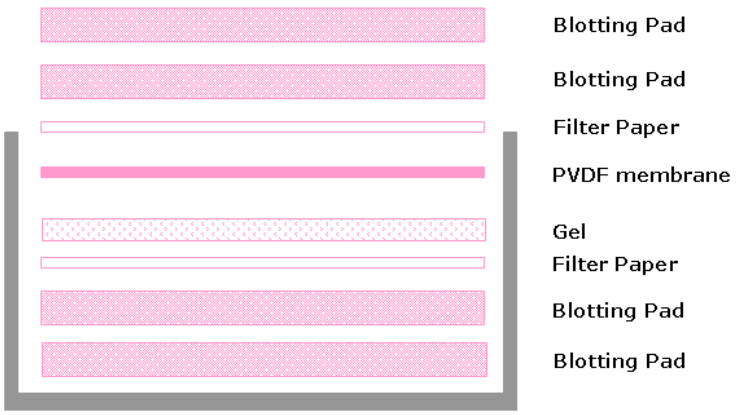

Figure 8. Diagrammatic representation of the polyacylamide gel/PVDF membrane blotting module assembles.

To facilitate protein transfer, the pre-soaked PVDF membrane is placed on top of the gel and a trans-blot sandwich is assembled between pre-wetted blotting pads and two layers of filter paper thoroughly soaked in transfer buffer. The gel/membrane assembly is placed in the module so that the gel is closest to the cathode plate. When an electric current is applied, transfer of proteins from the gel to the PVDF membrane takes place. This process is also known as immunoblotting.

2.14. Immunostaining

2.14.1. Immunocytochemistry

HTC were trypsinised, seeded into a 6-well tissue culture plate and fixed in ice cold methanol (1 minute, room temperature) once they reached ~70-80% confluency. After 3 washes with ice cold PBS (5 minutes each), blocking process was carried out using 5% (w/v) BSA in PBS (30 minutes at room temperature). Following blocking, the cells were treated with 2 ml primary antibody (diluted in 5% (w/v) BSA) overnight at 4°C. A FITC-conjugated secondary antibody was applied after 3 washes of PBS (5 minutes each). After incubation for 1 hour at room temperature (in a dark room), the cells were washed 3 times with PBS. For nuclear visualisation, 1µg/ml solution of DAPI (Sigma, UK) diluted in PBS was used and incubated for 10 minutes at room temperature. The cells were then washed with PBS (once, 5 minutes), covered with PBS and observed under a fluorescent microscope (Eclipse TE 2000-U, Nikon).

2.14.2. Immunohistochemistry

Immunohistochemistry is a different method from immunocytochemistry, which is used for detecting protein localisation in tissues. Tissues such as kidneys can be preserved by aldehyde fixation or rapidly frozen in liquid nitrogen. In the experiments described in this thesis, mouse kidneys were freshly removed and fixed in formalin overnight before being transferred into 70% (v/v) ethanol and stored at 4˚C. Embedding in paraffin wax was then carried out and slides of tissue sections (5μm) were prepared for immunostaining using antibodies against CRYM and MOSC2.

To start immunohistochemistry, the paraffin wax was first melted on a heated plate before being removed in xylene solution. The sections were then treated with a series of 100%, 95% and 70% (v/v) ethanol washes (5 minutes each) for rehydration. Once the excess ethanol had been removed (3 washes in PBS, 5 minutes each), the sections were treated with 3% hydrogen peroxide for 15 minutes at room temperature to stop peroxidase activity as well as undiluted swine serum for 10 minutes with 3 washes using PBS (5 minutes) in between (Table 9). The sections were then incubated with primary antibody diluted in PBS/0.25% (v/v) Triton X-100/0.25% BSA overnight at 4˚C. After removing residual primary antibody with 3 PBS washes, sections were exposed for 30 minutes to biotinylated link universal, a mixture of biotinylated anti-rabbit, anti-mouse and anti-goat immunoglobulins that recognise and bind to the primary antibody. Sections were then washed 3 times with PBS and for immunofluorescent staining; FITC-conjugated secondary antibodies were made up in PBS/0.25% (v/v) Triton X-100/0.25% BSA where the sections were incubated for 2 hours at 4˚C. Protein localisation was viewed under a fluorescent microscope (Eclipse TE 2000-U, Nikon) after glycerol mounting.

Table 9. Preparation of 10X phosphate buffered saline (PBS)

Reagent	Amount for 1L (10X)	Final Conc. of 1X PBS buffer
NaCl	80g	136mM
NaH_2PO_4	2g	1.7mM
Na_2PO_4	11.6g	8mM
KCl	2g	2.7mM

Reagents listed above were dissolved in ~900ml DI H_2O and the pH was adjusted to 7.2 before being made to a final volume of 1L with DI H_2O.

The 10X PBS buffer was diluted 10-fold with DI H_2O to make 1X working reagent.

2.15. Semi-quantitative analysis using ImageJ

ImageJ is a program that quantifies protein band intensity based on peak area. For analysing the protein expression, the densitometry of both target protein and reference protein was carried out using ImageJ (version 1.43: National Institutes of Health; www.rsb.info.nih.gov/ij). The amount of the target protein was expressed relative to the reference protein for each sample.

2.16. N-reductive assay

1) *In vivo*: 0.05mg homogenate proteins from kidneys and livers of mice were incubated in 100mM potassium-phosphate buffer pH 6.0 containing 3mM of the substrate benzamidoxime in a total volume of 150µl. After 3 minutes of pre-incubation, a reaction was started with the addition of 1mM NADH (cofactor) and stopped after 20 minutes for the liver and 50 minutes for the kidney by adding 150µl ice cold methanol. Samples were shaken at room temperature for 5 minutes, centrifuged at 11,000xg rpm for 5 minutes and supernatant injected to HPLC to identify and quantify each component.

2) *In vitro*: Human renal cells (HMCs, HEK293 and HTC) were seeded into a 6-well tissue culture plate. The media was then changed and cells were seeded in triplicate with normal glucose (5 mmol/L glucose), high glucose (25 mmol/L glucose) and normal glucose with mannitol (5 mmol/L+ 20 mmol/L mannitol) for four days. At day four of the experiment (reaching 100 % confluency), the medium was removed; cells were washed with 1ml incubation buffer (37°C; Table 10) and incubated with 1ml

pre-warmed incubation buffer at 37°C for 15 minutes. After removing the incubation buffer, 1ml pre-warmed substrate buffer was added to the cells and then incubated in at 37°C for 120 minutes. Next, the substrate buffer (6 mg benzamidoxime into 100 ml) was transferred to a universal tube and stored at -20°C for HPLC. The cells were scratched from and re-suspended into 1ml ice cold PBS. The samples were centrifuged for 3 minutes at 10,000xg, PBS was removed and the cells were then stored at -80°C for protein content determination.

Table 10. Preparation of incubation buffer

Reagent	Amount for 500ml	Final Conc.
HBSS buffer	50ml	1X
HEPES	1.19g	10 mM
$NaHCo_3$	175mg	4,2 mM

The reagents listed above were dissolved in DI H_2O to make up the final volume to 500ml; the PH was adjusted to 7.4 with concentrated KOH.

2.17. Statistical analysis

Data are expressed as mean ± standard deviations (SD). All statistical comparisons were made using SPSS 20 software and sigma plot 11. Descriptive statistics and multiple comparisons including Student's *t* tests, 1-way analysis of variance (ANOVA) and also post-hoc Tukey tests were performed. Differences between treatments were considered significant with p values <0.05 and highly significant with p values < 0.001.

Chapter 3

Is CRYM a glucose regulated gene in experimental models of diabetes *in vivo* and in human tubular cells *in vitro*?

Chapter 3. Is CRYM a glucose regulated gene in experimental models of diabetes *in vivo* and in human tubular cells *in vitro*?

3.1. Abstract

We previously found that the expression of CRYM, which is involved in the transport of intracellular thyroid hormone, is significantly up-regulated in response to high glucose *in vivo* and *in vitro.* The objective of this chapter was to investigate the expression of renal and cardiac CRYM in models of diabetes as well as in HTC to determine if its expression was altered in DN. Kidneys and hearts were obtained from (a) acute STZ-induced-diabetic, treated and control mice (n= 3) and (b) ß-*Phb2* KO mice. In addition, HTC grown in NG (5 mM), HG (25 mM) and NG with mannitol (5mM glucose + 20 mM mannitol) were used. The cellular location of CRYM protein was examined in sections of mouse kidneys and in cultured HTC using immunofluorescence.

Renal CRYM mRNA levels increased during hyperglycaemia in the STZ-induced diabetic mice and this increase was reverted by the treatment of diabetes ($P<0.001$). The hyperglycaemia-induced increase in renal CRYM was specific as we could not demonstrate any change in cardiac CRYM. We also could not demonstrate any change in renal and cardiac CRYM levels of KO mouse model ($P>0.05$). Immunohistochemistry revealed an abundant expression of CRYM protein in the cytosol of HTC, with less expression in HMCs. Surprisingly, CRYM mRNA levels showed a slight decrease in HTC under HG conditions.

In summary, we show for the first time that renal CRYM is regulated by glucose and its expression is increased in STZ-induced diabetic mice. CRYM protein is highly abundant in HTC and expressed at low levels in the glomerulus. Unlike earlier finding in HMCs, CRYM mRNA levels decreased in cultured HTC in response to HG. These data support the view that CRYM is regulated by glucose and suggest that it may be playing a specific role in HTC. Further studies will be required to determine the function of CRYM in DN.

3.2. Introduction

CDK108 was one of 25 clones isolated by differential screening. The sequence of rat CDK108 presented a strong hybridisation signal in the kidneys of progressively hyperglycaemic GK rat at 40 weeks compared to GK rat kidneys at 6 weeks (Malik et al., 1997). Northern blot analysis of RNA from GK rat kidneys at age 6, 16, 26 and 40 weeks old and aged-matched-Wistar control kidneys indicated a higher expression of CDK108 in the kidneys of the GK rat at 40 weeks (Zaidi, 1997). The DNA sequence of rat CDK108 showed that it represents μ-crystallin, an abundant protein normally found in the eye (Zaidi, 1997).

μ-crystallin has also been described as CRYM or NADP-regulated thyroid hormone binding protein (THBP) (Vie et al., 1997), and so for the purpose of this study we will refer to this gene as CRYM. The whole sequence of rat CRYM consists of 1227 bp with a polyA$^+$ tail of 17 bp, located 13 nucleotides downstream of putative polyadenylation signal (AATAAA), as well as a 31 bp 5′ untranslated region and 245 bp 3′ untranslated region (Ziadi, 1997). A putative coding region, which encodes a polypeptide of 314 amino acids, has a start codon (ATG) at position 32 and a putative stop codon (TGA) at position 790 bp in the second open reading frame (Zaidi, 1997). Previous studies showed that CRYM mRNA expression is altered in relation to progressive hyperglycaemia in the kidney of GK rat (Al-kafaji and Malik, 2010). This finding suggests a possible role for CRYM expression in early renal changes which contribute to DN. In order to further understand the possible role of CRYM in DN, we explored whether this gene was involved in the signalling pathways that lead to the damage in diabetic kidneys.

CRYM was first identified as μ-crystallin, a major lens structural protein in Australian marsupials and the whole sequence of μ-crystallin was obtained from a Kangaroo lens cDNA (Chen et al., 1992). RNA analysis in kangaroo tissues displayed that CRYM was most abundant in kangaroo's lenses (Kim et al., 1992) and was also expressed at much lower levels in neural tissues, retina and brain (Kim et al., 1992). Northern blot analysis of human tissues showed that the human homologue CRYM mRNA is abundant in the kidney, heart, brain, skeletal muscle and neural tissue whereas there is less CRYM mRNA in the liver and lung (Kim et al., 1992). Vie et al. (1997) also detected a full-length human CRYM cDNA from a brain cDNA library and showed

that it was identical to nicodinamide-adenine dinucleotide phosphate (NADPH)-regulated thyroid hormone binding protein (THBP) (Vie et al., 1997). The deduced 314-amino acid protein had a predicted molecular mass of approximately 34 kDa. High expression of human CRYM was shown in cochlear vestibular tissues in the inner ear (Abe et al., 2003). Lower but significant concentrations of CRYM mRNA have been observed in various non-lens tissues in marsupials and humans (Wistow and Kim, 1991).

Among the mouse tissues, CRYM mRNA is most abundant in the skin, whereas lower levels are detectable in the brain, eye, heart, kidney, liver and lung (Aoki et al., 2000). In the rat, mRNA expression of CRYM has been detected in a number of tissues such as kidney (Vie et al., 1997) and brain (Beslin et al., 1995). Also, CRYM mRNA expression has been observed in the spleen, stomach and urinary bladder (Vie et al., 1997).

The CRYM gene is located at chromosome 16 P13.11-P12.3 in the human genome (Chen et al., 1992). More specifically, Yokoyama et al. (1992) demonstrated that the CRYM gene is localised on the short arm in the region 16p13.11-p12.3.

● ***Involvement of CRYM in various diseases***

Hearing is one of the most important functions controlled by the thyroid hormone and CRYM is recognised as a candidate for hearing loss that is not related to other signs and symptoms (Abe et al., 2000). Abe et al. (2003) proposed that CRYM might be one of the genes responsible for non-syndromic deafness and demonstrated that mutant CRYM protein may affect clinical hearing ability. They suggest that T_3-binding properties affect the fibrocytes of the cochlea. Therefore, mutant CRYM could abrogate the affinity of the thyroid hormone, a pivotal factor for the development of the auditory system, and might be involved in the potassium ions recycling system (Abe et al., 2003).

Following the development of microarray techniques, numerous studies established specific regulation of CRYM expression. Malinowska et al. (2009) identified CRYM as one of the androgen-regulated genes and they reported elevated expression of CRYM in cancer tissue. They also demonstrated CRYM as a downregulated gene during tumour progression in prostate carcinoma (Malinowska et al., 2009). The expression of CRYM was significantly elevated in non-small cell lung carcinoma

(Chong et al., 2006), whereas the expression level was low in brain tumours (Khalil, 2007). Although the putative role of CRYM in prostate cancer is unknown, it has been determined that changes in CRYM mRNA levels are induced following anticancer drug suppression of prostate cancer cells *in vitro* (Mousses et al., 2002). Furthermore, screening of a breast cancer cDNA library from SKBR3 human breast cancer cells demonstrated that 13 genes, one of which was CRYM, were identified mainly by the breast cancer patient sera (Forti et al., 2002).

A recent article showed high CRYM RNA and protein expression levels in the muscle of patients with facioscapulohumeral muscular dystrophy (FSHD) (Klooster et al., 2009; Reed et al., 2007). FSHD is a genetic disease of muscular dystrophy that is thought to be caused by the deletion of the megasatellite repeat on chromosome 4q35 (Wijmenga et al., 1990). The disorder is linked to nonskeletal muscle manifestation including retinal and inner ear defects (Reed et al., 2007). High expression of CRYM may play a role in the pathogenesis of FSHD and it may also affect both hearing function and retinal development (Reed et al., 2007).

- ***CRYM* as a μ-crystallin**

μ-Crystallins are water-soluble structural proteins of a heterogeneous family which were discovered in the cells of a vertebrate lens. The family contains the major groups such alpha (α), beta (β), gamma (γ), delta (λ), mu (μ) and numerous minor groups. These groups are classified according to their charge, size, vertebrate source and immunological properties. Crystallins are different from each other; some are abundant only in certain groups of associated species, whereas the remainder are common to most vertebrates (Lee et al., 1993). CRYM is one of the μ-Crystallin proteins and is a major structural protein of the lens (Chen et al., 1992). The μ-Crystallin mRNA is most abundant in kangaroo lenses but is not abundant in human lenses (Vie et al., 1997). Hence, the non-lens expression of CRYM in humans and mice formulated the idea that the protein has a non-structural, probably enzymatic role in the retina and other tissues (Chen et al., 1992, Segovia et al., 1997). The complete predicted amino acid sequence of CRYM was similar to the ornithine cyclodeaminase (OCD) sequences (Kim et al., 1992; Witsow and Kim, 1991). The ornitine cyclodeaminase (OCD) is a bacterial enzyme which is encoded by tumour-inducing Ti plasmids of *Agrobacterium tumefaciens*. This enzyme converts ornithine to proline and it requires NAD^+ as a cofactor (Kim et al., 1992).

The superfamily relationship between CRYM and OCD suggests the possibility that mammalian CRYM has a non-structural, possibly enzymatic role (Kim et al., 1992). It has been reported that the (iodo) thyronine binding site of CRYM could be associated with the amino acid (ornithine, arginine, and lysine) binding sites of the cyclodeaminase enzymes (Segovia et al., 1997; Vie et al., 1997). The pyridine nucleotide binding site of CRYM could also be linked to that of OCD (Kim et al., 1992) since enzyme activity is stimulated by NAD^+ which acts as a catalyst, rather than a co-substrate. This suggests that the mammalian CRYM originated from an ancient family (Vie et al., 1997).

● ***Human homologue of CRYM encodes NADP-regulated-thyroid hormone binding protein***

CRYM is also known as a cytosolic thyroid hormone binding protein which is regulated by nicotinamide adenine dinuclotide phosphate (NADP) (Vie et al., 1997). The cloned cDNA sequence and peptide sequencing data showed that THBP is the same as human CRYM (Kim et al., 1992). A number of thyroid hormone-responsive tissues such as the kidney were known to contain a NADP-regulated-THBP responsible for most of the intracellular high-affinity thyroxine (T_4) and triiodothyronine (T_3) binding (Parker, 1993). The pivotal action of thyroid hormone occurs via the binding of T_3 to its nuclear receptors in the target tissues. These receptors are part of a superfamily of ligand-dependent transcription factors that contain the receptors for steroid hormones, retinoids and vitamin D (Guiochon-Mantel and Milgrom, 1993; Lazar, 1993). Many studies demonstrated that the binding of T_3 to cytosolic proteins in different types of cells and tissues are regulated. This indicates that these proteins could play a role in the control of intracellular T_3 homeostasis (Donovan et al., 1995).

Hashizume (1989) reported for the first time that T_3 binding was activated by NADPH and $NADP^+$ in rat kidney cytosol. Analysis of cytosolic T_3-binding from rat (Beslin et al., 1995) and human kidneys (Vie et al., 1997) demonstrated that binding is activated in the presence of NADPH, whereas $NADP^+$ inhibits the activation by NADPH (Hashizume et al., 1989; Vie et al., 1997). Accordingly, there is a similarity between cytosolic binding sites for T_3 and T_4 with thyroid hormone nuclear receptors (TRs) and also, the binding activity of THBPs is 100 times greater than TRs (Vie et

al., 1997). For this reason, they are responsible for most of the high affinity T_3 and T_4 binding in rat astrocytes and human kidney tissue (Vie et al., 1997). Binding of T_3 to cytosolic CRYM indicates that CRYM is involved in the regulation of intracellular T_3 homeostasis (Vie et al., 1997).

The relationship between the function of human THBP and the major lens protein in kangaroos is not clear. In fact, most of the crystallins which are expressed in lenses do not just act as structural proteins and their synthesis is not limited to the lens (Wistow and Piatigorsky, 1988). For instance, several multifunctional species-specific crystallins are NAD(P)H-binding proteins, which defend against oxidation in the lens and/ or help to filter UV radiation (Wistow, 1993). Notably, THBP has a high affinity for NADPH, which is known to regulate cellular redox (Beslin et al, 1995; Vie et al, 1996).

The crystal structure of human CRYM suggests it might have redundant functions as it binds not only to T_3, but also to NADPH (Cheng et al., 2007; Hashizume et al., 1989). However, the physiological importance of this coupling is still not clear. Since NADPH inhibits T_3 binding, oxidative stress might be another agent for control of T_3 binding to CRYM in cytoplasm (Kobayashi et al., 1991). According to these findings, it has been established that CRYM plays an essential physiological role in regulated thyroid-hormone-associated gene expression and transporting and reserving T_3 in the nuclei *in vitro*, and also has a clinical effect on hearing ability. However, the main role of CRYM remains to be elucidated *in vivo* (Suzuki et al., 2007).

● ***CRYM as a candidate gene for DN***

Previous studies by Al-Kafaji (2010) showed that CRYM is a glucose-regulated gene in DN and it was the first report on the regulation of CRYM in hyperglycaemia (Al-Kafaji and Malik, 2010). These studies displayed that CRYM mRNA is abundantly expressed in the GK rat and it is significantly increased by diabetes in the kidney and heart among other tissues. For instance, CRYM mRNA is highly expressed in the kidneys (326±50 vs 147±54, $p<0.05$) and hearts (326±277 vs 191±63, $p<0.05$) of GK rats compared to non-diabetic controls. These results suggested that rat CRYM mRNA is elevated in diabetic kidneys and supported a link between hyperglycaemia with rat CRYM mRNA expression (Figure 9a). Also, these studies demonstrated that CRYM can be directly regulated by glucose *in vitro* (Al-Kafaji and Malik, 2010).

To investigate the direct effect of glucose on CRYM, they analysed CRYM mRNA expression in cultured HMCs and a human mesangial cell line (HMCL) (Al-Kafaji and Malik, 2010). CRYM mRNA levels were increased in HMCs and were directly regulated by glucose (Figure 9b). For example, CRYM mRNA was significantly increased in HMCs ($P<0.005$) (Al-Kafaji and Malik, 2010). The glucose regulation of CRYM and elevated mRNA/ protein expression in HMCs suggested an important role for CRYM in hyperglycaemia-induced molecular pathways that lead to DN (Al-Kafaji and Malik, 2010).

ROS have been identified as signalling molecules in HMCs grown under HG (Hancock et al., 2001) and therefore studying ROS in HG condition is important. Al-Kafaji and Malik (2010) examined whether the increase in CRYM in HG was occurring in parallel with increased intracellular ROS. They found that ROS levels significantly increased in cells grown in HG and data demonstrated that CRYM mRNA levels were enhanced together with increased intracellular ROS in HMCLs grown in HG. This was the first report to show elevated CRYM mRNA levels in renal cells exposed to HG in association with increased intracellular ROS (Al-Kafaji and Malik, 2010).

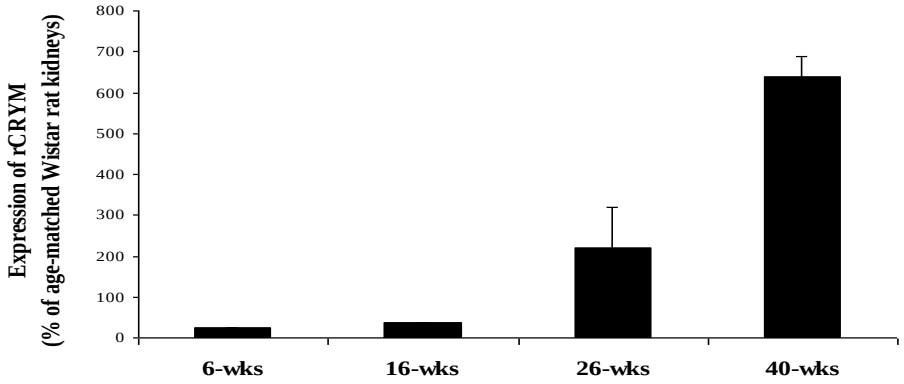

Figure 9a. Elevated rat CRYM mRNA expression in a diabetic kidney.

This data taken from Al-Kafaji (2008) shows that CRYM mRNA expression was elevated in 40 week old kidneys of progressively hyperglycaemic GK rats.

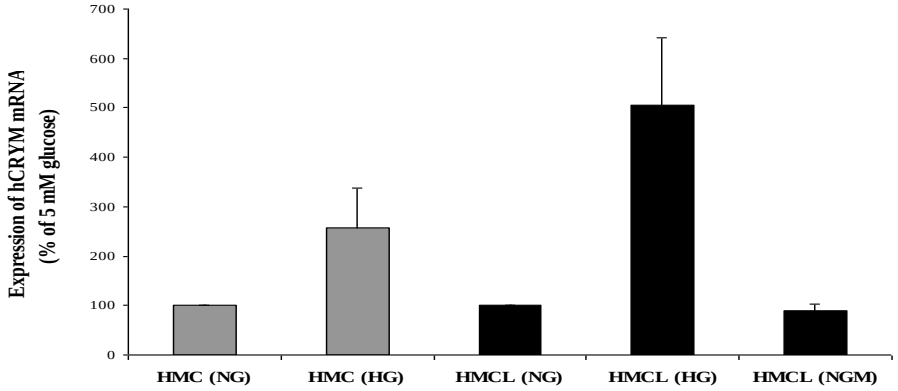

Figure 9b. The effect of high glucose on the expression of human CRYM mRNA in primary cultures of mesangial cells (HMCs) and in the human mesangial cell line (HMCL).

This data taken from Al-Kafaji (2008) shows that CRYM mRNA expression was increased in primary cultures of mesangial cells and in the human mesangial cell line.

The simultaneous increase in CRYM expression and in intracellular ROS suggests that CRYM may be involved in ROS induced pathways in the cell (Al-Kafaji and Malik, 2010). To examine the effect of CRYM on intracellular ROS, CRYM was over-expressed as a fusion protein in HMCs. The expression of CRYM as a fusion protein in transfected HMCs resulted in a decrease of glucose-induced intracellular ROS (Al-Kafaji and Malik, 2010). These observations suggested that CRYM levels might be increased to counteract oxidative stress caused by increased production of ROS resulting from hyperglycaemia (Al-Kafaji and Malik, 2010). Hence, ROS and oxidative stress play an important role in DN. CRYM expression is linked to increased intracellular ROS in response to glucose. The elevation of CRYM is accompanied by reduced glucose-induced ROS (Al-Kafaji and Malik, 2010). These results lead us to the hypothesis that CRYM may be acting as an antioxidant involved in reduction of intracellular ROS and to follow up on previous studies and further investigate CRYM mRNA/ protein expression in mouse and mammalian cells.

Aims and Objectives

1) To investigate whether CRYM is a glucose regulated gene in a mouse model of diabetes and is abnormally expressed in hyperglycaemia, we will use *in vivo* models of diabetes. Kidney and heart tissues from two experimental models (ß-*Phb2* KO and C57/BL6 mice) will be used. CRYM mRNA levels will be quantified using real-time qPCR; protein expression and localisation will be determined using immunofluorescence.

2) To further investigate glucose regulation of CRYM, we will use *in vitro* models of DN namely HTC. HTC will be grown in NG, HG and NGM (n=3) for 3 days and CRYM mRNA expression will be determined using qPCR. Protein expression will be examined using immunofluorescence under the same experimental conditions.

3.3. Results

3.3.1. Experimental models of diabetes used in this study

The *in vivo* diabetic mouse models and the *in vitro* renal cell model used in this study are shown in Table 11a. These were: a) ß-*Phb2* KO mouse, b) STZ- induced mouse and c) HTC.

a) ß-*Phb2* KO mouse: The diabetic and control kidneys and hearts from male and female mice (University of Geneva Medical Centre, Switzerland) used in this study were bred by crossing flox-*Phb2*-flox mice with rat-insulin promoter driven Cre mice so that *Phb*2 is specifically deleted in pancreatic beta cells (Section 2.4). ß-*Phb2* KO mice become diabetic at the age of 5-6 weeks and they were markedly diabetic at a later age i.e. 11 weeks when they have extensive polyurea (Table 11a). Kidney and heart tissues were collected at 11 weeks; by this time KOs had glycaemia ranging between 30-40mM. Indeed, ablation of *ph2* in mouse ß-cell sequentially resulted in impairment of insulin secretion, a loss of ß cells and severe diabetes (Supale et al., 2013). These mice represent a spontaneous model of diabetes development through a series of molecular events which do not require the administration of toxic diets or chemicals.

b) STZ-induced mouse: Eight week old C57Bl/6 mice were rendered diabetic by using STZ; the mice were then treated by islet transplantation (Section 2.4.). Tissues from this mouse model were provided by Dr Aileen King, King's College London. The untreated diabetic mice had blood glucose levels of >20 mmol/L and the treated mice had blood glucose levels of <11.1 mmol/L for a period of 4 weeks. In addition, non-diabetic, non-transplanted mice were used as controls (blood glucose <11.1 mmol/L). The right kidneys and the hearts were used to determine CRYM mRNA levels (Table 11a).

Table 11a: Mouse models of diabetes used in this study

Name	Group	N	Age	Gender	Blood Glucose levels mmol/L
ß-*Phb2* KO	KO	6	11 weeks	M/F	30-40
ß-*Phb2* KO	Control	4	11 weeks	M/F	<11.1
STZ	Control	3	8 weeks	M	<11.1
STZ	Diabetic	3	8 weeks	M	>20
STZ	Treated	3	8 weeks	M	<11.1

Kidneys and hearts were taken from control (n= 4) and KO (n= 6) of a ß-*Phb2* KO mouse model at 11 weeks and from an acute STZ-induced mouse model in which we obtained control (n= 3), diabetic (n= 3) and cured (n= 3) samples at 8 weeks.

C) Human renal tubular cells (HTC): HTCs (ATCC®, UK) were cultured in NG, HG and NGM for 3 days of experiments as described previously (Section 2.3). NGM was included to rule out the osmolarity effect. Samples were then stored in -80°C and used for mRNA and protein studies (Table 11b).

Table 11b. *In vitro* renal cells models used in this study

Name	Condition	N	Glucose mmol/L
HTC	NG	3	5
HTC	HG	3	25
HTC	NGM	3	5 mM glucose+20mM mannitol

Human renal tubular cells grown in normal glucose (NG, 5mM), high glucose (HG, 25mM) and normal glucose with mannitol (NGM, 5 mmol/L+ 20 mmol/L mannitol) for 3 days.

3.3.2. Gene expression assay for mouse and human CRYM

The aim of this part of the work was to set up a quantification assay for mouse and human CRYM to detect the mRNA levels of CRYM *in vivo* and *in vitro*.

1) Primer design and amplification of mouse and human CRYM

Oligonucleotide primers designed for both mouse and human CRYM based on the mRNA sequence of the gene (Accession number NM_016669 and L02950) were used to quantify the 61 bp and 62 bp fragments of mouse and human CRYM cDNAs respectively (Table 12a). The primers were designed using Roche Applied Science software and synthesised at Sigma-Aldrich (Figure 10a and 10b). The protein sequences of both mouse and human CRYM are shown in appendix 2.

Table 12a. Oligonucleotide primers used in PCR and RT-PCR

Gene name	Accession number	Product size	Sequence
mCRYM F_1: Forward primer	NM_016669	61 bp	ggg gct caa tca atg ct
mCRYM R_1: Reverse primer			gct cgt cat cca gtt ctc g
hCRYM F_1: Forward primer	L02950	62 bp	gcc ctg aag gag tct gag g
hCRYM R_1: Reverse primer			tct ccc agc tca gca aag at

The sequences shown in Table12a are 5' to 3' with F primers representing the sense strand and R primers representing the anti-sense strand of the CRYM F1 and CRYM R1 primers.

```
   1 atttagggct cagctcctgg aacgtggagt gtgtttcagc ccgggttcga aggcaggcgg
  61 cgagatgaag cgggcgccag cgttcctgag cgcagaggag gtgcaggatc accttcgcag
 121 ctccagcctt ctcatcccac ccctggaggc cgcactggcc aacttctcca aaggtcccga
 181 cggaggggtc atgcagccag tgcgcaccgt ggtgcctgta gccaagcacc gaggcttcct
 241 gggagtcatg cctgcctaca gtgctgctga ggatgcgctc accaccaagt tagtcacctt
 301 ctatgagggc cacagcaaca cagcggtccc ctcccatcag gcatcggtgc ttctctttga
 361 tcccagcaat ggctccctgc tggcggtcat ggatggaaat gtcataactg caaagagaac
 421 agcagcggtg tctgccattg ccacaaagct gttgaagccc ccaggcagtg atgtgctgtg
 481 catccttgga gcgggggtcc aggcgtacag tcactatgag atcttcacag agcagttctc
 541 cttcaaggag gtgagaatgt ggaaccgcac cagggaaaat gctgagaagt ttgcaagcac
 601 agtgcaagga gatgttcggg tctgttcatc agtgcaggag gctgtgacag gtgctgatgt
 661 catcatcaca gtcaccatgg caacagagcc cattttattt ggtgaatggg taaagccggg
 721 ggctcacatc aatgctgttg gagccagcag gcctgactgg cgagaactgg atgacgagct
 781 catgaggcaa gcggtgctgt atgtggactc ccgggaggct gccctgaagg agtcaggaga
 841 cgttctgttg tcaggggctg acatctttgc tgagcttgga gaagtgattt caggagcgaa
 901 gcctgcacac tgtgagaaga ccacagtgtt caaatctttg gggatggcag tggaagacct
 961 ggttgcagcc aaattagtat atgattcttg gtcatctggc aagtgagttg aaggaaccgt
1021 gcctgagttg gccatcacag ctcaacactg tttcacaagt gtcaaaatca aaggaggtcc
1081 agtccccagt gaatggtagt gattgtcatt cataagtact gacaccccta ttcatgtttg
1141 tggttggata gctaaaccag gtaaccattt cttctgttaa ggggtgatgg ccacattatc
1201 taccccttgat cttactagtc ttgtatctct ctgaaataaa tcatttccac ttcttc
```

Figure 10a. Nucleotide sequence of mouse CRYM mRNA, accession number NM-016669.

The forward primer (CRYM F_1) is represented in blue and reverse primer (CRYM R_1) in green. The putative initiation codon is at position 65 and is in red. The stop codon is also shown in red.

```
   1 agactgaggt tagaaggcac aggtggcgag atgagccggg taccagcgtt cctgagcgcg
  61 gccgaggtgg aggaacacct ccgcagctcc agcctcctca tcccgcctct agagacggcc
 121 ctggccaact tctccagcgg tcccgaagga ggggtcatgc agcccgtgcg caccgtggtg
 181 ccggtgacca agcacagggg ctacctgggg gtcatgcccg cctacagtgc tgcagaggat
 241 gcactgacca ccaagttggt caccttctac gaggaccgcg gcatcacctc ggtcgtccct
 301 tcccaccagg ctactgtgct actctttgag cccagcaatg gcaccctgct ggcggtcatg
 361 gatggaaatg tcataactgc aaagagaaca gctgcagttt ctgccattgc caccaagttt
 421 ctgaaacctc ccagcagtga agtgctgtgc atccttgggg ctggggtcca ggcctacagc
 481 cattatgaga tcttcacaga gcagttctcc tttaaggagg tgaggatatg gaaccgcacc
 541 aaagaaaatg cagagaagtt tgcagacaca gtgcaaggag aggtacgggt ctgttcttcg
 601 gtccaggagg ctgtggcagg tgcagatgtg atcatcacag tcaccctggc aacagagccc
 661 attttgtttg gtgaatgggt gaagccaggg gctcacatca atgctgttgg agccagcaga
 721 cctgactgga gagaactgga tgatgagctc atgaaagaag ctgtgctgta cgtggattcc
 781 caggaggctgccctgaagga gtctggagat gtcctgctgt caggggccga gatctttgct
 841 gagctgggag aagtgattaa gggagtgaaa ccagcccact gtgagaagac cacggtgttc
 901 aagtctttgg gaatggcagt ggaagacaca gttgcagcca aactcatcta tgattcctgg
 961 tcatctggta aataaaacaa aggaacttga tgttgagatg gatgcttgag gaatattgct
1021 gctggttctc ataatttcta gagtaaatga gggagtccag tccccagtga actctccttt
1081 tgtgcttatc atgttttacc ttaaatgctg agatcctcat ttatgtttgt agttggaaag
1141 caaagctagg tagccatttc ttctgttcta ccaagttata atagcattca tttcccttta
1201 tatttccctg aaataaagca cattccaatt gtgcagtg
```

Figure 10b. Nucleotide sequence of human CRYM mRNA, accession number L02950. The forward primer (CRYM F_1) is represented in blue and reverse primer (CRYM R_1) in green.The putative initiation codon is at position 31 and in red. The stop codon also is shown in red.

Figure 10a and 10b show the position of the primers. Primers for mouse CRYM F_1 and CRYM R_1 were used to amplify a fragment of mouse kidney cDNA (Figure 10c) and human CRYM F_1 and CRYM R_1 primers were used to to determine the CRYM mRNA transcript in HTC (Figure 10b). PCR was carried to confirm the product sizes of mouse and human CRYM genes using an annealing temperature of 60°C and 3 mM concentration of $MgCl_2$ (Figure 10c).

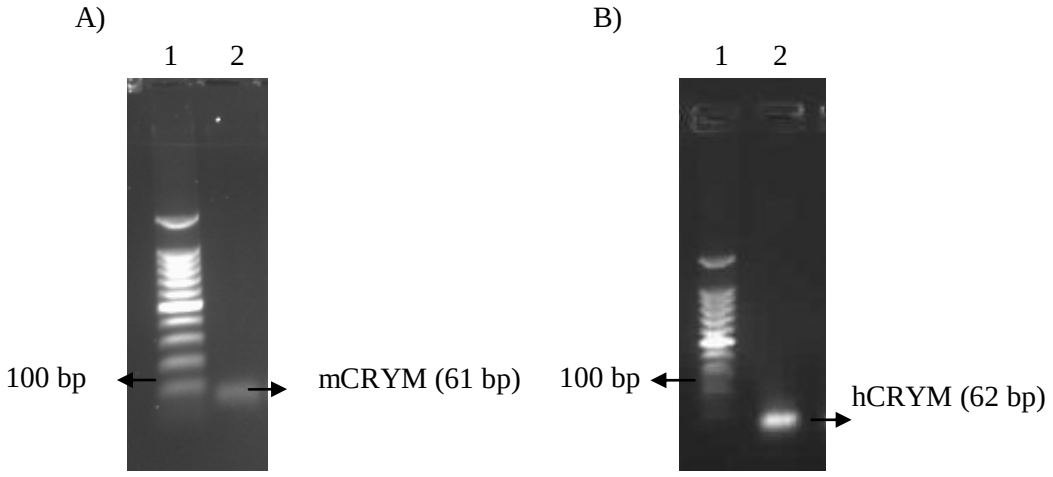

Figure 10c. Purification of mouse and human CRYM.

A): mCRYM, B): hCRYM. Approximately 30 µl of each PCR product was loaded on an agarose gel (1%, 1X TBE) and the DNA of each PCR product was excised from the gel band and purified. 10 µl of purified products was then gel electrophoresed along with a 100bp DNA ladder.

2) RNA isolation and cDNA synthesis from mouse tissues and human renal tubular cells

To determine the regulation of mouse and human CRYM mRNA expression *in vivo* and *in vitro* models total RNA was isolated from the kidneys and hearts of ß-*Phb2* KO and STZ mice and from HTC in each condition (Section 2.6.1). RNA concentration was determined by measuring the absorbance of RNA at A_{260} using nanodrop (Table 12b). For each condition, cDNAs were synthesised (Section 2.6.4.) and CRYM primers were used to detect CRYM mRNA expression in the kidney and hearts of mouse models *in vivo* and also in HTC *in vitro*. qPCR was carried out to measure copy numbers of mouse and human CRYM mRNA relative to the reference gene.

Table 12b. Concentration of RNA isolated from samples

Models	Samples	Condition	RNA Concentration (ng/µl)	Samples	Condition	RNA Concentration (ng/µl)
ß-*Phb*2 KO	Kidney1	Control	529.5	Heart1	Control	252.9
	Kidney2	Control	473.5	Heart2	Control	238.8
	Kidney3	Control	1283	Heart3	Control	135.2
	Kidney4	Control	566.2	Heart4	Control	106.4
	Kidney5	KO	750.6	Heart5	KO	280.2
	Kidney6	KO	658.6	Heart6	KO	298.1
	Kidney7	KO	638.9	Heart7	KO	169.8
	Kidney8	KO	405.3	Heart8	KO	295.4
	Kidney9	KO	1243.6	Heart9	KO	1211.6
	Kidney10	KO	311.8	Heart10	KO	2589
STZ	Kidney1	Control	16	Heart1	Control	177.9
	Kidney2	Control	37	Heart2	Control	160
	Kidney3	Control	75	Heart3	Control	130.7
	Kidney4	Diabetic	152	Heart4	Diabetic	94.6
	Kidney5	Diabetic	185	Heart5	Diabetic	20.84
	Kidney6	Diabetic	184.5	Heart6	Diabetic	68.9
	Kidney7	Treated	144	Heart7	Treated	99.9
	Kisney8	Treated	26	Heart8	Treated	126
	Kidney9	Treated	73	Heart9	Treated	102
HTC	HTC1	NG	1.30			
	HTC2	NG	1.12			
	HTC3	NG	1.19			
	HTC4	HG	1.65			
	HTC5	HG	1.22			
	HTC6	HG	1.98			
	HTC7	NGM	1.99			
	HTC8	NGM	1.22			
	HTC9	NGM	2.01			

RNA was extracted from kidneys and hearts of ß-*Phb*2 KO and STZ-induced mice *in vivo* and human tubular cells *in vitro*. Concentration of RNA in each condition was detected by measuring the absorbance at A_{260} using nanodrop.

3) Identification of most stable control gene for quantitative gene expression measurements *in vivo* and *in vitro*

a) *In vivo*: To evaluate the most stable and reliable reference gene *in vivo*, endogenous gene expression stability was measured using geNorm and NormFinder Programs (Vandesompele et al., 2002). Both geNorm and NormFinder are popular algorithms for identifying the optimal normalisation gene for a set of candidate reference genes by ranking them for normalisation according to their expression stability (Vandesompele et al., 2002; Andersen et al., 2004). In this experiment, we used the prepared cDNA samples from 6 samples of control, diabetic and treated C57/BL6 mice for kidney tissues. Then, we assessed mRNA expression of six different candidate reference genes for each sample: beta actin (β-actin), TATA-box

binding protein (TBP), 28S ribomosal RNA (Rn28s1), phosphoglycerate kinase (PGK), peptidylprolyl isomerise B (PPIB), and glyceraldehyde-3-phosphate dehydrogenase (GAPDH). A list of primers used in this part is shown in Section 2.7 (Table 5b).

All candidate reference genes were quantified and the normalisation factor (NF) was calculated based on the mean expression value of the best endogenous controls. Both software programs pick the most stable genes in terms of improved reduction of technical variation and more accurate appreciation of biological changes (Vandesompele et al., 2002; Andersen et al., 2004). The findings showed that all candidate reference genes in this experimental study are stable and they are similar to each other. geNorm identified mouse β-actin (M= 0.072) as the gene with least stability, as they have the highest M-value and more variation compared to other genes. GAPDH (M= 0.047) is the most stable gene in mouse kidney tissues (Appendix 3). Normfinder also identified mouse GAPDH (M = 0.01) as the most stable gene with the least overall variation and mouse β-actin was determined to be the least stable expressed gene (M= 0.042). Both geNorm and Normfinder determined GAPDH as the most stably expressed gene and we therefore used mouse GAPDH for our *in vivo* experiments to normalise the quantification of mouse CRYM most accurately.

b) *In vitro*: Gene expression was quantified by normalisation to 3 different endogenous reference genes: β-actin, PGK and PPIB (Section 2.7, Table 5a). In this experimental study, HTC (n= 4) and HMCs (n= 4), cultured in NG and HG respectively, were quantified relative to reference genes using real-time qPCR. geNorm and NormFinder software were used to normalise these expression patterns, independent of mRNA expression levels. Both programs picked two genes with the lowest M-value which were most stable, as well as the gene with the highest M-value which was the least stable reference gene. For both HTC and HMCs samples, PGK (M= 0.779) was selected as the most stable gene and PPIB (M= 1.049) was calculated to be the least stable gene. Thus, we used PGK as the most stable gene for our *in vivo* experiments.

4) Purification and generation of standard curves

To accurately measure the copy numbers of mouse CRYM and human CRYM *in vivo* and *in vitro*, standards were prepared from purified PCR products to use with qPCR. (section 2.8). The amount of amplicon in each purified PCR product was measured using nanodrop and the number of copies was calculated based on the molecular weight of each individual gene. The amount of DNA was calculated for each gene in 10 µl PCR products as presented in Table 12c.

Table 12c. Concentration and amount of DNA in the purified PCR products Using Nanodrop

Gene	Length of PCR product(bp)	Concentration of DNA	Amount of DNA (g/µl)	Cpoies of gene per µl (g/µl)
mCRYM	61	22.1	22.1×10^{-9}	$0.5x10^{11}$
mGAPDH	125	35	35×10^{-9}	$3.3x10^{11}$
hCRYM	62	10.6	10.6×10^{-9}	0.5×10^{11}
hPGK	121	14.5	14.5×10^{-9}	1.09×10^{11}

For each gene, a standard curve was created using a range of eight dilutions (10^9 to 10^2 copies per µl) of the PCR product containing the target cDNA. The first tube for CRYM contained 0.15×10^{-9} copies of the gene, and was applied in 10-fold serial dilutions by adding 10 µl of 0.15×10^{-9} to 85 µl of DEPC-treated water and 5 µl of tRNA (10 µg/ml; Sigma, UK). This process was repeated to make up $0.15x10^2$ concentrations. Amplification of the 10-fold dilution series was performed in qPCR by using the LightCycler 480 and QuantiFast DNA Master SYBR Green kit (QIAGEN, UK). The successful generation of standards for both target genes and reference genes are shown in Appendices 4 and 5.

5) Quantification of renal and cardiac CRYM copy numbers in ßeta-Prohibitin 2 knockout and streptozotocin-induced diabetic mice *in vivo*

To measure copy numbers of CRYM mRNA in control and diabetic kidneys and hearts of both a ß-*Phb2* KO mouse and an acute STZ-induced mouse, previously described in section 3.3.1., total RNA was extracted from each sample (Table 12b). From this, cDNA was synthesised and CRYM mRNA copy numbers relative to the reference gene (GAPDH) were determined.

The quantification of each sample was achieved by comparing the fluorescence of a PCR product of unknown concentration with the fluorescence of several dilutions of both mouse and human CRYM external standards (measuring Ct for each reaction and using the standard curve to determine starting copy number). Fluorescence values were calculated in the log-linear phase of amplification to produce a fluorescence curve which increases with each cycle as the product accumulates. To examine specificity, melting-curve analysis was performed. The result shows a fluorescence curve profile that was obtained during a slow denaturation of PCR products. Melting peaks have been generated by differentiation of melting curves, and defining the melting temperature of amplified product. Samples were normalised with respect to mRNA expression of the reference gene (GAPDH). The concentration of the nucleic acids used as standards for target genes and reference genes were known and prepared for absolute quantification. All qPCR experiments were performed in triplicate; cDNAs were used for each experimental condition. Statistical analysis of the data using student's *t* test provided the mean, standard deviation and the *p* values.

- ***Renal and cardiac mRNA levels of CRYM in the ßeta-Prohibitin2 knockout mouse***

Renal and cardiac CRYM copy numbers relative to mouse GAPDH mRNA copy numbers were detected using qPCR in ß-*Phb2* KO mice as shown in Table 13a. The results showed that there was no difference in diabetic renal CRYM mRNA levels compared to their control (0.0133 ± 0.00516 vs. 0.0200 ± 0.0200, P>0.05; Table 13b). We could not also demonstrate any change in cardiac CRYM mRNA levels in presence of hyperglycaemia. Statistical analysis of the data using student's *t* test showed a non-significant difference in diabetic hearts compared to control hearts (0.0060 ± 0.0054 vs. 0.00 ± 0.00, P>0.05; Table 13b).

Table 13a. Relative CRYM and GAPDH mRNA expression values of ß-*Phb*2 KO kidney and heart tissues

Tissues	Condition	CRYM	CRYM	CRYM	GAPDH	GAPDH	GAPDH	CRYM ratio
Kidney	Control1	1720	1350	2660	70700	528000	110000	0.01
	Control2	1310	754	646	72100	53100	71200	0.01
	Control3	1130	1100	1280	92700	103000	93800	0.01
	Control4	616	681	4660	39900	42100	44600	0.05
	KO1	618	606	535	56900	55000	66400	0.01
	KO2	578	596	521	71100	84300	76000	0.01
	KO3	779	1090	949	105000	36900	40500	0.02
	KO4	388	528	508	60500	64600	60200	0.01
	KO5	1070	837	796	51900	54000	465100	0.02
	KO6	621	697	516	53400	54500	60300	0.01
Heart	Control1	375	352	359	207000	236000	174000	0.00
	Control2	313	334	291	83800	115000	135000	0.00
	Control3	536	332	327	66300	102000	97500	0.00
	Control4	310	332	694	154000	77200	36300	0.00
	KO1	340	305	340	35000	67400	66100	0.01
	KO2	345	301	347	30300	120000	112000	0.00
	KO3	335	379	327	95000	61900	66800	0.00
	KO4	419	390	430	80200	97100	69800	0.01
	KO5	380	342	394	24600	32800	25700	0.01

CRYM mRNA copy numbers relative to GAPDH copy numbers were determined using qPCR in control and diabetic mouse kidneys and hearts of a ß-*Phb*2 KO mouse. For each condition, samples were used to prepare cDNA. Renal and cardiac CRYM mRNA levels were quantified from each sample in triplicate. Data are shown as relative expression values.

Table 13b. Relative copy numbers of CRYM mRNA in ß-*Phb*2 KO mice kidneys and hearts tissues

Tissue	Condition	N	Mean values ± SD of mouse CRYM copy numbers
Kidney	Control	4	0.0200 ± 0.0200
	KO	6	0.0133 ± 0.00516
Heart	Control	4	0.00 ± 0.00
	KO	5	0.0060 ± 0.0054

CRYM mRNA copy numbers relative to GAPDH copy numbers were detected in kidneys and hearts of ß-*Phb*2 KO mice. Values are shown as mean ± SD. P>0.05

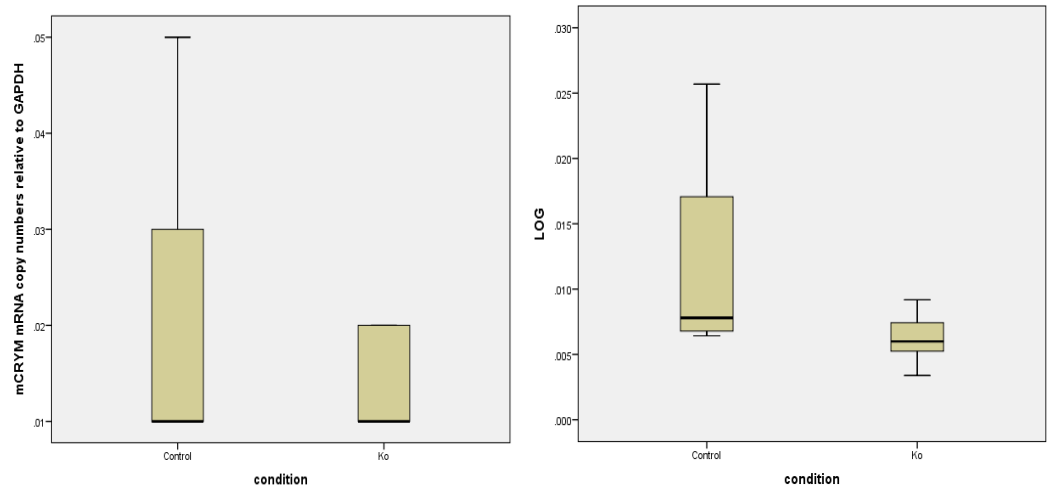

Figure 11a. Effect of high glucose on renal CRYM mRNA levels of ß-*phb2* KO mice.

Kidneys from diabetic (n= 6) and control (n= 4) of ß-*Phb*2 KO mice were used to examine the effect of hyperglycaemia on CRYM mRNA levels in the kidneys. A) Levels of expression of renal CRYM mRNA were quantified by qPCR and quantification being carried out and the results were expressed as levels of renal CRYM relative to GAPDH. B) The data were log transformed and showed a non-significant difference in renal CRYM levels when compared to their control, P>0.05.

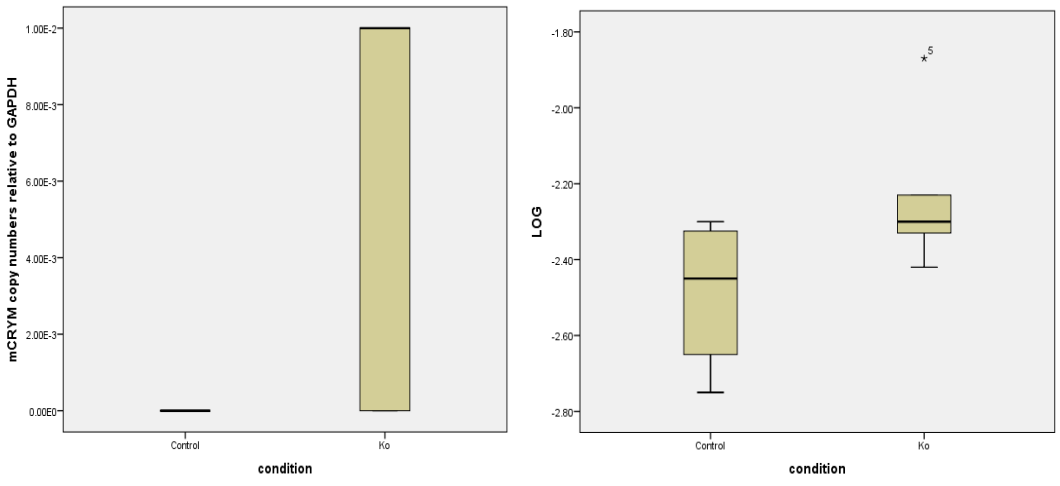

Figure 11b. Effect of high glucose on cardiac mRNA levels of ß-*Phb2* KO mice.

Hearts were collected from diabetic (n= 5) and control (n= 4) of ß-*Phb*2 KO mice. Cardiac CRYM copy numbers were detected using qPCR. The mean values and standard deviation of different experiments are shown. A) Values shown are copy numbers of cardiac CRYM mRNA relative to GAPDH. B) The data were log transformed and found not to change in cardiac CRYM mRNA levels in diabetic conditions, P>0.05.

As shown in Figures 11a and 11b, no difference was seen in diabetic conditions. This is the first study to examine the expression of renal and cardiac CRYM mRNA levels in a ß-*Phb2* KO mouse model and we could not demonstrate any change of renal and cardiac CRYM mRNA levels in diabetic conditions.

● ***Renal and cardiac mRNA levels of CRYM in streptozotocin-induced diabetic mice***

As described previously, renal and cardiac CRYM copy numbers were measured in control, diabetic and treated kidneys of mice relative to GAPDH, as shown in Table 14a. The data were log transformed as the actual CRYM copy number values were skewed and not normally distributed. Student's *t* test was used to obtain the mean, standard deviation and *p* values. The results showed that renal CRYM levels were increased by hyperglycaemia in the kidneys of STZ mice and this increase was attenuated by the treatment of diabetes (0.76 ± 0.33 vs. -2.17 ± 0.22, $P<0.001$; Table 14b).

The hyperglycaemia-induced increase in renal CRYM was specific as we could not demonstrate any change in cardiac CRYM ($P>0.05$; Table 14b); the results showed a non-significant difference between control and diabetic hearts (Figure 12b). The mean values of cardiac CRYM mRNA in control and treated kidneys were close to each other and were lower than in diabetic hearts.

Table 14a. Relative CRYM and GAPDH mRNA expression values of STZ mouse kidney and heart tissues

Tissue	Condition	CRYM	CRYM	CRYM	GAPDH	GAPDH	GAPDH	CRYM ratio
Kidney	Control1	334	247	359	79700	77500	86100	0
	Control2	964	880	948	87300	79500	87500	.01
	Control3	771	838	724	117000	111000	101000	.01
	Diabetic1	540	675	419	141	197	151	3.34
	Diabetic2	590	744	589	23	18	95	14.14
	Diabetic3	335	433	1210	155	266	43	4.26
	Treated1	1130	1080	730	7090	7930	6870	.13
	Treated2	818	1070	1080	639	575	581	1.65
	Treated3	605	648	768	64500	99800	87800	0.1
Heart	Control1	481	326	276	64000	71000	62800	0.01
	Control2	268	256	132	48500	47800	50100	0.00
	Diabetic1	282	293	300	148000	96200	36600	0.00
	Diabetic2	171	221	216	11900	10200	10200	0.02
	Diabetic3	322	271	304	41100	43300	60400	0.01
	Treated1	246	302	216	25500	27500	29400	0.01
	Treated2	100	288	272	2690	3760	7230	0.04

CRYM copy numbers relative to GAPDH copy numbers were determined using qPCR in control, diabetic and treated kidneys and hearts of STZ-induced diabetic mice. For each condition, samples were used to prepare cDNA and renal and cardiac CRYM mRNA levels were quantified from each sample in triplicate. Data are shown as relative expression values.

Table 14b. Relative copy numbers of CRYM mRNA in STZ mouse kidney and heart tissues

Tissue	Condition	N	Mean values ±SD of mouse CRYM copy numbers	Mean values ±SD of CRYM log
Kidney	Control	3	0.006 ± 0.005	-2.17 ± 0.22
	Diabetic	3	7.24 ± 5.98	0.76 ± 0.33**
	Treated	3	0.596 ± 0.914	-0.91 ± 1.57
Heart	Control	2	0.005 ± 0.0007	-2.3 ± 0.06
	Diabetic	3	0.009 ± 0.008	-2.1 ± 0.39
	Treated	2	0.028 ± 0.027	-1.6 ± 0.50

CRYM mRNA copy numbers relative to GAPDH copy numbers were detected in kidneys and hearts of STZ-induced diabetic mice. Values are shown as mean ± SD. There is a significant result between control and diabetic kidneys. **P<0.001

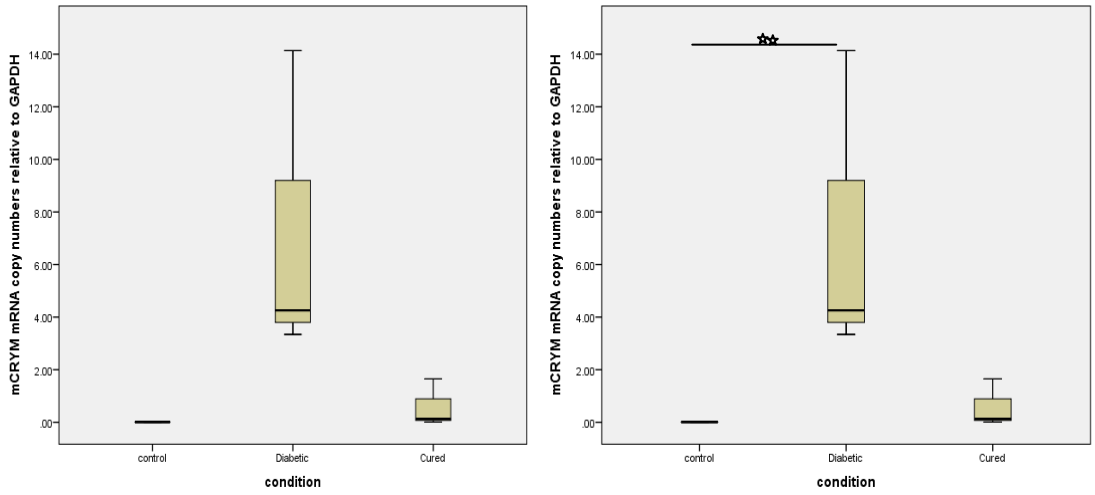

Figure 12a. The effect of high glucose on renal CRYM mRNA levels of STZ mice.

Kidneys were collected from control, diabetic and treated STZ-induced diabetic mice. Renal CRYM copy numbers were detected using qPCR. A) The mean values and standard deviation of different experiments are shown. Values shown are copy numbers of renal CRYM mRNA relative to GAPDH. B) Student's *t* test of the log-transformed values showed a significant increase of CRYM levels in diabetic kidneys. **P<0.001

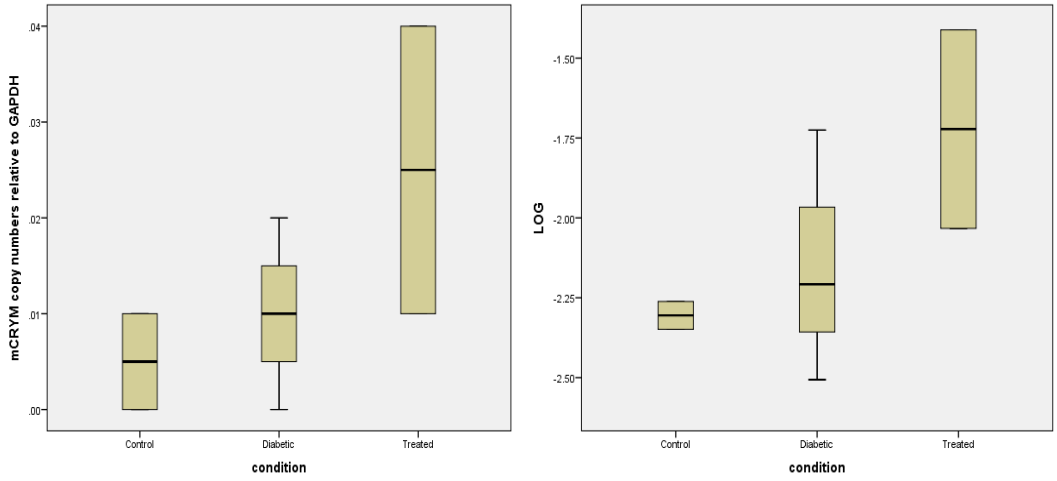

Figure 12b. Effect of high glucose on cardiac CRYM mRNA levels of STZ mice.

Hearts were collected from control, diabetic and treated STZ-induced diabetic mice. Cardiac CRYM copy numbers were detected using qPCR. A) The mean values and standard deviation of different experiments are shown. Values shown are copy numbers of cardiac CRYM mRNA relative to GAPDH. B) The data were log-transformed and showed a non-significant difference of cardiac CRYM levels in diabetic conditions, P>0.05

Figure 12a showed that diabetes leads to increased expression of renal CRYM mRNAs, which can be corrected in kidneys through treatment of diabetes. This increase in renal CRYM mRNAs of STZ mice supports previous finding, which showed that renal CRYM mRNA is up-regulated in the kidneys of a GK rat (Al-Kafaji and Malik, 2010). However, there are no changes in cardiac CRYM mRNAs of STZ-induced diabetic mice (Figure 12b).

3.3.3. CRYM protein expression is up–regulated in diabetic kidneys of streptozotocin-induced diabetic mice

In this part of the study, the expression and the localisation of CRYM protein was determined in control and diabetic kidney sections of STZ-induced diabetic mice using immunoflourescence. Mouse kidney sections of STZ mice which were previously used for mRNA study were incubated with the CRYM antibody overnight and anti goat FITC conjugated secondary antibodies for 2 hours; nuclei were stained blue with DAPI (Section, 2.14.1). Sections were examined under a fluorescence microscope (Eclipse TE 2000-U, Nikon).

The fluorescence probe was determined by a green emission indicating the location of CRYM protein in the kidney and it revealed that CRYM protein was located predominantly in the glomerulus and tubules of the kidney; it also showed that CRYM was more abundant in the tubules. CRYM protein was expressed at relatively higher levels in hyperglycaemia compared to control, suggesting increased protein expression of CRYM protein in diabetic kidney (Table 15). Besides the higher levels of CRYM protein, the tubules were bigger (hypertrophy) and distorted compared to control sections (Figure 13a).

To confirm the accuracy of CRYM protein expression, public domain image analysis software (ImageJ v3.91 http://rsb.info.nih.gov/ij) was applied to measure the fluorescence intensity in control and diabetic sections. Furthermore, it showed that the increase in FITC green fluorescence was not due to over-exposure of the images. Four images were selected for each condition and ImageJ analysis was used to calculate the optimal signal to noise ratio. The average of each condition was found and the data showed a 1.4-fold increase in the fluorescence intensity of the CRYM protein in the diabetic mouse compared to the control mouse sections (Figure 13b). These data

support previous results illustrating renal CRYM mRNA to be significantly increased in STZ diabetic mice.

Table 15. Statistical analysis of CRYM protein fluorescence intensity in STZ kidneys

Tissue	Condition	N	Mean values ± SD of mouse CRYM protein
Kidney	Control	4	45.76 ± 29.42
	Diabetic	4	65.73 ± 29.58*

Fluorescence intensity of FITC was obtained in control and diabetic mice kidneys of STZ-induced diabetic mice using ImageJ analysis. The data are shown as mean ± SD. *P<0.05

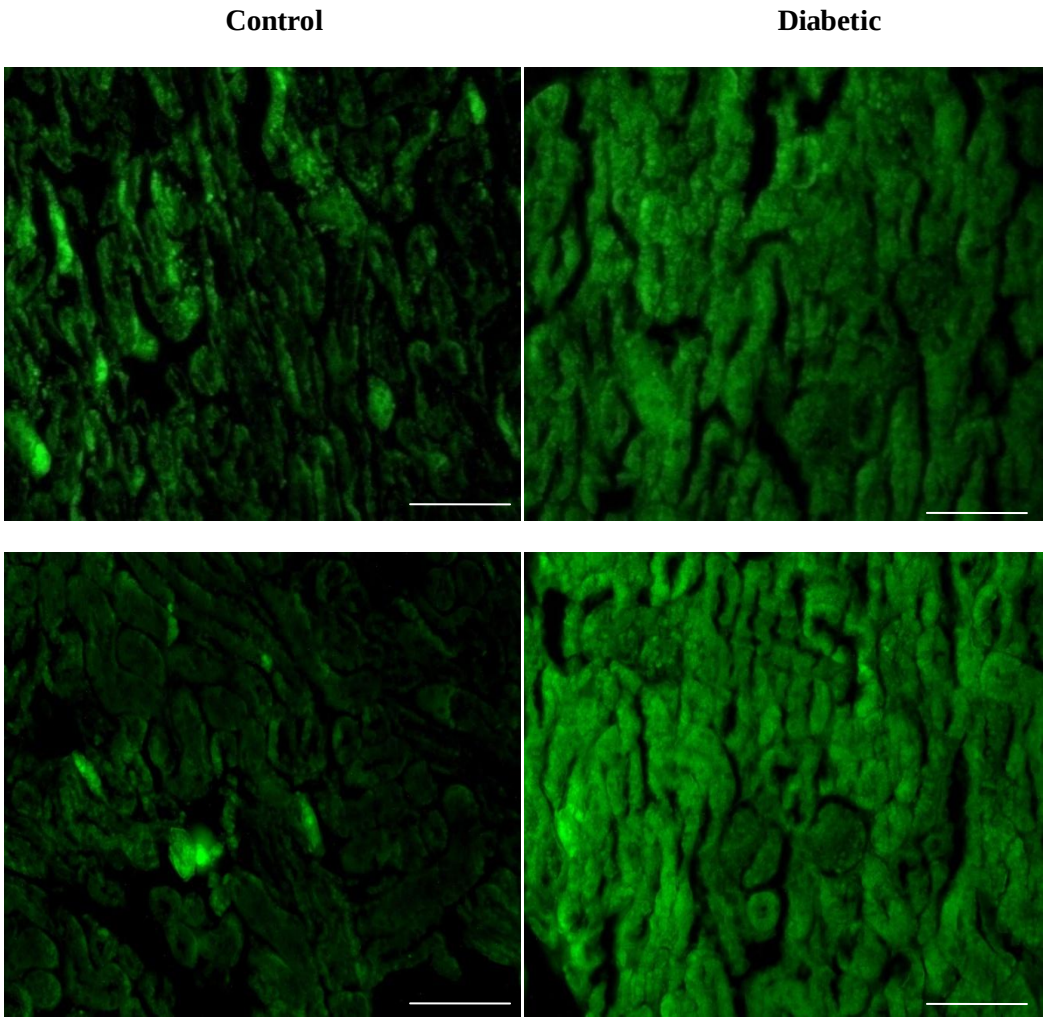

Figure 13a. Increased protein levels of CRYM are associated with diabetic mouse kidney.

Kidney sections of cortex from diabetic and control STZ- induced diabetic mice were labelled with the CRYM primary antibody and FITC conjugated secondary antibody. Green represents the CRYM protein. Scale bars are 250µM.

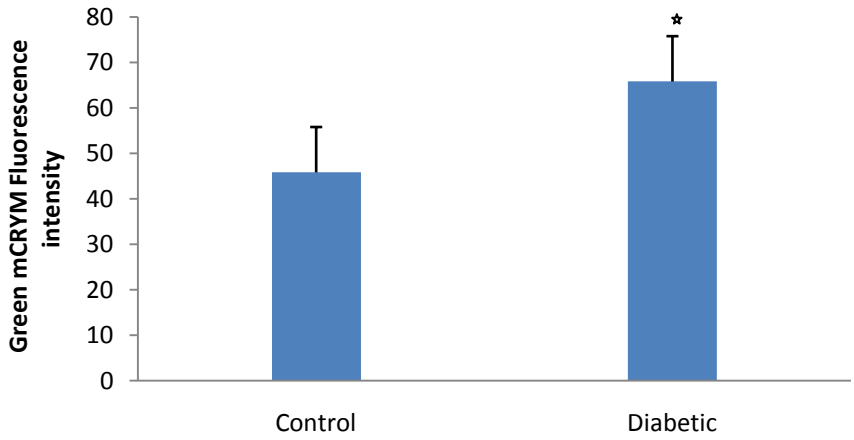

Figure 13b. Increase in fluorescence intensity in diabetic mice compared to controls.
CRYM protein was increased in diabetic kidneys of STZ mice. *P<0.05

• ***CRYM protein is more abundant in tubular cells compared to glomerular cells of streptozotocin-induced diabetic mice***

The fluorescent probe detected by the green emission determined that CRYM protein was located abundantly in tubules and less in the glomerulus of control and diabetic STZ mice kidneys (Figure 13c).

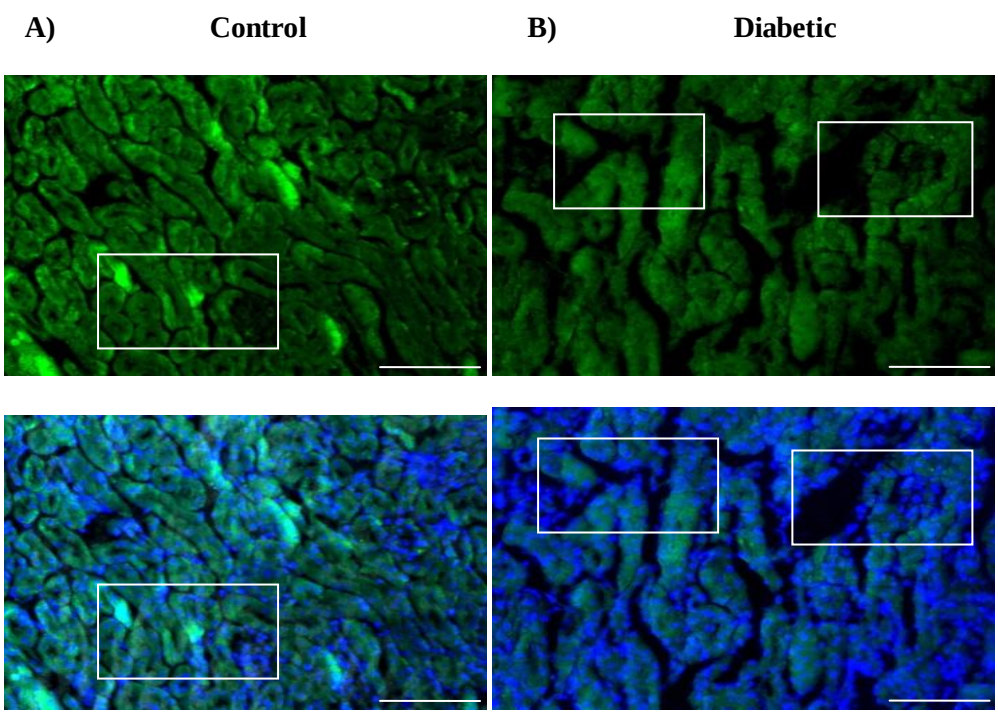

Figure 13c. CRYM protein is highly abundant in tubular and less present in glomerular cells from control and diabetic kidneys of mice.

Localisation and expression of mouse CRYM protein was assessed by CRYM primary antibody and FITC-conjugated secondary antibody; nuclei were stained with DAPI. These sections in the cortex of control and diabetic STZ mice showed kidney tubules and glomeruli. White boxes are showing less green staining in glomeruli and indicated higher expression of CRYM in the tubules as there is more green staining there. Scale bars are 250µM.

A higher magnification was used to further investigate the location of CRYM protein in mouse kidney sections. The CRYM protein was presented with green staining and the nuclei were labelled as blue. CRYM protein was found to be located in the cytoplasm, visible as green colour, in control and diabetic kidneys of the STZ mice (Figure 13d).

A) Control **B) Diabetic**

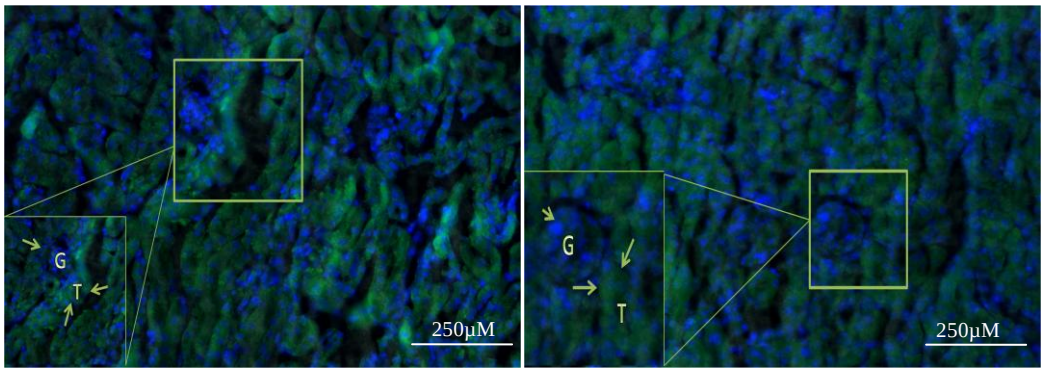

Figure 13d. CRYM protein expression in the cytoplasm in control and diabetic kidneys of mice.

Mouse kidney sections were labelled with CRYM primary antibody and FITC conjugated secondary antibody, and nuclei were stained with DAPI. A) These cortical sections of control and diabetic STZ-induced diabetic mice showed kidney tubules. One glomerulus and one tubule of each condition has been magnified and shows the cytoplasmic localisation of CRYM protein in the control and diabetic kidney. B) A higher magnification of a section in both the control and diabetic kidneys further confirmed cytoplasmic localisation of CRYM protein and more expression of CRYM in tubular cells, T: tubule and G: glomerulus.

3.3.4. Is renal CRYM mRNA regulated by glucose in cultured human tubular cells?

Our previous results showed that renal CRYM mRNA is up-regulated by glucose in the diabetic kidneys of STZ-induced diabetic mice. Immunohistochemistry study revealed an abundant expression of CRYM protein in renal tubular cells of the STZ mice. These results suggested that diabetes leads to an increased expression of renal CRYM which can be corrected in the kidneys by the treatment of diabetes, and although there are high levels of CRYM protein in renal tubular cells, the up-regulation may be taking place in mesangial or other renal cells. Previously, Al-Kafaji (2010) reported the up-regulation of renal CRYM mRNA by glucose in HMCs and HMCL.

Therefore, in this part we examined renal CRYM mRNA levels in HTC to see if they could be induced by high glucose. As described previously, HTC were cultured until highly confluent and cells were exposed to NG, HG and NGM for 3 days. NGM was used to test for any osmalarity effect. RNA concentration was determined by

measuring the absorbance of RNA at A_{260} using nanodrop (Table 12b; Section 3.3.1). cDNA was synthesised from RNA (Section 2.6.4.). For each condition, cDNAs were synthesised and CRYM primers were used to detect the CRYM mRNA expression in HTC. qPCR was carried out to measure copy numbers of renal CRYM mRNA relative to a reference gene.

● ***Quantification of renal CRYM copy numbers in human cultured renal tubular cells***

In HTC, renal CRYM mRNA copy numbers were measured relative to PGK using qPCR (Table 16a). Surprisingly, in HG, renal CRYM mRNA levels showed a slight decrease in HTC (Figure 14) whereas they had previously shown a significant increase in HMCs and HMCL (Al-Kafaji and Malik, 2010). Statistical analysis of the data using student's *t* test showed a significant decrease in cells exposed to HG when compared to NG (0.03 ± 0.05 vs. 0.5 ± 0.26, $P<0.05$; Table 16b). We also found no significant difference between NG and NGM ($p>0.05$), thereby showing the absence of osmolarity effect.

Table 16a. Renal CRYM mRNA expression values relative to PGK in human renal tubular cells cultured in different conditions

Cells	Condition	CRYM	CRYM	CRYM	PGK	PGK	PGK	CRYM ratio
HTC1	NG	3700	3310	3660	2360	3570	7360	0.79
HTC2	NG	3010	4680	2460	14900	17900	5840	0.26
HTC3	NG	3130	3540	4060	7770	7770	7770	0.45
HTC4	HG	4520	4720	4460	76000	50500	17500	0.10
HTC5	HG	3440	3540	3310	7600	8690	3700000	0.00
HTC6	HG	3660	4240	3900	ND	1020000	1110000	0.00
HTC7	NGM	5770	7050	7070	516000	25900	29400	0.19
HTC8	NGM	8120	7890	8040	21000	5070	7860	0.71
HTC9	NGM	6140	5510	5910	7600000	ND	4450000	0.00

Renal CRYM mRNA copy numbers relative to PGK mRNA copy numbers were detected using qPCR in human tubular cells, cultured in normal glucose (NG), high glucose (HG) and normal glucose with mannitol (NGM) for both experiments. For individual conditions, three separate samples were used to prepare cDNA and human CRYM was quantified for each sample in triplicate. Data are shown as relative expression values.

Table 16b. Relative copy numbers of CRYM mRNA in human cultured renal tubular cells

Cells	Condition	N	Mean values ± SD of human CRYM copy numbers
HTC	NG	3	0.50 ± 0.26
	HG	3	0.03 ± 0.05*
	Mannitol	3	0.30 ± 0.36

Renal CRYM mRNA copy numbers relative to PGK mRNA copy numbers were detected in in human tubular cell lines grown in normal glucose (NG), high glucose (HG) and in normal glucose plus mannitol (NGM). Copy numbers are shown as mean ± SD (n= 3). *P<0.05

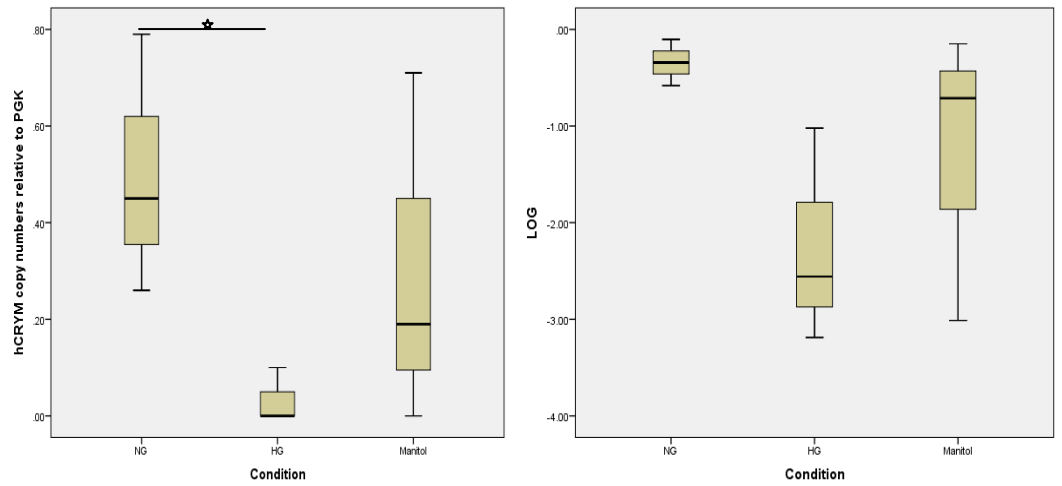

Figure 14. Effect of high glucose on renal CRYM mRNA levels in human tubular cells.

After being synchronised, tubular cells were incubated in normal glucose (5 mM), high glucose (25 mM) and normal glucose with mannitol (5 mM glucose + 20 mM mannitol) for 3 days. Renal CRYM copy numbers were detected using qPCR (n= 3). A) The mean values of three different experiments are shown. Values shown are copy numbers of renal CRYM mRNA relative to PGK. B) The data showed a decrease in CRYM mRNA level in cells exposed to HG. *P<0.05

1) Cellular localisation of CRYM protein in human embryonic kidney 293 (HEK293) cells

The aim of this part of the study was to test the specificity of the human CRYM antibody in human HEK293 cells before investigating the CRYM protein expression in HTC. To determine human CRYM protein in renal HEK293 cells, the cells were

maintained in DMEM media until they reached confluence and were then growth arrested for 24 hours. The quiescent cells were seeded on 6-well pellet at a density of 10,000 cells/well in DMEM media containing NG, HG and NGM and were incubated for 3 days. However, we only used HEK293 cells grown in NG to test the CRYM antibody for the first time.

The specificity of the purified antibody was assessed by immunostaining. Two different concentrations of the primary antibody were used (1:30, 1:50 dilutions). The HEK293 cells were incubated with a goat polyclonal IgG primary antibody made against CRYM and FITC-conjugated donkey anti-goat IgG secondary antibody at 1:30 and 1:50 dilutions for 2 hours. Immunostaining was carried out to detect the location of CRYM protein in HEK293 cells. The results showed successful detection of CRYM protein in HEK293 cells at different concentrations of the primary antibody and suggested that a 1:30 dilution would be the best working concentration for future immunostaining (Figure 15).

● ***Cellular localisation of CRYM protein in human renal tubular cells***

Previously, we found a moderate decrease in renal CRYM mRNAs in HTC in the presence of HG. The aim of this section was to determine the localisation and expression of CRYM protein in NG and HG conditions. Part of the cell pellets used for mRNA study was saved for the protein study. In this study, we used only cells grown in NG and HG.

Quiescent cells were subjected to immunofluorescence analysis. The cells were prepared as described above for the detection of CRYM protein in HEK293 cells. Localisation and expression of CRYM protein was assessed by confocal microscopy following staining of cells with a goat polyclonal IgG primary antibody against CRYM and FITC-conjugated donkey anti-goat IgG secondary antibody for fluorescence labelling. Cells were mounted with PBS and nuclei were counterstained with DAPI (blue). Figure 16a and 16b illustrates confocal microscope images of HTC expressing CRYM protein after exposure to NG and HG respectively for 3 days.

CRYM protein was distributed throughout the cytoplasm in cells both in NG and in HG. The fluorescent probe detected through the green emission indicated that CRYM protein is located in the cytoplasm of tubular cells and the blue staining represents the

nuclei, which were counterstained with DAPI. These results were in line with previous studies demonstrating CRYM protein to be located in the cytoplasm of HMCs (Al-Kafaji and malik, 2010) and HEK293 cells under NG. In addition to CRYM protein localisation, no difference in the expression level of CRYM protein was found in both NG and HG conditions (Figure 16a and 16b).

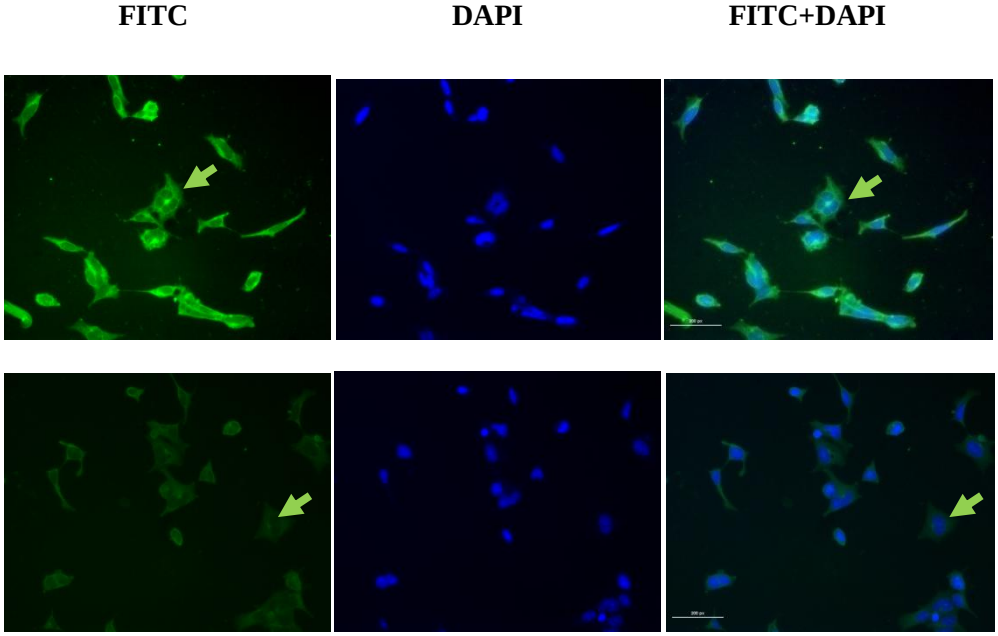

Figure 15. Detection of CRYM protein expression in normal glucose of human embryonic kidney 293 cells.

Human embryonic kidney 293 cells were cultured in normal (5 mM) glucose. Cells were incubated with goat polyclonal IgG primary antibody and FITC-conjugated secondary antibody (1:30 dilution) and they were stained with DAPI. The reactivity was visualised for FITC to detect the location of the protein. Arrows show that CRYM protein is localised to the cytoplasm.

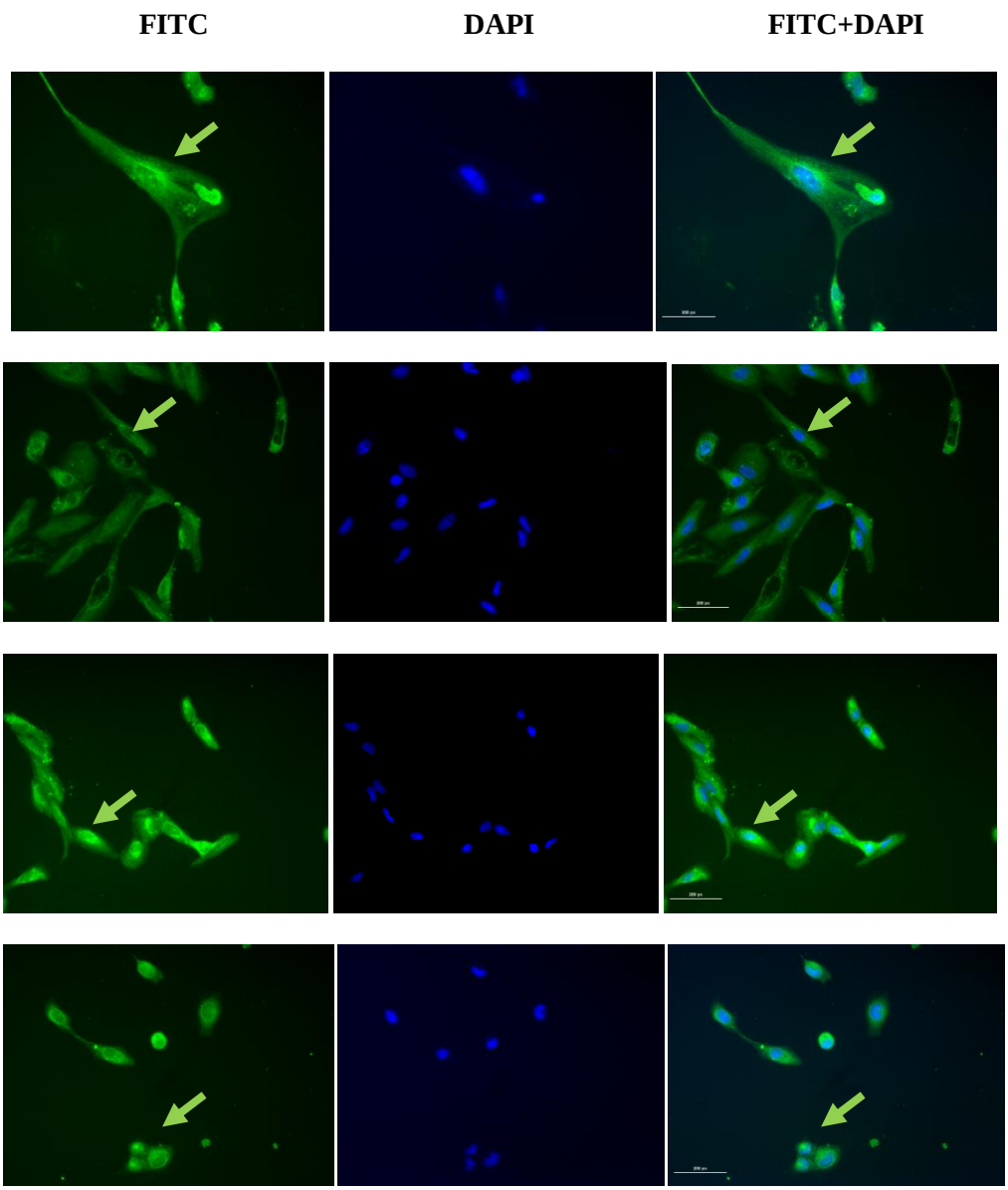

Figure 16a. Detection of CRYM protein expression in normal glucose of human tubular cells.

Human tubular Cells were cultured in normal (5 mM) glucose. Cells were incubated with goat polyclonal IgG primary antibody and FITC-conjugated secondary antibody and they were mounted using DAPI. The reactivity was visualised for FITC to detect the location of the protein. Arrows show that CRYM protein is localised to the cytoplasm.

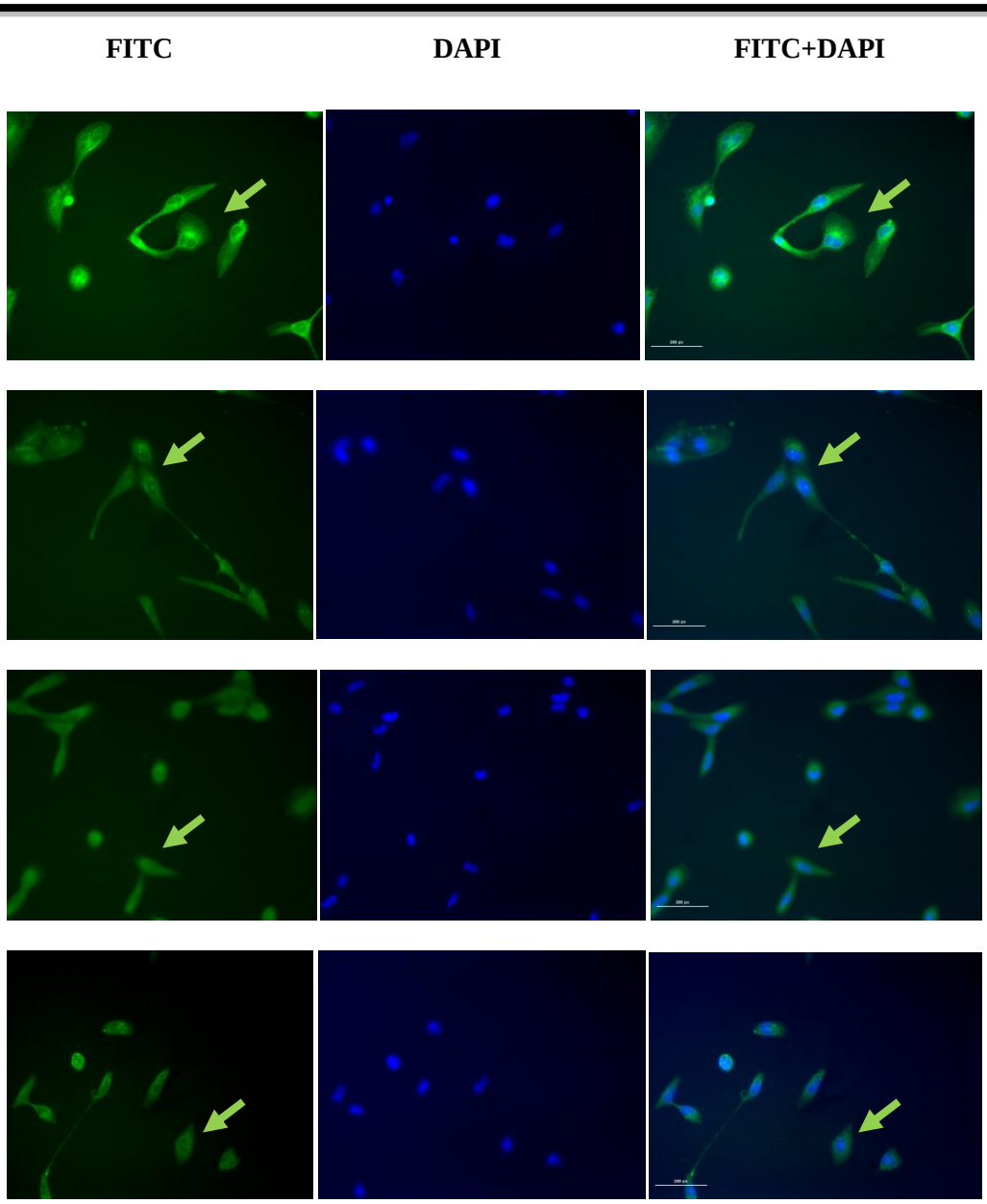

Figure 16b. Detection of CRYM protein expression in high glucose of human tubular cells.

Human tubular Cells were cultured in high (20 mM) glucose. Cells were incubated with goat polyclonal IgG primary antibody and FITC-conjugated secondary antibody and they were stained with DAPI. The reactivity was visualised for FITC to detect the location of the protein. Arrows show that CRYM protein is localised to the cytoplasm.

3.4. Discussion

We report that CRYM, also known as thyroid hormone binding protein and μ-crystallin is involved in the cell's glucose response in diabetes. In this part of the study we looked at CRYM expression *in vivo* and *in vitro*. The main focus of this study was to investigate whether renal CRYM mRNA and protein were regulated by the presence of HG in the *in vivo* and *in vitro* models and also to detect the location of CRYM protein in HTCs. In the first part of this study, we analysed renal and cardiac mRNA expression in ß-*Phb2* KO and STZ mice and also CRYM protein expression were measured in the kidneys of diabetic induced STZ mice compared to healthy controls. Secondly, CRYM copy numbers as well as were measured and the location of CRYM was examined in HTC.

Our study is the first to show that renal CRYM mRNA is regulated during the development of hyperglycaemia in the kidneys of STZ-induced diabetic mice. We found that renal CRYM mRNAs increased in response to hyperglycaemia in the kidneys of STZ-induced diabetic mice and this increase was attenuated by the treatment of diabetes ($P<0.05$). Renal CRYM mRNA expression was significantly increased in diabetic kidneys compared to control kidneys. The increase in renal CRYM in whole kidneys was specific as we could not demonstrate any change in cardiac CRYM. We also examined renal and cardiac CRYM mRNA levels in ß-*Phb*2 KO mice to see if they followed the same pattern of expression, however we could not find any change in renal and cardiac CRYM mRNAs in the presence of hyperglycaemia. The differential expression of CRYM in ß-*Phb2* KO and STZ-induced diabetic mice might be as a result of the difference between these biological models. Therefore, it is possible that the biological difference of these two models could be affecting renal and cardiac CRYM expression.

Following these results, immunofluorescence staining was carried out to determine the expression and location of CRYM protein in control and diabetic kidneys of the STZ mice. CRYM protein was widely expressed in diabetic kidneys, mostly in the tubules and it was expressed at lower levels in the glomerulus. By analysing the fluorescent intensity, it was found that CRYM protein expression was significantly higher in diabetic kidneys compared to the controls, which confirmed the mRNA data.

Further analysis of protein localisation showed that CRYM protein was localised in the cytoplasm of the HTC in the control and diabetic sections of the kidney.

We also examined renal CRYM mRNA levels in HTC to see if they could be induced by HG. However, we found a moderate decrease of renal CRYM mRNA levels in HTC in the presence of HG. In contrast, renal CRYM showed up-regulation by glucose in cultured HMCs in previous studies by Al-Kafaji (2010). We also showed that renal CRYM protein is predominantly found in HTC and its expression is not increased in HG condition.

It was previously shown that renal CRYM is differentially regulated by glucose and strongly hybridised to a cDNA probe prepared from poly (A)+ RNA isolated from the kidneys of a GK rat compared to the normoglycaemic kidneys of a wistar rat at 6 weeks (Malik et al., 1997). The detection of renal CRYM mRNA transcript in the kidneys of a GK rat but not in the normoglycaemic kidneys of a Wistar rat suggested the up-regulation of renal CRYM mRNA levels in diabetic kidneys (Zaidi, 1997). A study by Al-kafaji (2010) which reported a gradual elevation in CRYM mRNAs from the kidneys of GK rats from 6 weeks to 40 weeks is consistent with these results and therefore our data supports the notion that renal CRYM is up-regulated by glucose in diabetic kidneys and suggests glucose regulation of renal CRYM mRNA expression in a mouse model.

The location of CRYM has not been demonstrated in the kidney previously. The CRYM gene is located at human chromosome 16p13.11-p12.3 which contains several genes (Chen et al., 1992). These genes encode proteins that have both specific and unique renal localisation and function and some encode for proteins whose functions are still unknown, but whose alteration causes renal diseases (Stiburkova et al., 2000; Kamatani et al., 2000; Pirulli et al., 2001). Our observation of up-regulation in renal CRYM mRNAs occurring in the diabetic kidneys of STZ mice, rats and in HTC raises the idea that CRYM may be involved in the pathogenesis of DN.

In HG, ROS produces and increases glucose signalling in renal cells and it is also involved in excessive ECM deposition in DN (Ha and Lee, 2005; Lee et al., 2003). The increase of CRYM is parallel with increased ROS in HMCs in response to HG, suggesting that CRYM might be involved in protecting renal cells from the result of

high glucose-induced ROS formation and increases the hypothesis that CRYM may serve as an endogenous antioxidant.

Immunofluorescence showed that mouse CRYM protein expression is mostly localised in the tubules and less in the glomerulus. Consistent with this observation, human CRYM protein was also found to be more abundant in the renal tubules of a human kidney compared to the glomeruli (Suzuki et al., 2007). Therefore, they suggested that CRYM expression is cell–type specific.

We have also shown that CRYM protein localises into the cytoplasm in control and diabetic mice. This is consistent with the previous study by Al-Kafaji (2010) that showed CRYM protein was expressed in the cytoplasm. Interestingly, CRYM was identified as a cytosolic T_3-binding protein in rat cytosol by Suzuki (2007).

A study by Suzuki et al., (2007) demonstrated that CRYM has the capability to modulate the activity of T_3. Indeed, CRYM binds to T_3 and NADPH and holds T_3 in cytoplasm, which increases the concentration of T_3 (Hashizume et al., 1989; Vie et al., 1996). However, NADP inhibits T_3 binding and it is possible that for oxidative metabolism is another factor for control of T_3 binding to CRYM in cytoplasm (Kobayashi et al., 1991). It was reported that mutations in the CRYM gene have been linked to non-syndromic deafness in patients and this suggested that mutant CRYM could abrogate the affinity of thyroid hormone (Abe et al., 2003; Oshima et al., 2006). It is also notable that diabetic patients commonly suffer from thyroid dysfunction such as hyperthyroidism (Patricia, 2000). This finding supports the hypothesis that CRYM could have a possible role in thyroid hormone function.

The glomerulus mainly consists of endothelial cells, podocytes and mesangial cells and the mesangial cells have a contribution in ECM production and accumulation (Greenberg, 1998). The previous study by Al-Kafaji (2010) showed that CRYM protein was elevated in HMCs (Al-Kafaji and Malik, 2010). Therefore, over-expression of CRYM in these cells in diabetic mice might play an important role in diabetes-induced GBM thickening and ECM production. There are other factors such as hyperglycaemia which could be involved in this process and are consistent with these findings.

Hyperglycaemia is known to be a key factor in pathological changes in DN (Kanwar et al., 2011). HTC involved in DN and their central role in injury to DN has been extensively studied (Qi et al., 2007). Therefore, HTC are an ideal model in which to unravel the cellular mechanism such as proliferation, contributing to the tubulointerstitial changes in DN and leading to the progression of renal failure in DN (Qi et al., 2007). Furthermore, other abnormalities in diabetes may contribute to the cause of pathological alterations of HTC. Hyperglycaemia is believed to be the main factor and induces renal injury through various complex and overlapping biochemical pathways that are involved in several key molecules, for example; TGF-β1, AGE products, protein kinase C, the polyol pathway, the hexoamine pathway and oxygen free radicals (Sheetz and King, 2002).

In this study, we showed that CRYM is down-regulated by glucose in HTC. Human CRYM mRNA levels were reduced following exposure of cells to HG compared to NG. Unexpectedly, we found that when HTC were exposed to HG, its effect on CRYM was less; in fact, CRYM mRNA expression was decreased in HTC. Within 3 days of exposing HTC to HG, tubular expression of human CRYM mRNA was reduced. Hence, the low regulation of human CRYM mRNA in response to high glucose observed was unexpected in our tubular cell model, as we previously found that human CRYM was increased in association with hyperglycaemia in the primary and transformed mesangial cell line. These changes suggest that this effect might be specific for certain cell types such as mesangial cells, rather than having a non-specific cellular response. In response to this finding, we suggested that expression of CRYM might be cell–type specific.

CRYM protein expression in HTC was also examined by confocal microscopy and we found no changes in CRYM protein expression for HTC cultured in either NG or HG. In addition, cellular localisation of CRYM within HTC showed cytoplasmic localisation of CRYM protein in both NG and HG conditions. Therefore, this suggests that CRYM may be a cytosolic protein.

As mentioned previously, CRYM is known to be involved in ROS (Al-Kafaji and Malik, 2010) and its altered expression in diabetes may play a role in oxidative stress damage. However, the exact function of CRYM in DN remains to be determined.

Therefore, further studies are required to discover the potential role of CRYM in hyperglycaemia-induced ROS in DN.

Chapter 4

Circulating CRYM mRNA levels in peripheral blood of patients with diabetic retinopathy and nephropathy

Chapter 4. Circulating CRYM mRNA levels in peripheral blood of patients with diabetic retinopathy and nephropathy

4.1. Abstract

As we had shown that CRYM is regulated by glucose, the aim of this chapter was to determine if we can detect CRYM in peripheral blood and to see if its expression is associated with DN and DR.

Two cross sectional studies were carried out to compare the expression of circulating CRYM mRNA in T2DM patients with and without retinopathy (n= 36), as well as with and without nephropathy (n= 99). Circulating CRYM mRNA expression was quantified using qPCR relative to the reference genes. Resulting data were analysed using student's *t* test and $P<0.05$ was considered significant.

For the first time we demonstrated that low levels of CRYM mRNA can be detected in peripheral blood of patients with diabetes. We found that circulating CRYM mRNA levels were reduced by 2.9-fold in DR patients ($P<0.05$) compared to diabetic controls without retinopathy. Patients with retinopathy had a longer duration of diabetes and higher HbA1c and ACR in comparison to controls.

In contrast, circulating CRYM mRNA levels were 7.4-fold higher in patients with nephropathy when compared with a large group of patients without nephropathy. Patients with nephropathy had a long duration of diabetes, and they also had higher ACR in comparison to patients without nephropathy.

In summary, for the first time we were able to show that circulating CRYM mRNA is regulated in blood of patients with DR and DN. Circulating CRYM mRNA levels were decreased in patients with DR. However, they were increased in patients with DN. Therefore, it is currently unclear if this finding is indicative of different pathophysiological processes in DN and DR, or is owing to an experimental alteration.

4.2. Introduction

Patients with T1DM and T2DM have a much higher risk of complications involving many different systems within the body. DN and DR are major complications of diabetes which can result in end stage renal failure and blindness respectively (Brownlee, 2001). Currently, the presence of microalbuminuria is monitored in patients with DM (Cruickshanks et al., 1993). Microalbuminuria is defined as persistent albumin excretion rate of between 30 and 300mg/24 hours. Microalbuminuria is used as a marker for vascular damage (Stehouwer et al., 1992) and an indicator for nephropathy (Bojestig et al., 1996) and retinopathy of patients with diabetes (Cruickshanks et al., 1993). However, it is not indicative in the early stages and is usually detected once the microvasculature has been damaged (Mogensen et al., 1995) and is therefore not a predictive marker for diabetic complications.

Angiotensin-converting enzyme (ACE) inhibitors are current therapies for the treatment of DN which efficiently slow the development of DN (Lewis et al., 1993; Parving et al., 2001). Only 30% to 40% of patients with diabetes will develop disease. However, in all newly diagnosed diabetic patients the treatment is not desirable as these drugs have long-term side effects (Parving et al., 2001). Therefore, there is great demand for the identification of early markers and predictors, which will help to identify those patients with a higher risk of developing renal disease and this may prove beneficial for early treatments.

Microvascular diseases are the result of several factors such as hyperglycaemia, glycated proteins and oxidative stress which activate metabolic pathways and PKC isoforms (Brownle, 2001). These factors can generate various growth factors in the kidney and they could be a potential marker for diabetic complications. TGF-β1, CTGF and podocytes-derived VEGF are some of the markers which have been proposed for the detection of the progression of microvascular diseases (Ziyadeh et al., 2008).

TGF-β1 is believed to be an important profibrotic factor in the development of DN and it plays a role in GBM thickening which is the main characteristic of DN (Sharma and Ziyadeh, 1997; Ziyadeh, 2008). The increased activation of TGF-β1 is one of the main causes that leads to kidney fibrosis and this results in the accumulation of

extracellular matrix which may be an important contributor in DN (Loeffler and Wolf, 2013; Wada et al., 2002; Zhu et al., 2007). There are many studies that show an association between circulating and renal TGF-β1 activity in the progression of DN. Sharma et al. (1997) found an increase of renal TGF-β1 in patients with diabetes and the urinary levels of TGF-β1 were significantly increased in those patients. TGF-β1 mRNA levels and TGF-β1 receptor have also been shown to increase in *db/db* mice (Ziyadeh et al., 1999). Therefore, it can be used as a predictive marker for DN. However, further studies are required to define its role as a marker of DN progression (Jermus et al., 2008).

CTGF is a member of CCN matricellular proteins which is induced by TGF-β1. CTGF is downstream of TGF-β1 and it is involved in renal fibrosis. It also has capability to bind to a number of growth factors for modifying its function (Mason, 2009). Therefore, CTGF is a potential biomarker for DN. CTGF may act to meditate the actions of mesenchymal cells and also act as an effector of TGF-β1 (Grotendorst, 1997; Mason 2009). Indeed, it can stimulate TGF-β1 signalling by binding directly to the growth factor, and stimulating its interaction with the TGF-β1 receptor (Mason 2009). A number of findings showed the up-regulation of CTGF in DN. For example, Riser et al. (2003) showed that glomerular expression of CTGF is greatly up-regulated early in experimental and human diabetes. Urinary levels of CTGF were also elevated in STZ-diabetic animals (STZ-rats after 30 weeks) and they were increased in patients with DN compared to healthy controls (Riser et al., 2003).

Similar to these results, Wahab (2005) showed that the glomerular CTGF mRNA and protein were increased at early stages of DN and continued to increase as DN progressed. They also concluded that both CTGF and CTGF-independent pathways mediate increased synthesis of fibronectin in hyperglycaemia. High levels of CTGF plasma has been demonstrated in patients with renal disease and was established to be a self-regulating predictor of kidney failure and mortality in T1DM patients with nephropathy (Nguyen et al., 2008). CTGF mRNA expression and protein levels were also more expressed in the podocytes and mesangial cells of murine models of DN (Roestenberg et al., 2004). Protein levels of CTGF also increased in proximal tubular epithelial cells in rodent models of type 1 diabetic nephropathy in STZ-rats (after 30 weeks) and type 2 diabetes (db/db mouse) (Wang et al., 2001; Guha et al., 2007).

Nevertheless, CTGF regulation in DN is likely to be a key factor in the progression of glomerulosclerosis by affecting matrix synthesis (Wahab 2005).

While a number of studies indicated that the TGF-β1 pathway is a key mediator of mesangial matrix accumulation, there is doubt over the function of TGF-β1 as the main mediator of DN with albuminuria (Ziyadeh, 2008). Growing evidence suggests that VEGF has a pivotal role in microvascular complications of diabetes and perhaps it directly contributes to the proteinuria of diabetes rather than the extracellular matrix build up (Wolf et al., 2005). VEGF is a potent angiogenic and vasculogenesis factor, which is implicated in both DR and DN and also participates in the progression of albuminuria (Caldwell, 2003). In DR, VEGF is involved in the neovascularisation of PDR and plays a pivotal role in the retinal microvascular disease. Therefore, it has been proposed as an exciting target for therapeutic intervention in DR (Caldwell, 2003).

VEGF is involved in the progression of DN due to the reduction of hyperfilteration albuminuria and glomerular hypertrophy by neutralisation (Hovind et al., 2000; Flyvbjerg, 1998). Consistently, there was evidence which demonstrated that VEGF is up-regulated in the diabetic kidneys of diabetic animal models and also contributes to the progression of albuminuria (Chen et al., 2008). In patients with diabetes, VEGF is increased in both their urine and plasma. This phenomenon has been discussed in a study by Hovind (2000), who showed that plasma levels of VEGF were significantly increased in DN patients compared to patients with normalbuminuria. With regards to this, they suggest that VEGF is increased early in the course of DN in men with T1DM. A marked decrease in albuminuria of diabetic animals has been established through inhibition of VEGF activity by neutralising antibodies or small molecule inhibitors of VEGF receptor kinase in animal studies (Virese et al., 2001; Sung et al., 2006).

Taken together, it is noticeable that TGF-β1, CTGF and VEGF could be potential markers for diabetic complications and future therapeutic strategies might be based on their activity. For instance, anti-TGF-β1 treatments could counter the matrix accumulation. Therefore, strategies could reduce albuminuria by normalising over-activity of CTGF and VEGF signalling (Ziyadeh et al., 2008). However, it is very important to point out that any therapeutic approach should have normal levels of

activity for these signalling pathways and they should not be much lower than normal. This is because a basal activity for each is necessary to make the optimal homeostasis of all types of glomerular cells (Lindenmeyer et al., 2007). It is vital for anti-TGF-β1 strategies to be aware of the possible external inhibitions of the inflammatory properties of TGF-β1 (Ziadeh, 2008). One way to overcome this issue is to recognise other molecules as potential therapeutic markers in the TGF-β1 signalling pathway instead of inhibiting the whole signalling pathway.

NSA2 is also a new marker for diabetic complications which was recently reported by Shahni et al. (2011). NSA2 is a putative cell cycle regulator in mammalian cells which became elevated in the kidney of a GK rat, a spontaneous model of T2DM. Shahni et al. (2011) showed for the first time that renal and circulating NSA2 levels are increased in the presence of HG in the experimental models of diabetes. In DN patients with albuminuria, NSA2 is elevated in their peripheral blood. They concluded that the circulating NSA2 mRNA levels were related to renal impairment within the patient population independent of other risk markers and it may also play a role in the pathology of DN.

In the previous chapter we demonstrated that renal CRYM mRNA and protein levels were increased in STZ-induced diabetic mice. Previous studies have shown that CRYM is increased in cultured mesangial cells in response to glucose and the diabetic GK rats (Al-kafaji and Malik, 2010). Therefore, CRYM shows an increase in experiments like other putative biomarkers mentioned above such as NSA2, TGF-β1, CTGF and VEGF, all of which are increased in DN; for example, in circulating urine and/or renal cells. Therefore CRYM may be a new biomarker for diabetic complications.

Aims and objectives of this chapter

The main objective of this chapter was to evaluate circulating CRYM mRNA as a biomarker of DN and DR. The specific aims were as follows:

1) To detect CRYM mRNA in human blood

2) To quantify the mRNA levels of circulating CRYM mRNA relative to the reference gene from T2D patient samples with retinopathy

3) To determine the best reference gene for quantification of human blood mRNAs

4) To verify the circulating CRYM mRNA levels in type 2 DN patients

Two sets of patient samples were used, which had been collected separately for this study:

Diabetic retinopathy patient samples (DR): This set comprised of 36 patients from the study 07/H0806/120 recruited by Dr Sobha Sivaprasad (Section 2.5), of which 5 patients had no retinopathy and were used as controls (T2D with > 10 years duration of diabetes) and 31 patients had progressive retinopathy (T2D with NPDR and PDR respectively; Section 2.5).

Diabetic nephropathy patient samples (DN): Comprised of 99 patients with T2D, of which 30 patients had no nephropathy and 69 patients had DN. These samples were collected from SEEDA/JJ study (undertaken by Dr Malik and Professor Gnudi) and has been previously described (Section 2.5).

4.3. Results

4.3.1. Detection of CRYM mRNA in human blood

There are no previous reports of CRYM expression in human blood; cDNA was synthesised from RNA (Section 2.6.4) to determine whether CRYM is expressed in the blood of DN patients, RNA was isolated from whole blood (Section 2.6.1), cDNA was synthesised and human CRYM primers (Section 3.3.2) were used to amplify the CRYM gene (Figure 17). The expressed 62 bp CRYM PCR product could be detected in blood samples of patients with DN, suggesting that CRYM is expressed in human whole blood.

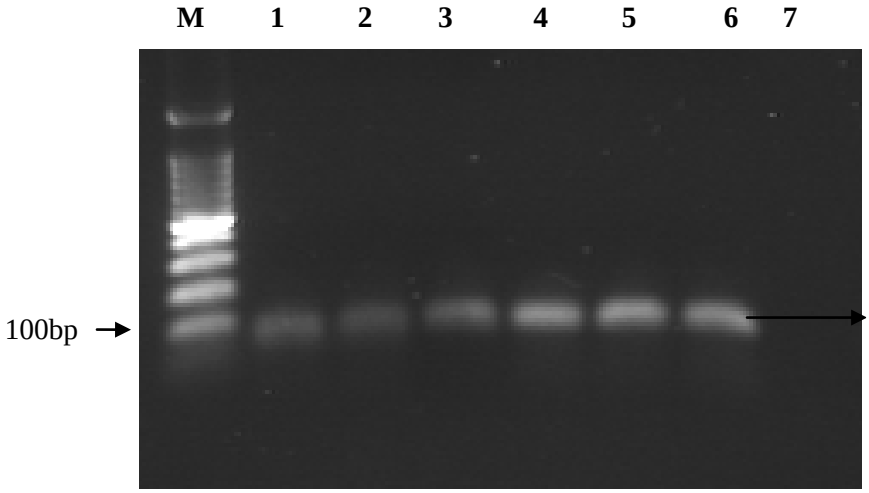

Figure 17. mRNA expression of human CRYM in whole blood.
Total RNA (1µg) was extracted from whole blood of patients with and without diabetic nephropathy. The RNAs were reverse transcribed to cDNA and amplified by qPCR with hCRYM F1 and hCRYM R1 primers. M: 100 bp ladder, lane 1-6: DN cDNAs, lane 7: negative control.

.

4.3.2. Circulating CRYM mRNA levels in type 2 diabetic retinopathy patients

CRYM mRNA levels were investigated in T2D patients with and without retinopathy. Samples were selected from the study 07/H0806/120, recruited by Dr Sobha Sivaprasad (Section 2.5). All the DR samples had been collected in PAXGENE tubes and RNA had been prepared by Dr Asif Butt, St Thomas' Hospital. cDNA corresponding to the set had also been previously prepared by Dr Shahni (KCL). The control samples from a separate SEEDA/JJ study were selected and converted to cDNA by Dr Shahni. This was used to determine circulating CRYM mRNA levels relative to GAPDH by measuring CRYM copy numbers and C_T values using qPCR.

- ***Absolute quantification of CRYM mRNA in the circulating blood of diabetic retinopathy patients, using qPCR* standards**

CRYM copy numbers were quantified with each sample being carried out in triplicate using qPCR (Appendix 6). For each replicate sample, the values of both CRYM and GAPDH were extrapolated from the respective melting curve and standard curve.

CRYM copy numbers showed a huge variation in each replicate in both DR and the control group. We found that CRYM mRNA levels were low in the blood samples and CRYM copy numbers ranged from non-detectable to several thousands (Table 17a). As shown in table 17a, CRYM copy numbers ranged from high (93650) to non-detectable (0) showing variability in their expression.

GAPDH mRNA levels were expressed more consistently in comparison to CRYM mRNA levels and their expression was much higher than CRYM mRNA levels (Table 17a). However, there was a major difference in the DR group when compared to control, as there was less RNA in the control samples. Table 17a shows that the range of GAPDH copy numbers was between 500-10,000 in the control group, whereas the range in the DR group was more than 10,000.

Table 17a. Range of CRYM and GAPDH copy numbers in all patients with and without retinopathy

Name	Range	Control	DR
CRYM copy numbers	ND	0/5	1/25
	<100	2/5	13/25
	>100-10,000	3/5	11/25
GAPDH Copy numbers	<500	1/5	0/25
	500-10,000	4/5	0/25
	>10,000	0/5	25/25

We also examined the frequency distribution of both CRYM and GAPDH copy numbers from the entire data. The frequency distributions of both CRYM and GAPDH copy numbers were found to be positively skewed, due to the high variation of both CRYM and GAPDH copy numbers. Figure 18a showed that mean and standard deviation for both CRYM and GAPDH values were slightly higher as there was a larger concentration at the lower end of the scores.

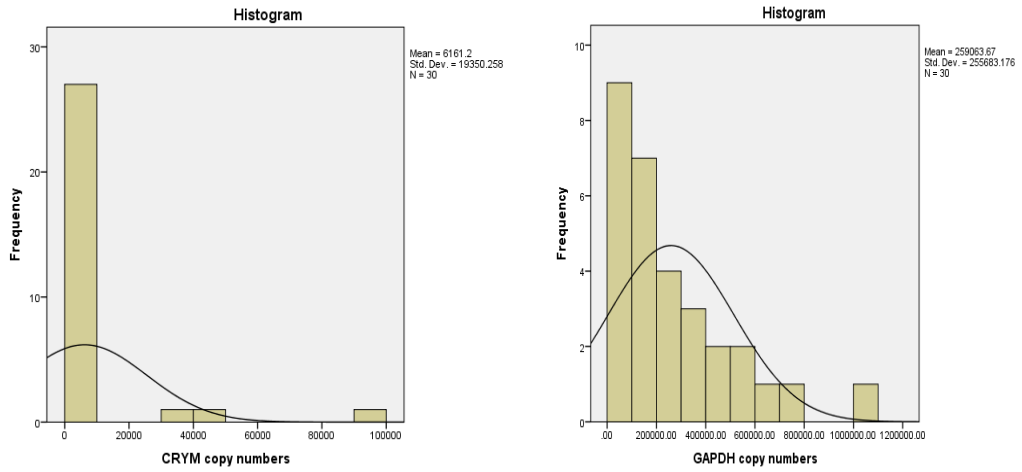

Figure 18a. Frequency distribution of CRYM and GAPDH values in patients with and without retinopathy.
Skewed distribution was obtained for both CRYM and GAPDH values. The mass distribution was concentrated on one side of the figures. The frequency distribution of both CRYM and GAPDH values showed a positive skew.

We also measured CRYM copy numbers relative to GAPDH and the data were analysed using SPSS 20 with results being expressed as mean ± standard deviation (Table 17b). A student's *t* test analysis was performed with DR as the grouping variable and CRYM copy numbers as test variables to test for significant differences between groups with no DR (n= 5) and DR (n= 31). Error bars were then generated to represent the trend of the mean CRYM ratio in the respective types of diabetes. The ratio of most samples was very low due to low expression of CRYM mRNA levels. As described previously, our data were positively skewed. Therefore, our data were log transformed to achieve a symmetric distribution (Figure 18b). An analysis of log CRYM mRNA copy numbers in DR patients versus those without retinopathy for the whole data set showed a significant decrease ($P<0.001$; Table 17b) in CRYM copy numbers in DR patients (-3.40 ± 1.04) compared to patients with no DR (-1.16 ± 0.53).

Table 17b. Relative copy numbers and log copy numbers of CRYM in all patients with and without retinopathy

Patient data set	Condition	N	CRYM copy number relative to GAPDH±SD	Log CRYM copy number relative to GAPDH±SD
All patients	No DR	5	0.12 ± 0.13	-1.16 ± 0.53
	DR	31	0.001 ± 0.002	-3.40 ± 1.04**

Circulating CRYM mRNA copy numbers relative to GAPDH mRNA copy numbers were detected in all type 2 diabetic patients and log values were calculated. No DR: No diabetic retinopathy, used as control, DR: Diabetic retinopathy. **P<0.001

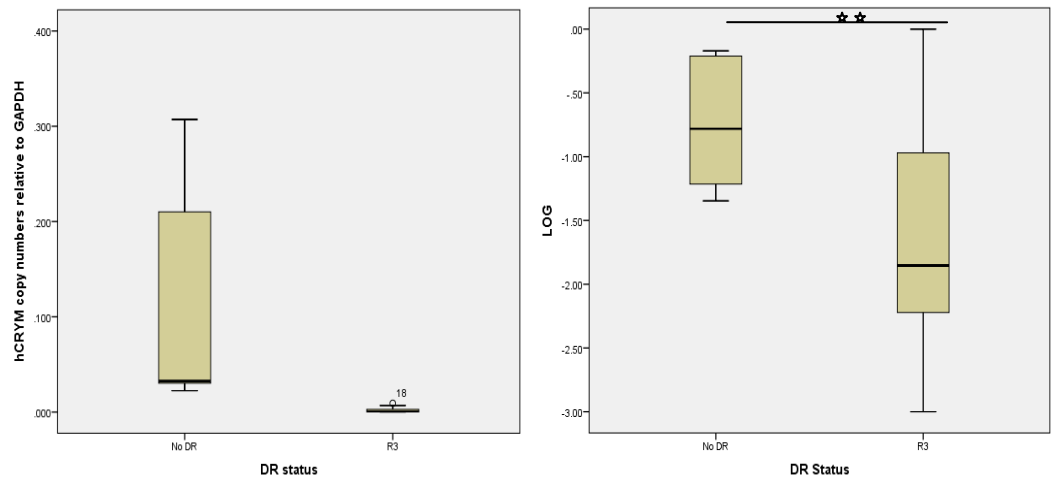

Figure 18b. CRYM mRNA copy numbers in circulating blood from patients with diabetic retinopathy.

A) Comparison of diabetic patients without retinopathy (No DR, n= 5) to those with retinopathy (DR, n= 31; -3.40 ± 1.04 vs. -1.16 ± 0.53) is illustrated as a boxplot (SPSS 20). B) A student's *t test* of the transformed values showed a highly significant difference in CRYM mRNA copy numbers of patients with and without retinopathy. **P<0.001

.

● ***Relative quantification of CRYM mRNA in circulating blood of DR patients, using the comparative C_T method, i.e., $2^{-\delta\delta C}{}_T$ method***

In this part, we used $C_T$values for relative quantification as well as absolute quantification. Relative quantification is the second most widely used method for processing qPCR data, where the PCR signal of the desirable gene in the experimental group is compared to that of a calibrator group such as the control group (Livak & Schmittgen, 2001). The main aim of relative quantification is to determine relative

difference in gene regulation among various groups. Conversely, absolute quantification is appropriate for resolving the exact number of gene copies present in a group. Thus, the comparative C_T method was used in this experimental study.

For this purpose, the average threshold cycle number (C_T) of the triplicates obtained for every sample and the C_T of target gene (CRYM) to control gene (GAPDH) was measured. Next, the Delta Delta C_T method was used with respect to the calibrator group (patients with only T2D, with a mean age of 50 ± 15 years and with > 10 years duration of diabetes). The fold difference in CRYM values was then worked out to determine the difference in CRYM ratio at different states, using the following equations (Livak & Schmittgen, 2001):

$$\delta C_T = \text{Average } C_T \text{ CRYM} - \text{Average } C_T \text{ GAPDH}$$

$$\delta\delta C_T = \delta C_T \text{ of specific retinopathy stage} - \text{Average } \delta C_T \text{ of calibrators}$$

$$\text{Fold difference in CRYM ratio} = 2^{-\delta\delta CT}$$

The fold difference in CRYM ratio (mean ± SD) at different stages of DR for each sample was then determined (Appendix 7). The DR risk factors of the respective data were examined for significant differences with DR status. The data were analysed statistically using SPSS 20 to assess the significance of the differences noted in mean fold change of CRYM values with severity of DR and was log-transformed to achieve a normal distribution.

A student's *t* test analysis was performed with DR as the grouping variable and CRYM fold difference as a test variable. The student's *t* test analysis showed a significant difference of CRYM log values between DR groups when compared with controls (-1.71 ± 1.77 vs. 1 ± 0.81, P<0.001, Table 17c). Patients with DR showed a 0.5-fold decrease in the mean fold difference in the circulating CRYM mRNA values when compared with controls. The data showed the same trend in the fold-difference of CRYM ratio which was observed previously with CRYM copy numbers (Figure 18c).

Table 17c. Fold difference in CRYM ratio with respect to calibrators, at varying stages of diabetic retinopathy for the complete data set

Patient data set	Condition	N	CRYM values relative to GAPDH±SD	Log CRYM values relative to GAPDH±SD
All patients	No DR	7	24 ± 29.63	1 ± 0.81
	DR	41	1.17 ± 2.57	-1.71 ± 1.77**

CRYM mRNA C_T values relative to GAPDH C_T values were calculated in all type 2 diabetic patients and log values were calculated. No DR: No diabetic retinopathy, used as control, DR: Diabetic retinopathy. **P<0.001

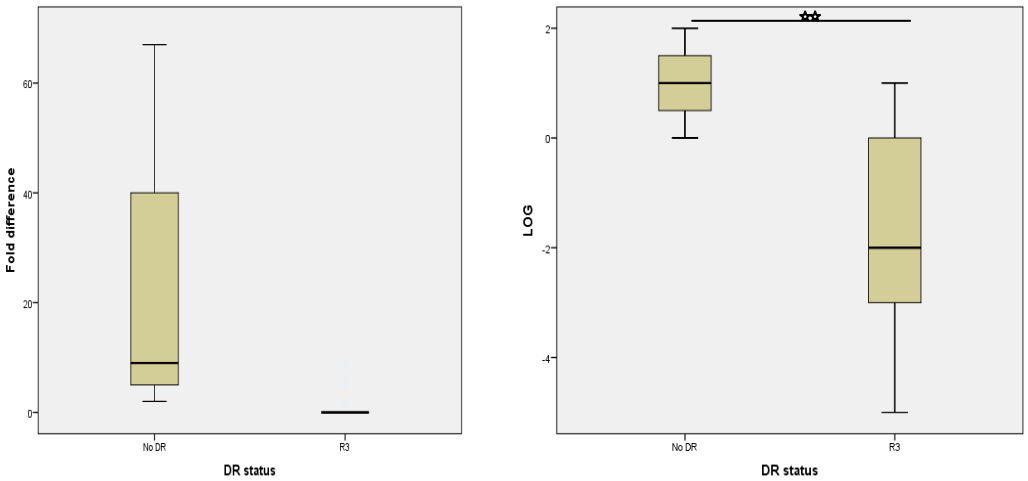

Figure 18c. CRYM mRNA C_T values in the circulating blood from patients with diabetic retinopathy.

A) Comparison of diabetic patients without retinopathy (no DR, n= 7) to those with retinopathy (DR, n= 41; -1.71 ± 1.77 vs. 1 ± 0.81) is illustrated as a box plot (SPSS 20). B) A student's *t* test of the transformed values showed a highly significant difference in CRYM mRNA C_T values of patients with and without retinopathy. **P<0.001

● ***Overall trend in the circulating blood CRYM mRNA regulation in DR***

Circulating CRYM mRNA expression was decreased in patients with DR compared to patients with no DR in both absolute (Figure 18b) and relative (Figure 18c) quantification. The relative quantification data support the absolute quantification data and they both demonstrated the same trend as each displayed a down-regulation of CRYM mRNA expression in patients with DR compared to controls.

GAPDH mRNA levels were not constant as they exhibited an altered expression in patients with PDR compared to patients with no DR. This could be due to different

strategies used to store blood and extracted RNA. However, it could also be because GAPDH is not a suitable reference gene for RNA normalisation from blood samples.

4.3.3. Determination of the most stable reference gene for blood RNA

To evaluate the most stable and reliable reference gene for our DN data, endogenous gene expression stability was measured using the geNorm and NormFinder Programs (Vandesompele et al., 2002). Both geNorm and NormFinder are the most popular algorithms for identifying the optimal normalisation gene for a set of candidate reference genes, by ranking them for normalisation according to their expression stability.

Gene expression was quantified by normalisation for three different widely used endogenous control genes: β-Actin, PGK and PPIB (Table 5a, section 2.7). The expression patterns for these three reference genes were determined in 6 whole blood samples from T2DM patients with and without DN using qPCR (Table 18). They represented RNAs from each of the two quantitative methods. geNorm and NormFinder software were used to normalise the expression patterns, independent of mRNA expression levels. As shown in table 18, normalising the data to β-actin introduces large and variable errors into the analysis. Both programs picked two genes with the lowest M value which was the most stable, and conversely the gene with the highest M value was the least stable control gene. For whole blood samples, PGK (M= 0.54) were selected as the most stable genes and β-Actin (M= 0.818) was calculated as the least stable gene. In the following study, we have used PGKvalues as the internal control for normalising our data.

Table 18. Quantification of reference gene values in circulating blood of type 2 diabetic patients with and without nephropathy

Samples	Group	PPIB	PPIB	Ave	PGK	PGK	Ave	actin	actin	Ave
18	T2DN	6.85	9.55	8.20	80.30	68.90	74.60	$2x\ 10^3$	$8x10^3$	$5x10^3$
51	T2DN	14.50	17.50	16.00	73.20	68.90	71.05	$5x10^3$	$7x10^2$	$2x10^3$
282	T2DN	15.00	25.30	20.15	95.00	70.80	82.90	0	0	0
172	T2D	17.10	38.40	27.75	84.00	73.60	78.80	0	0	0
131	T2D	24.50	14.10	19.30	96.20	94.30	95.25	0	0	0
140	T2D	12.60	17.80	15.20	111.00	83.20	97.10	0	0	0

PPIB, PGK and β-actin copy numbers were determined using qPCR. For each group, pre-used cDNAs was used and the average of each reference gene was quantified from each sample. T2DN: type 2 diabetic nephropathy, T2D: type 2 diabetes.

4.3.4. Quantification of CRYM mRNA in circulating blood of patients, with and without nephropathy

In this part of the study, CRYM mRNA levels in the circulating blood of type 2 diabetic patients with and without nephropathy were compared. To determine circulating CRYM mRNA levels, selected samples from the SEEDA/JJ study (Section 2.5) were used to measure CRYM mRNA copy numbers relative to PGK. A qPCR was carried out to measure the circulating CRYM copy numbers and the values were normalised by using the PGK. All samples were run in triplicate (Appendix 8).

CRYM mRNA levels expressed were low in the circulating blood of patients. As shown in table 19a, CRYM copy numbers ranged from the highest (106) to the lowest (0) in whole data. PGK values also showed a constant expression in all the samples and their range was from 10 to 68. Thus, normalising PGK improved the data as PGK values showed more stability in their expression than we had found for GAPDH (Table 19a). However, PGK copy numbers were very low in circulating blood.

Table 19a. Range of CRYM and GAPDH copy numbers in all patients with and without retinopathy

Name	Range	Control	DN-NA	DN-A
CRYM copy numbers	ND	2/30	0/31	1/38
	<10	18/30	16/31	28/38
	10-110	10/30	15/31	9/38
GAPDH Copy numbers	<10	8/30	28/30	37/38
	10-50	22/30	2/30	1/38
	50-100	0/30	1/30	0/38

We also examined the frequency distribution of both CRYM and PGK copy numbers from the entire data. The frequency distributions of both CRYM and PGK copy numbers were found to be positively skewed, as the tail was longer on one side (Figure 19a). This was because of high expression of CRYM and PGK in a few samples. Therefore, this affected the data distribution. CRYM values showed a mean of 13.2 and a standard deviation of 21.5 while PGK values had a mean of 6.5 and a standard deviation of 11.9. As figure 19a shows, the standard deviation for PGK values was 1.8-fold lower than CRYM values.

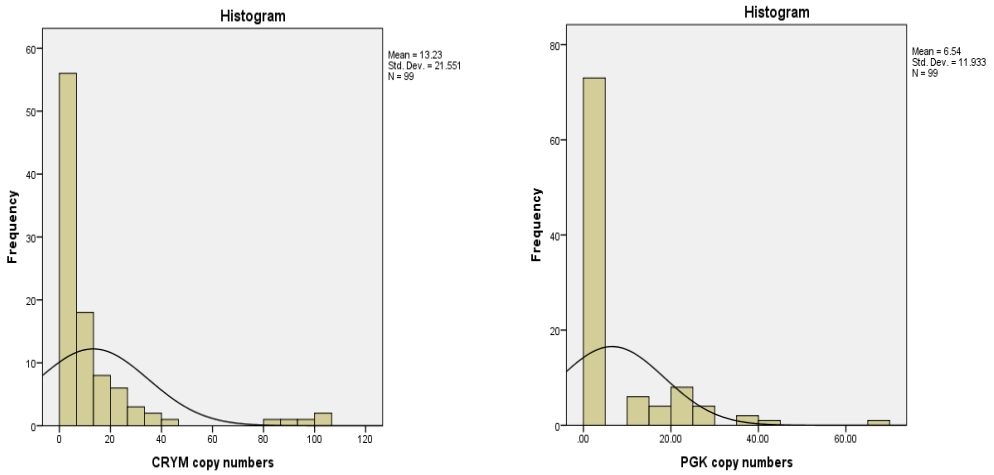

Figure 19a. Frequency distribution of CRYM and PGK values in patients with and without retinopathy.
Skewed distribution was obtained for both CRYM and PGK values. The mass of distribution was concentrated on one side of the figures. The frequency distribution of both CRYM and PGK values showed a positive skew.

A comparison of patients with no DN (n= 30) and patients with DN (n= 69) showed a significant 7.4-fold (P<0.001) increase in patients with DN (57.51 ± 98.17) compared to patients with no DN (7.76 ± 24.95; Table 19b). As the patient data were not normally distributed, the data were log transformed to achieve a symmetrical distribution (Figure 19b).

Table 19b. Relative copy numbers and log copy numbers of CRYM mRNA in patients with type 2 diabetes nephropathy and without nephropathy

Patient data set	Condition	Number of patients	CRYM copy number relative to PGK±SD	Log CRYM Copy number relative to PGK±SD
All patients	Control	30	7.76 ± 24.95	-0.17 ± 0.97
	DN	69	57.51 ± 98.17**	1.29 ± 0.71**

Circulating CRYM mRNA copy numbers relative to PGK copy numbers were determined in all patients and log values were calculated. DN: diabetic nephropathy. **P<0.001

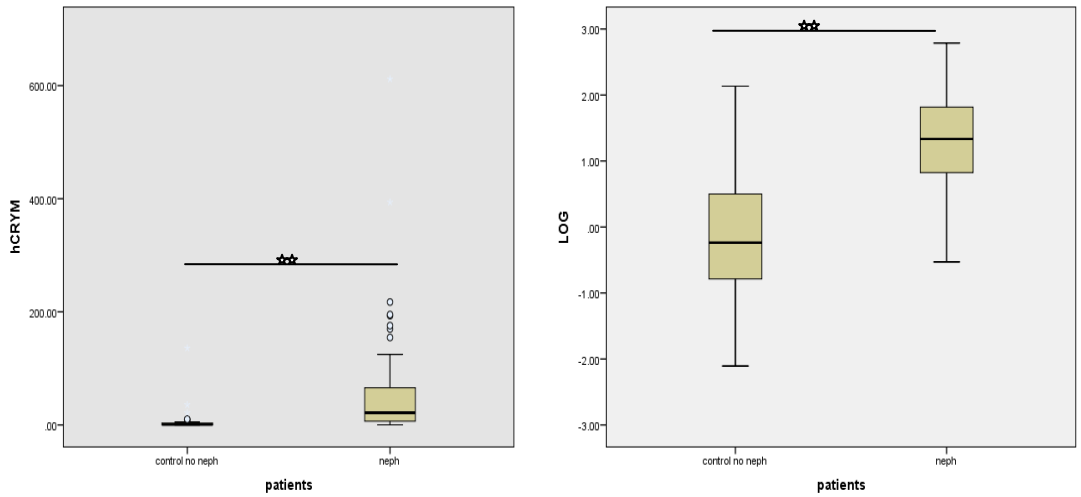

Figure 19b. CRYM mRNA copy in the circulating blood of patients with and without diabetic nephropathy.

A) Comparison of diabetic patients without nephropathy (control no neph, n= 30) to those with nephropathy (neph, n= 69; 57.51 ± 98.17 vs. 7.76 ± 24.9 and P<0.001) is illustrated as a boxplot (SPSSS 20). CRYM distribution is skewed and is increased in neph versus control no neph. B) The data were log transformed. A student's *t* test of the transformed values showed a highly significant difference. **P<0.001

For further analysis, our patients with a history of albuminuria in this study were divided into groups: (1) Control: Patients with type 2 diabetes with > 10 years duration of diabetes, respectively, without history of albuminuria, with normal renal function, normal blood pressure (<130/80 mmHg) and taking no antihypertensive agents. (2) Normoallbuminuria: ACR < 2.5 mg/mmol for men (albumin extraction rate AER <25 mg/day) and ACR < 3.5 mg/mmol for women (AER < 35 mg/day). (3) Albuminuria: ACR > 2.5 mg/mmol for men (AER >25 mg/day) and > 3.5 mg/mmol for women (AER > 35 mg/day). GFR was evaluated using the Modification of Diet in Renal Disease (MDRD) formula.

In order to see if CRYM could be a potential predictive or diagnostic marker, the circulating CRYM mRNA copy numbers were analysed in DN patients with normalbuminuria (DN-NA) and DN patients with microalbuminuria or proteinuria (NA-A). The data showed that patients with DN-NA had a significant 11.7-fold higher CRYM mRNA expression in their blood compared to diabetic controls (Table 19c and Figure 19c).

Table 19c. Relative copy numbers and log copy numbers of CRYM mRNA in patients with nephropathy

Patient data set	Condition	Number of patients	CRYM copy number relative to PGK±SD	Log CRYM Copy number relative to PGK±SD
Patient by diabetes types	T2D	30	7.67 ± 24.55	-0.14 ± 0.97
	DN-NA	31	90.32 ± 133.68*	1.48 ± 0.76**
	DN-A	38	31.79 ± 44.22*	1.13 ± 0.63**

Circulating CRYM mRNA copy numbers relative to PGK mRNA copy numbers were determined in patients with nephropathy and log values were calculated. DN-NA: nephropathy patients without microalbuminuria and DN-A: nephropathy patients with microalbuminuria. *P<0.05 and **P<0.001.

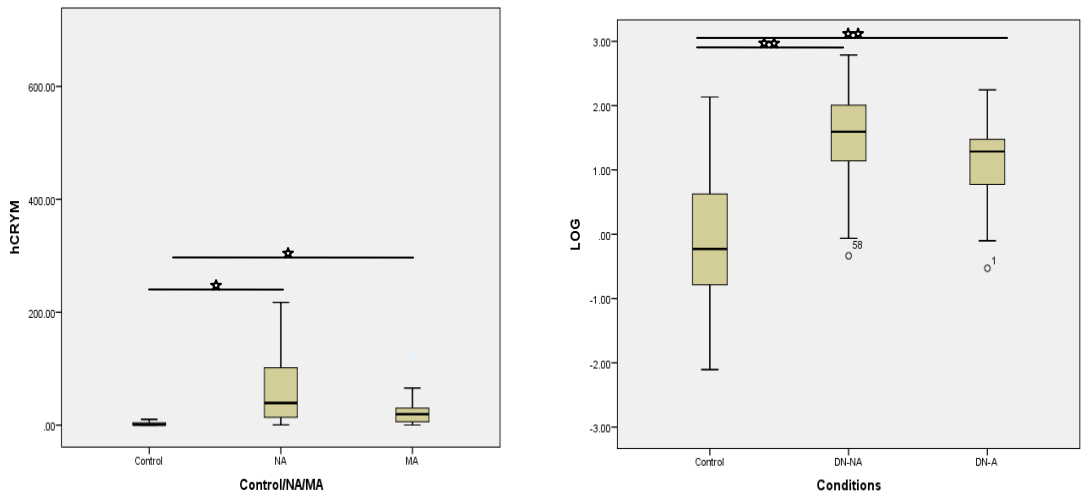

Figure 19c. CRYM mRNA copy number in the circulating blood of diabetic patients with and without nephropathy according to their blood function.

A) Comparison of nephropathy patients with microalbuminuria or proteinuria (DN-A, n= 38) and nephropathy patients who had reverted to normallbuminuria (DN-NA, n= 31) with diabetic controls (n= 30). The data are illustrated as a boxplot (SPSS 20). Circulating CRYM mRNA copy numbers were increased in patients with normalbuminuria (DN-NA) compared to control (90.32 ± 133.68 vs. 7.67 ± 24.55). B) The data were log transformed. A student's *t* test of the transformed values showed a significant difference in CRYM mRNA copy numbers. *P<0.05, **P<0.001

● ***Overall trend in circulating blood CRYM mRNA regulation***

Circulating CRYM mRNA regulation showed a 7.4-fold increase in patients with nephropathy compared to patients without nephropathy (57.51 ± 98.17 vs. 7.76 ± 24.95, P <0.001; Table 19b). In these patients, circulating CRYM mRNA levels was 2.8-fold higher in those receiving medication who had reverted to microalbuminuria (DN-NA, n= 31) compared with those receiving medication with microalbuminuria (DN-A, n= 38; 90.32 ± 133.68 vs. 31.79 ± 44.22, P<0.05; Table 19c).

In summary, the results showed that circulating CRYM mRNA levels were up-regulated in T2DN-NA even after adjusting for predictor variables. These data suggest that there might be an association between circulating CRYM mRNA levels and DN as they significantly increase in DN patients. However, CRYM mRNA levels were reduced in DN-A patients and this reduction suggested a further biological role for CRYM in the progression of kidney failure. Thus, this result suggests the need for future studies to determine the function of CRYM in the circulating blood of patients with kidney failure.

1) The association of clinical parameters in diabetic retinopathy and diabetic nephropathy patients

Parallel to the demonstration of circulating CRYM mRNA in each set, clinical parameters were investigated for each set separately:

● ***Diabetic retinopathy (DR set)***

Clinical parameters were also investigated in patients with type 2 diabetes with > 10 years duration of diabetes and without retinopathy as controls (No DR, n= 5), type 2 diabetes with severe retinopathy (DR, n= 31). The clinical parameters of the respective data were examined for significant differences with DR status. Student's *t* test analysis was performed with DR as the grouping variable and age, gender, diabetes duration, BMI, HbA1c, Systolic blood pressure, Diastolic blood pressure and cholesterol as test variables using SPSS 20.

DR patients had a significant association with duration of diabetes; they had a lengthy duration of diabetes compared to control groups (17.10 ± 9.37 vs. 12.17 ± 3.86, P<0.05, Table 20) and they had a significant correlation with HbA1c (8.6 ± 1.67, P<0.05). The DR groups also suffered from kidney disease as they had higher ACR

(51.89 ± 50.26, P<0.001) and lower eGFR compared to controls (57.71 ± 23.42, P<0.05). It is noteworthy that the DR groups had 52% more ACR compared to No DR group (Table 20).

Table 20. Baseline characteristic of diabetic patients with and without retinopathy

Parameters	**NO DR (n=5)**	**DR (n=31)**
Age (years)	64.86 ± 12.26	65.05 ± 11.08
Gender (F:M)	2:3	17:14
Diabetes duration (years)	12.17 ± 3.86	17.10 ± 9.37*
BMI (kg/m^2)	32.55 ± 2.92	32.35 ± 7.68
HbA1c (%)	6.45 ± 2.11	8.6 ± 1.67*
ACR (mg/mmol)	0.97 ± 0.54	51.89 ± 50.26**
eGFR (ml min^{-1} 1.73 $m^{-2)}$	79.83 ± 25.41	57.71 ± 23.42*
Systolic Bp (mmHg)	133.57 ± 17.67	161.66 ± 135.57
Diastolic Bp(mmHg)	71.43 ± 11.25	99.32 ± 145.07
Cholesterol (mmol/L)	4.2 ± 4.8	5.8 ± 4.9

BMI: body mass index, HbA1c: Haemoglobin A1c, ACR: albumin/creatinine ratio, eGFR: glomerular filtration rate, Bp: blood pressure, *P<0.05, **P<0.001

● ***Diabetic nephropathy (DN set)***

As previously described, DN set was only composed of T2D (n= 30) and T2DN (n= 69). For the control group, there were 17 women and 13 men with an average age of 56 ± 12 years and slightly overweight (BMI of 29 ± 8 kg/m2, Table 21). Despite diabetes, their blood glucose was controlled and they had good blood pressure control (126 ± 20 mmHg). They also had normal renal function as their ACR, eGFR and albuminuria were all within a normal range. In the patient group with DN, there were 34 women and 35 men with an average age of 63 ± 11 years (an average of 10 years older than the controls). Their blood glucose was high as their HbA1c was higher than the normal average (22 ± 32%) and their blood pressure was higher than the normal average (132 ± 24 mmHg). Their ACR was significantly higher when compared with the normal group (15.92 ± 41.92 vs. 1.36 ± 1.62, $P<0.001$) and they suffered from kidney disease as their ACR and albuminuria were higher than the normal range and eGFR was lower than controls (Table 21).

Clinical parameters were also examined separately in DN patients with a history of albuminuria. Patients with T2DN-NA (n= 31) and T2DN-A (n= 38) were older than controls (n=30). There were less male in the T2DN-NA group and more female in the T2DN-A group (Table 21). The T2DN-A group had higher blood pressure compared to the T2DN-NA group and their BMI and HbA1c were nearly identical. Both groups had nephropathy as they had higher ACR and lower eGFR compared to the control group. However, the most important difference between DN-NA and DN -A was the difference in their ACR as they had 24% more ACR compared to the DN-NA group (Table 21). This implies that the T2DN-A group is progressing more speedily towards end stage renal disease, compared to the T2DN-NA group, despite both groups taking medication.

A student's t test analysis was performed with DN as the grouping variable and age, gender, BMI, HbA1c, SBP and DBP and duration of diabetes as test variables using SPSS 20. Compared with diabetic controls, patients with DN showed a significant increase with their age, duration of diabetes and their ACR ($P <0.05$; Table 21). There was no significant difference between groups in terms of sex, BMI or eGFR.

Table 21. Baseline characteristic of diabetic patients with and without nephropathy

Parameters	Control (n= 30)	DN(Full Set) (n= 69)	DN-NA (n= 31)	DN-A (n= 38)
Age (years)	56.45 ± 12.33*	63.03 ± 11.72*	57.76 ± 11.03	66.79 ± 12**
Gender (F:M)	17:13	34:35	15:16	19:19
Diabetesduration (years)	14.66±27.41**	34.39±46.77**	35.16 ± 49.69*	32.89±44.57*
BMI (kg/m^2)	29.93 ±8.46	29.55 ± 10.74	30.21± 10.96	29.08±10.54
HbA1c (%)	13.38±22.24	22.18 ± 32.11	22.65 ± 31.65	21.35±32.59
ACR (mg/mmol)	1.36±1.62**	15.92±41.92**	12.52 ± 30.51	36.73±55.27*
eGFR($ml\ min^{-1}\ 1.73\ m^{-2)}$	102.38±25.56	64.41 ± 16.5	67.16 ± 18.17	62.61±32.26
Systolic Bp (mmHg)	126.1±20.49	132.56± 24.84	128.83±23.96	135.86±25.41
Diastolic Bp (mmHg)	77.2± 9.38	73.17± 14.55	73.86 ± 15.8	73.02±13.67

BMI: body mass index, HbA1c: Haemoglobin A1c, ACR: albumin/creatinine ratio, eGFR: glomerular filtration rate, Bp: blood pressure, *P<0.05, **P<0.001

4.4. Discussion

In this chapter, we demonstrated for the first time that CRYM mRNA can be detected in the circulating cells of patients with DN. We also found that circulating CRYM mRNA levels were decreased in patients with DR. However, CRYM mRNA levels showed an increase in patients with DN.

Circulating CRYM mRNA levels were measured in patients with type 2 DR (n= 31) and compared with patients with no DR (n= 5). CRYM copy numbers showed a large variation in their expression and CRYM copy numbers ranged from non-detectable to several thousand. GAPDH values were also not detected at constant levels. This difference in GAPDH levels in both the control and the DR groups is likely to be due to different RNA samples, as the samples for the control and the DR groups were collected by separate students and stored differently.

Statistical analysis showed that circulating CRYM mRNAs were significantly decreased in patients who had severe retinopathy, compared with patients with no DR. Both absolute and relative quantification methods showed the same trend. The student's *t* test analysis revealed a significant relation between DR and ACR. There was also a significant correlation in patients with DR with other risk factors such as the duration of diabetes, HbA1c and eGFR.

In the DN set, we found that circulating CRYM mRNA levels were significantly elevated in patients with T2DN (n= 69) compared to diabetic controls without DN (n= 30). CRYM copy numbers were more consistent in DN data when compared to CRYM levels in DR data. However, their expression was still very low in circulating cells.

Circulating CRYM mRNA levels were increased 7.4-fold in patients with T2DN and this effect was strongest in patients with well controlled nephropathy compared to those with proteinuria. This finding was contrary to our previous findings in the DR set. However, we used a different reference gene for the DN set, and samples were stored in different ways.

In the DN set, there were some correlations between the patients with DN risk factors. All patients with T2D, T2DN-NA and T2DN-A had a significant correlation with the duration of diabetes. Patients with DN-A as well as patients with no DN displayed a

correlation with age and ACR. The increase of circulating CRYM mRNA levels in patients with DN in this study is interesting however as we do not have CRYM values for healthy controls, it is difficult to make a conclusion.

As circulating CRYM mRNA levels increased in patients with DN and their mRNA expression pattern is similar to NSA2, it raises the theory that CRYM might be acting as a putative biomarker. However, we cannot confirm these results as circulating CRYM mRNA levels were expressed at low levels in whole blood. Furthermore, differences in how patient samples were stored may have affected the data. Thus, these results are an initial finding and they require further confirmation.

An early determination of diabetic complications is not very applicable or useful. For instance, to detect DN in patients with diabetes requires urinary albumin extraction and declining GFR. However, these methods usually identify renal dysfunction only after a long duration of clinical silence when kidney damage has already begun (Glassock, 2010). Hence, it is necessary to discover new biomarkers that have predictive power. Emerging candidate biomarkers of renal and retinal dysfunctions contained markers of oxidative stress, inflammation, glomerular damage and endothial dysfunction.

There are some promising new biomarkers which all show an increase in patients with DN. One such example is a cysteine protease inhibitor which is known as cystain C. Cystain C is elevated in the serum and urine of patients with DN (Pucci et al., 2007; Oddoze et al., 2011). Jeon (2011) has reported that patients with macroalbuminuria have higher levels of cystain C in their serum and urine along with an increasing degree of albuminuria. They also showed a significant correlation with GFR, ACR, and sex (Jeon et al., 2011). A renal liver-type fatty acid-binding protein (L-FABP), was another biomarker which was detected as increased in patients with type 2 diabetes compared to healthy controls and this increase was associated with HbA1c, eGFR and cholesterol (Kamijo-Ikemori, 2011).

It was surprising, in the context of our investigation, that circulating CRYM mRNA levels showed a different trend in the DR set compared to the DN set. This converse trend might be as a result of using different reference genes for DR and DN sets as they were expressed at different levels. PGK was determined as the most stable and reliable reference gene. The frequency distribution of GAPDH and PGK in both data

showed that the expression of PGK levels is more consistent when compared with GAPDH and their standard deviation was lower than GAPDH. However, PGK was expressed at lower levels in circulating cells and their expression was close to CRYM expression.

It would have been ideal to repeat our DR experiments with PGK to see if the same trend was followed or not. However, it was not possible to repeat the experiments with PGK owing to a lack of samples. Therefore, it is unclear if this observation is indicative of different pathophysiological processes in DR and DN, or is because of an experimental alteration.

This was the first study of an examination of circulating CRYM mRNA levels in the whole blood of patients with diabetes. Owing to restrictions regarding Ethics Approval for this research, we could not determine levels of circulating CRYM mRNA in healthy controls. The inability to compare circulating CRYM mRNA in healthy controls versus diabetic patients makes it unclear whether or not circulating CRYM is associated with DN. Moreover, the low levels of CRYM mRNA expression in human whole blood samples suggest that it may not be a useful biomarker. Therefore, it remains to be established whether alteration in CRYM mRNA levels is a cause or a consequence of microvascular disease. Further studies should include the evaluation of circulating CRYM mRNA levels in fresh, healthy samples as a control.

Chapter 5

Are MOSC2 and MOSC1 glucose regulated genes both *in vivo* and *in vitro*?

Chapter 5. Are MOSC2 and MOSC1 glucose regulated genes both *in vivo* and *in vitro*?

5.1. Abstract

We previously identified MOSC2 as one of several hyperglycaemia-induced renal genes in the GK rat, and showed that it was regulated by glucose *in vitro* in HMCs. In the current chapter we investigated the expression of MOSC2 and its homolog MOSC1 in models of diabetes and patient samples to explore their roles in the pathophysiology of DN.

Kidneys (n= 3) were obtained from an acute STZ-induced mouse, and a β-*phb2* KO mouse. Additionally, human renal (mesangial, embryonic kidney, tubular) cells grown in NG (5mM) and HG (25mM) and blood samples from diabetes patients with and without DN (n= 13) were used. mRNA levels were determined using qPCR relative to reference genes, and protein location/abundance was determined using immunofluorescence. Functional analysis included N-hydroxylation assays.

MOSC2 mRNAs increased during hyperglycaemia in diabetic kidneys of STZ-induced diabetic mice and this increase was attenuated by treatment of diabetes ($P<0.05$). However, we could not find any change of renal MOSC2 expression in β-*phb2* KO mice. Immunohistochemistry revealed abundant expression of MOSC2 protein in HTC, and very low expression in HMCs. We also found that MOSC1 was not regulated by glucose both *in vivo* and *in vitro*. Surprisingly, in HG, MOSC2 mRNAs showed a slight decrease in cultured HTC whereas they showed a significant increase in HMCs and HEK293 cells. Upon evaluation of MOSC2/MOSC1 mRNA levels as potential biomarkers of DN, we could detect low levels of MOSC1 but there was no expression of MOSC2. Biochemical analysis of MOSC protein showed that the N-reductive activity was increased in diabetic conditions. Our data suggested that MOSC2 is a glucose-regulated gene and its glucose induction may be involved in glucose-induced pathways. However, we could not find any evidence that MOSC1 is regulated or altered. Circulating MOSC1 showed no changes in patients with DN, suggesting that MOSC2/MOSC1 are unlikely to be useful biomarkers for DN but may be involved in pathology of DN.

5.2. Introduction

Hyperglycaemia contributes to DN and is the hallmark for diabetes mellitus (Christine et al., 1995). For the purposes of investigating novel therapeutic targets for DN, several novel genes that are regulated in the presence of hyperglycaemia in rodent models of DN and in HMCs were identified (Malik et al., 1998). Besides CRYM, there are a number of known glucose-regulated genes, such as CTGF (Burns et al., 2006), serum glucocorticoid-regulated kinase (Feng et al., 2005), beta-defensin-1 (Page et al., 2003), NSA2 (Shahni et al., 2011) and MOSC2 (CDK7) (Malik et al., 2007).

In this chapter, we will investigate the expression and function of MOSC2, a putative thiol-related gene; characterised as glucose regulated gene *in vivo* and *in vitro*. MOSC2 (CDK7) was first identified by the Malik group in 1997. They used differential display to determine genes that showed altered expression in the kidneys of the GK rat during the development of diabetes. A number of novel genes designated as candidate diabetes-associated kidneys (CDK) were recognised by cloning; MOSC2 was one of several differentially expressed fragments from diabetic kidneys and named CDK7 (Table 22; Page et al., 1997).

A cDNA library of the kidneys from a GK rat was probed and represented the MOSC2 mRNA (Malik et al., 2007). From 100,000 screening clones, 5 clones which showed a strong hybridisation signal were sequenced. Sequencing showed that two clones of 440 bp and two clones of 770 bp were partial cDNAs of the largest clone (1330 bp), which was named rat MOSC2 (Malik et al., 2007).

Table 22. MOSC2 (CDK7) as one of 26 clones from diabetic rat kidneys.

Clone	Identity
CDK1	Lactate dehydrogenase
CDK2	NADH ubiquinone oxidoreductase 42KD subunit precursor
CDK3	Enach, alpha subunit
CDK4	Beta-defensin
CDK5	NADH ubiquinone oxidoreductase 42KD subunit precursor
CDK6	Megalin
CDK7	MOSC2
CDK8	Ubiquitin-like gene BC084728
CDK9	Phosphatase inhibitor
CDK10	Ubiquitin like novel
CDK101	Hepatom a derived growth factor
CDK102	H-protein
CDK103	16s Rrna
CDK104	Chemokine CXC 16
CDK105	Novel, now called NSA2
CDK106	Zfn1. Novel zinc finger protein
CDK107	Schlafen 4
CDK108	CRYM
CDK109	RM 16S rRNA
CDK120	RM cytochrome C oxidase subunit II
CDK121	RM NAD dehydrogenase subunit 5
CDK122	RM 16S rRNA
CDK123	RM cytochrome C oxidase subunit I
CDK124	RM cytochrome C oxidase subunit I
CDK125	RM cytochrome C oxidase subunit I
CDK126	RM cytochrome C oxidase subunit I

MOC2 (CDK7) was one of 26 clones isolated by differential screening which showed a strong hybridisation signal in the kidneys of GK rat (Page et al., 1997).

MOSC2 mRNA expression was measured in rat tissues using qPCR (Malik et al., 2007). They showed that MOSC2 mRNA expression is abundant in the rat brain, heart, kidney, liver, lung, spleen, stomach and urinary bladder. They also found that MOSC2 mRNA is expressed at higher levels in the liver, kidney and urinary bladder and is expressed at lower levels in the heart and spleen. Furthermore, to investigate the expression of MOSC2 mRNA in renal diseases, Malik et al. (2007) examined MOSC2 mRNA expression in the kidneys of GK as hyperglycaemic and Wistar as normoglycaemic rat models respectively. qPCR was used to precisely quantify mRNA expression of MOSC2 at different ages from the kidneys of both GK and Wistar rats. When compared with Wistar rats, GK rats are normoglycaemic at 6 weeks and progressively develop hyperglycaemia, being hyperglycaemic by 26 weeks. Conversely, Wistar rats remain normoglycaemic at all ages. Development of

hyperglycaemia lead to elevation in Rat MOSC2 mRNA levels, compared to their control age-matched Wistar rats (Figure 20a).

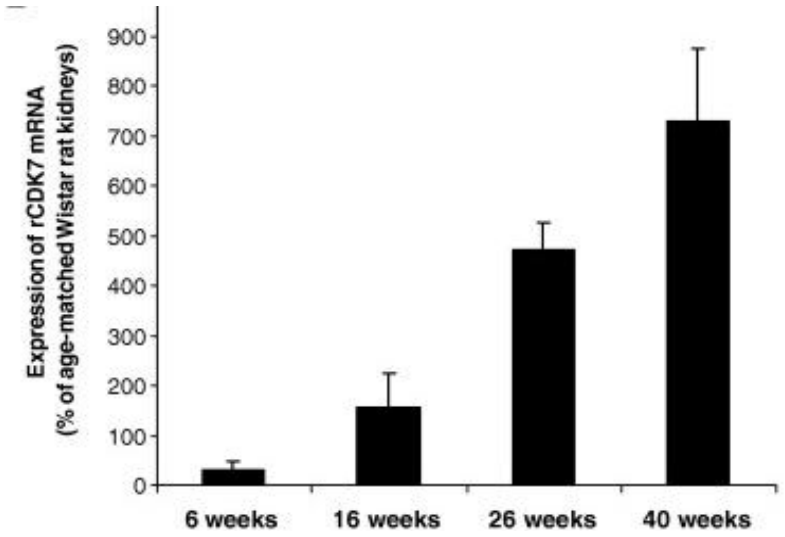

Figure 20a. Effect of hyperglycaemia on the expression of MOSC2 (CDK7) mRNA in the kidneys of a GK rat.
MOSC2 (CDK7) mRNA levels were quantitated in kidneys of GK rat at different ages using qPCR from at least two kidneys at each stage, with quantification being carried out in duplicate. The results are expressed as % values relative to those seen in age-matched Wistar rats (normoglycaemic controls). Taken from Malik et al., 2007.

Using Southern blot, Malik et al. (2007) found that MOSC2 is a highly conserved gene in humans and they identified a homologue of human MOSC2 using BLAST. A hypothetical protein FLJ20605, was a homologue of MOSC2 as it showed a high sequence similarty (84%) to rat MOSC2 when analysed by the IMAGE consortium (Accession No.BC011973). Human MOSC2 mRNA expression is abundant in both human foetal and adult kidneys as well as HMCs (Malik et al., 2007). MOSC2 mRNA is widely expressed in various human tissues such as the foetal brain, foetal lung and foetal heart, with the highest expression being in human foetal livers (Figure 20b).

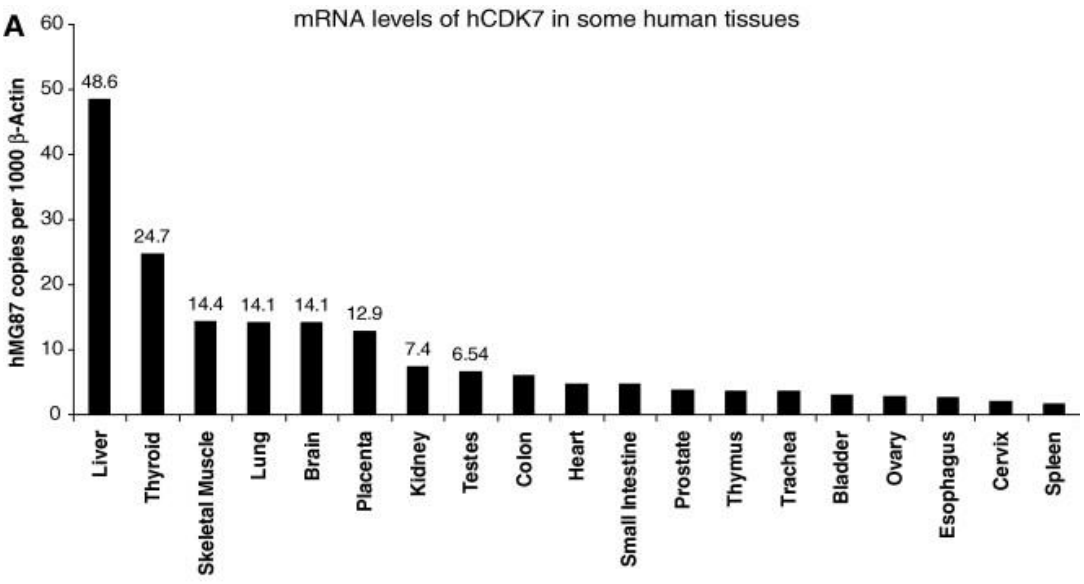

Figure 20b. mRNA levels of MOSC2 (CDK7) in some human tissues.

A) MOSC2 (CDK7) mRNA is widely expressed in various human tissues such as lung, brain and kidney. The greatest amount of human CDK7 was found in liver tissue and the lowest amount was in spleen tissue. Taken from Malik et al., 2007.

Malik et al. (2007) also looked at human MOSC2 mRNA expression in primary HMCs and a transformed HMCL which they cultured in NG, HG and NGM respectively (Malik et al., 2007). Human MOSC2 was significantly increased in cells exposed to HG compared to cells grown in NG; there was no significant difference in MOSC2 mRNA levels between human cells cultured in NG and NGM. They also reported that human MOSC2 mRNA was expressed in HMCs, confirming that MOSC2 is directly up-regulated by HG (Figure 20c).

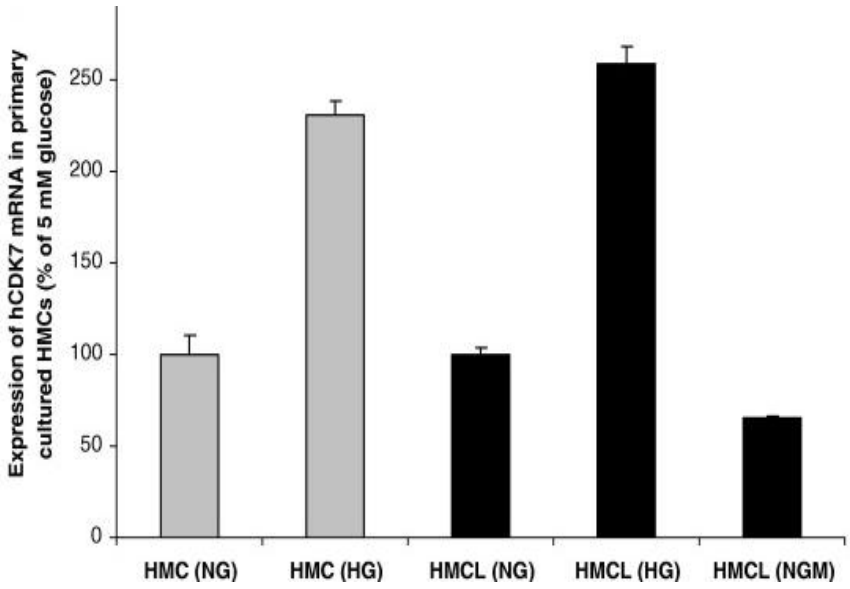

Figure 20c. MOSC2 (CDK7) is induced by glucose in cultured renal mesangial cells.

Primary cultures of mesangial cells (HMCs) and a transformed mesangial cell line (HMCL) were incubated in 5 mM glucose (NG), 25 mM glucose (HG) or 5 mM glucose and 20 mM mannitol (NGM). MOSC2 (CDK7) mRNA copy numbers were quantitated using qPCR (n = 3). The results are expressed as values relative to 5 mM glucose. Taken from Malik et al., 2007.

MOSC2 is a highly conserved gene in humans, rats, mice and monkeys and it is a highly conserved protein within MOSC and MOSC-N domains which are located at residues 35-155 and 169-313. Interestingly, the highly conserved cysteines found at position 269 and 272 within the motif CPRC, resembled the catalytic domain found in thioredoxin. Thioredoxin is an enzyme which is involved in regulating the redox balance of the cells and it provides a highly conserved oxidoreductase system with antioxidant and redox regulatory roles (Schulze et al., 2004). Indeed thioredoxin is an antioxidant protein which uses the thiol group in oxidation and reduction-based signalling (Glyn-Jones et al., 2007).

Thioredoxin is known to have an important role in hyperglycaemia-induced oxidative stress by interacting with protein through the inhibition of thioredoxin function (Schulze et al., 2004). The point of interest is the remarkable conservation of cysteines

within all MOSC2 homologues and its similarity to the thioredoxin protein catalytic domain, suggesting a functional link between thioredoxin and MOSC2. Furthermore, the thiol group found in cysteines can form disulphide bridges through oxidation. In many cellular proteins, the oxidation and reduction of thiol groups have a key role in the cellular antioxidant defense system as well as in intracellular signalling (Liang et al., 2007). They also showed that cellular thiol plays an important role in hyperglycaemia-induced tissue damage (Liang et al., 2007). In addition Ceriello (2000) found that the cellular antioxidant responses are defective in patients with DN (Ceriello et al., 2000). Morrison et al. (2004) also showed that changes in thiol protein levels are linked with DN progression. MOSC2, one of the genes involved in the thiol pathway, showed up-regulation in two experimental models of DN (Morrison et al., 2004). Consistently, there was a presence of highly conserved cysteines in MOSC2 protein, suggesting that MOSC2 is a novel thiol protein and is postulated to be involved in the cell response to oxidative stress (Malik et al., 2007).

Human MOSC2 is located at chromosome 1q42.11 and the human MOSC2 gene spans 35,917 and consists of eight exons. MOSC2 protein shows conservation in one tyrosine kinase phosphorylation domain and nine protein kinase C phosphorylation domains namely four N-myristilation sites and five casein kinase II sites. The MOSC domain has been detected in the molybdenum cofactor sulfurase and a number of proteins from both prokaryotes and eukaryotes; it is also a superfamily of β-strand-rich domains (Anantharaman et al., 2002). In relation, the proteins which have MOSC and MOSC-N domains are generated from the promitochondrial endosymbiont and have been involved in the synthesis of metal-sulfur clusters in the eukaryotic mitochondrion by their function as sulfur carrier proteins (Anantharaman et al., 2002). In the Malik laboratory, MOSC2 was used as a fusion protein which is localised to the cytosol and nucleus. They also purified the recombinant protein and sent it to Karolinska to be tested for thioredoxin-like activity (Shahni, 2011).

The mitochondrial amidoxime reducing component, mARC, is a newly discovered molybdenum enzyme which complexes with two other components in the mitochondria; the electron transport proteins NADH-cytochrome b5 reductase (CYB5R) and cytochrome b5 (CYB5). mARC was first identified in porcine liver mitochondria in 2006 (Hvemeyer et al., 2006). The human genome codes for two mARC genes, referred to as mARC1 or MOSC1 and mARC2 or MOSC2, which are

capable of catalysing the activation of N-hydroxylated prodrugs. Havemeyer (2011) found that mARC is the fourth molybdenum containing enzyme and mARC2/MOSC2 is the same as CDK7, which is located in the outer mitochondrial membrane. They also showed that mARC homologues contributed to the reduction of NOHA to L-arginine (Figure 20d; Kotthaus et al., 2011)

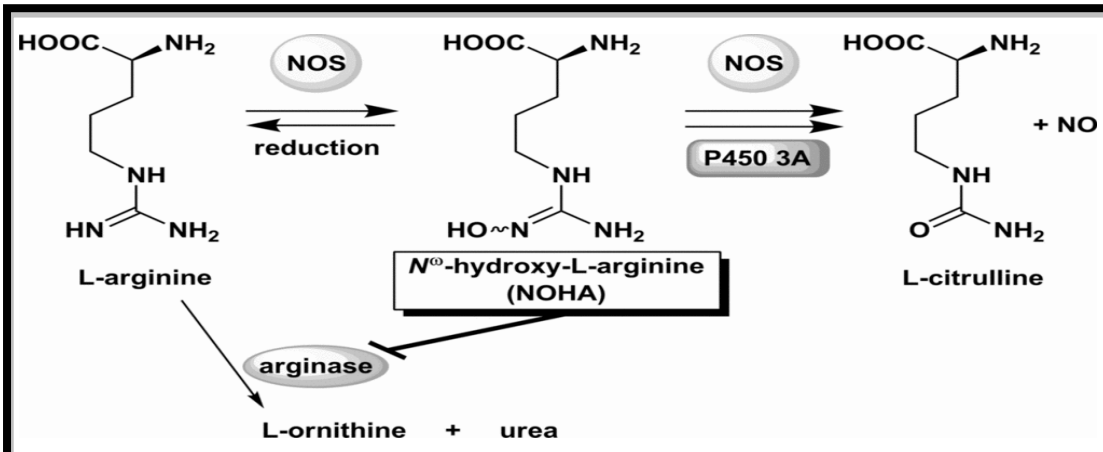

Figure 20d. Overview of L-arginine-dependent biosynthesis of Nitric Oxide (NO).

In the L-arginine-dependent biosynthesis of Nitric Oxide (NO), N-hydroxy-L-arginine (NOHA) is the physiological substrate which can be reduced by reconstituted enzyme systems which contain either MOSC1 or MOSC2. Taken from Kotthaus et al., 2011.

All analysed mammalian genomes include both MOSC1 and MOSC2 genes which share high sequence identity (Plitzko et al., 2013). On exploring the function of MOSC, they showed that both human MOSC proteins are involved in reduction of N-hydroxylated substrates *in vitro*. Plitzko et al. (2013) also showed that MOSC is not capable of reducing N-hydroxylated substrates without the electron transport proteins. MOSC proteins were reported to work on the same N-hydroxylated substrates and this could be one of their physiological activities (Plitzko et al., 2013).

The full-length transcript of MOSC1 encoded 385 amino acids which are homologue to moaA in *Escherichia coli*. The first cDNA from MOSC1 was homologue to various proteins which are involved in the synthesis of MOCO bacteria (Reiss et al., 2010). MALDI-TOF (matrix-assisted laser desorption ionisation-time-of-flight) mass spectrometry results from purified human MOSC protein showed that MOSC2 protein

is more localised at the outer mitochondrial membrane compared to MOSC1 (Katthaus et al., 2011). Recently, a genome wide association study (GWAS) found an association between MOSC1 with two important risk factors for coronary artery disease and accordingly, MOSC might play a role in lipoprotein metabolism (Neve et al., 2011).

Studying the functional activity of MOSC proteins and testing the hypothesis that MOSC acts as an antioxidant in response to ROS could provide a novel therapeutic target for DN. The strategies that were undertaken to test this assumption are explained below: first we looked at the effect of HG on MOSC2/MOSC1 mRNA expression in experimental models of DN and *in vitro*; secondly we examined MOSC2/MOSC1 protein expression to confirm the mRNA study. We also looked at MOSC2 protein localisation in the kidneys of control and diabetic mice to determine their function using N-reductive assay. Circulating MOSC1 mRNA expression was also examined in T2DN patients to test if they were expressed in whole blood.

Aims and objectives of this chapter

1) To confirm and extend previous findings that MOSC2 is a glucose-regulated gene by using models of diabetes (*in vivo* and *in vitro* models).

2) To determine if MOSC1 is regulated by glucose *in vivo* and *in vitro.*

3) To find out if N-reductive activity (associated to MOSC2 and MOSC1) is increased in diabetes.

4) To evaluate if MOSC1 is a biomarker in circulating blood of patients with T2DN

5.3. Results

5.3.1. Experimental models of diabetes used in this study

In this study, we used diabetic mouse *in vivo* models and renal cell *in vitro* models. There were: a) β-*Phb2* KO mouse, b) STZ mouse, c) HMCs, d) HEK293 cells and e) HTC.

For *in vivo* models, kidneys (n= 3) were obtained from a β-*Phb2* KO mouse and an acute STZ-induced mouse which we previously described (Section 3.3.1.). Human cultured renal cells (HMCs, HEK293, HTC) were incubated in different conditions until they reached confluence. They were growth arrested for 24 hours and were seeded in triplicate at a density of 10,000 in NG (5 mM), HG (25 mM) and NGM (5mM glucose+ 20 mM mannitol) for a 3-day experiment (Section 2.3.1.). Samples were then stored in -80°C and used for mRNA and protein studies (Table 23).

Table 23. *In vitro* renal cells models used in this study

Name	Condition	N	Blood glucose levels mmol/L
HMCs	NG	3	5
HMCs	HG	3	25
HMCs	NGM	3	5 mM glucose+20mM mannitol
HEK293	NG	4	5
HEK293	HG	4	25
HEK293	NGM	4	5 mM glucose+20mM mannitol
HTC	NG	3	5
HTC	HG	3	25
HTC	NGM	3	5 mM glucose+20mM mannitol

Human renal cells (human mesangial cells, human embryonic kidney cells, human tubular cells) grown in normal glucose (5mM), high glucose (25mM) and normal glucose with mannitol for 3 days.

5.3.2. Gene expression assay for mouse and human MOSC2/MOSC1

The aim of this part of the work was to set up a quantification assay for mouse and human genes of MOSC1 and MOSC2 to detect the mRNA levels of target genes in the *in vivo* and *in vitro* models.

1) Primer design and amplification of mouse MOSC2/MOSC1 *in vivo* and *in vitro*

a) *In vivo*: Oligonucleotide primers designed for the mouse MOSC2/MOSC1 mRNA sequence (Accession numbers NM_133684 and NM_001081361) were used to determine the MOSC2/MOSC1 transcript in mouse tissues. The MOSC2 sequence has 1883 bp which encodes 338 amino acids. The MOSC1 sequence has 2161 bp which

encodes 342 amino acids (Appendix 9). Primers were designed using Roche Applied Science software and synthesised at Sigma-Aldrich (Table 24a). Figures 21a and 21b show the position of the primers used in this part of the study.

Table 24a. Oligonucleotide primers used in PCR and RT-PCR

Gene name	Accession number	Product size	Sequence
mMOSC2F$_1$: Forward primer **mMOSC2R$_1$: Reverse primer**	NM_133684	67 bp	gga tcc cat ggg tga cag gga aga tgg cca tga gga
mMOSC1F$_1$: Forward primer **mMOSC1R$_1$: Reverse primer**	NM_001081361	60 bp	att gtc atc tcg gga tgt gg tcc aat gag aac ctc gtt cc
hMOSC2F$_1$: Forward primer **hMOSC2R$_1$: Reverse primer**	NM_017898	187bp	gac aca tgg tca ctg cc ttg cca cag tct ctg c
hMOSC1F$_1$: Forward primer **hMOSC1R$_1$: Reverse primer**	NM_022746	78 bp	cca cag tgg acc cag aca c ggt cac act ggc gat aac tct

The sequences are presented from 5` to 3` with F primers representing the sense strand and R primers representing the anti-sense strand of MOSC2 and MOSC1 primers.

```
   1 gtagcccagg cctgcccggg atagtgtaac atggttcct ccagctctac ggctctggct
  61 cgcctcggcc tccctgggca gccgcggtcc acctggctcg gcgtcgccgc gctggggctg
 121 gctgcggtgg cgctggggac cgtagcttgg cgtcgcacgc gtccccggcg gcgccggcag
 181 ctgcagcagg tgggcacggt gtcgaaggtt tggatctacc cgatcaagtc ctgcaagggg
 241 gtgtcggtgt gtgagaccga gtgcacggac atggggctgc gctgtggcaa agtgcgcgac
 301 aggttctgga tggtggtgaa ggaggacgga cacatggtca ctgcccgcca ggagcctcgc
 361 cttgtgctgg tctccatcac cctggagaac aattacctga cgctggaagc tccaggcatg
 421 gagcagatag ttctgccaat caagctccct tcttcgaata agatccacaa ctgcaggctg
 481 tttggtctcg acatcaaagg cagagattgt ggcgatgagg tagctcagtg gttcaccaac
 541 tacctgaaga cgcaagccta caggttggtt cagtttgata ccagcatgaa aggaagaaca
 601 acgaagaaac tttacccttc tgaaagttac cttcagaact atgaggtagc ctacccggac
 661 tgcagccctg tccacctgat ttctgaagcc tccttagtcg atctcaacac caggctgaag
 721 aagaaagtga agatggaata tttcaggcca aacatcgtgg tgtcaggctg tgaggctttc
 781 gaggaggata cttgggatga actcctgatt ggtgacgtgg agatgaaaag ggtgttgagc
 841 tgtcccaggt gcgttctgac tacagtggac ccagacaccg gcatcataga caggaaggag
 901 ccactggaga ccctgaagag ctatcgcctg tgtgatcctt ctgtgaagag tatataccag
 961 tcatctccac tttttgggat gtatttctcg gtggagaagc ttgggagcct gagagtgggt
1021 gaccctgtgt accggatggt ggattagtgg atcccatggc tgacacgctt ccaggtccga
1081 ggagacatat ctgcgagtcc tcatggccat cttcctggaa ccggatctct atttttcttt
1141 cggagctgtg tacgccttga cttaattcaa gaaaagtgcc agaggtggtt taggaatgtg
1201 aggctgtata aattttagat aatgaggttt ttagaaaaat aaatggaatt tgtctgcaat
1261 tattctgaat gctacacccg ctattacgtt tttctcattc ctgcctctac gattgctgaa
1321 gtttaaagac acagctcgaa agctgccact tttaaaaaat gtttatactt ttcagtaggt
1381 ctgtcgcttg agaaaggtaa gaaaaggagc cctcttgccc tgaatgtgca gggaatgtgc
1441 acatatctga tgtgctcgca tgctcacgaa agcctgttgg ccggtcttgg cctggctgtt
1501 gagccctgct gagtttggtt tcattattgt ttaccttgct gttatagaag tatgcttaca
1561 tacagaaatg acttcagagg tcatggggtt attttgttca tagactgtgg ctttacattt
1621 cattctgttc ctatcaagac aggtagaact tatctataat tgtgaattct tccaattcta
1681 caagagagtg gaccttaaag gaatggaatc ttccttcgga agaaggaaca aggagaaacc
1741 atgaactcag tcttaaaggc tcacggtagc acaggatgat gcactagctt gcagtaacag
1801 tacaaacact aagttaacat ggagccgagt tagctctctt acagctgtgt ggttccattg
1861 tcattaataa gtgcgagtct ctc
```

Figure 21a. Nucleotide sequence of mouse MOSC2 mRNA, accession number NM_133684 .

The forward primer (MOSC2 F_1) is shown in blue and the reverse primer (MOSC2 R_1) is in green. The putative initiation codon is at position 31 and is in red. The stop codon is also shown in red.

```
   1 ggtgagattc cacagctgag ccaccacctc ccgcccaggc cgaatgaaga tgcacaattt
  61 ggattggagg ggaagggtca ggagctgctg acctttgggc tcaggcccag gccgctggcc
 121 acagtagctc ttggtccagt cggcgccgga ggtgtatcaa gcgctcatcc cgccctctcc
 181 agtcatgggt gcggggtcct gggcgctgac cctcttcggc ttctccgcgt ttcgggtccc
 241 gggccagccg cggtccacct ggctcggcgt cgccgcgctg ggactggccg cggtggccct
 301 ggggacagtg gcctggcgtc gtgcgcgtcc ccggcgacgc cggcggctac agcaagtggg
 361 aacggtggca cagctctgga tctacccaat caagtcctgc aaggggttgt cggtgagcga
 421 ggcagagtgc actgccatgg ggctgcgcta tggccacctg cgcgacaggt tttggctcgt
 481 gatcaatgaa gaggggaaca tggtcactgc ccggcaggag cctcgattgg tcctgatttc
 541 tctgacctgt gaggacgaca ccttgactct cagtgcagct tacacaaagg acctgctgct
 601 gcctatcacc ccgcctgcca caaacccact cctccagtgc agagtgcatg gcctggagat
 661 acagggcagg gattgtggag aggatgcagc tcagtgggtc agcagcttct tgaagatgca
 721 gtcctgtcgc ctggtgcact tcgagccgca catgcgcccc agaagttctc ggcaaatgaa
 781 ggcttccaaa tcattttctc aaaataatga agtggcctac tcagatgcaa gtccattctt
 841 ggtcctttct gaggcatcct tggaagatct caactccagg ctggagcgca gagtgaaagc
 901 gacaaacttc aggcctaaca ttgtcatctc gggatgtggc gtttatgctg aggattcttg
 961 gaacgaggtt ctcattggag atgtggaact gaaacgggtg atggcttgta cccggtgcct
1021 tttaacaaca gtggatccag acactggcat ctcggacagg aaggagcctc tggaaacact
1081 gaagagctac cgcctgtgtg acccttccga gcaagcacta tatggaaagt tacccatctt
1141 tggacaatac ttcgctctgg aaaatccagg gacaatcaga gtgggagacc ctgtgtacct
1201 cctgggccag tgatgggaac tgttcgttct ggaagaacag atggctctta aaaaaaaact
1261 tttacaaaca gacatcgctt gaaacagttc ttcagcctgt tctttggatc ggccagttcc
1321 aagtttctct tctttcagat ttccgtctgt ttcaatgttt cctggggcca gcccacaaag
1381 caggcaaata cagctttgcg aacttagcag gtccctgtta tgtttcttgt agaatgaagg
1441 gattatcata ttgccctgtt tataaatacg gagtaatcct tctacgtcgg aattcacttg
1501 ccaagacatc atctccctag ccttcttttg ggaaagagaa gaaaaaggga gggacactgt
1561 gtaagccaga agaatgttcc agaatgttct gttacccctg gacatggtgc atacaacggg
1621 aattaaatac tctcccaagt aaagttggaa tgacggcttt tacttttctc cttgagccca
1681 ggctttggaa agagtttaaa gagcaagccc taaagatatt ggatgctgtt gcttactgac
1741 agtgtgaagt ttgacagacc ctttagccca agaacacgaa gtgtcagggt caaagccagc
1801 tctctacagc atccagacgg gctctcagct ctgtgaaaaa ggtgtttcca ctcttgaagc
1861 aaagtgttga tgcgcctcac taaaggattc aagatcgttc ctagcatgtg gggacagata
1921 gtgacaccag agagggagat acctccgcct gggtgtctaa gatgagattt gatcttgccc
1981 aggaaaatgg tggctctctt aatatgagca aaatgaaatg gtggcgcccc ctagtggtag
2041 tgaatggtag gtcggcccac cttgagaaaa atttaaaaag gggaaaaaca aaacaaaaca
2101 aaaccaaagc aatcttgtgc ttgttgttta gttttaaatt ttaaaacgtt ttaaaaactg
2161 a
```

Figure 21b. Nucleotide sequence of mouse MOSC1 mRNA, accession number NM-001081361.

The forward primer (MOSC1 F_1) is shown in blue and the reverse primer (MOSC1 R_1) is in green. The putative initiation codon is at position 185 and is in red. The stop codon is also shown in red.

Primers for mouse MOSC2/MOSC1 were used to amplify a fragment of mouse kidney cDNA. PCR was carried out to confirm the product size of MOSC2 and MOSC1 genes using an annealing temperature of 60°C and 3mM concentration of $MgCl_2$. Products with the expected sizes of 60 bp, corresponding to MOSC1, and 67 bp, corresponding to MOSC2, were observed (Figure 21C).

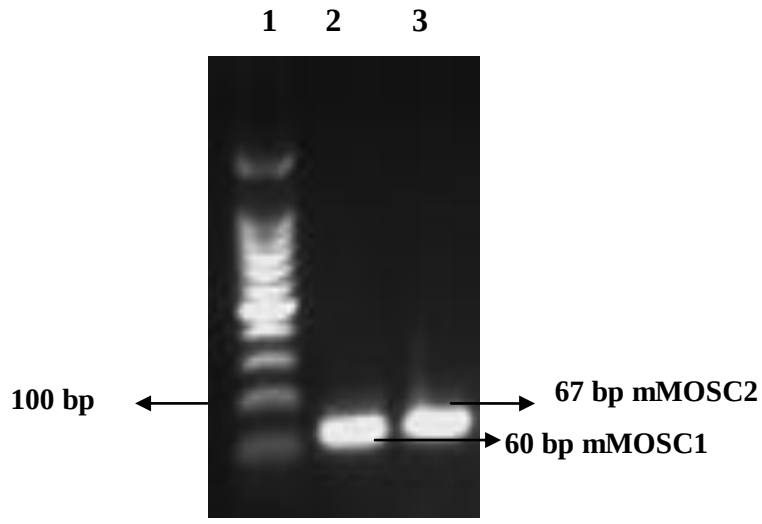

Figure 21c. PCR amplification of mouse MOSC2/MOSC1.

PCR was carried out to amplify fragments of genes from a mouse kidney cDNA (1µg) with mouse MOSC2/MOSC1 primers, using 3mM concentrations of $MgCl_2$ at 60°C. 10 µl of PCR products were subjected to electrophoresis on an agarose gel along with the 100 bp DNA ladder. Lane 1 shows the 100 bp DNA ladder and lanes 2 and 3 are the PCR products of mouse MOSC1 and mouse MOSC2 respectively.

b) ***In vitro:*** Oligonucleotide primers were designed for human as well as mouse MOSC2/MOSC1. Transcripts were based on the sequence of MOSC2 and MOSC1 mRNA (Accession number NM_017898 and NM_022746) and they were used to determine MOSC2/MOSC1 mRNA transcripts in human renal cells (Table 24a). The sequence of human MOSC2 is 1618 bp and it encodes a peptide of 335 amino acids. The sequence of human MOSC1 is 2258 bp and it encodes a peptide of 337 amino acids (Appendix 9). These primers were designed using Roche Applied software and synthesised by Sigma-Aldrich. Figure 21d and 21e show the position of the primers.

```
   1 ggcttggtca ccgcattaag gcattcccgc tctccgcgga actgctctgc cgtctcggcg
  61 gtgaaagtgt gagagggtcc gtagttgggt caactttgac tcctctcgcc tgcccggatc
 121 cttaagggcc tcctcgtcct cccggtctcc ggtcgctgcc gggtctgtgc gccggtccgc
 181 gcccgccctc gctctgccat gggcgcttcc agctcctccg cgctggcccg cctcggcctc
 241 ccagcccggc cctggcccag gtggctcggg gtcgccgcgc taggactggc cgccgtggcc
 301 ctggggactg tcgcctggcg ccgcgcatgg cccaggcggc gccggcggct gcagcaggtg
 361 ggcaccgtgg cgaagctctg gatctacccg gtgaaatcct gcaaaggggt gccggtgagc
 421 gaggctgagt gcacggccat ggggctgcgc agcggcaacc tgcgggacag gttttggctg
 481 gtgattaagg aagatggaca catggtcact gcccgacagg agcctcgcct cgtgctcatc
 541 tccatcattt atgagaataa ctgcctgatc ttcagggctc cagacatgga ccagctggtt
 601 ttgcctagca agcagccttc ctcaaacaaa ctccacaact gcaggatatt tggccttgac
 661 attaaaggca gagactgtgg caatgaggca gctaagtggt tcaccaactt cttgaaaact
 721 gaagcgtata gattggttca atttgagaca aacatgaagg gaagaacatc aagaaaactt
 781 ctccccactc ttgatcagaa tttccaggtg gcctacccag actactgccc gctcctgatc
 841 atgacagatg cctccctggt agatttgaat accaggatgg agaagaaaat gaaaatggag
 901 aatttcaggc caaatattgt ggtgaccggc tgtgatgctt ttgaggagga tacctgggat
 961 gaactcctaa ttggtagtgt agaagtgaaa aaggtaatgg catgccccag gtgtattttg
1021 acaacggtgg acccagacac tggagtcata gacaggaaac agccactgga caccctgaag
1081 agctaccgcc tgtgtgatcc ttctgagagg gaattgtaca agttgtctcc acttttgggg
1141 atctattatt cagtggaaaa aattggaagc ctgagagttg gtgaccctgt gtatcggatg
1201 gtgtagtgat gagtgatgga tccactaggg tgatatggct tcagcaacca ggagggattg
1261 actgagatct taacaacagc agcaacgata catcagcaaa tccttattat ccagccttca
1321 actatcttta ccctggaaaa caatctcgat ttttgacttt tcaaagttgt gtatgctcca
1381 ggttaatgca aggaaagtat tagaggggggg aatatgaaag tatatatata aattttaggt
1441 actgaaggct ttaaaaataa ttaagatcat caaaaatgct attttgaatg ttatcatggc
1501 tattacactt ttacttcctg actttaatat tgatgaataa agcaagttta atgaatcaac
1561 taaaaagctg caaaaaaaaa aaaaaaaaaa aaaaaaaaaa aaaaaaaaaa aaaaaaaa
```

Figure 21d. Nucleotide sequence of human MOSC2 mRNA, accession number NM_017898.

The forward primer is shown in blue (MOSC2 F_1) and the reverse primer (MOSC2 R_1) is shown in green. The putative initiation codon is at position 199 and is in red. The stop codon is at position 1204 and is also shown in red.

```
   1 acagcgccct gcagcgcagg cgacggaagg ttgcagaggc agtggggcgc cgaccaagtg
  61 gaagctgagc caccacctcc cactccccgc gccgcccccc agaaggacgc actgctctga
 121 ttggcccgga agggttcagg agctgcccag cctttgggct cggggccaaa ggccgcacct
 181 tcccccagcg gccccgggcg accagcgcgc tccggccttg ccgccgccac ctcgcggaga
 241 agccagccat ggcgccgccc ggctcctccg cgctggcgcg ctttgtcctc ctcgcgcaat
 301 cccggcccgg gtggctcggg gttgccgcgc tgggcctgac cgcggtggcg ctgggggctg
 361 tcgcctggcg ccgcgcatgg cccacgcggc gccggcggct gctgcagcag gtgggcacag
 421 tggcgcagct ctggatctac cctgtgaaat cctgcaaggg ggtgccggtg agcgaggcgg
 481 agtgcacggc catggggctg cgcagcggca acctgcggga caggttttgg cttgtgatca
 541 accaggaggg aaacatggtt actgctcgcc aggaacctcg cctggtcctg atttccctga
 601 cctgcgatgg tgacaccctg actctcagtg cagcctacac aaaggaccta ctactgccta
 661 tcaaaacgcc caccacaaat gcagtgcaca agtgcagagt gcacggcctg gagatagagg
 721 gcagggactg tggcgaggcc accgcccagt ggataaccag cttcctgaag tcacagccct
 781 accgcctggt gcacttcgag cctcacatgc gaccgagacg tcctcatcaa atagcagact
 841 tgttccgacc caaggaccag attgcttact cagacaccag cccattcttg atcctttctg
 901 aggcgtcgct ggcggatctc aactccaggc tagagaagaa agttaaagca accaacttca
 961 ggcccaatat tgtaatttca ggatgcgatg tctatgcaga ggattcttgg gatgagcttc
1021 ttattggtga cgtggaactg aaaagggtga tggcttgttc cagatgcatt ttaaccacag
1081 tggacccaga caccggtgtc atgagcagga aggaaccgct ggaaacactg aagagttatc
1141 gccagtgtga cccttcagaa cgaaagttat atggaaaatc accactcttt gggcagtatt
1201 ttgtgctgga aaacccaggg accatcaaag tgggagaccc tgtgtacctg ctgggccagt
1261 aatgggaacc gtatgtcctg gaatattaga tgccttttaa aaatgttctc aaaaatgaca
1321 acacttgaag catggtgttt cagaactgag acctctacat tttctttaaa tttgtgattt
1381 tcacattttt cgtcttttgg acttctggtg tctcaatgct tcaatgtccc agtgcaaaaa
1441 gtaaagaaat atagtctcaa taacttagta ggacttcagt aagtcactta aatgacaaga
1501 caggattctg aaaactcccc gtttaactga ttatggaata gttctttctc ctgcttctcc
1561 gtttatctac caagagcgca gacttgcatc ctgtcactac cactcgttag agaaagagaa
1621 gaagagaaag aggaagagtg ggtgggctgg aagaatatcc tagaatgtgt tattgcccct
1681 gttcatgagg tacgcaatga aaattaaatt gcaccccaaa tatggctgga atgccacttc
1741 ccttttcttc tcaagccccg ggctagcttt tgaaatggca taaagactga ggtgaccttc
1801 aggaagcact gcagatatta attttccata gatctggatc tggccctgct gcttctcaga
1861 cagcattgga tttcctaaag gtgctcagga ggatggttgt gtagtcatgg aggacccctg
1921 gatccttgcc attcccctca gctaatgacg gagtgctcct tctccagttc cgggtgaaaa
1981 agttctgaat tctgtggagg agaagaaaag tgattcagtg atttcagata gactactgaa
2041 aacctttaaa gggggaaaag gaaagcatat gtcagttgtt taaaacccaa tatctatttt
2101 ttaactgatt gtataactct aagatctgat gaagtatatt ttttattgcc attttgtcct
2161 ttgattatat tgggaagttg actaaacttg aaaaatgttt ttaaaactgt gaataaatgg
2221 aagctacttt gactagtttc agaaaaaaaa aaaaaaaa
```

Figure 21e. Nucleotide sequence of human MOSC1 mRNA, accession number NM_022746.

The forward primer is shown in blue (MOSC1 F_1) and the reverse primer is shown in green (MOSC1 R_1). The putative initiation codon is at position 249 and is in red. The stop codon is at position 1260 and is also shown in red.

cDNA from HEK293 cells in NG was used as a template in PCR to optimise MOSC2/MOSC1 primers. MOSC2 has previously been used by Malik et al. (2007), whereby the optimal conditions for both primers were established to be an annealing temperature of 55°C and 3mM concentration of $MgCl_2$. PCR products were analysed by agarose gel electrophoresis. Products of the expected sizes of 187 bp and 78 bp corresponding to MOSC2/MOSC1 were respectivel observed (Figure 21f). Therefore, the internal primers successfully amplified MOSC2 and MOSC1 fragments from the human kidney cDNA.

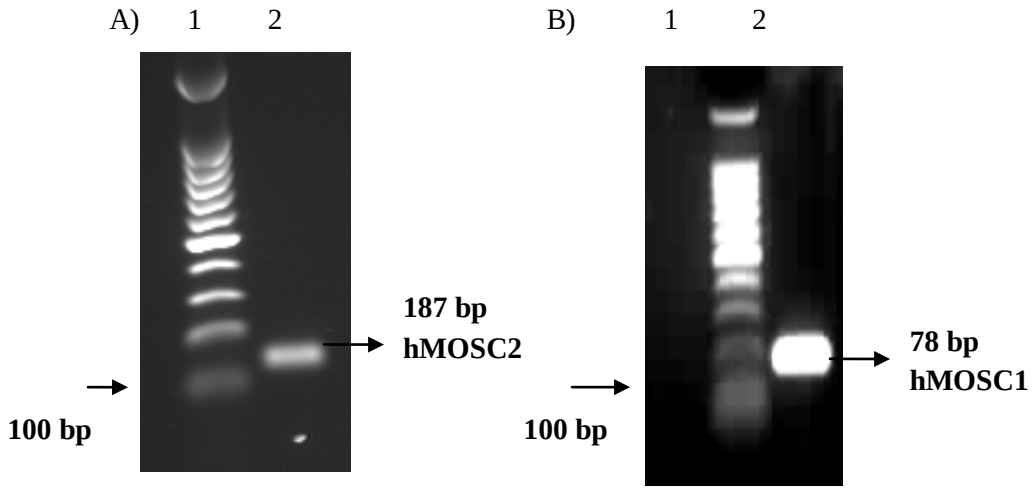

Figure 21f. PCR amplification of human MOSC2/MOSC1.

PCR was carried out to amplify fragments of MOSC2/MOSC1 genes from HEK293 cells cDNA (1µg) with MOSC1 and MOSC2 primers, using 3 mM concentrations of $MgCl_2$ at 55°C. The PCR products (10µl) were subjected to electrophoresis along with the 100 bp DNA Ladder. A) Lane 1: 100 bp DNA ladder, lane 2:187 bp of hMOSC2. B) Lane 1: 100bp DNA ladder, lane 2: 78 bp of hMOSC1.

3) RNA isolation and cDNA synthesis from mouse tissues and human renal tubular cells

To evaluate the regulation of MOSC2/MOSC1 mRNA in mouse tissues and human renal cells, RNA was isolated from each sample (Section 2.6.1.). The concentration and yield of RNA were determined by measuring the absorbance of RNA at A_{260} using Nanodrop (Table 24b and 24c). For each condition, cDNAs were synthesised and oligonucleotide primers were designed to detect mouse and human MOSC1/MOSC2 mRNA expression.

Table 24b. Concentration of RNA isolated from mouse tissues

Models	Samples	Condition	RNA Concentration (ng/µl)
ß-*Phb*2KO	Kidney1	Control	529.5
	Kidney2	Control	473.5
	Kidney3	Control	1283
	Kidney4	Control	566.2
	Kidney5	KO	750.6
	Kidney6	KO	658.6
	Kidney7	KO	638.9
	Kidney8	KO	405.3
	Kidney9	KO	1243.6
	Kidney10	KO	311.8
STZ	Kidney1	Control	16
	Kidney2	Control	37
	Kidney3	Control	75
	Kidney4	Diabetic	152
	Kidney5	Diabetic	185
	Kidney6	Diabetic	184.5
	Kidney7	Treated	144
	Kisney8	Treated	26
	Kidney9	Treated	73

RNA was extracted from kidneys of β-*Phb2* KO and STZ-induced diabetic mice *in vivo*. RNA concentration in each condition was detected by measuring the absorbance at A_{260} using Nanodrop.

Table 24c. Concentration of RNA from cultured human renal cells

Models	Samples	Condition	RNA Concentration (ng/µl)
HMCs	HMCs1	NG	92.7
	HMCs2	NG	74.2
	HMCs3	NG	116.3
	HMCs4	NG	119.9
	HMCs5	HG	66
	HMCs6	HG	117.7
	HMCs7	HG	87.3
	HMCs8	NGM	94.2
	HMCs9	NGM	64.4
	HMCs10	NGM	62.1
HEK293	HEK1	NG	434.9
	HEK2	NG	392.7
	HEK3	NG	215.7
	HEK4	NG	216.2
	HEK5	HG	431.3
	HEK6	HG	466.4
	HEK7	HG	148.2
	HEK8	HG	380.4
	HEK9	NGM	477.4
	HEK10	NGM	705.8
	HEK11	NGM	735.1
	HEK12	NGM	618.2
HTC	HTC1	NG	64.6
	HTC2	NG	28.1
	HTC3	NG	45.9
	HTC4	HG	58.4
	HTC5	HG	64.6
	HTC6	HG	56.6
	HTC7	NGM	32.3
	HTC8	NGM	1.22
	HTC9	NGM	9

RNA was extracted from cultured human renal cells (human mesangial cells, human embryonic kidney cells and human tubular cells). RNA concentration in each condition was detected by measuring the absorbance at A_{260} using Nanodrop.

4) Purification and generation of standard curves

To test the hypothesis that MOSC2/MOSC1 may be regulated by glucose in the experimental mouse models *in vivo* and *in vitro*, we performed a qPCR using LightCycler and QuantiFast DNA SYBR Green Kit (Qiagene, UK) to accurately quantify the copy numbers of MOSC2 and MOSC1 *in vivo* and *in vitro*. PCR products

of MOSC2 and MOSC1 genes were purified to prepare standards for the generation of standard curves.

A standard curve was created for mouse and human MOSC2/MOSC1 and the quantification of each sample was done in triplicate. To examine specificity, melting-curve analysis was performed. Samples were normalised with respect to mRNA expression of reference genes. The concentration of the nucleic acids used as standards for target genes and reference genes (Appendix 10 and 11) were known.

5.3.3. Glucose regulation of mouse and human MOSC2 *in vivo* and *in vitro*

In this part, we first tested the hypothesis that mouse MOSC2 is a glucose regulated gene in kidneys from experimental models of β-*Phb2* KO and STZ mice; their cDNA was used to test the effect of HG on their mRNA expression. To confirm the mRNA expression, we examined the protein expression in the kidneys of STZ mice by using western blot and we determined the location of the MOSC2 protein in control and diabetic kidneys of STZ mice by using immunofluresence. Following these findings, we observed the mRNA and protein expression of MOSC2 in human cultured renal cells (HMCs, HEK293 and HTC).

1) Quantification of renal CRYM copy numbers in βeta-*Prohibitin2* knockout and streptozotocin-induced diabetic mice *in vivo*

qPCR was performed with gene-specific primers to determine the expression of renal MOSC2 mRNA in control and diabetic kidneys of ß-*Phb2* KO mice and also in control, diabetic and treated kidneys from STZ mice. qPCR experiments were performed in triplicate; cDNAs from each condition were used. Statistical analysis of the data using student's *t* test provided the mean, standard deviation and the *p* values for all conditions.

- ***Renal mRNA levels of MOSC2 in the ß-Phb2 KO, a spontaneous model of diabetes***

Renal MOSC2 values were measured in control and diabetic kidneys of ß-*Phb*2 KO mice (Table 25a). The results showed no significant difference in renal MOSC2 mRNA copy numbers in diabetic kidneys compared to control kidneys (1.02 ± 0.61 vs. 0.59 ± 0.13, P>0.05; Table 25b). The data was log-transformed as the actual MOSC2 copy number values were skewed (Figure 22).

Table 25a. Relative renal MOSC2 and GAPDH mRNA expression values of β-*Phb2* KO mouse kidney

Samples	MOSC2	MOSC2	MOSC2	GAPDH	GAPDH	GAPDH	MOSC2 ratio
Control1	123000	121000	146000	237000	324000	141000	0.4
Control2	68700	84100	89000	116000	107000	97400	0.7
Control3	102000	125000	139000	182000	175000	189000	0.6
Control4	35200	40200	36500	118000	58600	55300	0.4
KO1	207000	213000	226000	105000	99000	106000	2.08
KO2	151000	136000	143000	171000	166000	163000	0.86
KO3	94800	115000	122000	162000	183000	162000	0.61
KO4	40700	38900	39500	54300	98500	72800	0.52
KO5	121000	146000	152000	102000	107000	85200	1.42
KO6	51200	56200	46200	85800	83800	77300	0.62

Renal MOSC2 copy numbers relative to GAPDH mRNA copy numbers were detected using qPCR in control and KO mouse kidneys. For control, 4 separate kidneys and for the diabetic condition, 6 separate kidneys were used to prepare cDNA. Renal MOSC2 was quantified from each sample in triplicate. Data are shown as relative expression values.

Table 25b. Relative renal copy numbers of MOSC2 mRNA in kidneys of ß-*Phb2* KO mice

Condition	N	Mean values ± SD of MOSC2 copy numbers	Mean values ± SD of MOSC2 log
Control	4	0.59 ± 0.13	-0.04 ± 0.23
KO	6	1.02 ± 0.61	-0.23 ± 0.09

Renal MOSC2 mRNA copy numbers relative to GAPDH copy numbers were detected in kidneys of the KO mice. Values are shown as mean±SD. P>0.05

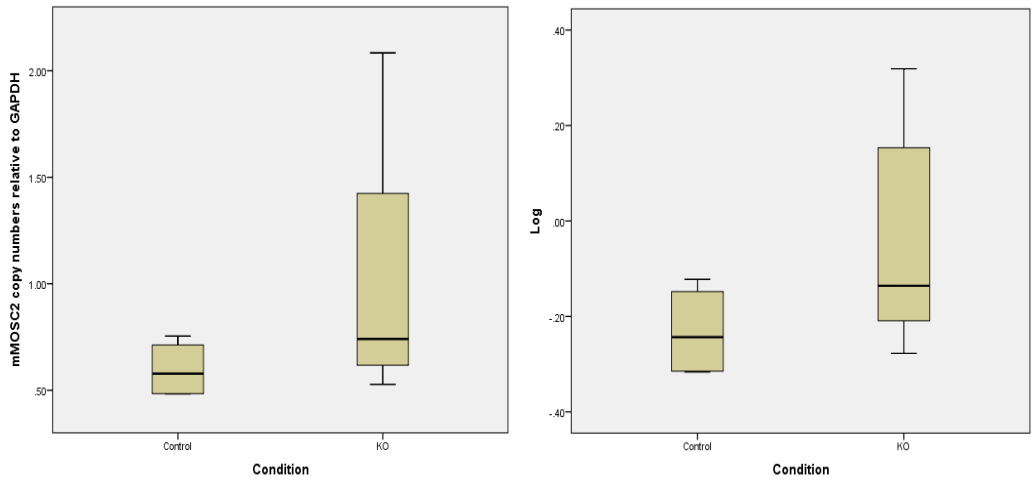

Figure 22. Renal MOSC2 mRNA levels were elevated in diabetic ß-*Phb2* KO mice kidneys.

Mouse kidneys were collected from diabetic and control KO mice. Renal MOSC2 copy numbers were detected using qPCR (n= 3). The mean values and standard deviation of different experiments are shown. A) Values shown are copy numbers of renal MOSC2 mRNA relative to GAPDH. B) The data were log-transformed. P>0.05

● ***Renal mRNA levels of MOSC2 in kidneys of streptozotocin-induced diabetic mice***

In the previous experiment, renal MOSC2 mRNA was found not to change in the presence of hyperglycaemia in ß-*Phb2* KO mice. To determine whether MOSC2 mRNA is regulated in the presence of hyperglycaemia in other diabetic mouse models, we investigated MOSC2 mRNA levels in control, diabetic and treated kidneys from STZ mice (Table 26a). The data showed a large increase in diabetic mice compared to control kidneys.

The data were log-transformed, and the log data showed a significant difference between control and diabetic (0.53 ± 0.25 vs. -0.2 ± 0.07, P<0.05; Table 26b*)* in the kidneys of STZ mice. The renal MOSC2 levels were higher in diabetic mice compared to control mice. This significant increase supports the association between renal MOSC2 mRNA expressions with hyperglycaemia. There was not a significant difference between renal MOSC2 levels of control and mice treated with STZ (-0.2 ± 0.07 vs. -0.07 ± 0.19, P>0.05). This data showed that hyperglycaemia can result in an increase of renal MOSC2 mRNA expressions in diabetic mouse models (Figure 23).

Table 26a. Relative renal MOSC2 and GAPDH mRNA expression in kidneys of STZ mice

Samples	MOSC2	MOSC2	MOSC2	GAPDH	GAPDH	GAPDH	MOSC2 ratio
Control1	8660	9820	12600	14200	15000	12900	0.73
Control2	23800	19600	19100	57000	48200	48200	0.51
Control3	1370	4080	8300	61800	7340	7340	0.63
Diabetic1	401	236	226	146	135	150	2.00
Diabetic2	187	243	191	29	39	30	6.30
Diabetic3	522	551	409	165	147	157	3.15
Treated1	2410	2970	150000	6600	3680	3300	0.59
Treated2	327	292	383	426	1890	529	0.69
Treated3	47800	44900	48200	32900	32400	35200	1.40

Renal MOSC2 copy numbers relative to GAPDH mRNA copy numbers were detected using qPCR in control, diabetic and treated mouse kidneys. For each condition, 3 separate samples were used to prepare cDNA and renal MOSC2 was quantified from each sample in triplicate. Data are shown as relative expression values.

Table 26b. Relative copy numbers of MOSC2 mRNA in kidneys of STZ mice

Condition	N	Mean values ± SD of MOSC2 copy numbers	Mean values ± SD of MOSC2 log
Control	3	0.63 ± 0.11	-0.2 ± 0.07
Diabetic	3	3.82 ± 2.22	0.53 ± 0.25*
Treated	3	0.89 ± 0.43	-0.07 ± 0.19

Renal MOSC2 mRNA copy numbers relative to GAPDH copy numbers were detected in the kidneys of STZ mice. Values are shown as mean ± SD. *P<0.05

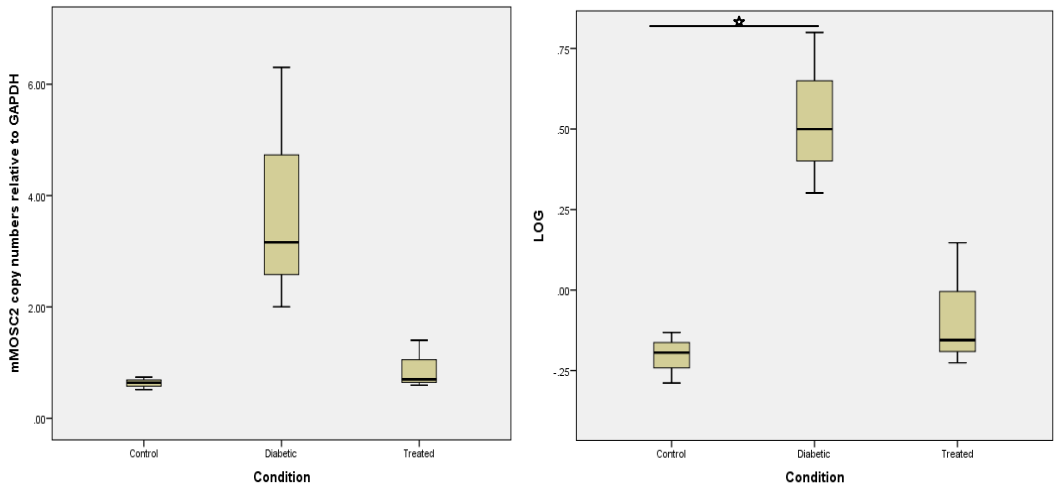

Figure 23. Renal MOSC2 mRNA levels were elevated in diabetic STZ mouse kidneys. Mouse kidneys were collected from control, diabetic and cured mice. Renal MOSC2 copy numbers were detected using qPCR (n= 3). The mean values and standard deviation of different experiments are shown. A) Values shown are copy numbers of renal MOSC2 mRNA relative to GAPDH. B) The data were log-transformed and showed an increase in renal MOSC2 mRNA expressions in diabeic kidneys. *P>0.05

2) Renal levels of MOSC2 proteins in streptozotocin-induced diabetic mice

The aim of this part of the study was to investigate the mouse MOSC2 protein expression in order to see whether hyperglycaemia enhanced protein expression of MOSC2. This part of the work was carried out in collaboration with Havemeyer group in Germany. Therefore, the same samples from the mouse MOSC2 mRNA expression experiments in a variety of kidneys from STZ mice were sent to Germany for protein analysis. Proteins from control, diabetic and treated kidneys (n= 3) of STZ mice were purified and assayed for total protein using a BCA protein assay kit (Pierce, UK). A dilution series of known concentrations of BSA protein was prepared (Section 2.11) and evaluated alongside protein samples from mice kidneys by measuring the absorbance at 450 nm using a plate reader (Table 27a). The concentration of protein samples was then determined according to the standard curve (Table 27b), which was produced by plotting A_{540} measurement for each BSA standard versus its concentration in mg/ml. The standard curve was used to detect the protein concentration of each particular sample (Figure 24a).

Table 27a. Concentration, Mean and SD absorbance of BSA

BSA concentration (mg/ ml)	Mean Absorbance (540 nm)	SD Absorbance
2	1.14	0.01
1	0.72	0.05
0.5	0.35	0.08
0.25	0.28	0.00
0.125	0.13	0.01
0	0.08	0.03

A dilution series of known concentrations of BSA protein was prepared and evaluated alongside protein samples from mouse kidneys by measuring the absorbance at 450 nm.

Table 27b. Concentration of protein from STZ mouse kidneys

Samples	BSA concentration (mg/ ml)	Absorbance (540 nm)
Control	16.2	0.1
Control2	12.9	0.1
Control3	17.8	0.4
Diabetic1	6	0.8
Diabetic2	13.3	0.1
Diabetic3	15.3	0.7
Treated1	16.8	0.4
Treated2	22.5	0.2
Treated3	17.1	2.1

The concentrations of protein samples from kidneys of STZ mice were determined using the standard curve shown in Figure 24a.

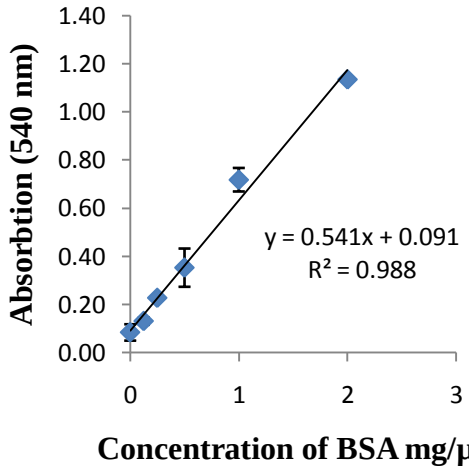

Figure 24a. Determination of protein concentration in STZ mice.
Dilution series of BSA protein was prepared and the concentration of each dilution was assayed by measuring the absorbance at 540 nm.

Immunoblot analysis was carried out by blotting extracted proteins (12µl) separated by 12.5% SDS-PAGE. The blot was incubated with anti-MOSC2 (MOCO sulfurase C-terminal-domain-containing) antibody raised against mouse MOSC2 (1:2500 dilution; Sigma-Aldrich), followed by horseradish peroxidise-conjugated anti-rabbit IgG secondary antibody (1:10000 dilution; Jackson Immuno Research, UK). Immunoreactive bands were detected by ECL (Enhanced chemiluminescence) system (ECL plus Western blotting detection system; GE Healthcare).

Figure 24b shows a representative immunoblot of the MOSC2 protein in control, diabetic and treated kidneys of STZ mice. The anti-MOSC2 antibody recognised an expected band of 34 kDa in STZ mouse kidneys. Induced expression of MOSC2 protein was observed in all types of STZ mouse kidneys, as detected by the strong intensity of the protein band. These results confirmed the increase of MOSC2 mRNA expression in diabetic mouse kidneys compared to control and showed that hyperglycaemia increased mouse MOSC2 protein expression as well as mRNA expression, shown previously in this chapter.

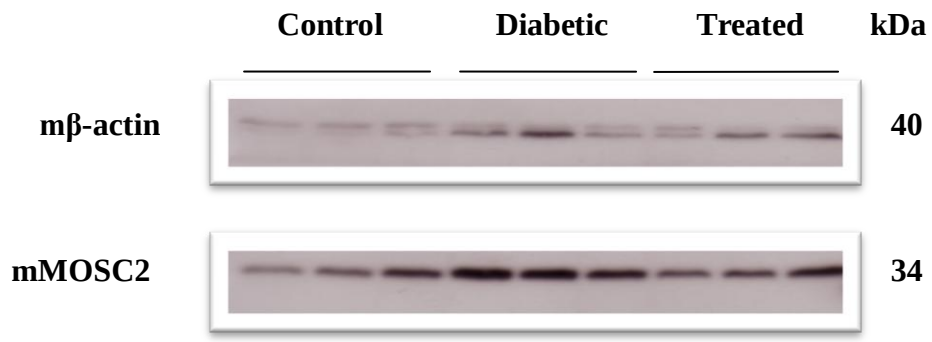

Figure 24b.Western blot analysis of mouse MOSC2 protein in kidneys of STZ mice.

Kidneys from control, diabetic and treated streptozotocin-induced diabetic mice were used to show the mouse MOSC2 protein expression. Equal amounts of proteins (12 µg) were subjected to SDS-PAGE and the expression of MOSC2 protein was detected by immunoblot analysis using a primary antibody anti-MOSC2 raised against MOSC2. The blot was re-probed with ß-actin antibody to demonstrate equal loading of protein in all lanes (This part of work was carried out in the Havemeyer lab, Kiel, Germany, by Heyka Jacob in collaboration with our group).

3) Determination of MOSC2 protein in diabetic and control kidneys of streptozotocin-induced diabetic mice

In this part of the study MOSC2 protein localisation was determined in control and diabetic mouse kidney sections using immunofluorescence. Mouse kidney sections were incubated with MOSC2 antibody overnight and anti-rabbit FITC conjugated secondary antibodies for 1 hour; nuclei were stained blue with DAPI (Section 2.14.2.). Sections were viewed under a fluorescent microscope (Eclipse TE 2000-U, Nikon). The fluorescent probe detected by the green emission indicated that the MOSC2 protein was located predominantly in the tubules and not in glomerulus of the mouse kidney. The MOSC2 protein was expressed at relatively higher levels in the tubules, suggesting MOSC2 protein expressed in tubular cells but not in mesangial cells. The data also showed that MOSC2 is more abundant in diabetic kidneys compared to control kidneys, which confirmed findings from the immunoblot analysis in kidneys of STZ mice. In addition to higher expression of MOSC2 protein, the tubules were bigger (hypertrophy) and distorted in comparison to the control kidney (Figure 25).

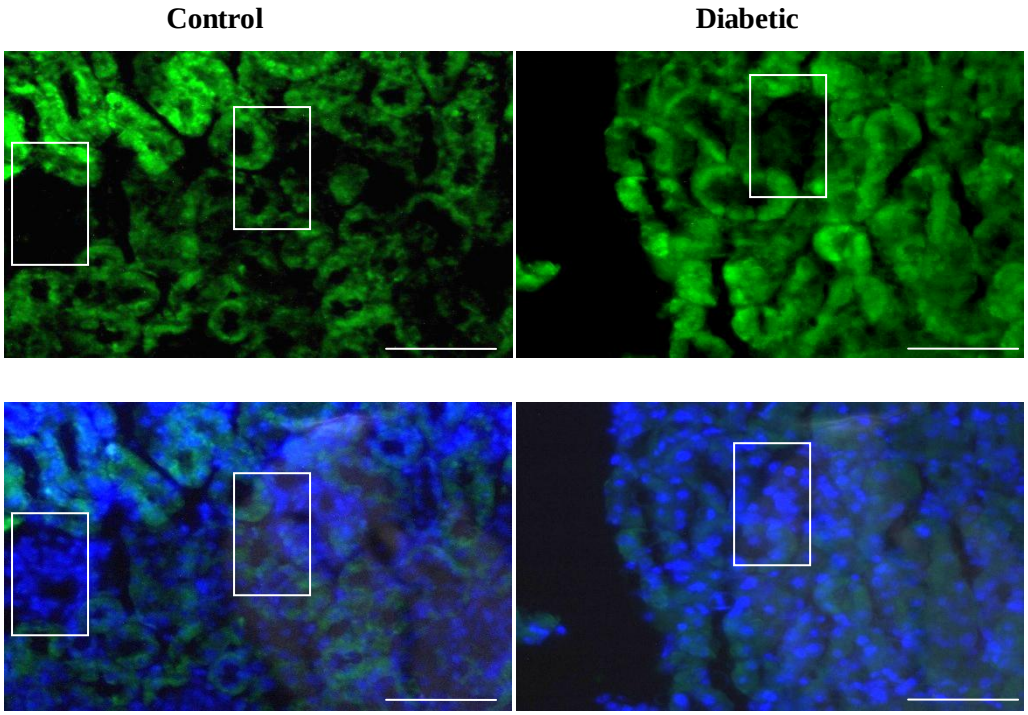

Figure 25. MOSC2 protein is highly abundant in tubular and less in glomerular cells from control and diabetic kidneys of STZ mice.
Sections of kidneys from control mice (blood glucose<11mmol/L) and diabetic mice (blood glucose level >20mmol/L) were labelled with mMOSC2 primary antibody and FITC conjugated secondary antibody and nuclei were stained with DAPI. White boxes are showing no green staining in glomeruli, which indicated renal expression of MOSC2 in tubules but not in glomeruli in cortex. Scale bars are 250µM.

4) ***Is renal MOSC2 mRNA regulated by glucose in human cultured renal cells?***

Previously, Malik (2007) showed that renal MOSC2 is increased in HMCs and HMCL when cells were exposed to HG. We subsequently tested the hypothesis that mRNA expression levels of renal MOSC2 were up-regulated in human renal cells (HMCs, HEK293, HTC). In order to measure copy numbers of renal MOSC2 mRNA under different conditions, human cultured renal cells were incubated in different conditions as previously described (Section 5.3.1.) and total RNA was isolated from each sample (Table 24c, Section 5.3.2.). cDNA was then synthesized, MOSC2 values relative to the reference gene (PGK) were determined and the data was normalised. All qPCR experiments were performed in triplicate for each particular sample in all conditions and a blank control was included in all runs.

● ***Effect of high glucose on renal MOSC2 mRNA expression in human cultured mesangial cells***

Copy numbers of renal MOSC2 mRNA relative to reference gene (PGK) were measured by qPCR (Table 28a). The data showed a significant elevation in renal MOSC2 copy numbers when the cells were exposed to HG compared to NG. This result was similar to the previous findings by Malik (2007). Statistical analysis of the data using student's *t* test showed that this elevation was significant (3.87 ± 1.07 vs. 0.85 ± 0.58, $P<0.05$; Table 28b). There was no significant difference between cells which were exposed to NG and NGM (0.09 ± 0.07 vs. 0.85 ± 0.58, $P>0.05$). This demonstrated that there was no osmalarity effect in play (Figure 26). This finding supports our previous results and demonstrates that the expression of renal MOSC2 is directly elevated by glucose in HMCs.

Table 28a. Renal MOSC2 mRNA expression values relative to PGK in human mesangial cells cultured under different conditions

Cells	Condition	MOSC2	MOSC2	MOSC2	PGK	PGK	PGK	MOSC 2 ratio
HMCs1	NG	2740	2050	1580	5420	6270	2260	0.46
HMCs2	NG	2530	1970	1920	110	1010	1220	1.92
HMCs3	NG	2350	1900	2280	1190	1790	1310	1.52
HMCs4	HG	2830	2860	4960	1040	918	821	3.11
HMCs5	HG	3890	3110	3610	776	724	791	4.63
HMCs6	HG	5550	4640	4100	32300	26400	29500	0.16
HMCs7	NGM	3900	790	1350	24300	17100	86200	0.12
HMCs8	NGM	173	12	0	6210	4850	14800	0.01
HMCs9	NGM	218	146	0	0	1260	952	0.16

Renal MOSC2 mRNA copy numbers relative to PGK mRNA copy numbers were detected using real time PCR in human renal mesangial cells cultured in normal glucose (NG), high glucose (HG) and normal glucose with mannitol (NGM). For individual conditions, 3 separate samples were applied to prepare cDNA and MOSC2 was quantified for each sample in triplicate. Data are shown as relative expression values.

Table 28b. Relative copy numbers of renal MOSC2 mRNA in human mesangial cells

Condition	N	Mean values ± SD of MOSC2 copy numbers	Mean values ± SD of MOSC2 log
NG	3	0.85 ± 0.58	-0.13 ± 0.27
HG	3	3.87 ± 1.07*	0.57 ± 0.12*
NGM	3	0.09 ± 0.07	-1.2 ± 0.64

Renal MOSC2 mRNA copy numbers relative to PGK mRNA copy numbers were detected in human mesangial cell line grown in normal glucose (NG) and high glucose (HG) and in normal glucose with mannitol (NGM). Copy numbers are shown as means ± SD. *P<0.05

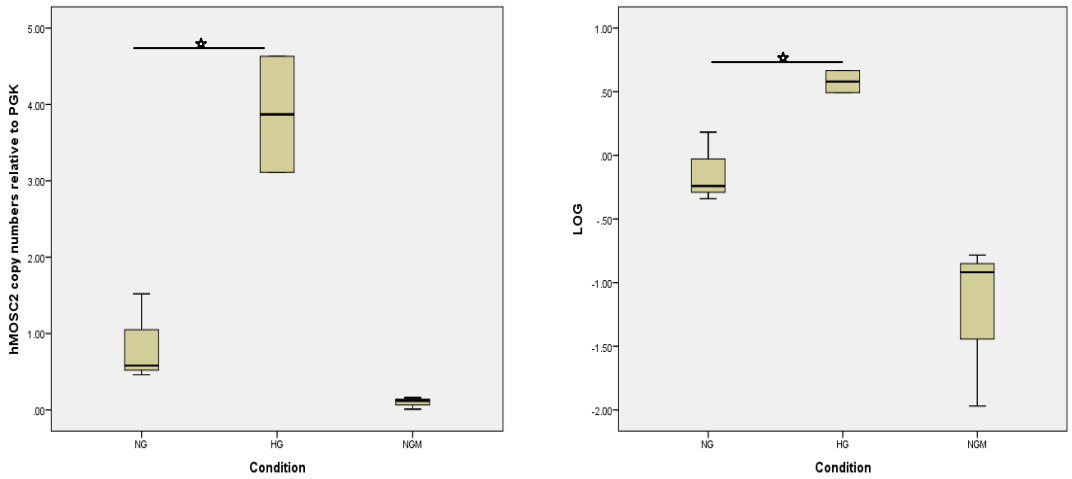

Figure 26. The effect of high glucose on renal expression of MOSC2 mRNA in mesangial cells.
After being synchronised, human mesangial cells were grown in 5mM glucose (NG), 25mM glucose (HG) and normal glucose with mannitol (5mM glucose + 20mM mannitol) for 3 days. Renal MOSC2 copy numbers were measured using real-time PCR (n = 3). The mean values of 3 different experiments are shown. A) Values shown are copy numbers of renal MOSC2 mRNA relative to PGK. B) The data showed an increase of renal MOSC2 levels in human mesangial cells exposed to HG. *P<0.05

● ***Effect of high glucose on renal MOSC2 mRNA expression in human cultured embryonic kidney 293 cells***

In the previous experimental study, we showed that renal MOSC2 was up-regulated in HMCs upon exposure of cells to HG. To test the hypothesis that renal MOSC2 also regulated in HEK293 cells, copy numbers of renal MOSC2 mRNA relative to PGK were measured by qPCR (Table 29a). Using student's *t* test for statistical analysis of the data, we found a significant increase in HG compared to NG (0.36 ± 0.03 vs. 0.04 ± 0.02, P<0.05; Table 29b). There was a non-significant difference between cells grown in NG with cells grown in NGM (0.15 ± 0.04 vs. 0.04 ± 0.02). The data were log-transformed as the actual copy values of MOSC2 were skewed. These results showed that renal MOSC2 was significantly up-regulated in HEK293 cells in HG.

Table 29a. Renal MOSC2 mRNA expression values relative to PGK in human embryonic kidney 293 cells cultured in different conditions

Cells	Condition	MOSC2	MOSC2	MOSC2	PGK	PGK	PGK	MOSC2 ratio
HEK1	NG	77890	9020	8070	31600	661000	34300	0.03
HEK2	NG	12200	15800	15000	136000	272000	263000	0.06
HEK3	HG	40500	34900	39600	89000	98300	107000	0.39
HEK4	HG	55500	36900	40800	120000	117000	115000	0.37
HEK5	HG	8550	8700	10900	35900	35500	33500	0.26
HEK6	NGM	8810	7520	7810	65400	62100	40400	0.14
HEK7	NGM	7130	6490	42	38000	42600	43900	0.1
HEK8	NGM	9430	8120	9290	48300	47200	41000	0.19

Renal MOSC2 mRNA copy numbers relative to PGK mRNA copy numbers were detected using real time PCR in human embryonic kidney 293 cells cultured in normal glucose (NG), high glucose (HG) and normal glucose with mannitol (NGM). For individual conditions, 3 separate samples were applied to prepare cDNA and renal MOSC2 was quantified for each sample in triplicate. Data are shown as relative expression values.

Table 29b. Relative copy numbers of renal MOSC2 mRNA in human embryonic kidney 293 cells

Condition	N	Mean values ± SD of hMOSC2 copy numbers	Mean values ± SD of hMOSC2 log
NG	2	0.04 ± 0.02	-1.32 ± 0.19
HG	3	0.36 ± 0.03*	-0.44 ± 0.04
NGM	3	0.15 ± 0.04	-0.83 ± 0.12

Renal MOSC2 mRNA copy numbers relative to PGK mRNA copy numbers were detected in human embryonic kidney 293 cells grown in normal glucose (NG), high glucose (HG) and in normal glucose with mannitol (NGM). Copy numbers are shown as means. *$P<0.05$

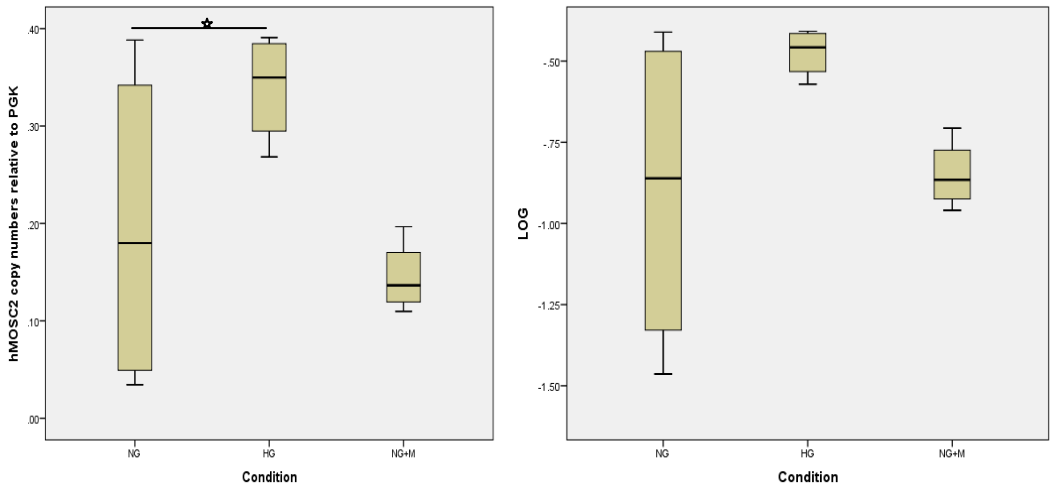

Figure 27. The effect of high glucose on renal expression of MOSC2 mRNA in human embryonic kidney 293 cells.

After being synchronised, human embryonic kidney 293 cells were incubated in 5mM (NG), 25 mM glucose (HG) and normal glucose with mannitol (5mM glucose + 20mM mannitol) for 3 days. Renal MOSC2 copy numbers were detected applying qPCR. The mean values of different experiments are shown. A) Values shown are copy numbers of renal MOSC2 mRNA relative to PGK. B) The data showed an increase of renal MOSC2 levels in cells exposed to HG.*P<0.05

● ***The effect of high glucose on MOSC2 mRNA expression in human cultured tubular cells***

As we found an up-regulation of renal MOSC2 by glucose in HMCs and HEK293, we examined the renal MOSC2 mRNA relative to reference gene (PGK) by qPCR (Table 30a). Surprisingly, we found a 2.15-fold decrease in renal MOSC2 copy numbers when cells were grown in HG compared to NG. Statistical analysis using student's *t* test showed a significant reduction of renal MOSC2 in cells grown in HG compared to NG (P<0.05; Table30b). However, the difference between NG and NGM was not significant, confirming no effect of osmolarity. HTC cultured in HG contained 0.2 ± 0.1 copies of renal MOSC2, whereas when cultured in NG, HTC contained 0.43 ± 0.05 copies of renal MOSC2 (Figure 28). These data showed that renal MOSC2 is decreased in HTC in hyperglycaemic conditions.

Table 30a. Renal MOSC2 mRNA expression values relative to PGK in human tubular cells cultured in different conditions

Cells	Condition	MOSC2	MOSC2	MOSC2	PGK	PGK	PGK	MOSC2 ratio
HTC1	NG	68	152	142	224	229	234	0.5
HTC2	NG	3380	2960	3280	6120	9780	714-	0.4
HTC3	NG	1110	1830	1700	3670	3600	4870	0.4
HTC4	HG	1130	346	286	7860	5450	6230	0.1
HTC5	HG	1460	2000	441	5720	5470	8120	0.2
HTC6	HG	1190	1570	838	2520	4190	4250	0.3
HTC7	NGM	81	155	143	1150	1380	1430	0.1
HTC8	NGM	713	290	329	2700	3480	1850	0.2
HTC9	NGM	100	112	0	42	46	43	2.4

Renal MOSC2 mRNA copy numbers relative to PGK mRNA copy numbers were detected using qPCR in human tubular cells cultured in normal glucose (NG), high glucose (HG) and normal glucose with mannitol (NGM). For individual conditions, 3 separate samples were used for preparation of cDNA and renal MOSC2 was quantified for each sample in triplicate. Data shown are relative expression values.

Table 30b. Relative copy numbers of renal MOSC2 mRNA in human tubular cells

Condition	N	Mean values ± SD of MOSC2 copy numbers	Mean values ± SD of MOSC2 log
NG	3	0.43 ± 0.05	-0.36 ± 0.07
HG	3	0.2 ± 0.1*	-0.7 3± 0.28
Mannitol	3	0.9 ± 1.3	-0.47 ± 0.75

Renal MOSC2 mRNA copy numbers relative to PGK mRNA copy numbers were detected in human tubular cells grown in normal glucose (NG) and high glucose (HG) and in normal glucose with mannitol (NGM). Copy numbers are shown as means. *P<0.05

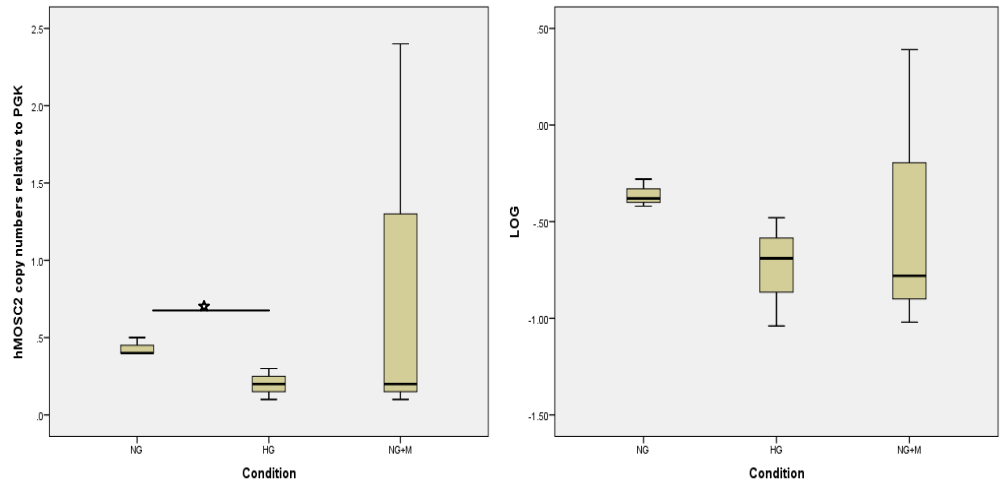

Figure 28. Effect of high glucose on renal expression of MOSC2 mRNA in human tubular cells.

After being synchronised, human tubular cells were incubated in 5mM (NG), 25mM glucose (HG) and normal glucose with mannitol (5 mM glucose + 20mM mannitol) for 3 days. MOSC2 copy numbers were detected by real-time PCR (n= 3). The mean values of 3 different experiments are shown. a) Values shown are copy numbers of renal MOSC2 mRNA relative to PGK. b) The data showed a decrease in human tubular cells exposed to HG. *P<0.05

5) Does hyperglycaemia result in increased renal MOSC2 protein levels in human cultured renal cells?

We have previously found that the human MOSC2 gene is directly up-regulated by glucose in HMCs and HEK293 cells. However, we found a down-regulation of MOSC2 mRNA expression in HTC. The aim of this part of the study was to determine the human MOSC2 protein levels to see the effect of HG on its protein expression. For the protein analysis, cell pellets from human cultured renal cells (HMCs, HEK293, HTC) grown in different conditions were saved from mRNA expression (Table 24c, Section 5.3.2.). For human MOSC2 protein, cell pellets were centrifuged and lysed in an appropriate lysis buffer and then cell lysate including the protein was recovered and examined.

A dilution series of known concentrations of BSA protein was prepared (Section 2.11.) and measured alongside protein samples from human renal cell lysates (HMCs, HEK293, HTC) by measuring the absorbance at 540 nm using a plate reader (Table 31a). The concentrations of the protein samples were then determined according to their respective standard curves (Table 31b). The standard curve was produced by plotting the A_{540} measurement for each BSA standard versus its concentration in

mg/ml. The standard curve was then used to assay the protein concentration of each particular sample (Figure 29a).

Table 31a. Concentration, mean and SD absorbance of BSA in human cultured renal cells

Cells	BSA concentration in cells (mg/ml)	Mean Absorbance (540 nm)	SD Absorbance
HMCs and HEK293	2	1.1	0
	1	0.6	0
	0.5	0.3	0
	0.25	0.2	0
	0.125	0.1	0
	0.025	0.1	0
	0	0	0
HTC	2	1.27	0.20
	1	0.67	0.09
	0.5	0.39	0.01
	0.25	0.26	0.01
	0.125	0.17	0.01
	0	0.10	0

A dilution series of known concentrations of BSA protein was prepared and evaluated alongside protein samples from human cultured renal cells (human mesangial cells, human embryonic kidney 293 cells, human tubular cells) by measuring the absorbance at 450 nm using a plate reader.

Table 31b. Concentration of protein from human renal cells

Cells	Condition	Concentration (mg/ ml)	Absorbance (540 nm)
HMCsl	NG	0.7	0.03
HMCs2	NG	0.8	0.03
HMCs3	NG	0.9	0.04
HMCs4	NG	0.7	0.06
HMCs5	HG	1.7	0.25
HMCs6	HG	1.7	0.25
HMCs7	HG	1.6	0.22
HMCs8	HG	1.6	0.24
HMCs9	NGM	0.6	0.19
HMCs10	NGM	0.6	0.21
HMCs11	NGM	0.5	0.27
HMCs12	NGM	0.6	0.29
HEK1	NG	3.6	0.03
HEK2	NG	3.0	0.03
HEK3	NG	4.5	0.04
HEK4	NG	3.6	0.06
HEK5	HG	3.9	0.25
HEK6	HG	4.8	0.25
HEK7	HG	4.4	0.22
HEK8	HG	3.1	0.24
HEK9	NGM	4.0	0.19
HEK10	NGM	3.9	0.21
HEK11	NGM	3.8	0.27
HEK12	NGM	3.9	0.29
HTC1	NG	0.2	0
HTC2	NG	0.2	0
HTC3	NG	0.4	0.3
HTC4	HG	0.3	0
HTC5	HG	0.2	0.1
HTC6	HG	0.3	-
HTC7	NGM	0.6	0
HTC8	NGM	0.2	0.1
HTC9	NGM	0.1	-

The concentrations of protein samples from human renal cells were determined using the standard curve shown in Figure 29a.

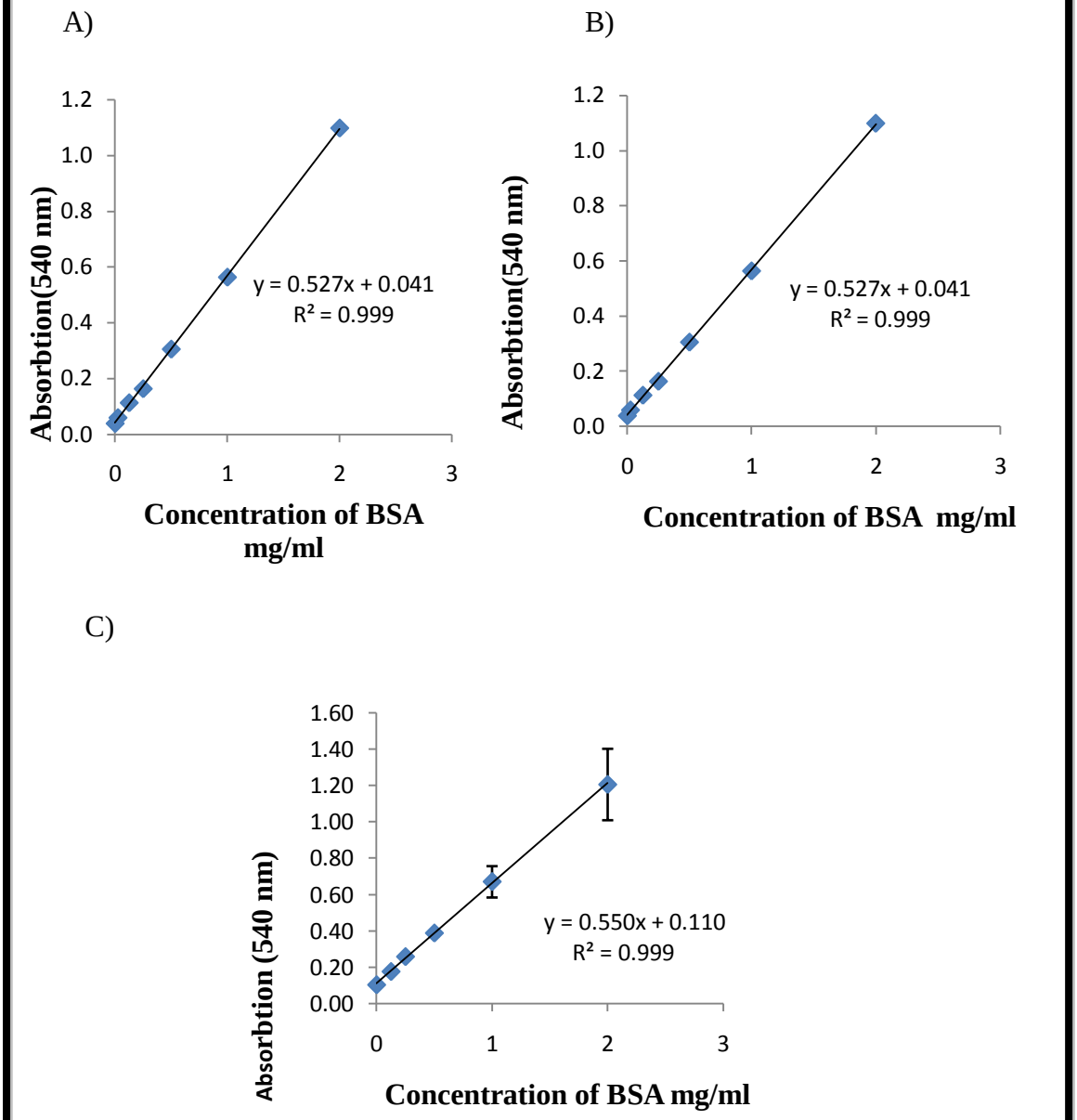

Figure 29a. Determination of protein concentration in human renal cells.

Dilution series of BSA protein was prepared and the concentration of each dilution was assayed by measuring the absorbance at 540 nm. A) Determination of BSA protein concentration in HMCs B) HEK293 and C) HTC.

Immunoblot analysis was carried out by blotting extracted proteins (25 µg) separated by 12.5% SDS-PAGE. The blot was incubated with anti-MOSC2 antibody raised against human MOSC2 (diluted 1:500; Abgent, USA; Sigma-Aldrich), followed by horseradish peroxidise-conjugated anti-rabbit IgG secondary antibody (1:10000 dilution; Jackson Immuno Research, UK). Immunoreactive bands were detected by ECL (Enhanced chemiluminescence) system (ECL plus Western blotting detection system; GE Healthcare).

● ***MOSC2 protein levels in human renal cells grown under different conditions***

Figure 29b shows a representative immunoblot of MOSC2 proteins in human renal cells grown under NG, HG and NGM conditions. The anti-MOSC2 antibody did not detect any band of the expected size of 34 kDa for all conditions of HMCs. In HEK293 cells, induced expression of MOSC2 protein was observed in cells exposed to HG compared to NG but the bands were faint (Figure 29b). For the HTC samples, the concentrations of protein samples from HTC (Table 31b) were determined using the standard curve shown in Figure 29a. The concentration of protein samples was too low to detect MOSC2 protein expression in HTC.

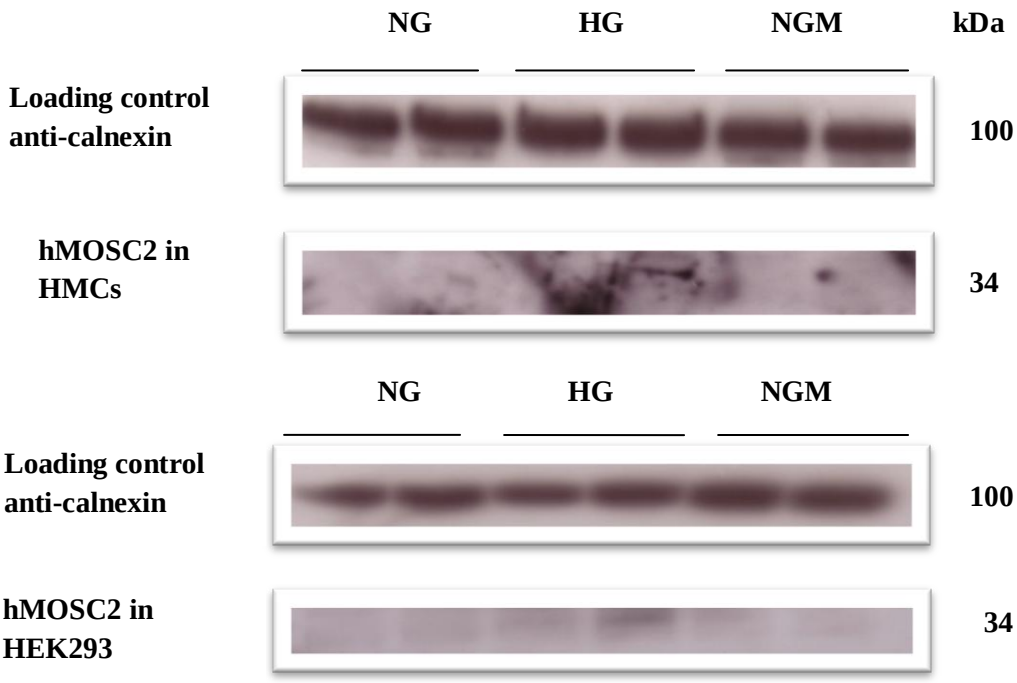

Figure 29b. Western blot analysis of MOSC2 protein in human mesangial and human embryonic kidney 293 cells.
Human cultured renal cells were serum-starved and exposed to normal glucose (5mM), high glucose (25mM) and normal glucose with mannitol (20+5 mM) for 3 days. Equal amounts of cell lysate proteins (25µg) were subjected to SDS-PAGE and the MOSC2 protein expression was determined by immunoblot analysis using rabbit polyclonal IgG primary antibody raised against MOSC2. The blot was re-probed with anti-calnexin antibody to determine the equal loading of protein in all lanes (This part of work was carried out in the Havemeyer lab, Kiel, Germany, by Heyka Jacob in collaboration with our group).

5.3.4. Is MOSC1 a glucose regulated gene *in vivo* and *in vitro* models?

In this section, we looked at the effect of hyperglycaemia on MOSC1 mRNA expression in STZ-induced diabetic mice *in vivo*. We also examined mRNA and protein regulation of MOSC1 in human renal cells (HMCs, HEK293, HTC) in the presence of hyperglycaemia.

● ***Renal mRNA levels of MOSC1 in kidneys of streptozotocin-induced diabetic mice***

First, we examined renal MOSC1 mRNA expression in control (n= 3), diabetic (n= 3) and treated (n= 3) kidneys of STZ-induced diabetic mice which were the same samples used previously for MOSC2 mRNA expression (Table 24b; Section 5.3.2). Copy

numbers were automatically measured from their concentration and samples were normalised with respect to expression of GAPDH mRNA. All qPCR experiments were performed in triplicate (Table 32a). Statistical analysis of the data using student's *t* test provided the *p* values for all conditions.

Table 32a. Relative Renal MOSC1 and GAPDH mRNA expression values in the kidneys of STZ mice

Sample	MOSC1	MOSC1	MOSC1	GAPDH	GAPDH	GAPDH	MOSC1 ratio
Control1	21	9	575	15200	14700	12600	0
Control2	9	9	59	44900	48900	39400	0
Control3	93200	2140		3460	3980	3560	13
Diabetic1	2980	2070	2450	132	137	122	19
Diabetic2	734	2960	1030	16	15	17	97
Diabetic3	983	238	0	126	208	181	2
Treated1	9	4	258	3100	2230	2330	0
Treated2	0	4890	592	518	350	487	4
Treated3	13	17	122	40800	36200	40500	0

Renal MOSC1 copy numbers relative to GAPDH mRNA copy numbers were detected using real-time qPCR in control, diabetic and treated mice kidneys. For each condition, 3 separate samples were used to prepare cDNA and renal MOSC1 was quantified from each sample in triplicate. Data are shown as relative expression values.

Renal MOSC1 mRNA copy numbers were elevated compared to control kidneys and they were corrected by treatment. However, statistical analysis of the data using student's *t* test showed that this increase was not significant (39.33 ± 50 vs. 4.33 ± 7.50, $P>0.05$; Table 32b). The standard deviation was very large in diabetic kidneys compared to control and treated kidneys (Figure 30). We also could not determine the MOSC1 protein levels in control, diabetic and treated kidneys as no antibody against mouse MOSC1 exists. With this in mind, we did not examine further models of diabetic mice for MOSC1, as the mRNA study showed non-significant changes.

Table 32b. Relative copy numbers of renal MOSC1 mRNA in kidneys of STZ mice

Condition	N	Mean values ± SD of MOSC1 copy numbers	Mean values ± SD of MOSC1 log
Control	3	4.33 ± 7.50	-1.33 ± 2.08
Diabetic	3	39.33 ± 50.65	1 ± 1
Treated	3	1.33 ± 2.30	-1 ± 2

Renal MOSC1 mRNA copy numbers relative to mGAPDH copy numbers were detected in the kidneys of STZ mice. Values are shown as mean ± SD.

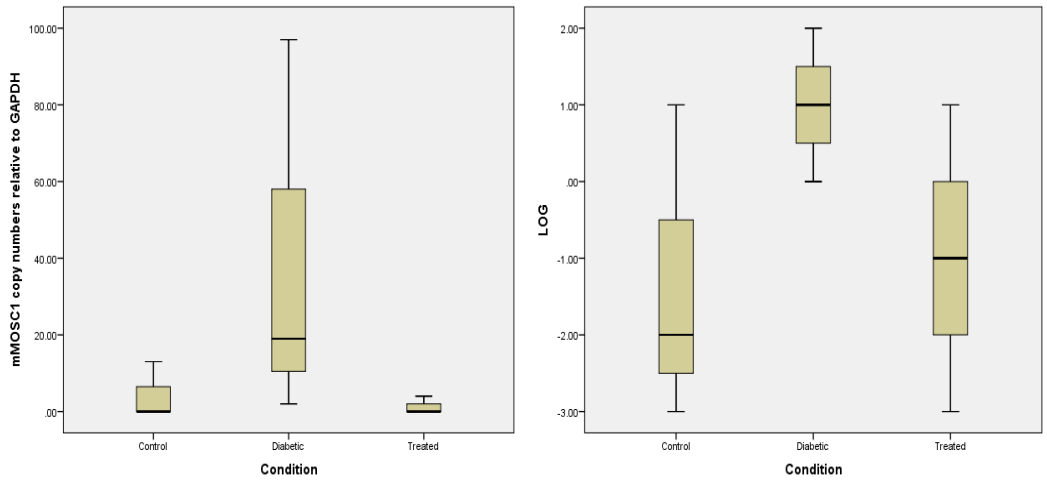

Figure 30. Effect of high glucose on renal MOSC1 mRNA levels in the kidneys of STZ mice.

Mouse kidneys were collected from control, diabetic and treated kidneys of STZ mice. Renal MOSC1 copy numbers were detected using real-time qPCR (n= 3). The mean values and standard deviation of different experiments are shown. A) Values shown are copy numbers of renal MOSC1 mRNA relative to GAPDH. B) The data were log-transformed and results were not significant. P>0.05

● ***Effect of high glucose on renal MOSC1 mRNA expression in human cultured mesangial cells***

To determine if MOSC1 is a glucose-regulated gene, we examined renal MOSC1 mRNA expression in human cultured renal cells (HMCs, HEK293, HTC) from the samples previously used for renal MOSC2 mRNA expression (Table 24c; Section 5.3.2). As renal MOSC2 was regulated by glucose in HMCs and HEK293 cells, we wanted to see if renal MOSC1 was also regulated by glucose in human cultured renal cells.

Renal copy numbers of MOSC1 mRNA relative to control gene (PGK) were measured by qPCR in HMCs (Table 33a). Statistical analysis of the data using student's *t* test showed that these results are non-significant (Table 33b) and there is no significant difference between each condition. The data were log-transformed, as the actual MOSC1 copy number values were not normally distributed (Figure 31).

Table 33a. Renal MOSC1 mRNA expression values relative to PGK in human mesangial cells cultured in different conditions

Cells	Condition	MOSC1	MOSC1	MOSC1	PGK	PGK	PGK	MOSC1 ratio
HMCs1	NG	1630	2430	3200	4920	4830	4970	0.49
HMCs2	NG	563	747	776	827	3490	2470	0.54
HMCs3	NG	615	529	523	1070	975	1022	0.31
HMCs4	HG	1410	1250	1220	1030	894	981	1.34
HMCs5	HG	10200	10100	9370	26200	23900	29300	0.37
HMCs6	HG	6450	10200	5390	26400	28800	23300	0.28
HMCs7	NGM	1290	1410	2520	8330	19100	6450	0.15
HMCs8	NGM	398	568	285	924	3330	982	0.24
HMCs9	NGM	1030	852	689	2530	2320	2840	0.33

Renal MOSC1 mRNA copy numbers relative to PGK mRNA copy numbers were detected using real time PCR in human renal mesangial cells, cultured in normal glucose (NG), high glucose (HG) and normal glucose with mannitol (NGM). For individual conditions, 3 separate samples were applied to prepare cDNA and renal MOSC1 was quantified for each sample in triplicate. Data are shown as relative expression values.

Table 33b. Relative copy numbers of MOSC1 mRNA in human mesangial cells

Condition	N	Mean values ± SD of MOSC1 copy numbers	Mean values ± SD of MOSC1 log
NG	3	0.44 ± 0.12	-.036 ± -0.13
HG	3	0.66 ± 0.58	-0.28 ± 0.36
NGM	3	0.24 ± 0.09	-0.36 ± 0.16

Renal MOSC1 mRNA copy numbers relative to PGK mRNA copy numbers were detected in human mesangial cell lines grown in normal glucose (NG), high glucose (HG) and in normal glucose with mannitol (NGM). Copy numbers are shown as means ± SD. $P>0.05$

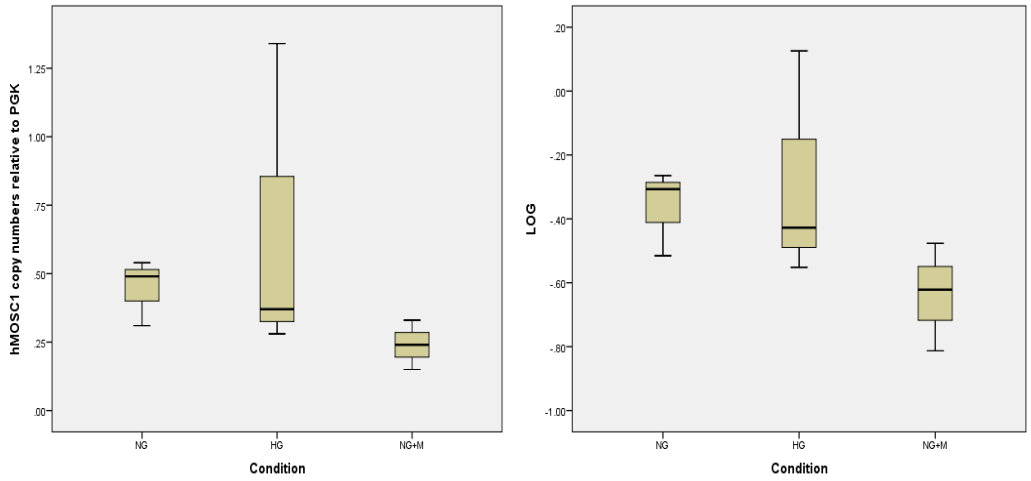

Figure 31. The effect of high glucose on renal expression of MOSC1 mRNA in human mesangial cell.

After being synchronised, human mesangial cells were grown in 5 mM glucose (NG), 25 mM glucose (HG) and normal glucose with mannitol (5 mM glucose + 20 mM mannitol) for 3 days. Renal MOSC1 copy numbers were measured using qPCR (n= 3). The mean values of 3 different experiments are shown. A) Values shown are copy numbers of renal MOSC1 mRNA relative to PGK. The results were not significant. B) After log-transformation of data, results were still not significant. P>0.05

● ***Effect of high glucose on Renal MOSC1 mRNA expression in human cultured embryonic kidney 293 cells***

Renal copy numbers of MOSC1 mRNA relative to reference gene (PGK) were measured by qPCR in HEK293 cells grown in NG, HG and NGM respectively (Table 34a). The data showed the same trend that we found in HMCs and it showed a non-significant difference between HEK293 cells cultured in HG compared to NG (0.87 ±0.24 vs. 1.62 ± 0.98, P>0.05; Table 34b). Statistical analysis of the data using student's *t* test showed a non-significant difference (Figure 32).

Table 34a. Renal MOSC1 mRNA expression values relative to PGK in human embryonic kidney 293 cells cultured in different conditions

Cells	Condition	MOSC1	MOSC1	MOSC1	PGK	PGK	PGK	MOSC1 ratio
HEK1	NG1	41300	24300	35000	22200	21400	13000	1.78
HEK2	NG2	51600	48300	21500	29600	8850	5230	2.78
HEK3	NG3	30400	34700	32900	26200	21000	15500	1.56
HEK4	NG4	235	267	147	516	615	553	0.39
HEK5	HG1	74500	85300	91100	75500	47900	76700	1.25
HEK6	HG2	83700	33300	96600	86500	98100	110000	0.73
HEK7	HG3	19900	16700	16200	13700	28000	62500	0.77
HEK8	HG4	69800	91400	52300	126000	4270	151000	0.76
HEK9	NGM1	33500	33900	38400	20800	23000	28500	1.46
HEK10	NGM2	82300	86200	74900	2600	24800	25300	3.2
HEK11	NGM3	55000	54800	52100	52900	41100	45100	1.16
HEK12	NGM4	61900	53500	56000	47100	52800	40700	1.22

Renal MOSC1 mRNA copy numbers relative to PGK mRNA copy numbers were detected using real time PCR in human renal embryonic kidney 293 cells cultured in normal glucose (NG), high glucose (HG) and normal glucose with mannitol (NGM). For individual conditions, 3 separate samples were applied to prepare cDNA and renal MOSC1 was quantified for each sample in triplicate. Data are shown as relative expression values.

Table 34b. Relative copy numbers of renal MOSC1 mRNA in human embryonic kidney 293 cells

Condition	N	Mean values ± SD of MOSC1 copy numbers	Mean values ± SD of MOSC1 log
NG	4	1.62 ± 0.98	0.11 ± 0.37
HG	4	0.87 ± 0.24	-0.06 ± 0.11
NGM	4	1.76 ± 0.98	0.20 ± 0.20

Renal MOSC1 mRNA copy numbers relative to PGK mRNA copy numbers were detected in human renal human embryonic kidney 293 cells grown in normal glucose (NG), high glucose (HG) and in normal glucose with mannitol (NGM). Copy numbers are shown as means ± SD. $P>0.05$

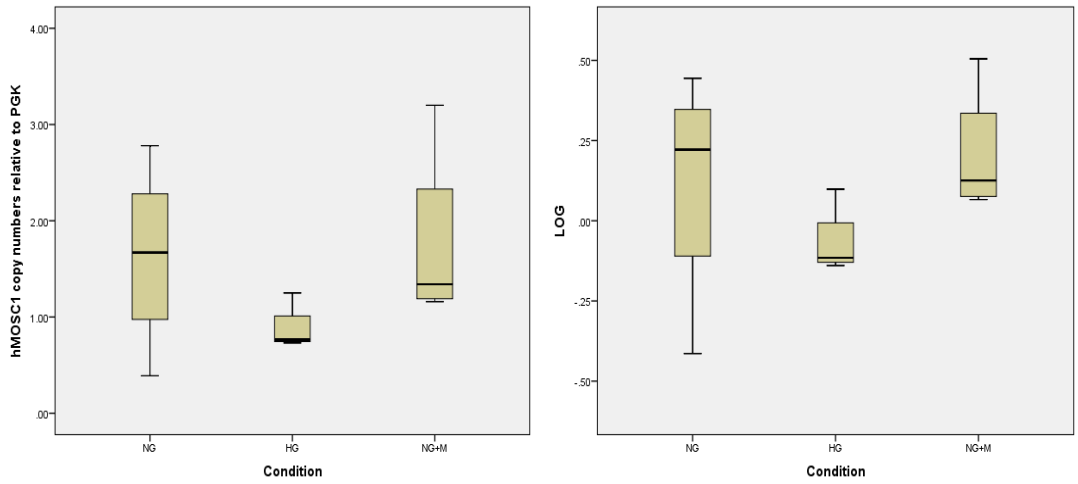

Figure 32. The effect of high glucose on renal expression of MOSC1 mRNA in human embryonic kidney 293 cells.

After being synchronised, human embryonic kidney 293 cells were grown in 5 mM glucose (NG), 25 mM glucose (HG) and normal glucose with mannitol (5 mM glucose+20mM mannitol) for 3 days. Renal MOSC1 copy numbers were measured using qPCR (n = 4). The mean values of 3 different experiments are shown. A) Values shown are copy numbers of renal MOSC1 mRNA relative to PGK. B) The data were log-transformed and results were not significant. P>0.05

● ***The effect of high glucose on renal MOSC1 mRNA expression in cultured human tubular cells.***

We could not demonstrate any change in renal MOSC1 mRNA expression in HTC. Renal copy numbers of MOSC1 mRNA relative to reference gene (PGK) in NG, HG and NGM of HTCs were measured by qPCR (Table 35a). Student's *t* test revealed no significant difference between NG and NGM (0.33 ± 0.15 vs. 0.61 ± 0.4, P>0.05; Table 35b), thereby suggesting the absence of osmolarity effect. Cells cultured in HG showed a non-significant difference in renal MOSC1 copy numbers when compared to those cultured in NG (P>0.05). HTC cultured in HG contained 0.27 ± 0.16 copies of renal MOSC1, whereas those cultured in NG contained 0.33 ± 0.15 copies of MOSC1 relative to PGK. The changes between MOSC1 mRNA levels were not significant (Figure 33).

Table 35a. Renal MOSC1 mRNA expression values relative to PGK in human tubular cells cultured in different conditions

Cells	Condition	MOSC1	MOSC1	MOSC1	PGK	PGK	PGK	MOSC1 ratio
HTC1	NG	64	52	59	147	164	57	0.48
HTC2	NG	568	984	651	4140	4140	4030	0.18
HTC3	NG	1340	1830	1160	4650	6040	3380	0.35
HTC4	HG	1440	2380	2090	4430	6040	5420	0.37
HTC5	HG	23	30	1470	4610	8220	6660	0.08
HTC6	HG	1220	1360	1610	3680	4150	3560	0.37
HTC7	NGM	766	537	689	1520	463	186	0.52
HTC8	NGM	1010	658	1300	4330	3620	3320	0.27
HTC9	NGM	34	-	-	26	32	36	1.06

Renal MOSC1 mRNA copy numbers relative to PGK mRNA copy numbers were detected using qPCR in human tubular cell lines cultured in normal glucose (NG), high glucose (HG) and normal glucose with mannitol (NGM). For individual conditions, 3 separate samples were applied to prepare cDNA and renal MOSC1 was quantified for each sample in triplicate. Data are shown as relative expression values.

Table 35b. Relative copy numbers of Renal MOSC1 mRNA in human tubular cells

Condition	N	Mean values ± SD of MOSC1 copy numbers	Mean values ± SD of MOSC1 log
NG	3	0.33 ± 0.15	-0.50 ± 0.21
HG	3	0.27 ± 0.16	-0.65 ± 0.38
Manitol	3	0.61 ± 0.40	-0.27 ± 0.30

Renal MOSC1 mRNA copy numbers relative to PGK mRNA copy numbers were detected in human tubular cell lines grown in normal glucose (NG), high glucose (HG) and in normal glucose with mannitol (NGM). Copy numbers are shown as means ± SD. P>0.05

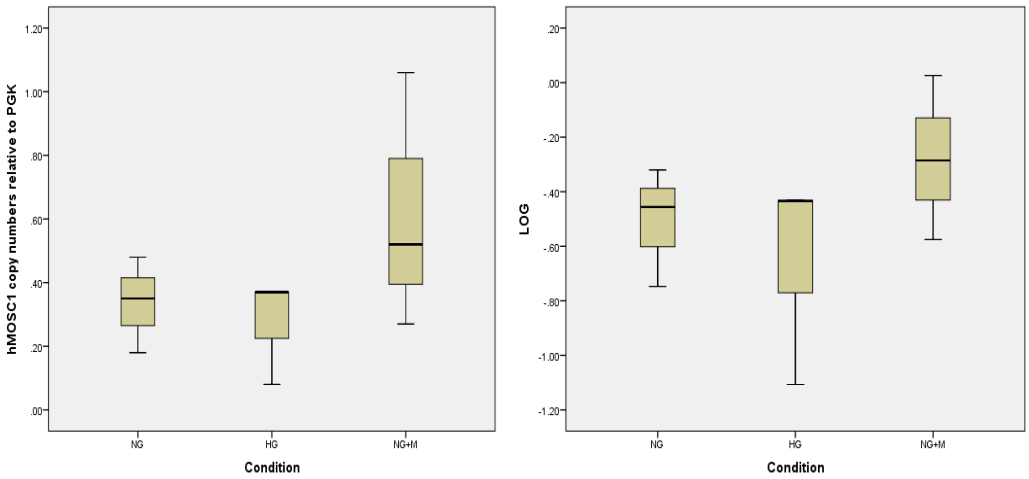

Figure 33. The effect of high glucose on renal expression of MOSC1 mRNA in human tubular cells.

After being synchronised, the tubular cells were incubated in 5 mM (NG), 25 mM glucose (HG) and normal glucose with mannitol (5 mM glucose + 20 mM mannitol) for 3 days.
Renal MOSC1 copy numbers were detected by qPCR (n= 3). The mean values of 3 different experiments are shown. A) Values shown are copy numbers of renal MOSC1 mRNA relative to PGK. B) The data were log-transformed and results were not significant. P>0.05

To conclude our observations, renal MOSC1 expression was found to remain unchanged in human renal cells (HMCs, HEK293, HTC) in HG.

3) Does hyperglycaemia result in increased MOSC1 protein levels in human cultured renal cells?

We have previously shown a non-significant difference in MOSC1 mRNA expression in human cultured renal cells. The aim of this part of the study was to determine MOSC1 protein levels *in vitro* in order to see the effect of HG on protein expression as well as mRNA expression. For the protein analysis, we used the same samples which were used for determining the expression of MOSC2 proteins in human cultured renal cells (Table 31b; Section 5.3.3).

Immunoblot analysis was carried out by blotting extracted proteins (25 µg) separated by 12.5% SDS-PAGE. The blot was incubated with anti-MOSC1 antibody raised against MOSC1 (diluted 1:1000; Abgent, USA) followed by horseradish peroxidise-conjugated anti-rabbit IgG secondary antibody (1:10000 dilution; Jackson Immuno Research, UK). Immunoreactive bands were detected by ECL (Enhanced chemiluminescence) system (ECL plus Western blotting detection system; GE

Healthcare). Figure 34 shows the representative immunoblot of MOSC1 protein in NG, HG and NGM of HMCs. The anti-MOSC1 recognised an expected band of 35 kDa which was very faint. In HEK293 cells, the anti-MOSC1 gave a band of 35 kDa corresponding to the expected molecular size of positive control (Figure 34). There was no major difference in MOSC1 protein expression in all conditions as the bands were almost identical. In HTC, MOSC1 was not determined as its concentration was too low in these cells (Table 31b; section 5.3.3).

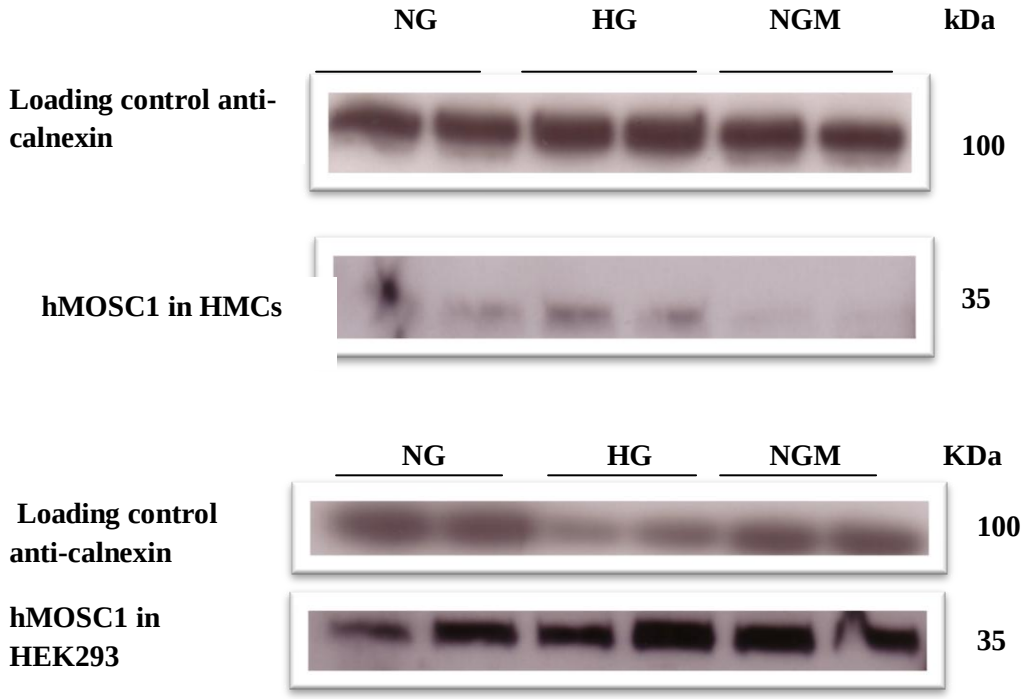

Figure 34. Western blot analysis of MOSC1 proteins in human mesangial and human embryonic kidney 293 cells.

Human mesangial cells and human embryonic kidney 293 cells were serum-starved and exposed to normal glucose (5 mM), high glucose (25 mM) and normal glucose plus mannitol (20+5 mM) for 3 days. Equal amounts of cell lysate proteins (25µg) were subjected to SDS-PAGE and MOSC1 protein expression was determined by immunoblot analysis using rabbit polyclonal IgG primary antibody raised against MOSC1.The blot was re-probed with anti-calnexin antibody to determine the equal loading of protein in all lanes (This part of work was carried out in the Havemeyer lab, Kiel, Germany by Heyka Jacob in collaboration with our group).

5.3.5. Investigation of N-reductive activity of MOSC *in vivo* and *in vitro*

In this part, we examined the N-reductive activity for both MOSC2 and MOSC1 *in vivo* and *in vitro*. The same samples saved from mRNA and protein studies were sent to Germany for N-reductive assay performed by the Havemeyer group. Previous studies by Havemeyer (2011) showed that MOSC2 is involved in the N-reductive pathway and it reduces N-hydroxylated compounds (Havemeyer et al., 2011). We previously showed that MOSC2 mRNA and protein were up-regulated in diabetic mice and HMCs, HEK293 cells under HG condition. Thus, it was interesting to determine whether N-reductive activity was also affected by glucose.

The endogenous function and substrates of the MOSC enzyme system are unknown. However, there is some evidence that MOSC is capable of reducing N-hydroxylated structures such as our model compound benzamidoxime (Havemeyer et al., 2011). Therefore, our hypothesis was to investigate whether N-reductive activity was increased in the presence of HG.

1) The effect of high glucose on N-reductive activity of MOSC *in vivo*

To test the hypothesis that N-reductive activity may be increased by glucose, we sent kidneys from control, diabetic and treated of STZ mice to Germany**.** The Havemayer group measured N-reductive activity for MOSC2 and MOSC1 in control, diabetic and treated kidneys of STZ mice. Samples were incubated with an incubation buffer and substrate buffer and their N-reductive activity were respectively calculated (Section 2.16). The protein activity for each sample was also measured for MOSC-activity as it reflects the complete reduction for both MOSC2 and MOSC1. Statistical analysis was performed for N-reductive activity and the results were shown as mean ± standard deviation (Sigma plot 11).

The results showed a 2.4-fold increase in the diabetic kidneys of mice when compared to control kidneys (Table 36). Statistical analysis of data using Tukey test showed a significant increase in N-reductive function (4.4 ± 0.6 vs. 1.8 ± 0.5, $P<0.05$) (Figure 35).

Table 36. The mean and SD of protein activity of MOSC in STZ mice kidneys

Condition	N	Mean values ± SD of protein activity (nmol Benzamide/ min × mg)
Control	3	1.8 ± 0.5
Diabetic	3	4.4 ± 0.6*
Treated	3	4.6 ± 0.03

The protein activity of MOSC was detected in kidneys of streptozotocin-induced diabetic mice. Values are shown as mean±SD. *P<0.05

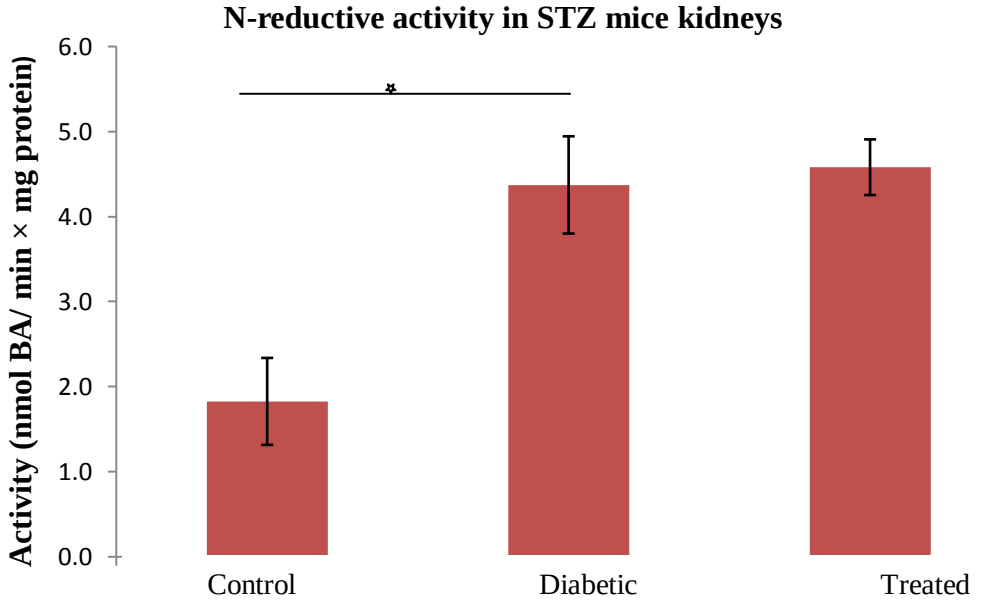

Figure 35. The increase of N-reductive activity in diabetic kidneys of mice.

The N-reductive activity for MOSC protein was measured in control (n= 3), diabetic (n= 3) and treated (n= 3) kidneys of streptozotocin-induced diabetic mice. The N-reductive activity showed a significant increase.* P<0.05 (This part of work was carried out in the Havemeyer lab, Kiel, Germany, by Heyka Jacob in collaboration with our group).

2) Effect of high glucose on N-reductive activity of MOSC *in vitro*

Human renal cells (HMCs, HEK293, and HTC) were cultured in NG, HG and NGM for 3 days. The culture media were then removed and divided for mRNA, protein expression and N-reductive assays. To determine N-reductive activity, the human renal cells were incubated with an incubation and substrate buffer. The incubation time and protein content were subsequently calculated (Section 2.16). The protein activity from each sample was also was measured for MOSC-activity as it reflects the

complete reduction for both MOSC2 and MOSC1. To determine the N-reductive activity, statistical analysis was used and results were shown as mean and standard deviation (Sigma plot 11).

Statistical analysis of data was performed using the Tukey test for analysis of variance and a significant increase between HG and NG of HMCs was found ($P<0.05$, Table 37). HMCs cultured in HG (0.59 ± 0.08) showed a 2-fold increase compared to NG (0.29 ± 0.03). Similar results were obtained with HEK293 cells: HEK293 cells cultured in HG showed 1.3-fold increase compared with those cultured in NG ($P<0.05$; Table 37). There was a significant difference between cells grown in HG and NG (0.58 ± 0.03 vs. 0.44 ± 0.02, $P<0.05$; Figure 36a).

Table 37. The mean and SD of MOSC protein activity in human renal cells

Cells	Condition	N	Mean values ± SD of protein activity (nmol BA/min × mg)
HMCs	NG	3	0.29 ± 0.03
	HG	3	0.59 ± 0.08*
	NGM	3	0.34 ± 0.05
HEK293	NG	4	0.44 ± 0.02
	HG	4	0.58 ± 0.03*
	NGM	4	0.39 ± 0.1
HTC	NG	3	0.7 ± 0.02
	HG	3	0.7 ± 0.04
	NGM	3	0.8 ± 0.5

The protein activity of MOSC was detected in human cultured renal cells (human mesangial cells, human embryonic kidney 293 cells, human tubular cells) separately. Values are shown as mean ± SD.*$P<0.05$

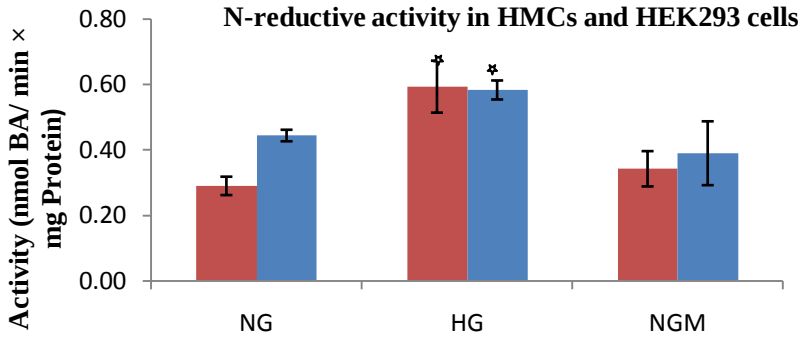

Figure 36a. The increase of N-reductive activity in human mesangial and human embryonic kidney 293 cells in the presence of high glucose.

The N-reductive activity for MOSC protein was measured in 5 mM (NG) or 25 mM glucose (HG) or 5 mM glucose + 20 mM mannitol (NGM) of both human mesangial cells (n= 3 for each condition) and human embryonic kidney 293 cells (n= 4 for each condition). The N-reductive activity showed a significant increase. **(**Red: HMCs, Blue: HEK293), *P<0.05 (This part of work was carried out in the Havemeyer lab, Kiel, Germany, by Heyka Jacob in collaboration with our group).

We found an increase of N-reductive activity in cells exposed to HG in both HMCs and HEK293 cells. In order to examine the N-reductive activity in HTC, MOSC2 and MOSC1 activity were measured. Statistical analysis of data using a Tukey test for analysis of variance showed a non-significant difference between all conditions as the protein concentration of HTC was low (Table 37). In these samples, the differences in the mean values among all groups were not great enough to exclude the possibility that the difference is due to random sampling variability; there was no statistically significant difference (P>0.05; Figure 36b).

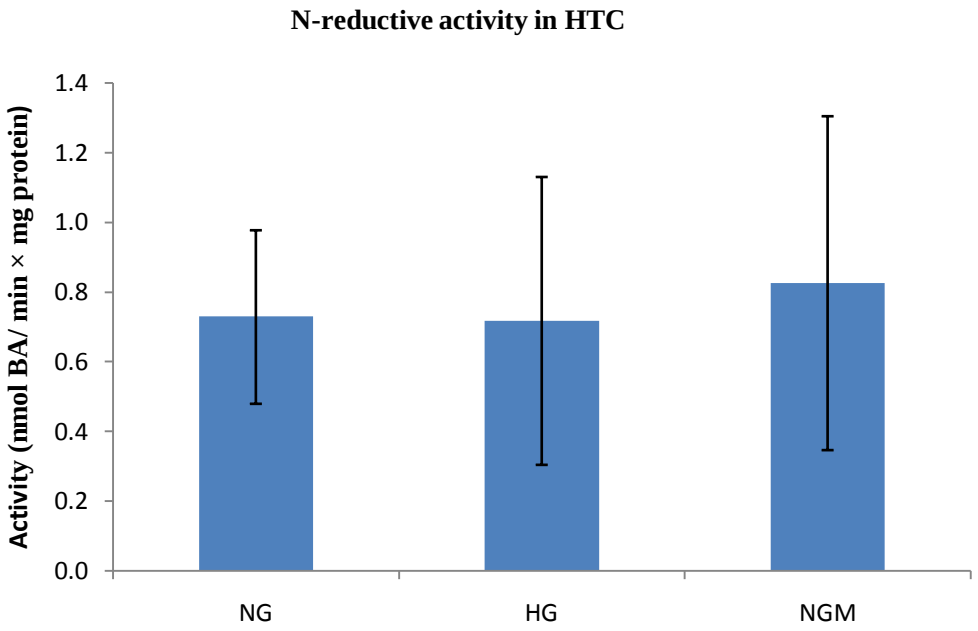

Figure 36b.The N-reductive activity in human renal tubular cells.

The N-reductive activity for MOSC protein was measured in 5 mM (NG) , 25 mM glucose (HG) and normal glucose with mannitol (5 mM glucose +20 mM mannitol) of human tubular cells (n=3 for each condition). The N-reductive activity did not show any change in HG. P>0.05 (This part of work was carried out in the Havemeyer lab, Kiel, Germany, by Heyka Jacob in collaboration with our group).

5.3.6. MOSC1 mRNA expression in peripheral blood of patients with DN

Previously, the Malik group showed that MOSC2 mRNA could not be determined in the circulating blood of patients with DN, suggesting that MOSC2 mRNA was not expressed in human blood (Shahni, Thesis 2011). Su (2004) established that human MOSC1 mRNA is expressed in white blood cells. Therefore, we tested MOSC1 mRNA expression in patients with T2DN to see if MOSC1 was expressed in circulating blood.

In this part of study and for the first time, MOSC1 mRNA levels in the circulating blood of patients with Type 2 diabetes and with no DN were compared. To determine MOSC1 mRNA expression, 0.2 ml of whole blood stored in RNAlater was used to measure MOSC1 mRNA copy numbers relative to the reference gene. mRNA was isolated (Section 2.6.1) and cDNA was synthesised for each sample. qPCR was carried

out using hMOSC1 F_1 and hMOSC1 R_1 primers (shown in table 24a; section 5.3.2.) and the data were normalised to PGK.

1) Grouping for analysis purposes

The data consisted of 13 patients with only T2D, of which 5 patients had no DN and 8 patients had T2DN with onset after the age of 35 and controlled by diet or established oral hypoglycaemic treatment and/or insulin. These samples were collected from SEEDA/JJ study (Section 2.5) and were previously used for CRYM study.

● ***Are circulating MOSC1 mRNA levels altered in patients with type 2 diabetic nephropathy?***

To confirm whether MOSC1 could be a potential predictive or diagnostic marker, circulating MOSC1 mRNA levels in the blood of patients with type 2 DN were compared with patients with no DN. All samples were analysed in triplicate. No change in MOSC1 mRNA levels was found upon comparing patients with no DN (30.27 ± 59.27) against patients with T2DN (21.62 ± 47.47; Table 38a). As the patient data were not normally distributed and were skewed, the data were log-transformed to achieve a symmetric distribution (Figure 37a).

Table 38a. Relative copy numbers and log copy numbers of circulating MOSC1 mRNA in patients with type 2 diabetic nephropathy and without nephropathy

Patient data set	Condition	Number of patients	MOSC1 copy number relative to PGK±SD	LogMOSC1Copy number relative to PGK±SD
All patients	Control	5	30.27 ± 59.27	0.69 ± 0.98
	DN	8	21.62 ± 47.47	0.51 ± 1.03

Circulating MOSC1 mRNA copy numbers relative to PGK copy numbers were determined in all patients and log values were calculated. DN: diabetic nephropathy. P>0.05

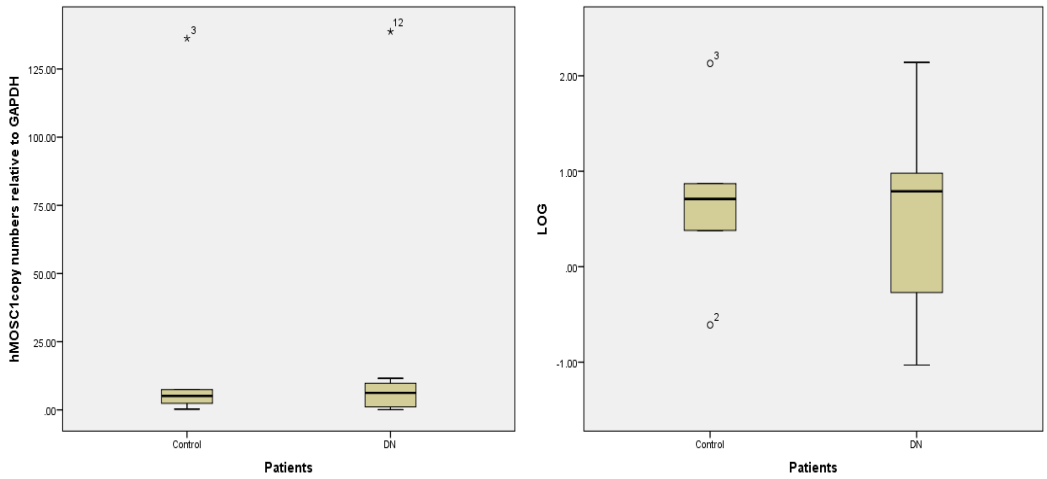

Figure 37a. MOSC1 mRNA copy in the circulating blood of patients with and without diabetic nephropathy.

A) Comparison of diabetic patients without nephropathy (control no neph, n= 5) to those with nephropathy (neph, n= 8; 30.27 ± 59.27 vs. 21.62 ± 47.47 and P>0.05) is illustrated as a boxplot (SPSSS 20). B) The data were log-transformed and showed a non-significant difference in circulating MOSC1 levels of patients with diabetic nephropathy. P>0.05

For further analysis, the patients in this study with a history of albuminuria were divided into groups: (1) Control: Patients with type 2 diabetes of > 10 years duration, with no history of albuminuria, with normal renal function, normal blood pressure (<130/80 mmHg) and taking no antihypertensive agents. (2) Normoalbuminuria; ACR < 2.5 mg/mmol for men (albumin extraction rate AER <25 mg/day) and ACR < 3.5 mg/mmol for women (AER < 35 mg/day). (3) Albuminuria; ACR > 2.5 mg/mmol for men (AER >25 mg/day) and > 3.5 mg/mmol for women (AER > 35 mg/day). GFR was evaluated using the Modification of Diet in Renal Disease (MDRD) formula. As the data were skewed, we performed log transformation (Figure 37b).

Table 38b. Relative copy numbers and log copy numbers of circulating MOSC1 mRNA in patients with nephropathy

Patient data set	Condition	Number of patients	MOSC1copy number relative to PGK±SD	Log MOSC1Copy number relative to pGK±SD
Patient by diabetes types	Control	5	30.27 ± 59.27	0.69 ± 0.98
	DN-NA	6	5.7 ± 4.13	0.5 ± 0.71
	DN-A	2	69.4 ± 98.01	0.55 ± 2.24

MOSC1 mRNA copy numbers relative to PGK mRNA copy numbers were determined in patients with nephropathy and log values were calculated. NA: nephropathy patients without microalbuminuria and NA-A: nephropathy patients with microalbuminuria. P>0.05

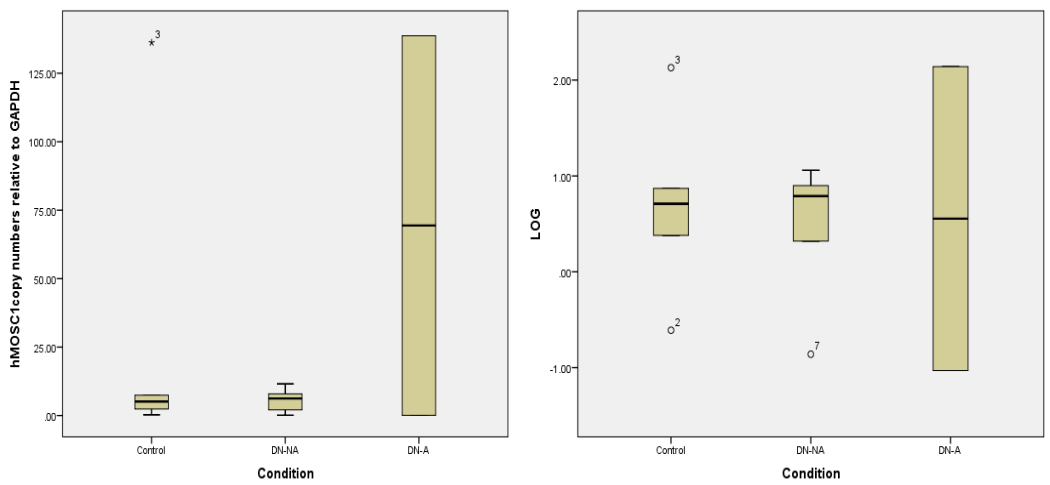

Figure 37b. MOSC1 mRNA copy number in circulating blood from diabetic patients with and without nephropathy according to their blood function.

A) Comparison of nephropathy patients with microalbuminuria or proteinuria (DN-A, n= 2) and nephropathy patients who had reverted to normallbuminuria (DN-NA, n= 6) with diabetic controls (n= 5). The data are illustrated as a boxplot (SPSS 20). B) The data were log-transformed and showed a non-significant result. P>0.05

● ***Association of clinical parameters***

The data was composed of controls (n= 5) and DN (n= 8). For the control group, there were 3 women and 2 men with an average age of 65 ± 10.51 years and who were slightly overweight (BMI of 25.28 ± 2.63 kg/m2; Table 38c). Despite having diabetes,

their blood glucose was controlled and they had good blood pressure control (119.4 ± 14.08 mmHg). They also had normal renal function as their ACR, eGFR and albuminuria were all within normal range. In the patient group with DN, there were 2 women and 6 men with an average age of 62.5 ± 11.01 (an average of 10 years older than the controls). Their blood glucose was high as their HbA1c was higher than the normal average (7.83 ± 2.31%). Their ACR was higher compared to the normal group (13.31 ± 28.06 vs. 52 ± 0.25, P>0.05) and they suffered from kidney disease as their ACR and albuminuria were higher than the normal range and eGFR was lower than controls (Table 38c).

Table 38c. Baseline characteristic of diabetic patients with and without nephropathy

Parameters	**Control (n= 5)**	**DN (Full Set) (n= 8)**	**DN-NA (n= 6)**	**DN-A (n= 2)**
Age (years)	65 ± 10.51	62.5 ± 11.01	62.5 ± 10.82	62.5 ± 16.26
Gender (F:M)	3:2	2:6	2:4	0:2
Diabetes duration (years)	25 ± 10.72	15.25 ± 6.38	17 ± 6.22	10 ± 4.24
BMI (kg/m^2)	25.28 ± 2.63	30.61 ± 8.39	32.08 ± 9.28	26.2 ± 3.11
HbA1c (%)	7.76 ± 1.6	7.83 ± 2.31	7.76 ± 2.25	8.05 ± 3.46
ACR (mg/mmol)	0.5 2± 0.25	13.31 ± 28.06	2.38 ± 1.4	46.1 ± 51.33*
eGFR (ml min^{-1} 1.73 $m^{-2)}$	89.4 ± 8.64	65.37 ± 36.5	60.66 ± 24.78	79.5 ± 75.66
Systolic Bp (mmHg)	119.4 ± 14.08	122.88 ± 14.99	117.67 ± 11.05	138.5 ± 17.67
Diastolic Bp (mmHg)	63.6 ± 6.65	66.88 ± 13.07	68.17 ± 6.16	78 ± 25.45

BMI: body mass index, HbA1c: Glycated haemoglobin, ACR: albumin/creatinine ratio, eGFR: glomerular filtration rate, Bp: blood pressure, *P<0.05,

Patients with T2DN were further subdivided into two groups as previously described. Patients with T2DN-NA (n= 6) and T2DN-A (n= 2) were older than controls (n= 5). The T2DN-A group had higher blood pressure compared with the T2DN-NA group and their BMI and HbA1c were nearly identical. Both groups had nephropathy as they had higher ACR and lower eGFR compared to the control group. However, the most important difference between T2DN-NA and T2DN-A was in ACR; they had 19% more ACR compared to the DN-NA group which was a sizeable figure (Table 38c) This implies that the T2DN-A group is progressing more rapidly towards end stage renal disease compared to the T2DN-NA group, despite both groups taking medication.

● ***Overall trend in circulating MOSC1 mRNA regulation***

Circulating MOSC1 mRNA expression was detected in blood of patients with DN. We could not determine a significant association between hyperglycaemia and MOSC1 mRNA expression in patients with DN. After adjustment for test variables such as age, gender, BMI, HbA1c, SBP, DBP and diabetes duration, a standardised increase of ACR was observed in patients with DN-A. This pilot study needs to be scaled up to understand the function of MOSC1 in the circulating blood of patients with kidney failure.

A student's *t* test analysis was performed with DN as the grouping variable and MOSC1 copy numbers, log MOSC1 copies, age, gender, BMI, HbA1c, SBP, DBP and diabetes duration as test variables using SPSS 20. Compared with diabetic controls and patients with DN-NA, only those patients with DN-A groups showed a significant increase with ACR ($P<0.05$). There was no significant difference between groups in terms of sex, BMI and eGFR.

5.4. Discussion

In this chapter, we looked at renal MOSC2 and MOSC1 expression *in vivo and in vitro*. In the first part of the study renal MOSC2 and MOSC1 mRNA and protein expression were measured in diabetic models of STZ-induced diabetic mice. During the second part, we investigated MOSC2 and MOSC1 mRNA and protein expression in human renal cells. Finally, we tested MOSC1 mRNA expression through measurement of MOSC1 copy numbers in the circulating blood of patients with DN compared to patients with no DN.

For the first time we were able to show that MOSC2 is increased during hyperglycaemia in the diabetic kidneys of STZ-induced diabetic mice and this increase was attenuated by the treatment of diabetes ($P<0.05$). However, we found no change in MOSC1 in the kidneys of diabetic mice. These results were consistent with the Malik studies, as MOSC2 (also known as CDK7) was found to increase in the GK rat. In addition, they showed that renal MOSC2 mRNA is not up-regulated in the normoglycaemic Wistar rat, suggesting that elevation of MOSC2 is a glucose-induced effect (Malik et al., 2007).

Western blot analysis showed that MOSC2 was highly expressed in the diabetic kidneys of STZ mice, whereas MOSC2 levels showed a decline in control samples. These findings confirmed the mRNA studies in the diabetic kidneys of STZ mice, suggesting that MOSC2 is a glucose-regulated gene in mice. However, we could not detect the MOSC1 protein expression in the mouse as there exists no commercial antibody against mouse mARC1. The immunofluorescent staining was performed to determine the location of MOSC2 protein in control and diabetic mouse kidneys. MOSC2 was abundantly expressed in the tubules of both control and diabetic kidneys and suprisingly not expressed in the glomerulus.

Previously, Malik et al. (2007) found that MOSC2 mRNA levels were up-regulated in cells exposed to HG compared to NG in HMCs and HMCL. Shahni (2011) showed that MOSC2 expression was 10-fold increased in HMCs grown in HG compared to those grown in NG. In this chapter, we looked at both renal MOSC2 and MOSC1 mRNA expression in NG, HG and NGM of three different types of human cultured renal cells (HMCs, HEK293, HTC). Renal MOSC2 showed a significant increase in cells grown in HG compared to NG for both HMCs and HEK293 cells. These results

confirmed our previous findings *in vivo,* and also confirmed the previous results by Malik et al. (2007). The hyperglycaemia-induced increase in renal MOSC2 was specific as we could not demonstrate any change in MOSC1.

Surprisingly, in HG, MOSC2 mRNA levels showed a slight decrease in HTC whereas they showed a significant increase in HMCs and HEK293 cells. This was the first time that renal MOSC2 and MOSC1 mRNA expression was measured in HTC. To confirm the mRNA studies, we used Western blot analysis for both MOSC2 and MOSC1 in human cultured renal cells (HMCs, HEK293, HTC). However, our Western blot experiments for both MOSC1 and MOSC2 were not successful and we could not detect any difference in the expression of both MOSC2 and MOSC1.

In this chapter, we showed the up-regulation of MOSC2 *in vivo* and *in vitro* in association with hyperglycaemia. As described previously, hyperglycaemia is a key factor in the progression of DN and it induces renal injury through chemical pathways (Sheets et al., 2002). This process involved several main molecules such as protein kinase C, TGF-β1 and glycation end products (Brownlee et al., 2001). There is a possible explanation for MOSC2, as its up-regulation in hyperglycaemia could be linked to its contribution in different aspects of regulating intracellular redox balance in the cell.

ROS is a key mediator in the progression of microvascular diseases by affecting the redox balance in the cell which can lead to abnormal activation of different pathways in the cell (Lee et al., 2003). For instance, hyperglycaemia can promote oxidative stress by inhibiting the thioredoxin function (Schulze et al., 2004). Thioredoxin is a small protein (12 kDa) which is involved in the redox regulation of the cell (Nordberg, 2001). Malik et al. (2007) showed that there is a notable conservation of cys-pro-arg-cys domain within the MOSC and MOSC-N domains of MOSC2 protein which is similar to the catalytic domain of thioredoxin. This similarity suggests a functional link between thioredoxin-like proteins and MOSC2. Hence, protein structures of MOSC2 contain the CPRC region, which could lead to a redox function of MOSC2. This could explain why MOSC2 is up-regulated in HG as it could protect cells from ROS-induced damage.

Malik et al. (2007) showed that MOSC2 mRNA expression appeared to be increased in the diabetic kidneys of GK rats and in human renal cells in the presence of

hyperglycaemia. Because of these findings, they named the molybdenum enzyme "CDK7" (Candidate Diabetes-associated Kidney) in their studies (Page et al., 1997; Malik et al., 2007).

It was shown by Havemeyer (2006) that MOSC protein purified from pig liver mitochondria was homologous to the C-terminal domain of Moco-Sulfurases (MOCO). They named this recently discovered protein "mitochondrial amidoxime-reducing component" (mARC), because initially the N-reductive activity of amidoxime was studied with this isolated mitochondrial enzyme. MOSC is identical to mARC, which is an N-reductive protein and part of a three component enzyme, consisting of mARC, cyt (cytochrome) *b5* and NADH cyt *b5* reductase. This molybdenum enzyme is capable of reducing nitrogen–containing groups (Havemeyer et al., 2011). mARC has been identified in the outer mitochondrial membrane of pig liver, which harboured the N-reductive system. They also showed that the human genome holds two mARC genes: mARC1/MOSC1 and mARC2/MOSC2. Both mARC1 and mARC2 genes were cloned and expressed in *Esherichia coli* (Havemeyer et al., 2006).

Havemeyer and co-workers identified MOSC2 and MOSC1 as outer mitochondria membrane proteins in pigs (Havemeyer et al., 2006). However, contrary to this result, other authors have purified MOSC2 and MOSC1 from the inner mitochondrial membrane of a mouse (Cruz et al., 2003). Shahni (2011) have shown subcellular localisation of MOSC2 using its specific antibody in HMCLs and determined that MOSC2 is localised to the mitochondria.

As the involvement of three enzymes in this reduction pathway was demonstrated, we therefore assessed the N-reductive activity for this molybdenum enzyme *in vivo* and *in vitro*. Biochemical analysis of MOSC protein showed that hyperglycaemia increased the N-reductive activity of MOSC protein in the kidneys of STZ mice *in vivo*. We also showed that the N-reductive activity is elevated in cells grown in HG compared to NG of both HMCs and HEK293 cells. However, we could not find any significant difference in HTC. This was the first occasion in which the function of MOSC in N-reductive activity with hyperglycaemia has been demonstrated. This result was consistent with our previous findings of MOSC2 being up-regulated in the presence of hyperglycaemia in *vivo* and *in vitro.*

MOSC and its N-reductive enzyme system are involved in drug metabolism, and they also play a role in the activation of amidoxime prodrugs. This recent discovery is a main target for drug research and the development of prodrugs (Clement et al., 2005). The Havemayer group demonstrated that MOSC2 is located in the outer mitochondrial membrane which harboured an N-reductive system and proposed that it was involved in the N-reductive system; MOSC2 was also postulated to protect cell from cytotoxic NO formation (Kotthaus et al., 2011).

To evaluate MOSC1 and MOSC2 mRNA levels as potential biomarkers of DN, we examined their expression in the peripheral blood of diabetic patients. There was no expression of MOSC2 (Shahni, 2011); however, the closely related homolog MOSC1 was expressed in the peripheral blood. Circulating MOSC1 mRNA did not change in association with complications. Therefore it is currently unclear if circulating MOSC1 is associated with DN.

We can conclude that up-regulation of MOSC2 in the presence of hyperglycaemia occurs in both mouse models and human cultured renal cells (HMCs, HEK293). This increase of MOSC2 and also its identity with cysteine domain suggests that MOSC2 is a novel thiol gene and it may play a role in response to oxidative stress. Despite not finding any significant results for MOSC1 *in vivo* or *in vitro,* its similarity with MOSC2 supports the assumption that it may be involved in hyperglycaemia-induced pathways. Also, its expression in circulating blood increases its chance of being a predictive marker for microvascular diseases.

Chapter 6
General Discussion

Chapter 6. General Discussion

DN is a frequent complication in patients with diabetes mellitus and it is the major cause of end stage renal disease (ESRD), which has been linked to cardiovascular morbidity and mortality. Previously, the Malik group (1997) used differential screening and differential display to isolate genes based on their differential expression from GK rat kidneys *in vivo* (Page et al., 1997; Page and Malik, 2003). CRYM and MOSC2 were identified as two of several hyperglycaemia-induced renal genes in the GK rat, and both were found to be regulated by glucose *in vitro* (Page and Malik, 2003).

In this thesis, we showed that the expression of CRYM and MOSC2 are altered in conditions of diabetes and may play a role in hyperglycaemia-induced pathways in the kidney that lead to renal failure. However, MOSC1 expression was found not to change in diabetic conditions *in vivo* and *in vitro*. Furthermore, circulating CRYM mRNA levels showed some change in patients with DR and DN but MOSC1 mRNA levels remained unchanged, suggesting that CRYM and MOSC2 are regulated but that MOSC1 is not. Unfortunately, it is unlikely that CRYM and MOSC2 could be useful biomarkers for DN or DR because of their low and variable levels of expression in circulating cells. However, our data supports the view that both genes may be involved in glucose-induced pathways.

CRYM

In the first part of this thesis, we demonstrated for the first time that renal CRYM mRNA expression is regulated during the development of hyperglycaemia in the kidneys of STZ-induced diabetic mice. In addition, when STZ-induced diabetic mice were treated by islet transplantation, renal CRYM mRNAs were normalised, providing direct evidence that hyperglycaemia-induced CRYM mRNA. The increase in renal CRYM mRNA levels in the STZ-induced model was specific as we could not show any change in cardiac CRYM, suggesting that up-regulation in CRYM in response to hyperglycaemia might be tissue specific.

Parallel to these findings, we also examined renal and cardiac CRYM mRNA levels for the first time in a ß-*Phb2* KO mouse where the loss of *phb2* in beta cells results in

type 1 diabetes. Surprisingly, we could not demonstrate any change in renal and cardiac CRYM mRNA levels in the diabetic kidneys of ß-*Phb2* KO mice when compared to control kidneys. Earlier studies with the GK rat have shown increased renal and cardiac CRYM in conditions of hyperglycemia (Al-Kafaji and Malik, 2010).

Differential expression of CRYM in ß-*Phb2* KO and STZ-induced diabetic mice might result from difference between these biological models; ß-*Phb2* KO mice are a unique model of spontaneous development of diabetes, through a series of molecular events and do not require the usage of chemicals such as STZ (Supale et al., 2013). Therefore, it is possible that the biological difference of these two models could affect renal and cardiac CRYM expression in both models. Furthermore, the difference between the duration of diabetes, blood glucose levels, and gender may have an effect. We used only kidneys from male mice in STZ-induced diabetic mice, whereas in the KO mice both genders were used. Therefore differences between these two models might cause the differential renal and cardiac CRYM mRNA regulation. Despite these issues, our data show that CRYM mRNA can be regulated in response to hyperglycaemia *in vivo.*

Previous studies have not managed to localise CRYM protein *in vivo.* We carried out immunofluorescence and found high levels of renal CRYM protein in the STZ mouse model, with particular abundance being noted in HTC, and less expression in the HMCs. Hyperglycaemia is known to affect different renal cells, affecting various renal cell types including glomerular mesangial cells, tubular epithelial cells as well as others (Kanwar et al., 2011). Therefore one question from our finding of high CRYM protein levels in HTC was whether hyperglycaemia can induce an increase in CRYM in these cells. However, we were not able to detect increased CRYM staining in the diabetic tubular cells compared to controls using immunofluorescence. It would be useful to carry out a Western blot for the confirmation of CRYM mRNA results and to complement the immunofluorescence findings. Unfortunately, we were unable to confirm the mRNA results by Western blot due to lack of tissues and time.

As the expression of CRYM was more abundant in renal tubular cells throughout the kidneys of STZ-induced diabetic mice, we examined renal CRYM mRNA levels in HTCs for the first time to see if it could be induced by HG. However, we found a moderate decrease in mRNAs in HTC in the presence of hyperglycaemia. Renal

CRYM mRNA levels were reduced following the exposure of cells to HG compared to NG. The Malik group previously found an increase of renal CRYM mRNA levels by hyperglycaemia in cultured HMCs (Al-Kafaji and Malik, 2010). Cellular localisation of CRYM within HMCs showed cytoplasmic localisation of CRYM protein in both NG and HG conditions. We also found CRYM protein staining in the cytoplasm of HTC as expected but we did not see any increase in the protein levels in HTC grown in HG.

The expression of CRYM mRNA in human peripheral blood mononuclear cells (PBMCs) has been previously reported (Suzuki et al., 2009). For the first time, we detected mRNA levels of CRYM in whole blood samples. We compared the levels of circulating CRYM mRNA in diabetic patients with and without DN and found that circulating CRYM mRNA levels were 7.4-fold increased in patients with T2DN. This effect was strongest in patients with a well controlled nephropathy compared to those with proteinuria. There was a significant correlation between some risk factors such as age, ACR, diabetic duration in patients with and without DN. In contrast, when we measured circulating CRYM in patients with DR, we found that levels were reduced compared to patients with no DR. This could suggest that DN and DR have different mechanisms; however, it may also be due to the way blood samples for the two studies were stored. The DN samples had been stored in RNAlater and the DR samples had been stored in Paxgene tubes, with the latter being more likely to be reliable. This part of the work showed potential but needs to be repeated.

Our results with CRYM from the *in vitro*, *in vivo* and patient studies support the view that CRYM is a regulated gene and could be induced by hyperglycaemia. With hyperglycaemia being widely accepted as a major cause of diabetic complications (Weiss and Sumpio, 2006; Brownlee, 2001), the up-regulation of CRYM in HG is interesting. In STZ-induced diabetic mice, we showed up-regulation of renal CRYM in diabetic kidneys. These findings and previous studies, which revealed increased renal CRYM mRNA in GK rat and HMCs (Al-kafaji and Malik, 2010; Ziadi, 1997), suggest a role for CRYM in hyperglycaemia-induced biochemical pathways that lead to the development of DN. However, the exact mechanism by which HG can result in increased renal CRYM mRNA remains to be determined. CRYM is likely to be of fundamental importance in the cell because 1) it is highly conversed in human, mouse, rat and other species (Kim et al., 1992) and 2) it is widely expressed in various

tissues showing the highest levels of expression in the kidney, heart and retina and lower levels in the lung, liver and other tissues (Osima et al., 2006, Abe et al., 2003, Aoki et al., 2000; Witsow and Kim, 1991). The exact cellular function of CRYM in the context of diabetes remains to be determined.

Several studies have described different functions for CRYM. For example, CRYM was shown to be a major structural lens protein in marsupial species (Chen et al., 1992) and proposed to have an enzymatic role (Witsow et al., 1993). In kangaroos and other species, CRYM acts as the major lens protein in the retina, brain and other tissues (Chen et al., 1992). In humans, another function for CRYM as a NADP-regulated thyroid hormone-binding protein has been shown (Kim et al., 1992, Vie et al., 1997). In fact, most of the lens proteins that act as crystallins are not specialised structural proteins and their synthesis is not limited to the lens (Wistow and Piatigorsky, 1988). Many of these crystallins are NADPH-binding proteins. Thus, they can protect against oxidation in the lens or help to filter UV radiation (Vie et al., 1996; Beslin et al., 1995).

When acting as an NADP-regulated thyroid hormone-binding protein, CRYM binds thyroid hormone T_3 in the presence of NADPH (Hashizume et al., 1989; Vie et al., 1997). CRYM was also related to non-syndromic deafness in humans and it was suggested that CRYM dysfunction may be involved in potassium ion recycling, and could also abrogate the thyroid hormone affinity as a vital factor for the progression of the auditory system (Abe et al., 2003). Interestingly, patients with DN exhibit an increased occurrence of thyroid dysfunction (Bando et al., 2002; Bando et al., 1999). Chen et al. (2007) proposed subclinical hypothyroidism as an independent risk marker for diabetic kidney and cardiovascular disease. It has been well documented that there is an association between thyroid and kidney function. Recently, Lin (2011) revealed that the use of T_3 prevented the development of kidney damage in a mouse with T2D (Hoeck and Daminet, 2009). Therefore, it is possible for regulation of CRYM to be involved in molecular events which have been linked to the pathogenesis of thyroid disease and diabetic kidneys.

We suggested that CRYM might be involved in a hyperglycaemia-induced polyol pathway as CRYM has NADPH binding activity and it is a NADP-regulated thyroid hormone binding protein (Hashizume et al., 1989; Vie et al., 1997). The polyol

pathway is one of the metabolic factors which are involved in the genesis of DN. In this pathway, aldose reductase reduces glucose to sorbitol in the presence of hyperglycaemia, which is later oxidised to fructose (Brownlee, 2005). In this process, a high rate of glucose elevates the turnover of cofactors including NADPH and NAD+. Therefore, NADPH is an essential co-factor for the reduction and regeneration of glutathione. By depleting glutathione, the polyol pathway increases its resistance to oxidative stress (Oates, 2002). Indeed, consumption of NADPH cofactor by aldose reductase may cause an impaired antioxidant defence system.

We have previously discovered that CRYM over-expression reduces glucose-induced intracellular ROS in cultured renal cells (Al-Kafaji and Malik, 2010). As CRYM binds to NADPH and its level is increased in the presence of hyperglycaemia where oxidative stress plays a role, we are lead to hypothesise that CRYM may play a role in the cellular response to oxidative stress caused by hyperglycaemia-induced ROS accumulation. Furthermore, various studies reported that hyperglycaemia resulted in ROS generation in HMCs (Xia et al., 2006; Frecker et al., 2005, Hua et al., 2003). ROS-induced oxidative stress has been proposed as a strong pathogenic co-factor in the progression of diabetic complications including DN and DR.

In HG, ROS produces and increases glucose signalling in renal cells and it is also involved in excessive ECM deposition in DN (Ha and Lee, 2005; Lee et al., 2003). CRYM and ROS increase simultaneously in HMCs in response to HG; suggesting that CRYM might be involved in protecting renal cells from the result of high glucose-induced ROS formation and increases the hypothesis that CRYM may serve as an endogenous antioxidant.

The demonstration that CRYM may act as an antioxidant suggests how important it is to investigate this area for the prevention or treatment of DN. Identifying the CRYM mechanism in inhibition of hyperglycaemia-induced intracellular ROS in HMCs may provide insight into its valuable role in protecting against oxidative stress, resulting in kidney damage in DN. It may provide a new direction for the treatment of DN. Future studies must investigate the *in vivo* consequences of the biochemical events by which CRYM play a role in reducing oxidative stress.

Diabetic patients have been reported to have high levels of oxidative stress because of lowered antioxidant function (Sindhu et al., 2005). In the current study we demonstrated that CRYM mRNA is present in the whole blood of patients with diabetes. However, its low levels of expression suggest it may not be a useful biomarker. Furthermore, our data showed that circulating CRYM mRNA levels were reduced in patients with severe DR and in patients with DN. Therefore, the regulation of CRYM can raise the theory that CRYM is involved in an antioxidant defence system.

MOSC

In this thesis, we also found that the expression of MOSC2 mRNA and protein was up-regulated in response to hyperglycaemia in the kidneys of STZ-induced diabetic mice. These findings support previous studies, which described MOSC2 to be a glucose-regulated gene in the diabetic kidneys of a GK rat and suggested that an increase in MOSC2 was a glucose-induced effect (Malik et al., 2007). The immunofluorescent staining was performed to demonstrate the location of MOSC2 protein in the kidneys of the control and diabetic mice. We found that MOSC2 was abundantly expressed in tubules of both control and diabetic kidneys and it was not expressed in the glomerulus. Parallel with MOSC2 studies, we have also looked at its homologue MOSC1. Unlike MOSC2, we found no changes in MOSC1 mRNA levels in any of our models or patient groups. As no antibody against mouse MOSC1 exists, we could not detect MOSC1 protein expression.

In keeping with our *in vivo* studies, we looked at renal regulation of human MOSC2 and MOSC1 *in vitro*. Previously, Malik et al. (2007) showed that human MOSC2 mRNA levels were up-regulated in cells exposed to HG compared to NG in HMCL. Shahni (2011) also reported that the expression of human MOSC2 was 10-fold increased in HMCs grown in HG compared to those grown in NG.

In the current study, we also found that the expression of human MOSC2 significantly increased in cells grown in HG compared to NG in both HMCs and HEK293 cells. These results confirmed our *in vivo* findings, and also confirmed the previous results by the Malik group (Malik et al., 2007). However, we found a decrease of MOSC2 mRNA levels in HTC grown in HG compared to HTC grown in NG, which was contrary to our previous findings. This was the first time that we had measured human MOSC2 mRNA expression in HTC, suggesting that further studies

are required to confirm this data. We also could not find any difference between all conditions of human MOSC1 expression in human cultured renal cells (HMCs, HEK293, HTC). To confirm the mRNA studies, we used Western blot analysis for both MOSC2 and MOSC1 protein in human renal cells (HMCs, HEK293, HTC). However, our western blot for both human MOSC1 and MOSC2 was inconclusive.

It was previously suggested by our group that MOSC2 may be acting as an antioxidant because of the presence of the CPRC domain and that it could be a thiol protein (Liang et al., 2007). The oxidation and reduction of thiol groups play a main role in the cellular antioxidant defence system as well as intracellular signalling which is found in various cellular proteins. This cellular antioxidant response has been identified to be defective in DN (Ceriello et al., 2000; Hodgkinson et al., 2003). Other studies have previously shown the up-regulation of certain genes involved in the thiol pathway (Liang et al., 2007; Morrison et al., 2004). We have also demonstrated that MOSC2 expression is up-regulated in both *in vivo* and *in vitro* models. One possible clarification for the up-regulation of MOSC2 in the presence of hyperglycaemia and the presence of highly conserved cysteine in the protein could be consistent with the theory that MOSC2 is a novel thiol protein playing a role in the cellular response to oxidative stress (Malik et al., 2007). Thus, our observations suggest a possible function for MOSC2 in DN, either as a regulator of intracellular ROS or as being involved in protecting the cells from ROS-induced damage.

Some groups have reported MOSC2 cellular localisation by using an antibody specific to MOSC2. Havemeyer and co-workers purified native MOSC2 from the outer membrane of a pig liver mitochondria (Havemeyer et al., 2006). However, Da Cruz et al. (2003) showed that MOSC1 and MOSC2 proteins were located in the inner membrane of the liver mitochondria using a proteomic approach (referred to as Q9CW42 and Q922Q1). Although these two findings were in contrast to the specific sub-compartment of MOSC, they both suggested mitochondrial membrane localisation. Interestingly, another study reported a dual subcellular localisation of MOSC2 (referred to as O88994) in both peroxisomes and mitochondria. In keeping with the current observation, the Malik group has shown that the full length mARC2/CDK7 is localised to the cytosol and nucleus of HEK cells in NG (Shahni, 2011).

Havemeyer (2006) reported that human MOSC2 is exclusively localised in mitochondria and it is expressed at higher levels in the kidney, liver and thyroid (Clement et al., 2005). Malik et al. (2007) also revealed that MOSC2 mRNA was expressed in most tissues and they also showed that MOSC2 mRNA levels were highly expressed in the kidney, liver and thyroid.

Havemeyer et al. (2011) mentioned that MOSC and its N-reductive enzyme system are involved in drug metabolism and play a role in the activation of amidoxime prodrugs. This recent discovery is a main target for drug research and development of prodrugs (Clement et al., 2005, Havemeyer et al., 2011). Human MOSC2 is proposed to be involved in the N-reductive system and also, it has been postulated to protect cells from cytotoxic NO formation (Kotthaus et al., 2011).

As the involvement of three enzymes in this reduction pathway was demonstrated, we sent our samples to the Havmeyer group to assess the N-reductive activity for this molybdenum enzyme *in vivo* and *in vitro.* We found that N-reductive activity increased in the diabetic kidneys of STZ-induced diabetic mice. We also showed that N-reductive activity is elevated in cells grown in HG, compared to NG of both HMCs and HEK293 cells. However, we could not find any significant difference in HTC as their protein concentration was very low. This was the first time the function of MOSC in N-reductive with hyperglycaemia was demonstrated. This result was consistent with our previous findings of MOSC being up-regulated in the presence of hyperglycaemia *in vivo* and *in vitro,* suggesting that MOSC played a role in N-reductive activity in the presence of hyperglycaemia.

In this thesis, we also examined circulating MOSC1 mRNA levels in patients with DN. This was the first study which detected MOSC1 mRNA expression in whole blood of patients with DN. Previously, Shahni (2011) reported a lack of MOSC2 mRNA expression in human peripheral blood and suggested that it was not a good candidate as predictive marker of DN. In this experimental study, we looked at only a few samples in diabetic patients with and without DN. Circulating MOSC1 mRNA was not changed in association with complications, suggesting that it is unlikely to be a useful biomarker for DN but may be involved in the pathways that lead to DN. However, as it was our first study with a few samples, further investigation is required.

Our previous hypothesis was that levels of MOSC2 mRNA increased in hyperglycaemia in GK rat and in HMCs. In this thesis, we showed that N-reductive activity was up-regulated in the diabetic kidneys of STZ diabetic mice, in HMCs and in HEK293 cells, suggesting that MOSC could play a role in N-reductive activity in the presence of hyperglycaemia.

Overall conclusion

In conclusion, we have shown that renal CRYM and MOSC2 can be regulated by glucose in the diabetic kidneys of STZ-induced diabetic mice, suggesting that diabetes leads to increased expression of renal CRYM and MOSC2 mRNAs which can be corrected in the kidneys by treatment of diabetes. Further studies are needed for both CRYM and MOSC2 to determine their exact function in the progression of DN.

Taken together, it appears likely that both CRYM and MOSC2 genes play a role in hyperglycaemia-induced signalling pathways in DN, and their glucose regulation raises the hypothesis that both CRYM and MOSC2 levels are up-regulated to correct for oxidative stress caused by increased hyperglycaemia-induced ROS. Our findings suggested that both CRYM and MOSC2 are involved in a cellular response to oxidative stress and it might be an association between CRYM and MOSC2 as they followed the same pattern of expression in response to hyperglycaemia. It would be interesting to investigate the role of both genes in oxidative stress, whether regulation of CRYM and MOSC2 is specific to hyperglycaemia-induced ROS production, or if it is as a result of activation of other hyperglycaemia-induced biochemical pathways. Further consideration to discover the antioxidant effect of CRYM and MOSC2 are of great interest and additional investigation might provide more insight into their function.

One aspect of DN is the abnormal activation of hyperglycaemia–induced metabolic and haemodynamic pathways (Brownlee, 2001). As described previously, hyperglycaemia can be the cause of increased intracellular ROS, both through NADPH oxidase and via electron leakage from mitochondrial electron transport chains. NADPH is known as a main mediator for different fundamental biological processes, such as mitochondrial function, energy metabolism and oxidative stress (Ying et al., 2008). Therefore, it would be interesting to see whether altered

expression of CRYM and MOSC2 can affect the NADPH/NADP+ ratio in the cell, as this ratio plays a role in the control of redox environment inside cells.

As circulating CRYM mRNA levels showed changes in patients with DN and DR, MOSC1/2 remained unchanged. These data suggest that CRYM or MOSC1 are unlikely to be useful biomarkers for DN but may be involved in the pathways that lead to DN. Further studies should examine the mRNA levels of CRYM and MOSC1 in patients as well as in healthy controls.

References

Abe S, Katagiri T, Saito-Hisaminato A, Shin-ichi Usami S, Inoue Y,et al. (2003) Identification of CRYM as a candidate responsible for non-syndromic deafness, through cDNA microarray analysis of human cochlear and vestibular tissues. *Am J Hum Genet*. **72:**73-82.

Al-Kafagi G (2008) Elevated levels of thyroid hormone binding protein in experimental diabetic nephropathy. Phd Thesis.

Al-Kafaji G, Malik AN (2010) Hyperglycaemia induces elevated expression of thyroid hormone binding protein in vivo in kidney and heart and in vitro in mesangial cells *Biochemical Biophys Res Commun.* **391**: 1585-1591.

Ahmed N (2005) Advanced glycation endproducts-role in pathology of diabetic complications. *Diabetes Research and Clinical Practice.* **67:** 3-21.

Amemiya T, Sasamura H, Mifune M, Kitamura Y, Hirahashi J, et al. (1999) Vascular endothelial growth factor activates MAP kinase and enhances collagen synthesis in human mesangial cells. *Kidney In.* **56**:2055–2063

American Diabetes Association (2004) Gestational diabetes mellitus.*Diabetes Care* **27:** 88-90.

American Diabetes Association (2004) Nephropathy in diabetes. Clinical Practice Recommendations. *Diabetes Care.* **27:** 79-83.

American Diabetes Association (2006) Standards of medical care in diabetes. Clinical Practice Recommendations. *Diabetes Care.* **29:** 4-42.

Anantharaman V, Aravanid L (2002) MOSC domains, ancient predicted sulfure-carrier domains, present in diverse metal-sulfur cluster biosynthesis proteins including molybdenum cofactor sulfurases *FEMS Microbiol Lett.* **207:** 55-61.

Andersen CL, Jensen JL and Qrntoft TF (2004) Normalisation of Real-Time Quantitative Reverse Transcription-PCR Data: AModel-Based Variance Estimation Approach to Identify Genes Suited forNormalisation, Applied to Bladder and Colon Cancer Data Sets. *Cancer Res.* **64**: 5245-5250.

Andersen JS, Lam YW, Leung AK, Ong SE, Lyon CE, et al. (2005) Nucleolar proteome dynamics. *Nature.* **433**:77–83.

Andersen NH, Mogensen CE (2002) Angiotensin converting enzyme inhibitors and angiotensin II receptor blockers: evidence for and against the combination in the treatment of hypertension and proteinuria. *Curr Hypertens Rep*. **4**:394-402.

Anderson S, Jung FF, Ingelfinger JR (1996). Renal rennin-angiotensin system in diabetes: Functional, immunohistochemical, and molecular biological correlations. *Am J Physiol.* 271: 595-602.

Aoki N, Ito K, Ito M (2000) Mu-Crystallin, thyroid hormone-binding protein, is expressed abundantly in the murine inner root sheath cells. *J Invest Dermatol.* **115**: 402-405.

Bando Y, Ushiogi Y, Okafuji K, Toya D, Tanaka N, et al. (2002) Non-Autoimmune Primary Hypothyroidism in Diabetic and Non-Diabetic Chronic Renal Dysfunction. *Exp Clin Endocrinol Diabetes.* **110:** 408-415.

Bando Y, Ushigoi Y, Toya D, Tanaka N, Fujisawa M (1999) Diabetic nephropathy accompanied by iodine-induced non-autoimmune primary hypothyroidism: two case reports. *Endocr J*. **46:** 803-810.

Bank N, Mower P, Aynedjian HS, Wilkes BM, Silverman S (1989) Sorbinil prevents glomerular hyperfusion in diabetic rat. *Am J Physiol*. **256:** F1000-F1006.

Bell GI, Burant CF, Takeda J, Gould GW (1993) Structure and function of mammalian facilitative sugar transporters. *J Biol Chem*. **268:** 19161-19164.

Beslin A, Vie M, Blondeau J, Francon J (1995) Identification by photoaffinity labeling of a pyridine nucleotide-dependent tri-iodothyronine-binding protein in the cytosol of cultured astroglial cells. *Biochem J*. **305:**729-737.

Blayer AJ, Fumo P, Snipes ER, et al. (1994) Polyol pathway mediates high glucose-induced collagen synthesis in proximal tubule. *Kidney Int*. **45**: 659-666.

Bojestig, M, Arnqvist, HJ, Karlberg, BE, Ludvigsson, J (1996) Glycemic control and prognosis in type I diabetic patients with microalbuminuria. *Diabetes Care*. **19**:313–317.

Border WA, Yahamoto T, Noble NA (1996) Transforming growth factor–β in diabetic nephropathy. *Diabetes Metab Rev*. **12**:309–339.

Bork P (1993) The modular architecture of a new family of growth regulators related to connective tissue growth factor. *FEBS Lett*. **327**:125-30

Bradham DM, Igarashi A, Potter RL, Grotendorst GR (1991) Connective tissue growth factor: a cysteine-rich mitogen secreted by human vascular endothelial cells is related to the SRC-induced immediate early gene product CEF-10. *J Cell Biol*. **114**:1285–1294.

Breyer MD, Bottinger E, Brosius FC, Coffman TM, Harris RC et al. (2005) Mouse models of diabetic nephropathy. *J Am Soc Nephrol*. **16:**27-45.

Brigstock DR (2003) The CNN Family: a new stimulus package. *J Endocrinol*. **178:** 169-175.

Brosius FC, Heilig CW (2005) Glucose transporters in diabetic nephropathy. Pediatr Nephrol. **20:** 447-451.

Brownlee M (2001) Biochemistry and molecular cell biology of diabetic complications.*Nature*. **4:** 813-820.

Brownlee M (2005) The pathobiology of diabetic complications. *Diabetes*. **54:** 1615-1625.

Bruno G, Runzo C, Cavallo-Perin P, Merletti F, Rivetti M, et al. (2005) The piedmont study group for diabetes epidemiology. Incidence of type 1 and type 2 diabetes in adults aged 30-49 years: the population-based registry in the province of Turin, Italy. *Diabetes Care*. **28**: 2613-9.

Burns WC, Twigg SM, Forbes JM, Pete J, Tikellis C, et al. (2006) Connective tissue growth factor plays an important role in advanced glycation end product-induced tubular epithelial-to-mesenchymal transition: implications for diabetic renal disease. *J Am Soc Nephrol*. **17:** 2484-2494.

Caramori ML, Fioretto P, Mauer M (2000) The need for early predictors of diabetic nephropathy risk: Is albumin excretion rate sufficient? *Diabetes*. **49**:1399–1408,

Carey RM, Siragy HM (2003) The intrarenal renin–angiotensin system and diabetic nephropathy. *Trends Endocrinol Metab*. **14**: 274–281.

Carven PA, Davidson MC, Deruberits FR (1990) Increase in diacylglycerol mass in isolated glomeruli by glucose from de novo synthesis of glycerolipids. *Diabetes.* **39:** 667-674.

Cefalu WT (2005) Glycemic control and cardiovascular disease - Should we reassess clinical goals? *N Engl J Med.* **22**: 2707-2709.

Ceolotto G, Gallo A, Miola M, Sartori M, Trevisan R, et al. (1999) Protein kinase C activity acutely regulated by plasma glucose concentration in human monocytes in vivo. *Diabetes.* **48:** 1316-1322.

Ceriello A, Ihnat MA, and Thorpe JE (2009) The "Metabolic Memory": Is More Than Just Tight Glucose Control Necessary to Prevent Diabetic Complications? *J Clin Endocrinol Metab*. **94**: 410-415.

Ceriello A, Morocutti A, Mercuri F, Quagliaro L, Moro M, et al. (2000) Defective intracellular antioxidant enzyme production in type 1 diabetic patients with nephropathy. *Diabetes.* **49**: 2170-2177.

Cha DR, Kim NH, Yoon JW, Jo SK, Cho WY, et al. (2000) Role of vascular endothelial growth factor in diabetic nephropathy. *Kidney Int Suppl.* **77:** 104–112.

Chen H, Phillips H, Callen D, Kim R, Wistow G, et al. (1992) Localisation of the human gene for μ-crystallin to chromosome 16p. *Genomics.* **14:** 1115-1116.

Cheng Z, Sun L, He J, Gong W (2007) Crystal structure of human μ-crystallin complexed with NADPH. *Protein Science.* **16:** 329-335.

Chen S, Cohen MP, Lautenslager GT, Shearman CW, Ziyadeh FN (2001) Glycated albumin stimulates TGF-ß1 production and protein kinase C activity in glomerular endothelial cells. *Kidney Int.* **59**:673–681.

Chen QX, Lv C, Huang LX, Cheng BL, Xie GH, et al. (2007) Genomic variations within DEFB1 are associated with the susceptibility to and the fatal outcome of severe sepsis in Chinese Han population. *Genes Immun*. **8**: 439-43.

Chen X, Li X, Wang P, et al. (2010) Novel association strategy with copy number variation for identifying new risk Loci of human diseases. *PLoS One.* **5**:12185.

Chen Y, Ruan XZ, Li Q, Huang A, Moorhead JF, et al. (2007) Inflammatory cytokines disrupt LDL-receptor feedback regulation and cause statin resistance: a comparative study in human hepatic cells and mesangial cells. *Am J Physiol Renal Physiol.* **293**(3): 680- 687.

Chistiakov DA (2011) Diabetic retinopathy: pathogenic mechanisms and current treatments. *Diabetes Metab Syndr.* **5**: 165-72.

Choi KC, Kim NH, An MR, Kang DG, Kim SW, et al. (1997) Alterations of internal rennin-angiotensin and nitric oxide systems in treptozotocin-induced diabetic rats. *Kidney Int*. **52**: 23-57.

Chong IW, Chang MY, Chang HC, Yu YP, Sheu CC, et al. (2006) Great potential of a panel of multiple hMTH1, SPD, ITGA11 and COL11A1 markers for diagnosis of patients with non-small cell lung cancer. *Oncol Rep.* **16**: 981-988.

Chouinard RF, Meek RL, Cooney SK, Tuttle KR (2002) Effects of amino acids and glucose on mesangial cell aminopeptidase A and angiotensin receptors. *Kidney Int.* **61**:106–109.

Christin K (1995) Diabetic nephropathy mechanisms of mesangial matrix expansion. *West J Med.* **162**: 318-321.

Chung SS, Ho EC, Lam KS, Chung SK (2003) Contribution of polyol pathway to diabetes-induced oxidative stress. *J Am Soc Nephrol.* **14**: S233-S236.

Clarkson MR, Murphy M, Gupta S, Lambe T, Mackenzie HS, et al. (2002) High glucose-altered gene expression in mesangial cells. Actin-regulatory protein gene expression is triggered by oxidative stress and cytoskeletal disassembly. *J Biol Chem.* **277**: 9707-9712.

Claudi VD, Berl T (2004) Pathogenesis of diabetic nephropathy. *Endocrine & Metabolic Disorders.***5:** 237-248.

Clement B, Mau S, Deters S, Havemeyer A (2005) Hepatic, extrahepatic, microsomal, and mitochondrial activation of the N-hydroxylated prodrugs benzamidoxime, guanoxabenz, and Ro 48-3656([[1-[(2s)-2-[[4-[(hydroxyamino)iminomethyl]benzoyl]amino]-1-oxopropyl]-4-piperidinyl]oxy]-acetic acid). *Drug Metab Dispose.* **33**:1740-7.

Clinical Trials Gov (2009) Study of GC1008 in Patients with Idiopathic Pulmonary Fibrosis (IPF).

Cooper ME, Vranes D, Youssef S, Stacker SA, Cox AJ, et al. (1999) Increased renal expression of vascular endothelial growth factor (VEGF) and its receptor VEGFR-2 in experimental diabetes. *Diabetes.* **48**:2229–2239.

Cortes P, Zhao X, Riser BL, Narins RG (1996) Regulation of glomerular volume in normal and partially nephrectomized rats. *Am J Physiol.* **270**: 356–370.

Cruickshanks KJ, Ritter LL, Klein R, Moss SE (1993) The association of microalbuminuria with diabetic retinopathy. The Wisconsin Epidemiologic Study of Diabetic Retinopathy. Ophthalmology. 6

Cruz D, Xenarios I, Langridge J, Vilbois F, Parone PA, et al. (2003) Proteomic analysis of the mouse liver mitochondrial inner membrane. *J Biol Chem.* **278:** 41566-41571.

Da Cruz S, Xenarios I, Langridge J, Vilbois F, Parone PA, et al. (2003) Proteomic analysis of the mouse liver mitochondrial inner membrane. *J Biol Chem.* **17**: 41566-71.

Danaei G, Finucane MM, Lu Y, Singh GM, Cowan MJ, et al. (2011) National, regional, and global trends in fasting plasma glucose and diabetes prevalence since 1980: systematic analysis of health examination surveys and epidemiological studies with 370 country-years and 2.7 million participants. *Lancet.* 378: 31–4.

De Cosmo S, Bacci S, Piras GP, Cignarelli M, Placentino G, et al. (1997) High prevalence of risk factors for cardiovascular disease in parents of IDDM patients with microalbuminuria. *Diabetologia.* **40**: 1191-1196.

Diabetes Control and Complications Trial Research Group (1995) Effect of intensive therapy on the development and progression of diabetic nephropathy in the Diabetes Control and Complications Trial. *Kidney Int.* **47:** 1703-1720.

Diabetes Control and Complications Trial Research Group (1993) The effect of intensive treatment of diabetes on the development and progression of long-term complications in insulin-dependent diabetes mellitus. *N Engl J Med.* **329:** 977-986.

Diabetes Control and Complications Trial/Epidemiology of Diabetes Interventions and Complications Study Research Group (2005). Intensive diabetes treatment and cardiovascular disease in patients with type 1 diabetes. *N Engl J Med.* **22**: 2643-53.

Diabetes Control and Complications Trial/Epidemiology of Diabetes Interventions and Complications Research Group (2003) Retinopathy and nephropathy in patients with type 1 diabetes four years after a trial of intensive therapy. *N Engl J Med.* **342:** 381-389.

Diabetes Control and Complications Trial/Epidemiology of Diabetes Interventions and Complications Research Group (2003) Sustained effect of intensive treatment of type 1 diabetes mellitus on development and progression of diabetic nephropathy: The Epidemiology of Diabetes Interventions and Complications study. *JAMA.* **290:** 2159-67.

Diabetes Control and Complications Trial/Epidemiology of Diabetes Interventions and Complications Research Group (2011) *N Engl J Med.*

Diamond JR (1993) Analogous pathobiologic mechanisms in glomerulosclerosis and atherosclerosis. *Kidney Int.* **39:** S29-S34.

Djk CV, Berl T (2004) Pathogenesis of diabetic nephropathy. *Endocrine & Metabolic disorders.* **5:** 237-248.

Dobson M (1776) Nature of the urine in diabetes. *Medical Observations and Inquiries.* **5:** 298-310.

Dolan V, Murphy M, Sadlier D, Lappin D, Doran P, et al. (2005) Expression of gremlin, a bone morphogenetic protein antagonist, in human DN. *Am J Kidney Dis.* **45**:1034–1039.

Donovan M, Olofsson B, Gustafson A, Dencker L, Eriksson U (1995) The cellular retinoic acid binding proteins. *J Steroid Biochem Mol Biol.* **53**: 459-465.

Du XL, Edelstein D, Rossetti L, Fantus IG, Goldberg H, et al. (2000) Hyperglycaemia-induced mitochondrial superoxide overproduction activates the hexosamine pathway and induces plasminogen activator inhibitor-1 expression by increasing Sp1 glycosylation. *Proc Natl Acad Sci.* **97**: 12222–12226.

Eddy AA (2005) Progression in chronic kidney disease. *Adv Chronic Kidney Dis.* **12**: 353-365.

Engerman RL, Kern TS, Larson ME (1994) Nerve conduction and aldose reductase inhibition during 5 years of diabetes or galactosaemia in dogs. *Diabetologia.* **37**: 141–144,

Engerman RL, Kern TS (1987) Progression of incipient diabetic retinopathy during good glycemic control. *Diabetes.* **36**: 808–812.

Epidemiology of Diabetes Interventions and Complications (EDIC) (1999) Design, implementation, and preliminary results of a long-term follow-up of the Diabetes Control and Complications Trial cohort. *Diabetes Care.* **22**: 99-111.

Epidemiology of Diabetes Interventions and Complications (EDIC) (2011) *New Engl J Med.*

Feng Y, Wang Q, Wang Y, Yard B, Lang F (2005) SGK1-mediated fibronectin formation in diabetic nephropathy. *Cell Physiol Biochem.* **16**: 237-244.

Fessele S, Maier H, Zischek C, Nelson PJ, Werner T (2002) regulatory context is a crucial part of gene function. *Trends Genet.* **18:** 60-63.

Flyvbjerg A, Gronbek H, Bak M, et al. (1998) Diabetic kidney disease: the role of growth factors. *Nephrol Dial Transplant.* **13**: 1104-1107.

Fogarty DG, Moczulski DK, Makita Y, Warram JH, Krolewski AS (1999) Evidence for a susceptibility locus for diabetic nephropathy on chromosome 7q in Caucasian families with type 2 diabetes. *Diabetes.* **48:** 47.

Forti S, Scanlan M, Invernizzi A, Castiglioni F, Pupa S, et al. (2002) Identification of breast cancer-restricted antigens by antibody screening of SKBR3 cDNA library using a preselected patient's serum. *Breast Cancer Res Treat.* **73**: 245-56.

Frecker H, Munk S, Wang H, and Whiteside C (2005) Mesangial cell reduced Ca^{2+} signalling in high glucose is due to inactivation of phospholipase C_3 by protein kinase C. *Am J Physiol Renal Physiol* **289:** 1078-1087.

Fukada Y, Yasui K, Kitayama M, Doi K, Nakano T, et al. (2007) Gene expression analysis of the murine model of amyotrophic lateral sclerosis: Studies of the Leu126delTT mutation in SOD1. *Brain Research.* **1160**: 1-10.

Fumo P, Kuncio GS, Ziadeh FN (1994) PKC and high glucose stimulate collagen alphal (IV) transcriptional activity in a receptor mesangial cell line. *Am J Physiol.* **267**: 632-638.

Gentle A, Anastasopoulos F, McBrien N (2001) High resolution semi-quantitative real-time PCR without the use of a standard curve. *Bio Techniques.* **31**:502-508.

Gilbert RE and Cooper ME (1999) The tubulointerstitium in progressive diabetic kidney disease: more than an aftermath of glomerular injury? *Kidney Int.* **56**: 1627-1637.

Gilbert RE, Akdeniz A, Weitz S, Usinger WR, Molineaux C, et al. (2003) Diabetes Urinary connective tissue growth factor excretion in patients with type 1 diabetes and nephropathy. *DiabetesCare.* **26**:2632-2636.

Glassock RJ (2010) Is the presence of microalbuminuria a relevant marker of kidney disease? *Curr Hypertens Rep.* **12**: 346-368.

Glyn- Jones S, Black MA, Phillips AR, Choong SY, et al. (2007) Transcriptomic analysis of the cardiac left ventricle in a rodent model of diabetic cardiomypathy: molecular snapshot of a severe myocardial disease. *Physiol. Genomics.* **28**: 284-293.

Greenberg A (1998) Primer on kidney diseases, 2nd edition, London: National kidney foundation.

Greene DA, Lattimer SA, Sima AA (1987) Sorbitol, phospho inositides, and sodium-potassium-ATPase in the pathogenesis of diabetic complications. N Eng J Med. **316**: 599-606.

Griendling KK, Sorescu D, Ushio-Fukai M (2000) NAD(P) H oxidase: Role in cardiovascular biology and disease. *Circ Res.* **86**: 494-501.

Grotendorst GR (1997) Connective tissue growth factor: a mediator of TGF-beta action on fibroblasts. *Cytokine Growth Factor Rev*. **8**:171–179.

Grzeszczak W (2001) Role of GLUT1 gene in susceptibility to diabetic nephropathy in type 2 diabetes.*Kidney Int.* **59**: 631-636.

Grone EF, Walli AK, Grone H-J, Miller B, Seidel D (1994) The role of lipids in nephrosclerosis and glomerulosclerosis. *Atherosclerosis.* **107:** 1-13.

Grossman E, Messerli FH (2008) Hepertention and siabetes.*Cardiovascular Diabetology*. **45:** 82-106.

Gruenewald S, Wahl B, Bittner F et al. (2008) The Fourth Molybdenum Containing Enzyme mARC: Cloning and Involvement in the Activation of *N*-Hydroxylated Prodrugs*J Med Chem.* **51**: 8173–8177.

Gudehithlu KP, Pegoraro AA, Dunea G, et al. (2004) Degradation of albumin by the renal proximal tubule cells and the subsequent fate of its fragments. *Kidney Int.* **65**: 2113–2122.

Guha M, Xu Z-G, Tung D, Lanting L, Natatajam R (2007) Specific down-regulation of connective tissue growth factor attenuates progression of nephropathy in mouse models of type 1 and type 2 diabetes.*FASEB J.* **21**:3355-6.

Guiochon-Mantel A, Milgrom E (1993) Cytoplasmic-nuclear trafficking of steroid hormone receptors. *Trends Endocrinol Metab.* **4**: 322-328.

Guzki TJ,West NE.,Black E., McDonald D, Ratnatanuga C, et al. (2000). Vascular superoxide production by NAD(P)H oxidase: Assosiation with endothial dysfunction and clinical risk factors. *Cric Res.* **86**: 85-90.

Ha H, Lee HB (2005) Reactive oxygen species amplify glucose signalling in renal cells cultured under high glucose and in diabetic kidney. *Nephrology.* **10**: 7-10.

Ha H, Yu MR, Choi YJ, Kitamura M, and Lee HB (2002) Role of high glucose-induced nuclear factor-κB activation in monocyte chemoattractant protein-1 expression by mesangial cells. *J Am Soc Nephrol* **13**: 894-902.

Han DC, Isono M, Hoffman BB, Ziadeh FN (1999). High glucose stimulates proliferation and collagen type I synthesis in renal cortical fibroblasts : mediation by autocrine activation of TGF-beta. *J Am Soc Nephrol.* **10**: 1891-1899.

Hancock JT, Desikan R, Neli SJ (2001) Role of reactive oxygen species in cell signalling pathways. *Biochem Soc Trans.* **29:** 345-350.

Haneda M, Koya D, Isono M, Kikkawa R (2003)Overview of Glucose Signalling in Mesangial Cells in Diabetic Nephropathy. *J Am Soc Nephrol.* **14**: 1374-1382.

Hashizume K, Kobayashi M, Miyamoto T (1986) Active and inactive forms of 3,5,3'-triiodo-L-thyronine (T3)-binding protein in rat kidney cytosol: possible role of nicotinamide adenine dinucleotide phosphate in activation of T3 binding. *Endocrinology.* **119:** 710-719.

Hashizume K, Miyamoto T, Ichikawa K, Yamauchi K, Sakurai A, et al. (1989)Evidence for the presence of two active forms of cytosolic 3,5,3'- triiodo-L-thyronine (T3)-binding protein (CTBP) in rat kidney. Specialized functions of two CTBPs in intracellular T3 translocation. *J Biol Chem.* **264**: 4864-4871.

Hashizume K, Miyamoto T, Ichikawa K, Yamauchi K, Kobayashi M, et al. (1989) Purification and characterization of NADPH-dependent cytosolic 3,5,3'- triiodo-L-thyronine binding protein in rat kidney. *J Biol Chem.* **26:** 4857-4863.

Havemeyer A, Bittner F, Wollers S, Mendel R, Kunze T,et al. (2006) Identification of the missing component in the mitochondrial benzamidoxime prodrug-converting system as a novel molybdenum enzyme. *J Biol Chem.* **17**: 281.

Havemeyer A, Grünewald S, Wahl B, Bittner F, Mendel R, et al. (2010) Reduction of N-hydroxy-sulfonamides, including N-hydroxy-valdecoxib, by the molybdenum-containing enzyme mARC. *Drug Metab Dispos.* **38**: 1917-21.

Havemeyer A, Lang J, Clement B (2011) The fourth mammalian molybdenum enzyme mARC: current state of research. *Drug Metabolism Reviews.* **43**: 524-539.

Heilig, C, Guo L, Brosius, F (2000) Antisense-GLUT1 inhibits angiotensin-II (AT) mediated TGFβ1 and fibronectin (FN) expression in mesangial cells (MC). *J Am Soc Nephrol.* **11**: 3387.

Heilig CW, Brosius FC, Cunningham C (2006) Role for GLUT1 in diabetic glomerulosclerosis. *Expert Rev Mol Med.* **6**:1-18.

Heilig CW, Deb DK, Abdul A, Riaz H, James LR, et al. (2013) Glut1 regulation of the pro-sclerotic mediators of diabetic nephropathy. *Am J Nephrol.* **38:** 39-49.

Heilig CW (2003) Glucose transporter-1- deficient mice exhibit impaired development and deformities that are similar to diabetic embryopathy. *Proc Natl Acad Sci USA.* **100**:15613-15618.

Heilig CW, Liu Y, England RL, Freytag SO, Gilbert JD, et al. (1997) D-glucose stimulates mesangial cell GLUT1 expression and basal and IGF-1-sensitive glucose uptake in rat mesangial cells: Implications for diabetic nephropathy. *Diabetes.* **46**: 1030–1039.

Heilig, K (2004) Overexpression of GLUT1 in glomeruli produces features of diabetic nephropathy (DN) in mice. *J Am Soc Nephrol.* **15**: 263A.

Heino J, Ignotz RA, Hemler ME, Crouse C, Massague J (1989) Regulation of cell adhesion receptors by transforming growth factor-β.Concomitant regulation of integrins that share a common β_1 subunit. *J Biol Chem.* **264**: 380-388.

Hellmich B,Schellner M, Schatz H (2000) Activation of transforming growth factor-β_1 in diabetic kidney disease. *Metabolism.* **3**: 353-359.

Henry DN, Buski JV, Concepcion LA, Brosius FC, Heilig CW (1999) Glucose transporters control the expression of aldose reductase, PKCα, GLUT1 genes in mesangial cells in vitro. *Am J Physiol.* **277:** 97-104.

Hill C, Flyvbjerg A, Grønbæk H, Petrik J, Hill DJ et al. (2000) The renal expression of transforming growth factor-ß isoforms and their receptors in acute and chronic experimental diabetes in rats. *Endocrinology.* **141**: 1196–1208.

Hirrata C, Nakano K, Nakamura N, Kitagawa Y, Shigeta H et al. (1997) Advaced glycation end products induce expression of vascular endothelial growth factor by retinal muller cells. *Biochem Biophys Res Commun.* **263**: 712-715.

Hodgkinson AD, Bartlett T, Oates PJ, Millward BA, Demaine AG (2003) The response of antioxidant genes to hyperglycaemia is abnormal in patients with type 1 diabetes and diabetic nephropathy. *Diabetes.* **52**: 846-851.

Hoek IV, Daminet S (2009) Interactions between thyroid and kidney function in pathological conditions of these organ systems: a review. *Gen Comp Endocrinol.* **160**: 205-215.

Hoffman BB, Sharma K, Zhu Y, Ziadeh FN (1998) Transcriptional activation of transforming growth factor-β1 in mesangial cell culture by high glucose concentration. *Kidney Int.* **54**: 1107-1116.

Holmes DI, Abdel Wahab N, Mason RM (1997) Identification of glucose-regulated genes in human mesangial cells by mRNA differential display. *Biochem Biophys Res Commun.* **238**:179-184.

Hong SW, Isono M, Chen S, Iglesias-De La Cruz MC, Han DC, et al. (2001) Increased glomerular and tubular expression of transforming growth factor-beta1, its type II receptor, and activation of the Smad signalling pathway in the db/db mouse. *Am J Pathol.* **158**: 1653 –1663.

Hostetter TH, Rennke HG, Brenner BM (1982) The case for intrarenal hypertension in the initiation and progression of diabetic and other glomerulopathies. *Am J Med.* **72**: 375–380.

Hovind P, Tarnow L, Oestergaard PB, Parving H (2000) Elevated vascular endothelial growth factor in type 1 diabetic patients with diabetic nephropathy. *Kidney Int.* **75:** 56-61.

Hovind P, Tarnow L, Rossing P, Jensen BR, Graae M**,** Torp I, et al. (2004) Predictors for the development of microalbuminuria and macroalbuminuria in patients with type 1 diabetes: inception cohort study. *BMJ.* **328:** 1105.

Hua H, Munk S, Goldberg H, Fantus IG, Whiteside CI (2003) High glucose-suppressed endothelin-1 Ca^{2+} signalling via NADPH oxidase and diacylglycerol-sensitive protein kinase C isozymes in mesangial cells. *J Biol Chem.* **278:** 33951-33962.

Idris I, Gray S, Donnelly R (2001) Protein kinase C activation: isozyme-specific effects on metabolism and cardiovascular complications in diabetes. *Diabetologia.* **44:** 659-673.

Imperatore G, Hanson RL, Pettitt DJ, Kobes S, Bennett PH, et al. (1998) Sib-pair linkage analysis for susceptibility genes for microvascular complications among Pima Indians with type 2 diabetes. Pima Diabetes Genes Group. *Diabetes.* **47:** 821-830

Inoguchi T, Li P, Umeda F, Yu HY, Kakimoto M, Imamura M, et al. (2000) High glucose level and free fatty acid stimulate reactive oxygen species production through protein kinase C-dependent activation of NAD(P)H oxidase in cultured vascular cells. *Diabetes.* **49**:1939-1945.

Ingolia TD, Craig EA (1982) Four small Drosophila heat shock proteins are related to each other and to mammalian alpha-crystallin. *Proc Natl Acad Sci USA.* **79:** 2360-2364.

Ishii N, Patel KP, Lane PH, Taylor T, Bian K, et al. (2001) Nitric oxide synthesis and oxidative stress in the renal cortex of rats with diabetes mellitus. *J Am Soc Nephrol.* **12**:1630–1639.

Ito Y, Aten J, Bende RJ, Oemar BS, Rabelink TJ, et al. (1998) Expression of connective tissue growth factor in human renal fibrosis. *Kidney Int.* **53**:853–861.

Itoh H, Mukoyama M, Pratt RE, Gibbons GH, Dzau VJ (1993). Multiple autocrine growth factors modulate vascular muscle cell growth response to angiotensin II. *J Clin Invest.* 91: 2268-2274.

Iwano M and Neilson EG (2004) Mechanisms of tubulointerstitial fibrosis. *Kidney Intr.* **13**:279–28.

Jahn D, Verkamp E, Soll D (1992) Glutamyl-transfer RNA: a precursor of heme and chlorophyll biosynthesis. *Trends Biochem Sci.* **17**: 215-218.

Jakus V, Rietbrock N (2004) Advance glycation end-products and the progress of diabetic vascular complications. *Physiol Res.* **53:** 131-142.

James LR, Catherine L, Doherty H, Kim H, Maeda N (2013) Connective tissue growth factor (CTGF) expression modulates response to high glucose. *PLOS One.* **8:** 1-11.

Jeon YK, Kim MR, Huh JE, et al. (2011) Cystatin C as an early biomarker of nephropathy in patients with type 2 diabetes. *J Korean Med Sci.* **26**: 258-263.

Jefferson J A, Shankland S J and Pichler R H (2008) Proteinuria in diabetic kidney disease: A mechanistic view point Proteinuria in diabetes. *Kidney Intr.* **74**: 22-36.

Jerums G, Premaratne E, Panagiotopoulus S, Clarke S, Power DA, et al. (2008) New and old markers of progression of diabetic nephropathy. *Diabetes Res Clin Prac*. 30-37.

Kahn BB, and Flier JS (2000) obesity and insulin resistance. *J Clin Invest.* **106**:473-481

Kafaji-Al G, and Malik AN (2010) Hyperglycaemia induces elevated expression of thyroid hormone binding protein in vivo in kidney and heart and in vitro mesangial cells. *Biochem Biophys Res Commun.* **391** (4): 1585-1591.

Kamatani N, Moritani M, Yamanaka H, Takeuchi F, Hosoya T, et al. (2000) Localisation of a gene for familial juvenile hyperuricemic nephropathy causing underexcretion-type gout to 16p12 by genome-wide linkage analysis of a large family *Arthritis Rheum.* **43:** 925-9.

Kamijo-Ikemori A, Sugaya T, Yasuda T, et al. (2011) Clinical significance of urinary liver-type fatty acid-binding protein in diabetic nephropathy type 2 diabetic patients. *Diabetes Care*. **34**: 691-696.

Kanwar YS, Sun L, Xie P, Liu FY, Chen S (2011) A glimpse of various pathogenetic mechanisms of diabetic nephropathy. *Annu Rev Pathol.* **6**: 395-423.

Kennefick TM, Oyama TT, Thampson MM (1996) Enhanced renal sensitivity to angiotensin actions in diabetes mellitus in the rat. *Am J Physiol.* **271**: 595-602.

Khalil AA (2007) Biomarker discovery: a proteomic approach for brain cancer profiling. *Cancer Sci.* **98**: 766.

Kim R, Gasser R, Wistow G (1992) µ-crystallin is a mammalian homologue of Agrobacterium ornithine cyclodeaminase and is expressed in human retina. *Proc Natl Acad Sci USA*. **89**: 9292-9296.

Kobayashi M, Hashizume K, Suzuki S, Ichikawa K, Takeda T (1991) A novel NADPH-dependent cytosolic 3,5,3'-triiodo-L-thyronine-binding protein (CTBP;5.1S) in rat liver: a comparison with 4.7S NADPH-dependent CTBP. *Endocrinology*. **129:** 1701-1708.

Kobayashi T, Uehara S, Ikeda T, Itadani H, Kotani H (2003)Vitamin D3 up-regulated protein-1 regulates collagen expression in mesangial cells. *Kidney Int.* **64:** 1632-1642.

Klooster R, Straasheijm K, ShahB,Sowden J, FrantsR, et al.(2009) Comprehensive expression analysis of FSHD candidate genes at the mRNA and protein level. *Eur J Hum Genet.* **17**(12): 1615-1624.

Komers R, Anderson S (2003) Paradoxes of nitric oxide in the diabetic kidney. *Am J Physiol Renal Physiol.* **284**: 1121–113.

Kone BC, and Baylis C (1997) Biosynthesis and homeostatic roles of nitric oxide in the normal kidney. *Am J Physiol*. **272**: 561–578.
Kotthaus J, Wahl B, Havemeyer A, Kotthaus J, Dennis S (2011) Reduction of N-hydroxyl-L-arginine by the mitochondrial amidoxime reducing component (mARC). *Biochem J*. **433**: 383-391.

Koya D, Haneda M, Nakagawa H, Isshiki K, Sato H, Maeda S, et al. (2000) Amelioration of accelerated diabetic mesangial expansion by treatment with a PKC beta inhibitor in diabetic db/db mice, a rodent model for type 2 diabetes. *FASEB J*. **14:** 439-447.

Koya D, Jirousek MR, Lin YW, Ishii H, Kuboki K, King GL (1997) Characterization of protein kinase C ß isoform activation on the gene expression of transforming growth factor-ß, extracellular matrix components, and prostanoids in the glomeruli of diabetic rats. *J Clin Invest*. **100**: 115–126.

Koya D, and King GL (1998) Protein kinase C activation and the development of diabetic complications. *Diabetes.* **47**: 859–866.

J Radnik R, Ayo S, Garoni J, Saikumar P (1994). High glucose elevates c-fos and c-jun transcripts and protein in mesangial cell culture. *Kidney Int.* **46**: 105-112.

Lebreton A, Saveanu C, Decourty L, Jacquier A, Fromont-Racine M (2006) Nsa2 is an unstable, conserved factor required for the maturation of 27 SB pre-rRNAs. *J Biol Chem.* **281**: 27099-108.

Lai KN, Leung JC, Chan LY, Guo H, Tang CS (2007) Interaction between proximal tubular epithelial cells and infiltrating monocytes/T cell in the proteinuric state. *Kidney Int.***71**: 526-538.

Lai KN, Leung JC, Lai KB, To WY, Yeung VT, LaiFM (1998) Gene expression of the renin-angiotensin system in human kidney. *J Hypertens.* **16**:91–102.

Lappin DW, Hensey C, McMahon R, Godson C, Brady HR (2000) Gremlins, glomeruli and diabetic nephropathy. *Curr Opin Nephrol Hypertens*. **9**: 469–472.

Lazar M (1993) Thyroid hormone receptors: multiple forms, multiple possibilities. *Endocr Rev.* **14:** 184-193.

Leask A (2004) TGF-β signalling and fibrotic response. *FASEB J.* **18**: 816-827.

Lee D, Gonzalez P, Rao P, Zigler J, Wistow G (1993) Carbonyl-metabolizing enzymes and their relatives recruited as structural proteins in the eye lens. *Adv Exp Med Biol.* **328:** 159-68.

Lee BH, Yu MR, Yang Y, Jiang Z, Ha H (2003) Reactive oxygen species-regulated signalling pathways in diabetic nephropathy. *J Am Soc Nephrol*. **14:** S241-S245.

Lee JM, Dedhar S, Kalluri R, Thompson EW (2006) The epithelial-mesenchymal transition: new insights in signalling, development, and disease. *J Cell Biol.* **172**: 973–981.

Lee TN, Alborn WE, Knierman MD, Konrad RJ (2006) The diabetogenic antibiotic streptozotocin modifies the tryptic digest pattern for peptides of the enzyme O-GlcNAc-selective N-acetyl-beta-d-glucosaminidase that contain amino acid residues essential for enzymatic activity. *Biochem Pharmacol*. **72**: 710–18.

Lehmann R, and Schleicher ED (2000) molecular mechanism of diabetic nephropathy. *Clinica Chimica Acta.* **297**: 135-144.

Lewis EJ, Hunsicker LG, Bain RP, Rohde RD (1993) The effect of angiotensin-converting-enzyme inhibition on diabetic nephropathy. The Collaborative Study Group. *N Engl J Med.* **329**: 1456–1462.

Li J, Gobe G (2006). Protein kinase C activation and its role in kidney disease.*Nephrology.* **11**: 428-434.

Lindenmeyer MT, Kretzler M, Boucherot A et al. (2007) Interstitial vascular rarefaction and reduce VEGF-Aexpression in human diabetic nephropathy. *J Am Soc Nephrol*. **18**: 1765-1776.

Liang M, Cowley AW Jr, Greene AS (2003) High throughput gene expression profiling: A molecular approach to integrative physiology. *J Physiol*. **554:** 22-30.

Liang M, and Pietrusz JL (2007) Thiol-related genes in diabetic complications: a novel protective role for endogenous thioredoxin 2. *Arterioscler Thromb Vasc Biol*. **27**(1): 77-83.

Lin Y, and Sun Z (2011) Thyroid hormone potentiates insulin signalling and attenuates hyperglycaemia and insulin resistance in a mouse model of type 2 diabetes. *Br J Pharmacol.* **162(3):** 597-610.

Liu X, Lu F, Pan K, Wu W and Cen H (2007) High glucode upregulates connective tissue growth factor expression in human vascular smooth muscle cell. *BMC Cell Biol*. **8**:1.

Liu Y (2006) Renal fibrosis: new insights into the pathogenesis and therapeutics. *Kidney Int.* **69**: 213-217.

Liu ZH (1999) Glucose transporter (GLUT1) allele (XbaI-) associated with nephropathy in non-insulin-dependent diabetes mellitus. *Kidney Int.* **55**:1843-1848.

Livak KJ, and Schmittgen TD (2001) Analysis of relative gene expression data using real-time quantitative PCR and the 2(-Delta Delta C(T)) method. *Methods.* **25**(4): 402-408.

Loeffler I, Wolf G (2013) Transforming growth factor-β and the progression of renal disease. *Nephrol*. 1-9.

Malik AN, Rossios C, Al-Kafaji G, Shah A, Page RA (2007) Glucose regulation of CDK7, a putative thiol related gene, in experimental diabetic nephropath. *Biochem Biophys Res Commun*. **25:** 237-44.

Malik A, Zaidi Q, Morris C, Williams J (1997) Cloning of abundantly expressed candidate diabetes associated kidney genes. *J Am Soc Nephro*. **8**: A2995-A2997.

MalinowskaK, Cavarretta IT, SusaniM, WrulichOA, ÜberallF, et al. (2009) Identification of μ-Crystallin as an androgen-regulated in human prostate cancer. *The Prostate.* **69**(10): 1109-1118.

Marletta MA (1989). Nitric oxide: biosynthesis and biological significance. *Trends Pharmacol Sci*. **158**: 348-352.

Mason E, Lagarde M, Wiernsperger N, El Bawab S (2006) Hyperglycaemia and glucosamine-induced mesangial cell cycle arrest and hypertrophy: Common or independent mechanisms. *IUBMB Life*. **58**:381-388.

Mason RM (2009) Connective tissue growth factor (CCN2), a pathogenic factor in diabetic nephropathy, what does it do? How does it do it? *J Cell Common Signal.* **3**: 95-104.

Matsui T, Yamagishi S, Ueda S, Nakamura K, Imaizumi T, et al. (2007) Telmisartan, an angiotensin II type 1 receptor blocker, inhibits advanced glycation end-product (AGE)-induced monocyte chemoattractant protein-1 expression in mesangial cells through downregulation of receptor for AGEs via peroxisome proliferator-activated receptor-gamma activation. *J Int Med Res.* **35**: 482-9.

McMahon R, Murphy M, Clarkson M, Taal M, Mackenzie HS, et al. (2000) IHG-2, a mesangial cell gene induced by high glucose, is human gremlin. Regulation by extracellular glucose concentration, cyclic mechanical strain, and transforming growth factor-β_1. *J Biol Chem.* **275**:9901–9904.

Meleth DA, Agron E, Chan C, Reed G, Arora K (2005) Serum Inflammatory markers in diabetic nephropathy. *Ophthalmol*. **11**: 4295-4301.

Melham MF et al. (2001) Effects of dietry suplimentation of alpha lipoic acid on early glomerular injury in diabetes mellitus. *J Am Soc Nephrol.* **12**: 124-133.

Menini S, Amadio L, Oddi G, Ricci C, Pesce C, et al. (2006) Deletion of $p66^{Shc}$ Longevity Gene Protects Against Experimental Diabetic Glomerulopathy by Preventing Diabetes-Induced Oxidative Stress. *Diabetes.* **55:**1642-1650.

Mishra R, Emancipator SN, Ken T, Simonson MS (2007) High glucose evokes an intrinsic proapoptotic signalling pathway in mesangial cells. *Kidney Int*. **67**:82-93.

Mishra R, Emancipator SN, Kern T, Simonson MS (2005) High glucose evokes an intrinsic proapoptotic signalling pathway in mesangial cells. *Kidney Int*. **67**:82-93.

Mitsuhashi T, Nakayama H, Ithoh T, et al. (1993). Immunohistochemical detection of adnanced glycation end products in renal cortex from STZ-induced diabetic rat.*Diabetes.* **42**: 826-832.

Mogensen, CE, Keane, WF, Bennett, PH, et al. (1995) Prevention of diabetic renal disease with special reference to microalbuminuria. *Lancet.* **346**: 1080–1084

Morgensens CE (1989) Natural history of renal functional abnormalities in human diabetes mellitus: from microalbuminuria to overt nephropathy, in: Stein (Ed.), Contemporary Issues in Nephrology: The Kidney in Diabetes Mellitus, *Churchill Livingstone*. 426.

Morris C (1997) The molecular biology of diabetic nephropathy. PhD Thesis. University of Wales.

Morrison J, Knoll K, Hessner M, Liang M (2004) Effect of high glucose on gene expression in mesangial cells: upregulation of the thiol pathway is an adaptational response. *Physiol Genomics.* **17:**271-82.

Mousses S, Bubendorf L, Wagner U, Hostetter G, Kononen J, Cornelison R, et al. (2002) Clinical Validation of Candidate Genes Associated with Prostate Cancer Progression in the CWR22 Model System using Tissue Microarrays. *Cancer Res.* **62:** 1256-1260.

Murphy M, Docherty NG, Griffin B (2008) IHG-1 amplifies TGF-β1 signalling and is increased in renal fibrosis. *J Am Soc Nephrol*. **19:** 1672–1680.

Murphy M, Godson C, Cannon S, kato S, Mackenzie HS, et al. (1999) Suppression subtractive hybridisation identifies high glucose levels as a stimulus for expression of connective tissue growth factor and other genes in human mesangial cells. *J Biol Chem.* **274**: 5830–5834.

Murphy M, McMahon R, Lappin DW, Brady HR (2002) Germlins: Is this what renal fibrogenesis has come to? Exp. Nephrol. **10**: 241-244.

Nathan DM, Buse JB, Davidson MB, Heine RJ, Holman RR, Sherwin R, Zinman B (2006) Management of hyperglycaemia in type 2 diabetes: a consensus algorithm for the initiation and adjustment of therapy. *Diabetes Care.* **29**: 1963-1972.

Neufeld G, Cohen T, Gengrinovitch S, Poltorak Z (1999) Vascular endothelial growth factor (VEGF) and its receptors. *FASEB J*. **13**: 9–22.

Neve EP, Nordling A, Anderson TB, Hellman U, Diczfalusy U et al. (2011) An amidoxime reductase system in adipocyte mitochondria containing cytochrome b5 type B (CYB5B) and molybdenunm cofactor sulfurase C-terminal containing 2 (MOSC2) of importance for lipid synthesis. *J Biol Chem.* **287**(9): 6307-6317.

Nguyen G, Delarue F, Burckle C et al. (2002) Pivotal role of the renin/prorenin receptor in angiotensin II production and cellular responses to renin. *J Clin Invest.* **109**: 1417–1427.

Nguyen TQ, Tarnow L, Jorsal A, et al. (2008) Plasma connective tissue growth factor is an independent predictor of end-stage renal disease and mortality in type 1 diabetic nephropathy. *Diabetes Care*. **31**:1177–1182.

Nishikawa T, Edelstein D, Du XL, Yamagishi S, Matsumura T, et al. (2000) Normalising mitochondrial superoxide production blocks three pathways of hyperglycaemic damage. *Nature.* **404:** 787-790.

Noh H, Ha H, Yu MR, Kang SW, Choi KH, et al. (2002) High glucose increases inducible NO production in cultured rat mesangial cells. Possible role in fibronectin production.*Nephron.* **90**: 78–85.

Nordberg J, Arner ES (2001) Reactive oxygen species, antioxidants, and the mammalian thioredoxin system. *Free Radic Biol Med.* **31:** 1287-1312.

Oates PJ (2002) Polyol pathway and diabetic peripheral neuropathy.*Intern Rev Neurobiol.* **50:** 325-92.

Oddoze C, Morange S, Portugal H, et al. (2001) Cystatin C is not more sensitive than creatinine for detecting early renal impairment in patients with diabetes. *Am J Kidney Dis.* **38**:310-316.

Okada H, Kikuta HT, Kobayashi T, Inoue T, Kanno Y, et al. (2000) Connective tissue growth factor expressed in tubular epithelium plays a pivotal role in renal fibrogenesis. *J Am Soc Nephrol*. **16**:133 – 143.

Oshima A, Suzuki S, Takumi Y, Hashizum K, Ab S, et al. (2006) CRYM mutations cause deafness through thyroid hormone binding properties in the fibrocytes of the cochlea. *J Med Genet.* **43**: 25.

Olson AL and Pessin JE (1996) Structure, function and regulation of the mammalian facilitative glucose transporter gene family.*Annu Rev Nulr*. **16**: 235-56.

Osterby R (1992) Glomurlar structural changes in type I (insulin-dependent) diabetes mellitus: causes, consequences and prevention. *Diabetologia.* **35:** 803-819.

Page R, Malik A (2003) Elevated levels of beta defensin-1 mRNA in diabetic kidneys of GK rats. *Biochem Biophy Res Comm.* **310**:513-521.

Page R, Morris C, William J, voc Ruhland, Malik AN (1997) Isolation of diabetes associated kidney genes using differential display. *Biochem Biophy Res Comm.* **323**: 49-53.

Pardianto G (2005) Understanding diabetic retinopathy. *Mimbar Ilmiah Oftalmologi Indonesia.* **2**:65-6.

Parving HH, Lehnert H, Brochner-Mortensen J et al. (2001) The effect of irbesartan on the development of diabetic nephropathy in patients with type 2 diabetes. *N Engl J Med.* **345**: 870–878.

Patricia W (2000) Thyroid disease and diabetes. *Clinical Diabetes.* **18:** 1**.**

Phillips A, Janssen U, Floege J (1999) Progression of Diabetic Nephropathy Insights from Cell Culture Studies and Animal Models. *Kidney Blood Press Res.* **22**: 81-97.

Pickup J, and Williams G (2003) Text book of diabetes 2nd volume *Blackwell publisher*.

Piek E, Heldin CH, Ten Dijke P (1999) Specificity, diversity, and regulation in TGF-ß superfamily signalling. *FASEB J.* **13**: 2105–2124.

Pirulli D, Puzzer D, De Fusco M, Crovella S, Amoroso A, et al. (2001) Molecular analysis of uromodulin and SAH genes, positional candidates for autosomal dominant medullary cystic kidney disease linked to 16p12. *J Nephrol.* **14:** 392-396.

Pfaffl MW, Vandesompele J, Kubista M (2009) Data analysis software in real-time PCR: Current technology and application. *Caister Academic Press.*

Plitzko B, Ott G, Reichmann D, Henderson CJ, Wolf R, et al. (2013) The involvement of mitochondrial amidoxime reducing components 1 and 2 and mitochondrial cytochrome b5 in N-reductive metabolism in human cells. *J Biol Chem.* **288**(28): 20228-20237.

Portilla D, Dai G, Peter JM, Gonzalez FJ, Crew MD, et al. (2000) Etomoxir-induced PPAR alpha-modulated enzymes protect during acute renal failure. *Am J Physiol Renal Physiol.* **278**: 667-675.

Pucci L, Triscornia S, Lucchesi D et al. (2007) Cystatin C and estimates of renal function: searching for a better measure of kidney function in diabetic patients. *Clin Chem.* **53**: 480-488.

Pupilli C, Lasagni L, Romaganani P, Bellini F, Menelli M, et al. (1999) Angitensin II stimulates the synthesis and secretion of vascular permeability factor/vascular endothelial growth factor in human mesangial cells. *J Am Soc Nephrol.* **10**: 245-255.

Qi W, Chen X, Zhang Y, Holian J, Mreich E, et al. (2007) High glucose induces macrophage inflammatory protein-3{alpha} in renal proximal tubule cells via a transforming growth factor-{beta}1 dependent mechanism. *Nephrol Dial Transplant.* **22**(11): 3147-3153.

Raptis A, and Viberti G (2001) Pathogenesis of diabetic nephropathy. *Exp Clin Endocrinol Diabetes.* **109**: 424-437.

Ravid M, Savin H, Jutrin I, Bental T, Katz B, et al. (1993) Long-term stabilizing effect of angiotensin-converting enzyme inhibition on plasma creatinine and on proteinuria in normotensive type II diabetic patients. *Ann Intern Med.* **118**:577–581.

Reed P.W, Andrea M.C, Neli C.P, Kevin M.F, Robert J.B (2007) Abnormal expression of mu-crystallin in facioscapulohumeral muscular dystrophy. *Experimental Neurology.* **205:**583-586.

Reiss J,and Hahnewald R (2010) Molybdenum cofactor deficiency: Mutations in GPHN, MOSC1, and MOSC2. *Human Mutation.* **32**(1): 10-18.

Rippin JD, Patel A, Bain SC (2001) Genetics of diabetic nephropathy. *Best Pract Res Clin Endocrinol Metab*. **15**: 345-358.

Riser BL, Cortes P, DeNichilo M, Deshmukh PV, Chahal PS, et al. (2003) Urinary CCN2 (CTGF) as a possible predictor of diabetic nephropathy. *Kidney Int.* **64**:451-458.

Riser BL, Denichilo M, Cortes P, Baker C, Grondin JM, et al. (2000) Regulation of connective tissue growth factor activity in cultured rat mesangial cells and its expression in experimental diabetic glomerulosclerosis. *J Am Soc Nephrol.* **11**: 25–38.

Ritz E (2001) Advances in nephrology: successes and lessons from diabetes mellitus. *Nephrol Dial Transplant.* **16**: 46-50.

Ritz E, and Tarng D (2001) Renal disease in type 2 diabetes. *Nephrol Dial Transplant*. **16**:11-18.

Rizvi AA (2004) Type 2 diabetes: Epidemiologic trends, evolving pathogenic concepts, and recent changes in therapeutic approach. *South Med J.* **97**: 1079-1087.

Robinson CJ and Stringer SE (2001) The splice variants of vascular endothelial growth factor (VEGF) and their receptors. *J Cell Sci.* **114:** 853-865.

Rocoo MV, Chen Y, Goldfarb S, Ziadeh FN. (1992). Elevated glucose stimulates TGF-β gene expression and bioactivity in proximal tubule. *Kidney Int.* **41**: 107-114.

Roestenberg P, van Nieuwenhoven FA, Wieten L et al. (2004) Connective tissue growth factor is increased in plasma of type 1 diabetic patient with nephropathy. *Diabetes Care*. **27**:1164-70.

Rother KI (2007) "Diabetes Treatment – Bridging the Divide".*N Engl J Med.* **356**(15): 1499-1501.

Roy S, Sala R, Cagliero E, Lorenzi M (1990) Overexpression of fibronectin induced by diabetes or high glucose: phenomenon with a memory. *Proc Natl Acad Sci USA.* **87**: 404–408.

Ryan A, Murphy M, Godson C, Hickey FB (2009) Diabetes mellitus and appotosis: inflammatory cells. *Apoptosis.* **14**:1435-1450.

Ruilope L, Kjeldsen SE, de la Sierra A, Mancia G, Ruggeneti P, et al. (2007) The kidney and cardiovascular risk--implications for management: a consensus statement from the European Society of Hypertension. *Blood Press.* **16**(2): 72-79.

Sambrook J, Fritsch EF, Maniatis T (1989) Molecular Cloning: A laboratory Manual, 2nd Edn. Cold Spring Harbor Laboratory Press, Cold Spring Harbor, New York, NY.

Schaeffner ES, Kurth T, Curhan GC, Glynn RJ, Rexrode KM, et al. (2003) Rubin A.L, Jarvis S (2011) Diabetes for dummies, 3rd edition, England: Willey & Sons, Ltd.

Schena FB, and Gesualdo L (2005) Pathogenetic mechanisms of diabetic nephropathy. *J Am Soc Nephrol.* **16**:S30-S33.

Schulze PC, Yoshioka J, Takahashi T, He Z, King GL, et al. (2004) Hyperglycaemia promotes oxidative stress through inhibition of thioredoxin function by thioredoxin-interacting protein. *J Biol Chem.* **279**: 30369–30374.

Segovia L, Horwitz J, Gasser R, Wistow G (1997) Two roles for mu-crystallin: a lens structural protein in diurnal marsupials and a possible enzyme in mammalian retinas. *Mol Vision.* **3**: 9-15.

Sell DR, and Monnier VM (1990) End-stage renal disease and diabetes catalyze the formation of a pentose-derived crosslink from aging human collagen. *J Clin Invest.* **85:** 380-384.

Sellitti F, Puggina E, Lagranha C, Doi Q, Pithon-Curi T, et al. (2007) TGF-beta-like Transcriptional Effects of Thyroglobulin (Tg) in Mouse Mesangial Cells. *Endocr J*. **54**: 449-58.

Senger DR, Galli SJ, Dvorak AM, et al. (1983) Tumour cells secrete a vascular permeability factor that promotes accumulation of ascties fluid. *Science.* **219**: 983-985

Shahni R (2011) The Role of Two Novel Genes, NSA2 and CDK7, in Diabetic Nephropathy. PhD thesis.

Shahni R, Gnudi L, King A, Jones P, Malik AN (2011) Elevated levels of renal and circulating Nop-7-associated 2 (*NSA2)* in rat and mouse models of diabetes, in mesangial cells in vitro and in patients with diabetic nephrpathy. *Diabetologia.* **55**: 828-834.

Sharma K, McCue P, Dunn SR (2003) Diabetic kidney disease in the db/db mouse. *Am J Physiol Renal Physiol.* **284**: 1138– 1144,

Sharma K, Ziyadeh FN (1997) Biochemical events and cytokine interactions linking glucose metabolism to the development of diabetic nephropathy. *Semin Nephrol.* **17**: 80–92.

Sharma K, Ziyadeh FN, Alzahabi B, McGowan TA, Kapoor S, et al. (1997) Increased renal production of transforming growth factor-ß1 in patients with type II diabetes. *Diabetes.* **46**: 854–859.

Sheehan A (2001) Cholesterol Update: Oxidized and Nonoxidized LDL Cholesterol. Do We Have to Worry about Both? *Dynamic Chiropractic.* **19** (11).

Sheetz MJ, King GL (2002) Molecular understanding of hyperglycaemia's adverse effects for diabetic complications. *J Am Med Assoc.* **288:** 2579-2588.

Shigeta Y, and Kikkawa R (1991) A role of mesangial dysfunction in the development of diabetic nephropathy. *Jpn J Med.* **30**(6): 622-623.

Shinohara M, Thornalley PJ, Giardino I, Beisswenger P, Thorpe SR, et al. (1998) Overexpression of glyoxalase-I in bovine endothelial cells inhibits intracellular advanced glycation endproduct formation and prevents hyperglycaemia-induced increases in macromolecular endocytosis. *J Clin Invest.* **101**: 1142–1147.

Shiose A, Kuroda J, Tsuruya K, Hirari M, Hirakata H, et al. (2001) Anovel superoxide-producing NAD (P)H oxidase in kidney. *J Biol Chem.* **276**: 1417-1423.

Sindhu RK, Ehdaei A, Farmand F, Dhaliwal KK, Nguyen T, et al. (2005) Expression of catalase and glutathione peroxidase in renal insufficiency. *Biochim Biophys Acta*. **1743**: 38-92.
.
Singh Ak, Gudehtihlu KP, Pegoraro AA, et al. (2004) Vascular factors altered in glucose-treated mesangial cells and diabetic glomeruli. Changes in vascular factor (VEGF) and its receptor VEGFR-2 in experimentn al diabetes.*Diabetes.* **48:** 597-606**.**

Singh DK, Winocour P and Farrington K (2008) Mechanisms of disease: the hypoxic tubular hypothesis of diabetic nephropathy.*Nature*. **4(4):** 216-225.

Singh LP, and Crook ED (2000) Hexosamine regulation of glucose-mediated laminine synthesis in mesangial cells involves protein kinase A and C. *Am J Physiol*. **279:** 646-654.

Singh R, Alavi N, Singh AK, Leehey DJ (1999) Role of angiotensin II in glucose-induced inhibition of mesangial matrix degradation. *Diabetes.* **48**: 2066–2073.

Stehouwer CD, Nauta JJ, Zeldenrust GC, et al. (1992) Urinary albumin excretion, cardiovascular disease, and endothelial dysfunction in non-insulin-dependent diabetes mellitus. *Lancet.* **340**:319–323.

Steinberg D, Parthasarathy S, Carew TE, Khoo JC, Witztum JL (1989) Beyond cholesterol. *N Engl J Med.* **320**: 915-924.

Stiburkova B, Majewski J, Sebesta I, Zhang W, Ott J, et al. (2000) Familial juvenile hyperuricemic nephropathy: localisation of the gene on chromosome 16p11.2-and Evidence for genetic heterogeneity. *Am J Hum Genet.* **66:** 1989-1994.

Supale S, Thorel F, Merkwirth C, Gjinovic A, Herrera PL (2013) Loss of prohibitin induces mitochondrial damages ß-cell function and survival and responsible for gradual diabetes development. *Diabetes.* **10:** 1-40.

Suzuki S, Suzuki N, Mori JI, Oshima A, Usami S, et al. (2007) micro-Crystallin as an intracellular 3,5,3'-triiodothyronine holder in vivo. *Mol Endocrionl.* **21**(4): 885-894.

Suzuki S, Mori JI, Hashizume K (2007) mu-crystallin, a NADPH-dependent T(3)-binding protein in cytosol. *Trends Endocrinol Metab.* 18(7): 286-289.

Suzuki S, Takei M, Nishio H, Inba A, Sato M, et al. (2009) Spiking expression of µ-Crystallin mRNA during treatment with methimazole in patients with graves Hyperthyroidism. *Horm Metab Res.* **41**: 548-553.

Tang SCW and Lai KN (2012) The pathogenic role of the renal proximal tubular cell in diabetic nephropathy. *Nephrol Dial Transplant.* **27**(8): 3049-3056.

Tan Al, Forbes JM, Cooper ME (2007) AGE, RAGE and ROS in diabetic nephropathy. *Semin Nephrol.* **27**: 130-143.

Tang S, Lai KN, Chan TM, et al. (2001) Transferrin but not albumin mediates stimulation of complement C_3 biosynthesis in human proximal tubular epithelial cells. Am Kidney Dis. **37:** 49-103.

Tanji N, Markowitz GS, Fu C, Kislinger T, Taguchi A (2000). Expression of advanced glycation end products and their cellular receptor.*J Am Soc Nephrol.* **11**: 1656-1666.

Tarnow L, Rossing P, Gall MN, Nielsen F, Parving H (1994). Hypertension in Diabetic Patients Before and After the JNC-V. *Diabetes Care.* **11**:1274-1251.

Teixeira PC, Iwai LK, Kuramoto ACK, Honorato R, Fiorelli A, Stolf N, et al. (2006) Proteomic inventory of myocardial proteins from patients with chronic Chagas' cardiomyopathy. *Braz J Med Biol Res.* **39**(12): 1549-1562.

Tesch GH, and Allen TJ (2007) Rodent models of streptozotocin-induced diabetic nephropathy. *Nephrology (Carlton).* **12**:261-266.

Thomas S, Vanuystel J, Gruden G, Rodriguez V, Burt D, et al. (2000) Vascular endothelial growth factor receptors in human mesangium *in vitro* and in glomerular disease. *J Am Soc NephroL.* **11**:1236–1243.

Tichopad A, Pfaffl M, Didier A (2003) Tissue-specific expression pattern of bovine prion gene: quantification using real-time RT-PCR. *Mol CellProbes.* **17:** 5-10.

Trachtman H, Koss I, Bogart M, Abramowitz J, Futterweit S, et al. (1998) High glucose enhances growth factor-stimulated nitric oxide production by cultured rat mesangial cells. *Res Commun Mol Pathol Pharmacol.* **100**:213–225.

Tsakas S and Goumenos DS (2006) Accurate measurement and clinical significance of urinary transforming growth factor-beta1. *Am J Nephrol.* **26**:186-93

UKPDS (1998) Intensive blood-glucose control with sulphonylureas or insulin compared with conventional treatment and risk of complications in patients with type 2 diabetes (UKPDS 33). *Lancet.* **352:** 837-853.

Unnikrishnan R, Anjana RM, Mohan V (2011) Importance of controlling diabetes early-the concept of metabolic memory, legacy effect and the case for early insulinisation. *JAPI.* **59:** 8-12.

Valko M, et al. (2006) "Free radicals, metals and antioxidants in oxidative stress-induced cancer. *Chem Biol Interact.* **160**:1-40.

Valko M, Leibfritz D, Moncol J, Cronin MT, Mazur M, Telser J (2007) Free radicals and antioxidants in normal physiological functions and human disease. *Int J Biochem Cell Biol.* **39**: 44-84.

Valko M, Morris H, Cronin M (2005) "Metals, toxicity and oxidative stress". *Curr Med Chem.* **12**: 1161-208.

Vandesompele J, De peter K, Pattyn F, Poppe B, Van Roy N, et al. (2002) Accurate normalisation of real-time quantitative RT-PCR data by geometric averaging of multiple internal control genes. *Genome Biol.* **3**: 0034.1.

Vestra MD**,** Saller A, Bortoloso E, Mauer M, Fioretto p (2000) Structural involvement in type 1 and type 2 diabetic nephropathy. *Diabetes Metab.* **26**: 8-14.

Vie M, Blanchet P, Samson M, Francon J, Blondeau J (1996) High affinity thyroid hormone-binding protein in human kidney: kinetic characterization and identification by photoaffinity labeling. *Endocrinol.* **137**: 4563-4570.

Vie M, Evrard C, Osty J, Breton-Gilet A, Blanchet P, et al. (1997) Purification, molecular cloning, and functional expression of the human nicodinamide-adenine dinucleotide phosphate-regulated thyroid hormone-binding protein. *Mol Endocrinol.* **11:** 1728-1736.

Vittorio C, Mancuso C, Sapienza M, Puleo E, Calafato S, et al. (2007) Oxidative stress and cellular stress response in diabetic nephropathy. *Cell stress & Chaperones.* **12**(4): 299-306.

Vlassara H, Palace MR (2002) Diabetes and advanced glycation end products. *J Intern Med.* **251:** 87-101.

Wada J, Kumar A, Ota K, Wallner EI, Batlle DC, et al. (1997) Representational difference analysis of cDNA of genes expressed in embryonic kidney. *Kidney Int.* **51**: 1629-1638.

Wada J, Makino H, Kanwar YS (2002) Gene expression and identification of gene therapy targets in diabetic nephropathy. *Kidney Int.* **61:** 73-78.

Wada H, Hashimoto K, Wada Y, Kobayashi M, Izumi A, et al. (2002) Extensive oligonucleotide microarray transcriptome analysis of the rat cerebral artery and arachnoid tissue. *J Atheroscler Thromb.* **9**: 224-232.

Wada T, Miyata T, Inagi R, Nangaku M, Wagatsuma M, et al. (2001) Cloning and characterization of a novel subunit of protein serine/threonine phosphatase 4 from mesangial cells. *J Am Soc NephroL.* **12**: 2601-2608.

Wahab NA, Cox D, Witherden A, Mason RM (2007) Connective tissue growth factor (CTGF) promotes activated mesangial cell survival via up-regulation of mitogen-activated protein kinase phosphatase-1 (MKP-1). *Biochem J.* **406:** 131-138.

Wahab NA, Parker S, Sraer JD, Mason RM (2000) The decorin high glucose response element and mechanism of its activation in human mesangial cells. *J Am Soc Nephrol*. **11**: 1607-1619.

Wahab NA, Schaefer L, Weston BS, Yiannikouris O, Wright A, Babelova A, Schaefer R, Mason RM (2005) Glomerular expression of thrombospondin -1, transforming growth factor beta and connective tissue growth factor at different stages of diabetic nephropathy and their interdependent roles in mesangial responses to diabetic stimuli. *Diabetologia*. **48**: 2650–2660.

Wahab NA, Weston BS, Mason RM (2005) Modulation of the TGFβ/Smad signalling pathway in mesangial cells by CTGF/CCN2. Exp Cell Res. **307**:305–314.

Wahab NA, Yevdokimova N, Weston BS, Roberts T, Li XJ, et al. (2001) Role of connective tissue growth factor in the pathogenesis of diabetic nephropathy. *Biochem J.* **359:** 77–87.

Wani J, Carl M, Henger A, Nelson PJ, Rupprecht H (2007) Nitric oxide modulates expression of extracellular matrix genes linked to fibrosis in kidney mesangial cells. *Biol Chem.* **388**:497-506.

Wasada T, Kawahara R, Katsumori K, Naruse M, Omori Y (1998) Plasma concentration of immunoreactive vascular endothelial growth factor and its relation to smoking. *Metabolism.* **47**:27–30.

Way KJ, Katai N, King GL (2001) Protein kinase C and the development of diabetic vascular complications. *Diabet Med.* **18:** 945-959.

Weigert C, Brodbeck K, Brosius FC, Huber M, Lenhmann R, et al. (2003) Evidence for a novel TGF-β1 independent mechanism of fibrosis in mesangial cells overexpressing glucose transporters. *Diabetes.* **52:** 537-535.

Weiss J, Sumpio B (2006). "Review of prevalence and outcome of vascular disease in patients with diabetes mellitus." *Eur J Vasc Endovasc Surg*. **31**:143-50.

Wendt T, Tanji N, Guo J, Hudson BI, Bierhaus A, et al. (2003) Glucose, glycation, and RAGE: implications for amplification of cellular dysfunction in diabetic nephropathy. *J Am Soc Nephrol.* **14**:1383–1395.

Whiteside CI, and Dlugosz JA (2002) Mesangial cell protein kinase C isozyme activation in diabetic milieu. *Am J Physiol Renal Physiol.* **282:** 975-980.

Wijmenga C, Frants RR, Brouwer OF, Weber JL, Padberg GW (1990) Location of facioscapulohumeral muscular dystrophy gene on chromosome 4. *Lancet*. **336**: 651-653.

Wild S, Roglic G, Green A, Sicree R, King H (2004) Global prevalence of diabetes: estimates for the year 2000 and projections for 2030. *Diabetes Care.* **27**:1047-1053.

Williams B, Gallacher B, Patel H, Orme C (1997) Glucose-induced protein kinase C activation regulates vascular permeability factor mRNA expression and peptide production by human vascular smooth muscle cells in vitro. *Diabetes.* **46**: 1497-1503.

Williams R, Van Gaal L, Lucioni C (2002) Assessing the impact of complications on the costs of Type II diabetes. *Diabetologia*. **45**: 13-17.

Wistow G (1993) Lens crystallins: gene recruitment and evolutionary dynamism.*Trends Biochem Sci.* **18:** 301-306.

Wistow G, and Kim H (1991) Lens protein expression in mammals: taxon-specificity and the recruitment of crystallins. *J Mol Evol*. **32:** 262-269.

Wistow GJ, and Piatigorsky J (1988) Lens crystallins: the evolution and expression of proteins for a highly specialized tissue. *Annu Rev Biochem.* **57:** 479-504.

Witzum JL, Miyata T, MAEDA K, et al. (1997) Immunohistochemical colocalisation of glycoxidation products and lipid peroxidation products in diabetic renal glomerular lesions. Implication for glycoxidative stress in the pathogenesis of diabetic nephropathy. *J Clin Invest.* **100**: 2995-3004.

Wolf G, Sharma K, Chen Y, Ericksen M and Ziyadeh FN (1992) High glucose-induced proliferation in mesangial cells is reversed by autocrine TGF-β. *Kidney Int.* **42:** 647–656.

Wolf G and Ziyadeh FN (1999) Molecular mechanisms of diabetic renal hypertrophy. *Kidney Int.* **56**: 393-405.

Wolf G, Chen S and Ziyadeh FN (2005) From the periphery of the glomerular capillary wall toward the centre of disease: podocyte injury comes of age in diabetic nephropathy, *Diabetes.* **54**: 1626–1634.

World Health Organisation.Definition, Diagnosis and Classification of Diabetes Mellitus and its Complications.Part 1: Diagnosis and classification of diabetes mellitus. Department of Noncommunicable Disease Surveillance, Geneva, 1999.

Wu X, Ivanova G, Merup M, Jansson M, Stellan B, et al. (1999) Molecular analysis of the human chromosome 5q13.3 region in patients with hairy cell leukemia and identification of tumour suppressor gene candidates. *Genomics.* **60**: 161-171.

Xia L, Wang H, Goldberg HJ, Munk S, Fantus IG, et al. **(**2006) Mesangial cell NADPH oxidase upregulation in high glucose is protein kinase C dependent and required for collagen IV expression. *Am J Physiol Renal Physiol.* **290:** 345-356.

Yamaoka T, Nishimura C, Yamashita K, Itakura M, Yamada T, et al. (1995) Acute onset of diabetic pathological changes in transgenic mice with human aldose reductase cDNA. *Diabetologia.* **38**: 255–26.

Yamamoto T, Noble NA, Cohen AH, Nast CC, Hishida A, et al. (1996) Expression of transforming growth factor-ß isoforms in human glomerular diseases. *Kidney Int.* **49**:461–469.

Yan HD, Li XZ, Xie JM, Li M (2007) Effects of advanced glycation end products on renal fibrosis and oxidative stress in cultured NRK-49F cells. *Clin Med J (Engl).* **120**: 787-93.

Yan HD, Lou MF, Fernando MR, Harding JJ (2006) Thioredoxin, thioredoxin reductase, and α-crystallin revive inactivated glyceraldehyde 3-phosphate dehydrogenase in human aged and cataract lens extracts. *Molecular Vision.* **12:** 1153-1159.

Yang J, Moravec CS, Sussman MA, DiPaola NR, Fu D, et al. (2000) Decreased SLIM1 expression and increased gelsolin expression in failing human hearts measured by high-density oligonucleotide arrays. *Circulation.* **102**(25): 3046-3052.

Yang Y, Ha H, Lee HB (2003) Role of reactive oxygen species in TGF-β1-induced epithelial-mesenchymal transition.*Nephrol Dial Transplant.* **18**(suppl 4) 300.

Yashpal SK, Wada J, Sun L, Xie P, Elisabeth IW, et al. (2008) Diabetic nephropathy:mechanisms of renal disease progression. *Exp Biol Med.* **10:** 4-11.

Yasuda T, Kondo S, Homma T, Harris RC (1996) Regulation of extracellular matrix by mechanical stress in rat glomerular mesangial cells. *J Clin Invest.* **98**:1991–2000.

Yokoyama Y, Narahara K, Tsuji K, Ninomiya S, Seino Y (1992) Autosomal dominant congenital cataract and microphthalmia associated with a familial t (2; 16) translocation. *Hum Genet.* **90**: 177-178.

Zaidi Q (1997) Characterization of candidate differentially expressed genes in developing and diabetic kidney. PhD thesis.

Zhang H, Ma X, Shi T, Song Q, Zhao H, et al. (2010) NSA2, a novel nucleolus protein regulates cell proliferation and cell cycle. *Biochem Biophys Res Commun*. **391**: 651-8.

Zhang L, Ma J, Gu Y, Lin S (2006) Effects of blocking the renin-angiotensin system on expression and translocation of protein kinase C isoforms in the kidney of diabetic rats .*Nephron Exp Nephrol.* **104**: 103-111.

Zhang SL, Filep JG, Hohman TC, Tang SS, Ingelfinger JR, et al. (1999) Molecular mechanisms of glucose action on angiotensinogen gene expression in rat proximal tubular cells. *Kidney Int.* **55**:454–464.

Zhang Z, Sun L, Wang Y, Ning G, Minto AW, et al. (2008) Renoprotective role of the vitamin D receptor in diabetic nephropathy. *Kidney Int.* **73**:163-71.

Zhu, Y., Usui, H.K. and Sharma, K (2007) Regulation of transforming growth factor beta in diabetic nephropathy: implications for treatment. *Seminars in Nephrology.* **27**: 153-160.

Zimpelmann J, Kumar D, Levine DZ, Wehbi G, Imig JD, et al. (2000) Early diabetes mellitus stimulates proximal tubule renin mRNA expression in the rat. *Kidney Int.* **58**: 2320–2330.

Ziyadeh FN (2008) Different roles for TGF-β and VEGF in the pathogenesis of the cardinal features of diabetic nephropathy. *Diabetes Res Clin Pract.* S38-S41.

Ziyadeh FN and Wolf G (2008) Pathogenesis of the podocytopathy and proteinuria in diabetic glomerulopathy, *Curr Diabetes Rev.* **4**:39–45.

Ziyadeh FN, Han DC, Cohen JA, Guo J, Cohen MP (1998) Glycated albumin stimulates fibronectin gene expression in glomerular mesangial cells: involvement of the transforming growth factor-beta system. *Kidney Int.* **53**:631-8.

Ziyadeh FN, Sharma K, Ericksen M, Wolf G (1994) Stimulation of collagen gene expression and protein synthesis in murine mesangial cells by high glucose is mediated by autocrine activation of transforming growth factor-ß. *J Clin Invest.* **93**:536–542.

Ziyadeh FN, Snipes ER, Watanabe M, Alvarez RJ, Goldfarb S, et al. (1990) High glucose induces cell hepertrophy and stimulates collagen gene transcription in proximal tubule. *Am J Physiol.* **90:** 704-71.

Ziyadeh FN, Hoffman BB & Han DC et al. (2000) Long-term prevention of renal insufficiency, excess matrix gene expression, and glomerular mesangial matrix expansion by treatment with monoclonal anti-transforming growth factor-beta antibody in db/db diabetic mice. *Proc Natl Acad Sci USA*. **97**: 8015–8020.

Appendix 1: List of chemicals, reagents and their suppliers

Materials and kits	Supplier
Bacto-agar, Mannitol	Difco
Dulbecco's Modified Eagle's Medium (DMEM)-low glucose, DMEM-high glucose, Penicillin-Streptomycin, Ampicillin, Trypsin-EDT, Phenol: Chloroform, transfer ribonucleic acid (tRNA), Bromophenol blue, Ethidium bromide, Glycerol, Trypan blue, Sodium dodecyl lsulfate (SDS), Acrylamide, Tris base (Tris-HCl), Ammonium persulphate, TEMED, Glycine, Nonfat milk, Tween 20, ox-LDL, n-LDL, TGF-β1,TNF-α, Formaldehyde, Acetone, Bovine serum albumine (BSA)	Sigma-Aldrich Ltd (UK)
RPMI 1640 media, Insulin-transferrin-selenium (ITS), HEPES buffer, Foetal bovine serum (FBS), Phosphate buffer saline (PBS), L-glutamine, Sodium bicarbonate (NaHCO3), Sodium acetate, Sodium hydroxide (NaOH)	GIBCO® Life Technologies (UK)
Goat polyclonal IgG antibody, Rabbit polyclonal IgG antibody, FITC-conjugated donkey anti-goat IgG, Rat kidney extract	Sant Cruz Biotechnology Inc (USA)
Vectashield mounting medium with propidium iodide	Vector Laboratories Peterborough (UK)
Hybond nitrocellulose filter, Horseradish peroxidase (HRP)-conjugated donkey anti-goat IgG antibody	Amersham Biosciences Ltd (UK)
3MM Chromatography papers	Whatman Ltd (UK)
Bio-Rad Protein Assay Dye Reagents Concentrate	BioRad Laboratories Ltd (UK)
S.N.A.P.™ MidiPrep kit, β-Gal assay kit, Lipofectamine™ LTX, anti-V5-FITC conjugated antibody, anti-His-FITC conjugated antibody, SeeBlue® Plus2 Pre-Stained Standard marker, Image-iT™ LIVE Green ROS detection kit, Luria Bertani broth, Agarose	Invitrogen (UK)
Wizard miniprep kit, UV quartz cuvettes, Taq DNA polymerase, Restriction endonucleases, DNA Ladders, dNTPs	Promega Ltd (UK)
GFX PCR DNA and Gel Purification Kit, Enhanced chemiluminensce (ECL) detection system	Amersham Biosciences Ltd (UK)
Totaly RNA isolation kit, RNAqueous™- 4PCR kit, DNase-1 treatment and DNase inactivation kit, ENDOFREE RT ™ kit, Nuclease-freetubes, Oligo-dT primer, AMV reverse transcriptase, Nuclease-free water, DEPCE-treated water, Rnase*Zap*	Ambion Inc (UK)
Cell culture flask (25; 75; 162 cm^2), 6-well cell culture cluster, Polypropylene conical Falcon tube (15; 50 ml), sterile pipette (5; 10; 25	Beckton Dickinson Ltd (UK)

ml), 0.22 ml sterile filters, 1 ml Cryo-vials	
4-glass chamber slides	Electron Microscopy Sciences, Lab-Tek (UK)
Sterile non pyrogenic DNase and RNase free freezing tube	Greiner BIO-one Ltd (UK)
FastStart DNA ^{Master} SYBR Green 1; LC-capillaries	Roche Diagnostics Ltd (Germany)
Filter tips	STar Lab (UK)
Molecular Biology Grade Solutions, Ethanol, Methanol, Glacial acetic acid, Isopropanol, Boric acid	VW International Ltd (UK)

Appendix 2: The Protein sequence of mouse and human CRYM

MKRAPAFLSAEEVQDHLRSSSLLIPPLEAALANFSKGPDGGVMQPVRTVVPVAKHRGFLGVMPAYSAAE
DALTTKLVTFYEGHSNTAVPSHQASVLLFDPSNGSLLAVMDGNVITAKRTAAVSAIATKLLKPPGSDVL
CILGAGVQAYSHYEIFTEQFSFKEVRMWNRTRENAEKFASTVQGDVRVCSSVQEAVTGADVIITVTMAT
EPILFGEWVKPGAHINAVGASRPDWRELDDELMRQAVLYVDSREAALKESGDVLLSGADIFAELGEVIS
GAKPAHCEKTTVFKSLGMAVEDLVAAKLVYDSWSSGK

Figure 2a.Protein sequence of mCRYM.
The protein sequence of mouse CRYM, sequence length: 313 amino acids.

MSRVPAFLSAAEVEEHLRSSSLLIPPLETALANFSSGPEGGVMQPVRTVVPVTKHRGYLGVMPAYSAAE
DALTTKLVTFYEDRGITSVVPSHQATVLLFEPSNGTLLAVMDGNVITAKRTAAVSAIATKFLKPPSSEV
LCILGAGVQAYSHYEIFTEQFSFKEVRIWNRTKENAEKFADTVQGEVRVCSSVQEAVAGADVIITVTLA
TEPILFGEWVKPGAHINAVGASRPDWRELDDELMKEAVLYVDSQEAALKESGDVLLSGAEIFAELGEVI
KGVKPAHCEKTTVFKSLGMAVEDTVAAKLIYDSWSSGK

Figure 2b. Protein sequence of hCRYM .
The protein sequence of human CRYM, sequence length: 314 amino acids

Appendix 3: Average expression stability values of remaining control genes in mouse kidneys

Samples	PGK	TBP	GAPDH	β-Actin	PPIB	Rn28s1	**Normalisat -ion Factor**
2587	1.85E+01	2.33E+01	1.57E+01	1.74E+01	2.38E+01	9.09E+00	**0.9368**
2613	2.06E+01	2.41E+01	1.70E+01	1.87E+01	2.77E+01	1.01E+01	**1.0258**
2615	2.04E+01	2.33E+01	1.61E+01	1.85E+01	2.52E+01	9.69E+00	**0.9803**
2458	2.18E+01	2.31E+01	1.71E+01	2.01E+01	2.76E+01	9.97E+00	**1.0366**
2589	2.12E+01	2.35E+01	1.64E+01	1.80E+01	2.73E+01	1.08E+01	**1.0187**
2609	2.08E+01	2.41E+01	1.67E+01	1.78E+01	2.75E+01	9.72E+00	**1.0052**
M < 1.5	**0.057**	**0.071**	**0.047**	**0.072**	**0.061**	**0.071**	

Appendix 4: Standard Curve of mouse CRYM and GAPDH produced by real-time qPCR

A) **B)**

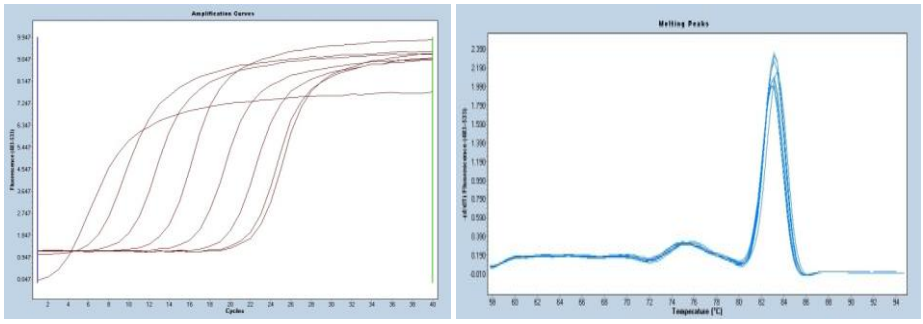

C)

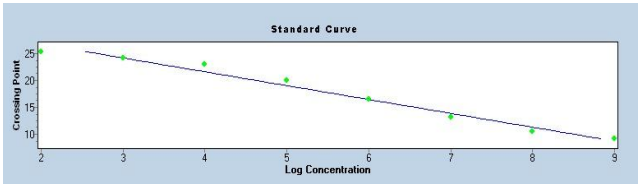

Figure 4a. Amplification of mCRYM in 10-fold dilutions and standardcurve generation.

Dilution series from 10^9 to 10^2 copies of the mCRYM PCR product were prepared and amplified by real time PCR. A) Amplification of mCRYM PCR product plotted versus cycle number. B) Melting curve derived from the amplification of mCRYM PCR product and after the last cycle, melting point analysis of mCRYM was obtained at 83°C. Also, the single melting peak for each amplified product is shown. C) Crossing point plotted against the known concentration of mCRYM standard (number of cycles needed to determine the PCR product plotted versus log concentration) to give the linear standard curve over 5 logs (10^9 to 10^2 dilutions) with correlation coefficient(r) = 1.00 and error = 0.0404.

A) **B)**

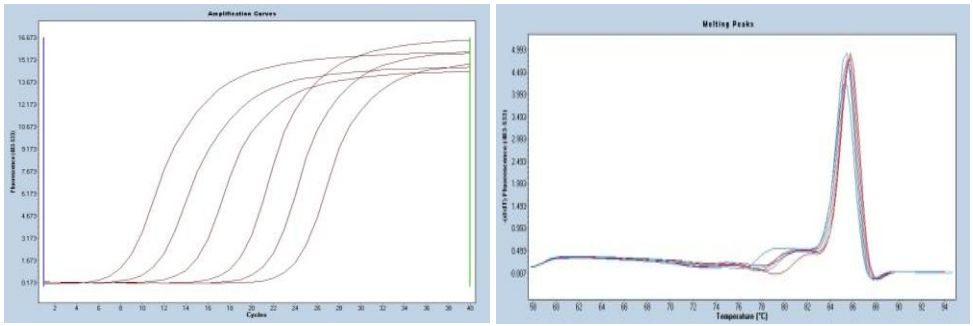

C)

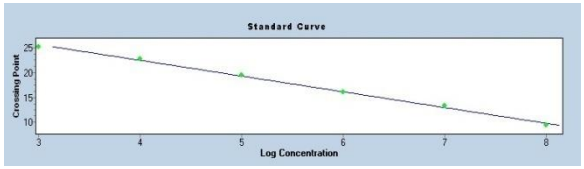

Figure 4b. Amplification of mGAPDH in 10-fold dilutions and standard curve generation.

Dilution series from 10^8 to 10^3 copies of the mGAPDH PCR product were prepared and amplified by real time PCR. A) Amplification of mGAPDH PCR product plotted versus cycle number. B) Melting curve derived from the amplification of mGAPDH PCR product and after the last cycle, melting point analysis of mGAPDH was obtained at 83°C. Also, the single melting peak for each amplified product is shown. C) Crossing point plotted against the known concentration of mGAPDH standard (number of cycles needed to determine the PCR product plotted versus log concentration) to give the linear standard curve over 5 logs (10^8 to 10^3 dilutions) with correlation coefficient(r) = 1.00 and error = 0.0404.

Appendix 5: Standard Curve of human CRYM and PGK produced by real-time qPCR

A) **B)**

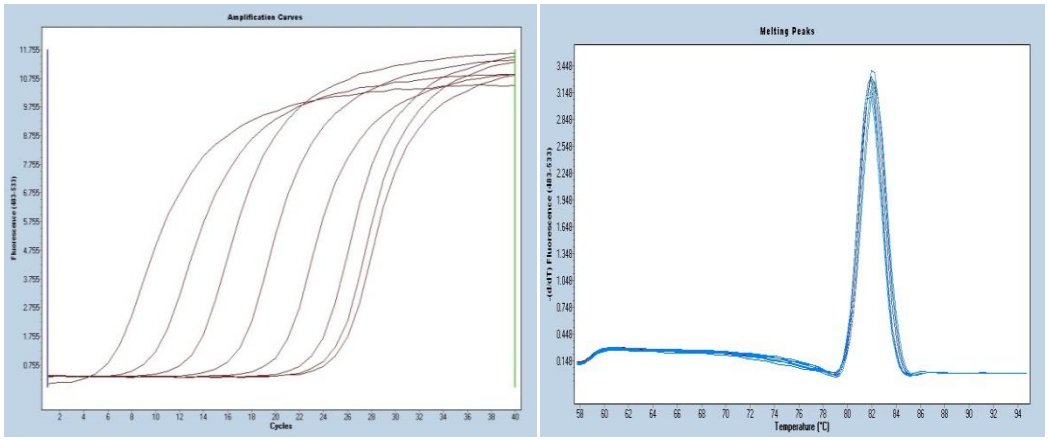

C)

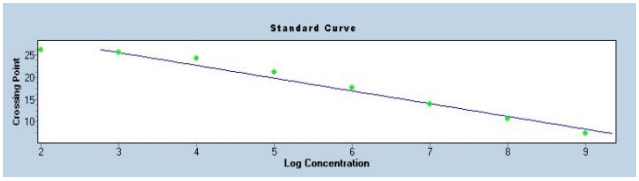

Figure 5a.Amplification of hCRYM in 10-fold dilutions and standard curve generation.

Dilution series from 10^9 to 10^2 copies of the hCRYM PCR product were prepared and amplified by real time PCR. A) Amplification of hCRYM PCR product plotted versus cycle number. B) Melting curve derived from the amplification of hCRYM PCR product and after the last cycle, melting point analysis of hCRYM was obtained at 83°C. Also, the single melting peak for each amplified product is shown. C) Crossing point plotted against the known concentration of hCRYM standard (number of cycles needed to determine the PCR product plotted versus log concentration) to give the linear standard curve over 5 logs (10^9 to 10^2 dilutions) with correlation coefficient(r) = 1.00 and error = 0.0404.

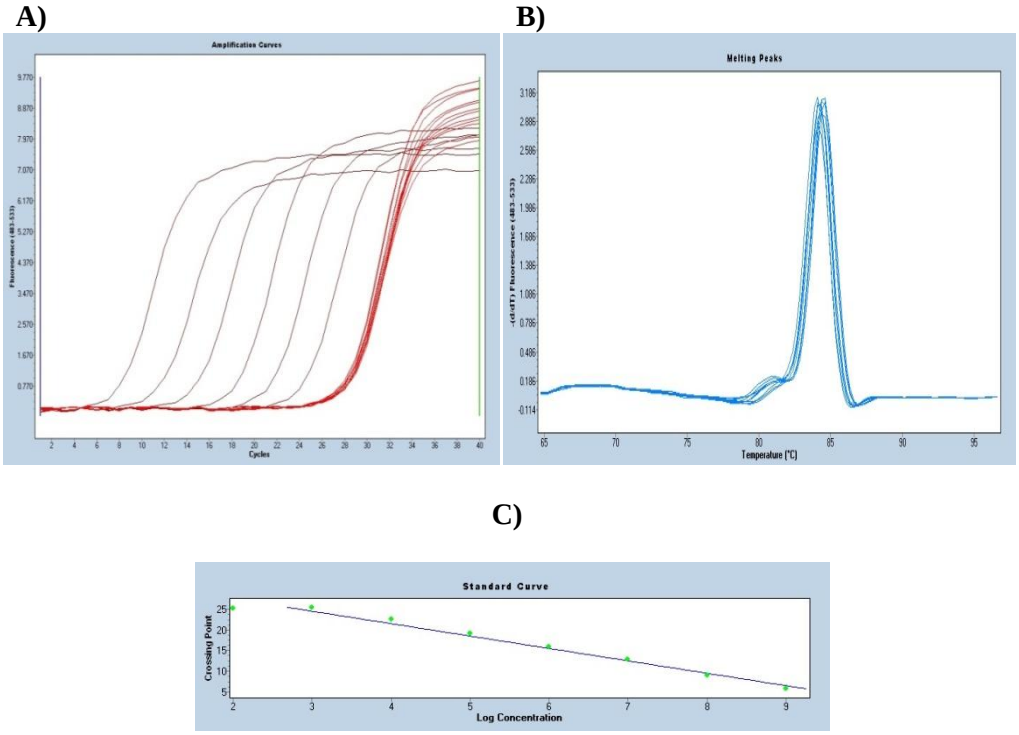

Figure 5b. Amplification of hPGK in 10-fold dilutions and standard curve generation.

Dilution series from 10^9 to 10^2 copies of the hPGK PCR product were prepared and amplified by real time PCR. A) Amplification of hPGK PCR product plotted versus cycle number. B) Melting curve derived from the amplification of hPGK PCR product and after the last cycle, melting point analysis of hPGK was obtained at 83°C. Also, the single melting peak for each amplified product is show. n) Crossing point plotted against the known concentration of hPGK standard (number of cycles needed to determine the PCR product plotted versus log concentration) to give the linear standard curve over 5 logs (10^9 to 10^2 dilutions) with correlation coefficient(r) = 1.00 and error = 0.0404

Appendeix 6. Quantification of CRYM mRNA copy numbers in the circulating blood of patients with type 2 diabetes, with and without retinopathy.

T2DR	CRYM(1)	CRYM(2)	CRYM(3)	GAPDH(1)	GAPDH(2)	GAPDH(3)
158	1970	371	91	173000	211000	227000
177	237	17	14	57800	59300	109000
186	41300	NA	146000	249000	388000	495000
79	111	299	1490	244000	232000	637000
39	34	984	22	169000	183000	200000
107	NA	33600	NA	438000	468000	635000
132	503	486	537	92400	110000	117000
100	663	261	234	198000	211000	221000
66	NA	5100	NA	583000	785000	873000
151	421	NA	NA	596000	964000	1610000
67	NA	NA	45400	184000	195000	514000
114	NA	NA	328	622000	711000	729000
20	0.79	2.36	4.53	184000	200000	229000
40	NA	20.60	0.30	170000	191000	207000
33	0.12	NA	18.70	536000	597000	502000
46	NA	NA	0.51	128000	129000	176000
68	NA	38.90	19.40	112000	113000	166000
39	1.33	58.70	14.30	24700	30300	35800
28	NA	NA	6.35	358000	366000	574000
56	NA	NA	8.90	410000	426000	628000
233	2.37	0.05	NA	274000	305000	354000
244	NA	0.36	NA	107000	46200	89700
42	NA	11.80	NA	198000	130000	209000
246	NA	7.4	NA	53200	75800	117000
176	2.91	NA	1.70	102000	102000	132000
Control						
39	70	96	78	284	374	503
139	49	193	220	2780	3250	3430
346	35	54	62	6360	6600	7650
356	75	331	103	1140	1620	1880
368	2650	1410	4920	481	483	693

Appendix 7. Quantification of CRYM CT values in the circulating blood of patients with type 2 diabetes, with and without retinopathy.

T2DR	CRYM-CT	GAPDH-CT	delta CT	delta delta CT	fold difference
174	19.54	16.13	3.41	4.91	0.06
179	12.99	14.43	-1.44	0.05	0.52
158	25.50	16.36	9.14	10.64	0.0013
177	28.61	17.89	10.72	12.22	0.0004
186	18.61	15.50	3.11	4.61	0.0819
79	25.63	15.63	9.99	11.49	0.0007
39	27.48	16.50	10.97	12.47	0.0004
86	18.81	15.08	3.72	5.22	0.0534
130	12.70	14.55	-1.85	-0.35	2.5521
84	18.87	13.77	5.10	6.60	0.0206
107	19.71	15.21	4.50	6	0.0313
123	21.54	15	6.54	8.04	0.0076
132	25.21	16.86	8.34	9.84	0.0022
100	25.72	17.48	8.23	9.73	0.0023
66	22.18	16.47	5.71	7.21	0.0135
150	17.56	16.15	1.41	2.91	0.2661
151	25.45	14.17	11.27	12.77	0.0003
156	16.20	15.22	0.97	2.47	0.3601
67	19.31	16.12	3.18	4.68	0.0777
115a	15.49	14.61	0.87	2.37	0.3851
141	14.86	14.08	0.78	2.28	0.4113
114	25.78	14.70	11.07	12.57	0.0003
146	19.83	16.68	3.15	4.65	0.0797
20	34.42	16.81	17.61	19.11	0.0000
40	34.17	16.92	17.25	18.75	0.0000
33	34.80	15.31	19.49	20.99	0.0000
46	36.18	17.34	18.83	20.33	0.0000
68	31.12	17.51	13.60	15.10	0.0001
39	32.35	19.72	12.63	14.13	0.0001
28	32.98	15.70	17.28	18.78	0.0000
56	32.55	15.50	17.04	18.54	0.0000
32	24.40	16.07	8.33	9.83	0.0022
233	36.64	16.17	20.46	21.96	0.0000
187	32.18	19.22	12.96	14.46	0.0001
244	36.63	19.75	16.87	18.37	0.0000
57	37.62	19.46	18.16	19.66	0.0000
42	32.19	18.51	13.67	15.17	0.0001
215	32.09	20	12.09	13.59	0.0002
197	30.12	18.49	11.62	13.12	0.0002
157	31.04	18.18	12.85	14.35	0.0001
27	32.78	20.53	12.25	13.75	0.0001
176	34.31	19.19	15.11	16.61	0.0000
246	32.78	19.72	13.06	14.56	0.0001

Control T2D					
71	26.8	24.20	2.6	2.6	0.3399
139	26.2	22.70	3.5	3.5	0.1797
346	27.4	25.2	2.2	2.2	0.4373
356	26.1	26.8	0.7	-0.7	3.2792
368	22.2	22.1	0.1	0.1	1.8277

Appendix 8. Quantification of CRYM mRNA in the circulating blood of patients with type 2 diabetes, with and without nephropathy

T2DN-A	CRYM(1)	CRYM(2)	CRYM(3)	PGK(1)	PGK(2)	PGK(3)
18	2.03	1.24	7.10	34.10	0.55	0.48
82	2.49	1.29	5.05	0.07	0.11	0.07
68	NA	6.95	3.30	0.73	0.62	0.00
25	7.35	3.49	1.30	0.25	NA	0.25
60	NA	1.14	21.30	1.02	0.38	0.11
16	5.68	1.43	1.61	0.05	0.13	0.18
56	NA	3.02	7.77	0.33	0.22	0.16
51	NA	1.26	NA	4.32	0.31	0.14
21	19.90	3.86	20.80	6.55	0.43	0.52
26	5.28	5.86	3.31	0.03	0.07	0.12
64	13.00	5.00	7.79	0.04	0.17	0.36
11	41.20	17.20	6.59	0.12	0.08	0.17
66	9.63	10.20	11.00	8.92	0.19	0.47
40	4.31	7.05	2.85	0.17	0.28	0.25
77	NA	6.62	22.00	0.15	0.10	0.12
36	5.83	2.44	6.23	0.49	0.05	0.00
59	3.13	4.19	1.30	6.00	0.07	0.24
67	3.19	3.54	3.42	0.16	0.20	0.18
75	5.82	2.57	1.70	0.39	0.40	0.17
83	57.50	4.13	18.60	1.07	0.59	0.24
110	123.00	46.00	97.10	0.38	0.62	0.72
111	2.05	3.93	7.43	2.07	0.40	0.82
210	NA	4.60	6.16	0.26	0.05	0.08
20	6.79	7.26	4.17	0.16	14.20	0.15
376	0.11	8.56	25.10	0.17	0.24	0.18
4	49.20	1.21	0.53	0.17	0.11	0.02
267	1.34	3.25	0.19	0.00	0.14	0.07
325	NA	3.42	2.83	0.25	0.86	0.45
305	4.33	2.22	0.40	0.84	0.39	0.25
278	2.44	2.67	7.02	0.09	0.13	0.35
183	NA	0	0.93	0.39	0.10	0.02
208	3.97	0.66	2.56	0.01	0.78	0.17
390	NA	4.43	4.25	0.04	0.25	0.85
117	NA	1.24	NA	0.19	0.09	0.19
212	1.65	2.67	NA	0.22	1.28	0.56
376	NA	4.25	NA	0.38	0.71	2.98
121	2.85	0	NA	0.15	0.16	0.08
271	8.65	0	3.13	0.23	0.17	0.19
T2DN-NA						
102	1.36	1.16	0.87	3.59	0.16	0.18
122	NA	4.31	2.23	0.26	0.17	0.28
141	2.47	1.96	3.43	0.05	0.41	0.31
133	4.11	6.21	3.74	0.04	0.03	0.08
113	3.88	2.77	3.18	1.70	2.48	1.38
19	2.32	0.79	0.08	0.26	0.25	0.21
15	2.17	2.84	1.59	0.15	0.16	0.13
3	NA	6.38	2.91	0.19	0.16	0.37
31	1.30	2.61	8.50	0.09	0.12	0.01
155	NA	26.30	22.40	0.28	0.21	0.10
159	11.50	30.40	2.75	0.11	0.33	0.13
175	NA	NA	21.50	0.78	0.29	0.50

191	17.40	1.87	4.92	0.11	0.14	0.52
174	NA	38.40	NA	0.22	0.14	0.17
204	6.01	2.86	2.39	0.09	1.32	0.18
207	0.16	1.40	1.07	0.08	0.34	0.18
211	211.00	NA	1.07	0.14	0.13	0.25
262	1.45	4.81	23.20	0.11	0.07	0.11
232	196.00	NA	0.95	0.20	0.38	0.17
221	2.00	3.52	3.52	0.13	0.15	0.30
243	31.70	NA	NA	0.39	0.48	205.0
217	39.00	29.90	47.00	0.21	0.14	0.25
322	NA	8.66	NA	0.14	0.53	0.57
283	NA	20.30	18.90	0.32	0.43	0.13
292	24.20	8.35	29.30	0.30	0.41	0.21
297	1.27	314.00	2.75	0.54	0.21	0.88
342	38.90	35.80	61.40	0.21	0.13	0.54
326	27.50	13.20	1.27	0.49	0.61	0.26
339	5.58	10.90	9.04	0.37	0.12	0.16
350	11.20	8.99	2.21	24.90	16.10	24.90
120	10.90	236.00	12.40	26.80	17.10	23.00
Control T2D						
123	11.70	11.30	14.60	21.80	19.80	23.30
127	22.20	2.71	7.18	16.00	16.30	10.50
131	10.30	31.80	4.84	52.70	37.80	43.80
138	55.50	8.62	9.25	34.10	29.10	16.30
140	10.40	7.88	4.26	38.70	27.00	41.20
154	11.50	32.10	11.90	31.60	33.00	20.40
157	11.00	80.70	2.39	11.40	10.30	14.70
187	9.81	21.80	4.87	19.70	13.10	13.70
185	11.50	NA	NA	17.10	18.10	22.50
229	19.10	30.40	19.20	18.70	23.60	21.70
235	1.38	1.54	1.87	33.00	15.30	13.30
284	5.83	2.13	1.40	12.70	10.70	12.80
252	10.00	1.24	1.32	28.90	11.00	11.20
182	0.08	0.05	0.73	81.60	4.75	23.60
152	NA	3.24	0.22	26.10	25.90	15.90
368	3.34	0.40	1.03	16.80	16.10	12.00
142	0.04	0.63	0.41	19.20	21.30	31.10
143	0.02	0.85	1.44	23.00	31.20	26.70
101	0.71	1.55	1.52	30.80	22.00	28.10
100	0.50	0.09	28.70	18.10	18.50	23.80
312	NA	1.37	1.49	9.22	8.78	15.90
330	4.93	1.17	7.01	10.00	13.80	12.60
379	7.91	2.56	11.00	0.51	1.08	0.50
317	NA	4.44	1.53	0.38	0.18	0.40
47	NA	2.93	3.64	0.34	0.37	0.41
23	NA	4.06	17.70	0.05	0.12	0.07
48	NA	5.84	1.74	0.30	0.18	0.05
302	NA	16.80	2.97	0.13	0.35	0.35
2	NA	10.70	0.07	3.31	0.12	0.08
378	NA	6.95	0.33	0.33	0	1.19

Appendix 9: The Protein sequence of mouse and human MOSC2/MOSC1.

MGSSSSTALARLGLPGQPRSTWLGVAALGLAAVALGTVAWRRTRPRRRRQLQQVGTVSKVW
IYPIKSCKGVSVCETECTDMGLRCGKVRDRFWMVVKEDGHMVTARQEPRLVLVSITLENNYL
TLEAPGMEQIVLPIKLPSSNKIHNCRLFGLDIKGRDCGDEVAQWFTNYLKTQAYRLVQFDTSM
KGRTTKKLYPSESYLQNYEVAYPDCSPVHLISEASLVDLNTRLKKKVKMEYFRPNIVVSGCEA
FEEDTWDELLIGDVEMKRVLSCPRCVLTTVDPDTGIIDRKEPLETLKSYRLCDPSVKSIYQSSPL
FGMYFSVEKLGSLRVGDPVYRMVD

Figure 9a. Protein sequence of mMOSC2.
The protein sequence of mouse MOSC2, sequence length: 338 amino acids.

MGAGSWALTLFGFSAFRVPGQPRSTWLGVAALGLAAVALGTVAWRRARPRRRRRLQQVGT
VAQLWIYPIKSCKGLSVSEAECTAMGLRYGHLRDRFWLVINEEGNMVTARQEPRLVLISLTCE
DDTLTLSAAYTKDLLLPITPPATNPLLQCRVHGLEIQGRDCGEDAAQWVSSFLKMQSCRLVHF
EPHMRPRSSRQMKASKSFSQNNEVAYSDASPFLVLSEASLEDLNSRLERRVKATNFRPNIVISG
CGVYAEDSWNEVLIGDVELKRVMACTRCLLTTVDPDTGISDRKEPLETLKSYRLCDPSEQALY
GKLPIFGQYFALENPGTIRVGDPVYLLGQ

Figure 9b. Protein sequence of mMOSC1.
The protein sequence of mouse MOSC1, sequence length: 342 amino acids.

MGASSSSALARLGLPARPWPRWLGVAALGLAAVALGTVAWRRAWPRRRRRLQQVGTVAKL
WIYPVKSCKGVPVSEAECTAMGLRSGNLRDRFWLVIKEDGHMVTARQEPRLVLISIIYENNCLI
FRAPDMDQLVLPSKQPSSNKLHNCRIFGLDIKGRDCGNEAAKWFTNFLKTEAYRLVQFETNM
KGRTSRKLLPTLDQNFQVAYPDYCPLLIMTDASLVDLNTRMEKKMKMENFRPNIVVTGCDAF
EEDTWDELLIGSVEVKKVMACPRCILTTVDPDTGVIDRKQPLDTLKSYRLCDPSERELYKLSPL
FGIYYSVEKIGSLRVGDPVYRMV

Figure 9c. Protein sequence of hMOSC2.
The protein sequence of human MOSC2, sequence length: 335 amino acids.

MGAAGSSALARFVLLAQSRPGWLGVAALGLTAVALGAVAWRRAWPTRRRRLLQQVGTVAQ
LWIYPVKSCKGVPVSEAECTAMGLRSGNLRDRFWLVINQEGNMVTARQEPRLVLISLTCDGD
TLTLSAAYTKDLLLPIKTPTTNAVHKCRVHGLEIEGRDCGEATAQWITSFLKSQPYRLVHFEPH
MRPRRPHQIADLFRPKDQIAYSDTSPFLILSEASLADLNSRLEKKVKATNFRPNIVISGCDVYAE
DSWDELLIGDVELKRVMACSRCILTTVDPDTGVMSRKEPLETLKSYRQCDPSERKLYGKSPLF
GQYFVLENPGTIKVGDPVYLLGQ

Figure 9d. Protein sequence of hMOSC1.
The protein sequence of human MOSC1, sequence length: 337 amino acids.

Appendix 10: Standard Curve of mouse and human MOSC2 produced by real-time qPCR

A) **B)**

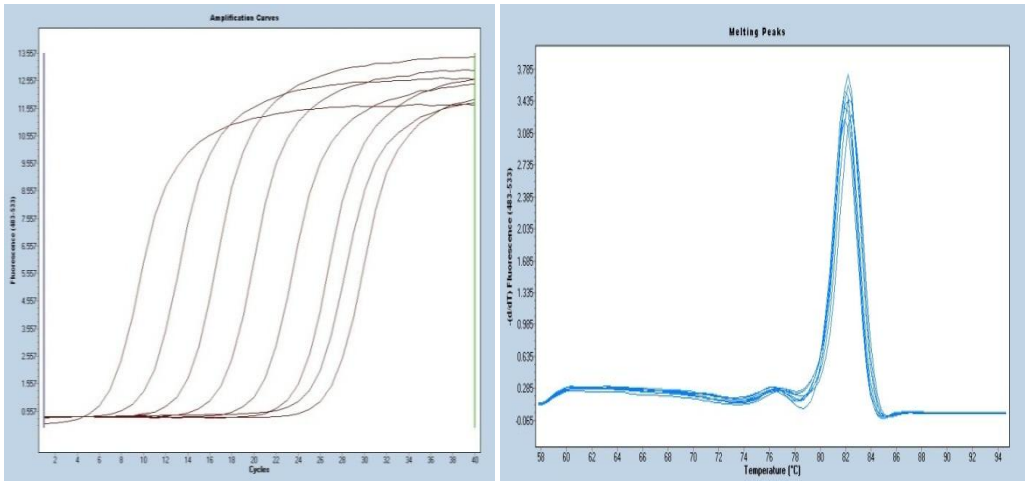

C)

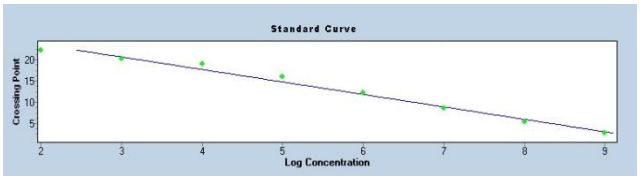

Figure 10a. Amplification of mMOSC2 in 10-fold dilutions and standard curve generation.

Dilution series from 10^9 to 10^2 copies of the mMOSC2 PCR product were prepared and amplified by real time PCR. A) Amplification of mMOSC2 PCR product plotted versus cycle number. B) Melting curve derived from the amplification of mMOSC2 PCR product and after the last cycle, melting point analysis of mMOSC2 was obtained at 83°C. Also, the single melting peak for each amplified product is shown. C) Crossing point plotted against the known concentration of mMOSC2 standard (number of cycles needed to determine the PCR product plotted versus log concentration) to give the linear standard curve over 5 logs (10^9 to 10^2 dilutions) with correlation coefficient(r) = 1.00 and error = 0.0404

A) **B)**

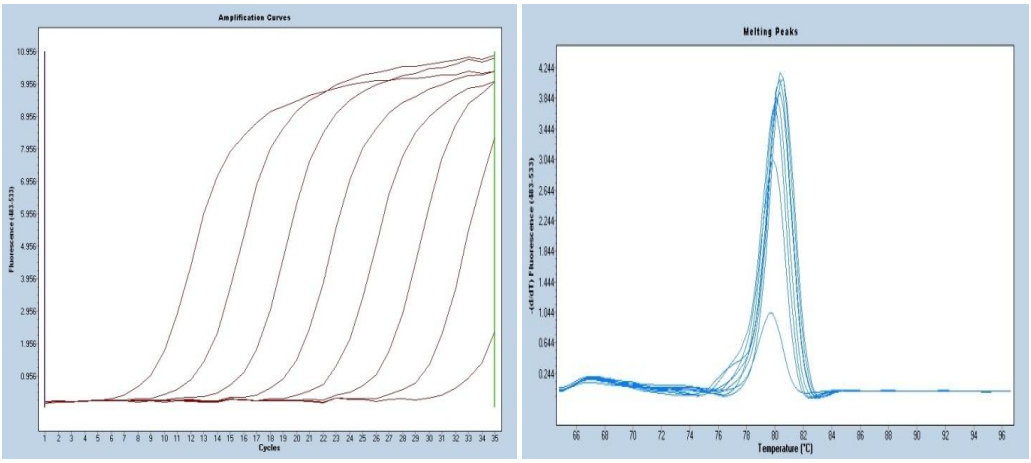

C)

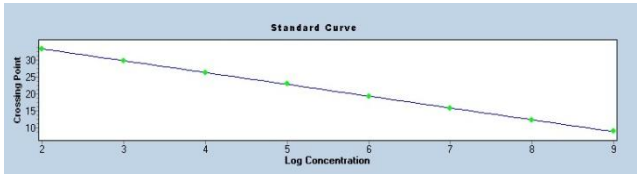

Figure 10b.Amplification of hMOSC2 in 10-fold dilutions and standard curve generation.

Dilution series from 10^9 to 10^2 copies of the hMOSC2 PCR product were prepared and amplified by real time PCR. A) Amplification of hMOSC2 PCR product plotted versus cycle number. B) Melting curve derived from the amplification of hMOSC2 PCR product and after the last cycle, melting point analysis of hMOSC2 was obtained at 83°C. Also, the single melting peak for each amplified product is shown. C) Crossing point plotted against the known concentration of hMOSC2 standard (number of cycles needed to determine the PCR product plotted versus log concentration) to give the linear standard curve over 5 logs (10^9 to 10^2 dilutions) with correlation coefficient(r) = 1.00 and error =0.0404

Appendix 11: Standard Curve of mouse and human MOSC1 produced by real-time qPCR

A) **B)**

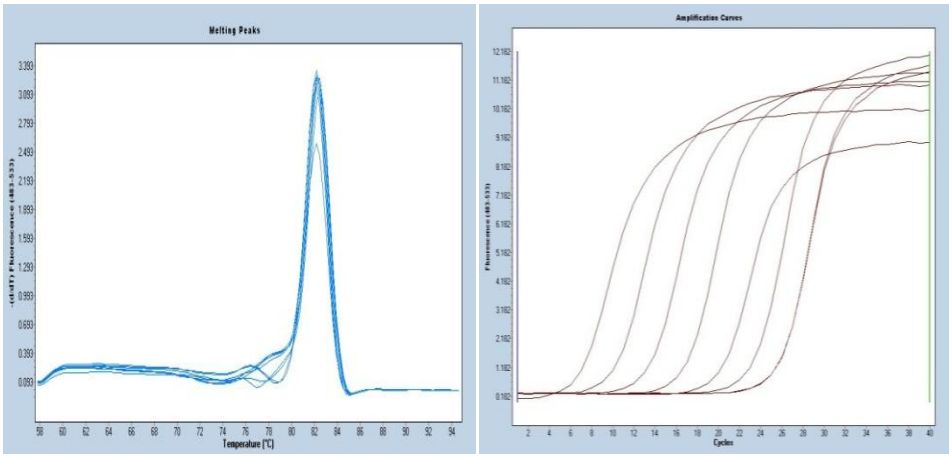

C)

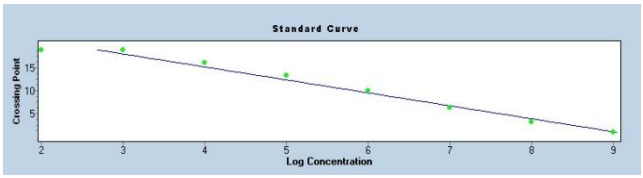

Figure 11a. Amplification of mMOSC1 in 10-fold dilutions and standard curve generation.

Dilution series from 10^9 to 10^2 copies of the mMOSC1 PCR product were prepared and amplified by real time PCR. A) Amplification of mMOSC1 PCR product plotted versus cycle number. B) Melting curve derived from the amplification of mMOSC1 PCR product and after the last cycle, melting point analysis of mMOSC1 was obtained at 83°C. Also, the single melting peak for each amplified product is shown. C) Crossing point plotted against the known concentration of mMOSC1 standard (number of cycles needed to determine the PCR product plotted versus log concentration) to give the linear standard curve over 5 logs (10^9 to 10^2 dilutions) with correlation coefficient(r) = 1.00 and error = 0.0404.

A) **B)**

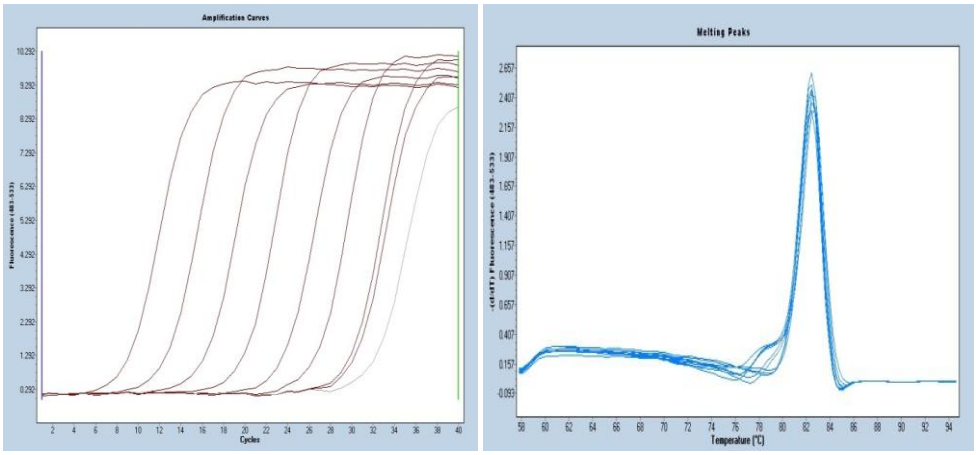

C)

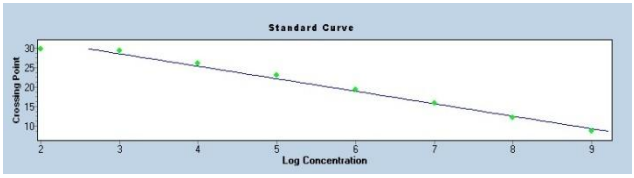

Figure 11b.Amplification of hMOSC1 in 10-fold dilutions and standard curve generation.

Dilution series from 10^9 to 10^2 copies of the hMOSC1 PCR product were prepared and amplified by real time PCR. A) Amplification of hMOSC1 PCR product plotted versus cycle number. B) Melting curve derived from the amplification of hMOSC1 PCR product and after the last cycle, melting point analysis of hMOSC1 was obtained at 83°C. Also, the single melting peak for each amplified product is shown. C) Crossing point plotted against the known concentration of hMOSC1 standard (number of cycles needed to determine the PCR product plotted versus log concentration) to give the linear standard curve over 5 logs (10^9 to 10^2 dilutions) with correlation coefficient(r) = 1.00 and error = 0.0404.

Abbreviations

$1,25(OH)_2D_3$	1,25-DihydroxyvitaminD3
ACE	Angiotensin-converting enzyme
AD	Aldose reductase
ADA	American Diabetes Association
AGEs	Advanced glycation end products
Ang	Angiotensinogen
BSA	Bovine serum albumin
***Phb2* KO**	βeta-*Prohibitin2* knockout
C_T	Threshold cycle
CDKs	Candidate diabetes associated kidney clones
CKD	Chronic kidney disease
CRYM	μ-crystalline
CTGF	Connective tissue growth factor
CVD	Cardiovascular disease
DAG	Diacylglycerol
DCCT	Dibetes Control and Complications Trial
DMEM	Dulbecco's Modified Eagle's Medium
DMSO	Dimethyl Sulfoxide
DN	Diabetic nephropathy
DR	Diabetic retinopathy
ds DNA	Double stranded DNA
ECM	Extracellular matrix
EDIC	Epidemiology of Diabetes Interventions and Complications Study Research Group
eNOS	Endothelial nitric oxide synthase

ERK1/2	Extracellular-signal regulated kinase 1 and 2
ESRD	End stage renal disease
FITC	Fluorescein isothiocyanate
FN	Fibronectin
GAPDH	Glyceraldehyde-3 phosphate dehydrogenase
GBM	Glomerular basement membrane
GFAT	Glutamine:fructose-6 phosphate amidotransferase
GFR	Growth filtration rate
GH	Growth hormone
GK	Goto Kakizaki
G-6-P	Glucose 6-phosphate
GLUT	Glucose transporter
HDL	High density lipoprotein
HEK	Human embryonic kidney
HG	High glucose
HMCs	Human mesangial cells
HMCLs	Human mesangial cell line
HRP	Horseradish peroxidase
HSP	Heat shock proteins
HTC	Human tubular cells
IDDM	Insulin dependent diabetes mellitus
IGF	Insulin-like growth factor
ITS	Insulin-transferrin-selenium
LC	Light cycler
LDL	Low-density lipoprotein
mARC	mitochondrial Amidoxime-Reducing Component

MnSOD	Manganese superoxide dismutase
MOPS	3-(N-morpholino) propanesulfonic acid
MOSC	Molybdenum Cofactor Sulfurase C-Terminal
NADP	Nicotinamide adenine dinucleotide phosphate
NOHA	N-hydroxyl-L-arginine
NG	Normal glucose
NGF	Nerve growth factor
NGM	Normal glucose plus mannitol
NF-$_K$B	Nuclear factor kappa B
NIDDM	Non insulin dependent diabetes mellitus
n-LDL	Native low density lipoprotein
nNOS	Neuronal nitric oxide synthase
NO	Nitric oxide
OD	Optical density
PAGE	Polyacrylamide gel electrophoresis
PBS	Phosphate buffer saline
PBMCs	Peripheral Blood Mononuclear Cells
PGK	Phosphoglycerate kinase
PKC	Protein kinase C
PPIB	Peptidylprolyl isomerase B
qPCR	Quantitative real time PCR
RAS	Renin-angiotensin system
RAGE	Receptor for advanced glycation end products
ROS	Reactive oxygen species
RT-PCR	Reverse transcriptase polymerase chain reaction
SD	Sorbitol dehydrogenase

SDS	Sodium dodecyl sulphate
SNP	Single nucleotide polymorphism
SOD	Superoxide dismutase
TBP	TATA box binding protein
T1D	Type 1 diabetes
T2D	Type 2 diabetes
TGF-β1	Transforming growth factor beta 1
tRNA	Transfer ribonuclease
UKPDS	UK Prospective Diabetes study
USRDS	US Renal Data System Annual Data Report